Illinois U Library

The American Mineralogist

Journal of the Mineralogical
Society of America

VOL. 43 JANUARY-FEBRUARY, 1958 Nos. 1 and 2

Contents

Foshagite: composition, unit cell and dehydration .... J. A. Gard and H. F. W. Taylor 1
Simplotite, a new quadrivalent vanadium mineral from the Colorado Plateau. .... M. E. Thompson, C. H. Roach and Robert Meyrowitz 16
New method for orienting electron microscope replicas .... Robert V. Rice and Alvin J. Cohen 25
Chrome mica-clay, Temple Mountain, Utah .... Paul F. Kerr and P. K. Hamilton 34
Hardness of single ice crystals .... T. R. Butkovich 48
Relationships among impurity contents, color centers and lattice constants in quartz .... A. J. Cohen and G. G. Sumner 58
The system $Fe_3O_4 - Mn_3O_4$ .... H. J. Van Hook and M. L. Keith 69
Relation between lattice constants and composition of the Ca-Mg carbonates .... Julian R. Goldsmith and Donald L. Graf 84
Some properties of diamond .... E. N. Bunting and A. Van Valkenburg 102
A chlorine-rich biotite from Lemhi County, Idaho .... Donald E. Lee 107
Notes on tapiolite, with special reference to tapiolite from southern Westland, New Zealand .... C. Osborne Hutton 112
Alteration of olivine and orthopyroxene in basic lavas and shallow intrusions. .... H. G. Wilshire 120
On chlorine in serpentinized dunite .... J. W. Earley 148
Notes and News: An occurrence of molybdenian stolzite in Arizona .... John N. Faick and Fred A. Hildebrand 156
Huntite from Tea Tree Gully, South Australia .... Brian J. Skinner 159
Chromian muscovite from Baker Mountain, Virginia .... R. V. Dietrich 162
A complex form of natural nepheline from Iivaara, Finland .... Th. G. Sahama 165

(*Continued on Cover 2*)

EDITOR: LEWIS S. RAMSDELL

BOARD OF ASSOCIATE EDITORS:

CHARLES L. CHRIST
ROBERT GARRELS
D. JEROME FISHER
E. WM. HEINRICH (1957–58)
JOSEPH MURDOCH (1957–59)
GEORGE T. FAUST (1958–60)

Published bi-monthly by the Society

(*Contents continued*)

Chart showing the sphere of influence of atoms and ions in minerals.... ....**Jerome H. Remick** **166**

Nonfibrous ulexite from the Kramer District, California................ ....**Robert D. Allen** **169**

Magnetic susceptibilities of minerals in the Frantz Isodynamic magnetic separator..........................**Sam Rosenblum** **170**

The structure and properties of natural and synthetic minerals......... ....**P. Saha and J. B. Smith** **174**

Book Reviews.. **176**

New mineral names... **180**

Mineralogical Society of America

ASSOCIATED WITH THE GEOLOGICAL SOCIETY OF AMERICA

President: **George E. Goodspeed,** University of Washington, Seattle 5, Washington.
Vice-President: **Ralph E. Grim,** University of Illinois, Urbana, Illinois.
Secretary: **C. S. Hurlbut, Jr.,** Harvard University, Cambridge 38, Massachusetts.
Treasurer: **Earl Ingerson,** U. S. Geological Survey, Washington 25, D. C.
Editor: **Lewis S. Ramsdell,** University of Michigan, Ann Arbor, Michigan.
Councilors: **Chester B. Slawson,** University of Michigan, Ann Arbor, Michigan.
Alfred O. Woodford, Pomona College, Claremont, California.
Samuel S. Goldich, University of Minnesota, Minneapolis 14, Minnesota.
Brian H. Mason, American Museum of Natural History, New York 24, New York.
Richard H. Jahns, California Institute of Technology, Pasadena, California.
Charles Milton, U. S. Geological Survey, Washington 25, D. C.
D. Jerome Fisher, University of Chicago, Chicago 37, Illinois.

The enlarged issues of this journal for 1958 are made possible by a grant from the Penrose Fund of the Geological Society of America.

The American Mineralogist—Journal of the Mineralogical Society of America

The journal, containing articles on mineralogy, crystallography, and allied sciences, is issued every two months. Contributions are invited.

The general conduct of the journal is in the hands of the editor, Lewis S. Ramsdell, Department of Mineralogy, University of Michigan, to whom all manuscripts should be submitted. To assist the editor, the Council of the Society has appointed the following Board of Associate Editors:

Charles L. Christ, U. S. Geological Survey, Washington 25, D. C.
E. Wm. Heinrich, Department of Mineralogy, University of Michigan, Ann Arbor, Michigan.
Robert M. Garrels, Harvard University, Cambridge 38, Massachusetts.
Joseph Murdoch, University of California at Los Angeles, Los Angeles, California.
D. Jerome Fisher, University of Chicago, Chicago 37, Illinois..
George T. Faust, U. S. Geological Survey, Washington 25, D. C.

Authors are requested to submit two copies of each manuscript, typewritten on standard size paper, 8½×11 inches. Photographs submitted for cuts should be glossy prints.

Beginning with Vol. 43, 1958, authors are entitled to 50 free reprints, without covers, of each article published.

Sent to all members and fellows of the Mineralogical Society of America. Membership dues $4.00 annually, fellowship dues $5.00 annually. Subscriptions for libraries, college, institutions, companies and similar organizations $6.00 annually.

Entered as second class matter at the post office at Menasha, Wis., under Act of March 3, 1879. Acceptance for mailing at the special rate of postage provided for in section 1103, Act of Oct. 3, 1917, paragraph 4 section 429 P. L. & R. authorized March 13, 1922.

Notice of change of address, orders, and remittances should be sent to Dr. Earl Ingerson, U. S. Geological Survey, Washington 25, D. C.

Printed by the George Banta Company, Inc., Menasha, Wisconsin
Printed in the United States of America

Leitz

first in precision optics

NEW

POLARIZING

MICROSCOPE SM-pol

Leitz sets a new standard with this student polarizing and chemical microscope of modern design, with dual, low-position focusing controls and large field of view. A reasonably priced polarizing microscope, the model SM-pol, has rugged, one-piece construction with Bertrand lens and pinhole diaphragm built into the tube. Inclined monocular tube will accommodate wide-field eyepieces and the microscope can be used faced away from the observer, permitting easy accessibility to the stage.

A reputation for integrity and a tradition of service have led thousands of scientific workers to bring their optical problems to Leitz. If you have problems in this field, why not let us help you with them?

See your Leitz dealer and examine these Leitz instruments soon. Write for information.

E. LEITZ, INC., Dept. AM-2
468 Fourth Avenue, New York 16, N. Y.

Please send me the Leitz____________brochure.

NAME____________________

STREET____________________

CITY__________ZONE______STATE______

E. LEITZ, INC., 468 FOURTH AVENUE, NEW YORK 16, N. Y.
Distributors of the world-famous products of
Ernst Leitz G. m. b. H., Wetzlar, Germany—Ernst Leitz Canada Ltd.
LEICA CAMERAS · LENSES · MICROSCOPES · BINOCULARS

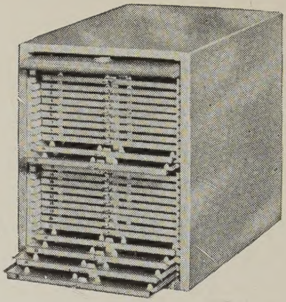

Eberbach

PETROGRAPHIC SLIDE
FILING CABINETS

These cabinets provide an expandable filing system. They may be stacked beside or on top of each other as the collection increases. The cabinet holds 750 slides, each of the 25 aluminum trays holding thirty 45 by 26 mm. slides. The door disappears, as shown, into the top of the cabinet which measures 10" high, 8½" wide by 12" deep. The cabinets are sturdily constructed of seasoned hardwood which is carefully filled and lacquered to retain the attractive light oak hue. The cabinet carries catalog number 60-664 and sells for $52.50.

Eberbach SCIENTIFIC INSTRUMENTS & APPARATUS CORPORATION
ANN ARBOR, MICH. ESTABLISHED 1843

MINERAL SPECIMENS

Large variety of crystals, crystal groups, rare minerals, and ore minerals for collectors, universities and museums.

1958 Mineral Catalog 25¢, or sent free when requested on official letterhead.

Filer's are interested in buying or exchanging for good quality minerals, especially from foreign countries. Correspondence is invited.

FILER'S
P. O. Box 372, Redlands, California

Our Specialty is
SELECTED MINERAL SPECIMENS
FROM WORLD-WIDE LOCALITIES FOR COLLECTORS AND MUSEUMS
we also carry a complete line of
MINERALIGHTS, DETECTRON GEIGER COUNTERS, ESTWING PROSPECTOR PICKS, MINERALOGICAL BOOKS, ETC.
Send for free current bulletin
SCHORTMANN'S MINERALS
6 McKinley Avenue Easthampton, Massachusetts

LET'S GET ACQUAINTED" OFFER

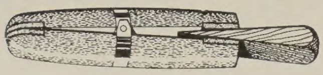

YOU BUY A RING CLAMP No. T33-I
REGULAR PRICE OF $1.35

'E WILL GIVE YOU ABSOLUTELY FREE A LADIES
ERLING SILVER RING IN ANY SIZE FROM 4 THRU 8.

ORD YOUR ORDER LIKE THIS:
ND ME I No. T33-I $1.35
I FREE RING X30-14. SEND SIZE - - -

U MAY SEND A $ BILL PLUS 35c IN STAMPS OR YOUR CHECK.
L ITEMS SENT POSTAGE PREPAID.

YOU SHOULD ALSO GET ACQUAINTED WITH —

RIEGER'S FABULOUS TREASURE CHEST OF JEWELRY VALUES

EY CHAINS
RACELET CHAINS
ARIAT CORDS
ELL CAPS
AROQUE RINGS
AROQUE CUFF LINKS
AROQUE STONES
ING MOUNTINGS
UCKY CLOVER
ARWIRES

QUALITY
LOW PRICES
VARIETY
SEND FOR OUR LATEST BARGAIN BULLETIN FOR A LISTING OF MANY OF THESE ITEMS.

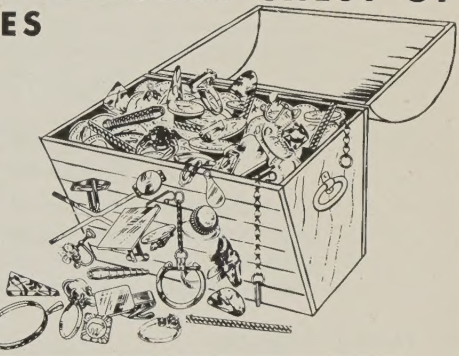

DO YOU HAVE THE FOLLOWING FREE CATALOGS?

PS-12 A 16-page Catalog of Synthetic Boules in color, Carved Jade items, Rock Crystal novelties, and new Safety Set Gem Mounts.

PS-13 A 24-page Catalog of Faceted Gem Stones printed in actual colors.

PS-14 A 16-page Catalog of Gold Rings to fit gems in Catalog PS-13.

S-15 A Catalog devoted Exclusively to **Rough Gem Materials.** Contains FIRST OFFERINGS of the exciting **NEW BLUE** AND **BLACK** ITALIAN **GOLDSTONE. GRIEGER'S ARE THE "FIRST" TO OFFER MANY NEW ITEMS!**

S-16 A **NEW CATALOG** listing all of our **"MONEY SAVING" PREMIUM OFFERS. YOU CAN SAVE** UP TO **50%.**

REQUEST CATALOGS YOU DO NOT HAVE BY NUMBER!

COME TO OUR STORE

UGE NEW SHIPMENT OF TIGER EYE JUST ARRIVED direct from Africa.

SK FOR YOUR FREE SAMPLE OF I dozen 7 prong one piece **bell caps.** REGULAR etail VALUE 75c. Ask for it by #X30-7—Only **I dozen** free to each store customer r with a mail order.

GRIEGER'S INC. • Mailing Address: P. O. Box 4185 • CATALINA STATION, PASADENA, CALIF.
Dep't K9-178 Store Address: 1633 E. WALNUT ST. • PASADENA 4, CALIF.
OUR STORE IS OPEN EVERY DAY 8:30 A.M. UNTIL 5:00 P.M. — CLOSED ALL DAY SUNDAY

For Mineralogists:

Index of Refraction Liquids

Range: 1.35 to 2.11 index; available in sets of limited range, or in sets with various intervals, or in any selection. Note that liquids 2.01 to 2.11 are now available.

See detailed price list of index liquids in our three-page advertisement in the July-August and September-October issues of the American Mineralogist. Or, write for Price List Nd-AM

Allen Reference Sets for Microscopical Studies in Mineralogy and Petrology

Six sets of Authentic materials for use as standards for refractive index, for standard materials mounted in balsam to be compared with unknowns, and for demonstration of typical optical characteristics under microscopical study.

Write for descriptive material A-AM

Text: Practical Refractometry by Means of the Microscope

By Roy M. Allen, D.SC.

Describes the technique of the immersion method of microscopy, with particular reference to the identification of minerals. Written primarily for elementary instruction, but this text will be very useful also to advanced workers. Price $1.00. Copy will be sent on approval.

Heavy Liquids

Formulated especially for determination of specific gravity of minerals, but special formulations are being made to order for various procedures. If you have any special problem in this field of separation of minerals or other materials by differences in specific gravity, please write us about your problem. Or, just write for leaflet HL-AM.

Lovins Field Finder

For re-locating any point of interest on microscope slide. Same size as a 3″ x 1″ microscope slide; has 1012 1mm. squares, each square numbered and lettered, with sides graduated into tenths. A beautiful example of micro-photography.

Write for Leaflet LFF-AM

Gems, Testing For Identity and For Defects

The CARGILLE-ALLEN GEM TESTING SET is the title of our new book describing the properties of gems and also the equipment for certain identification of gems by a new simple procedure. Price $1.00; this amount applicable to purchase price of any of the items listed in the book.

R. P. Cargille Laboratories, Inc.
117 Liberty St., New York 6, N.Y.

THE AMERICAN MINERALOGIST

JOURNAL OF THE MINERALOGICAL SOCIETY OF AMERICA

Vol. 43 JANUARY–FEBRUARY, 1958 Nos. 1 and 2

FOSHAGITE: COMPOSITION, UNIT CELL AND DEHYDRATION

J. A. GARD AND H. F. W. TAYLOR, *University of Aberdeen, Scotland.*

ABSTRACT

Foshagite is confirmed as a mineral species. A new analysis gives the composition $4CaO \cdot 3SiO_2 \cdot H_2O$; the ionic constitution is probably $Ca_4Si_3O_9(OH)_2$, with infinite metasilicate chains similar to those in wollastonite. The unit cell has been determined from a combination of single-crystal electron diffraction and oriented fibre x-ray methods; it is A-centred monoclinic with a 10.32, b 7.36, c 14.07 Å, β 106.4°, $Z=4$. The crystals are markedly fibrous with length b, and principal cleavage (001). Reflections with k odd are weak and diffuse, and the pseudo-cell is primitive monoclinic with a 10.32, b 3.68, c 7.04 Å, β 106.4°. Foshagite is dehydrated at about 700°, when it undergoes oriented transformation to β-$CaSiO_3$ and β-Ca_2SiO_4. The relationship of orientations in this transformation has been determined. In conjunction with other evidence, it gives a preliminary indication of the crystal structure.

INTRODUCTION

Foshagite was discovered at Crestmore, California by Eakle (1925). He showed that it was a white, fibrous mineral of approximate composition $5CaO \cdot 3SiO_2 \cdot 3H_2O$ and concluded from its optical properties that it was probably orthorhombic. Vigfusson (1931) concluded from optical and x-ray powder evidence that it was identical with hillebrandite, as did Berman (1937), but later x-ray powder work (Flint, McMurdie, and Wells, 1938; McMurdie and Flint, 1943; Heller and Taylor, 1956) showed that this was incorrect. Taylor (1952) obtained a fibre rotation pattern which indicated a 7.3 Å repeat distance along the fibre axis, with strong pseudo-halving. In this respect, foshagite resembles several other calcium silicate minerals such as xonotlite, hillebrandite, and tobermorite. Heller (1952) showed that dehydration caused ordered (or partly ordered) transformation to β-$CaSiO_3$ and β-Ca_2SiO_4. Flint, McMurdie, and Wells (1938) described the synthesis. Jander and Franke (1941) prepared a compound which they considered to be $3CaO \cdot 2SiO_2 \cdot H_2O$, the powder data for which agreed with those of foshagite. Newman (1956) made a new analysis and determined the heat of solution. The unit cell has not previously been determined.

TABLE 1. CORRELATION OF THE *X*-RAY POWDER DATA OF HELLER AND TAYLOR (1956) WITH *d*-SPACINGS CALCULATED FOR THE MONOCLINIC PSEUDO-CELL, WITH *k*-INDICES DOUBLED. CuKα RADIATION. CAMERA DIAMETERS 6 CM. AND 19 CM.

X-ray powder data		Monoclinic pseudo-cell	
d-spacings (Å)	*k*-indices	*hkl*-indices	*d*-spacings (Å)
10.0 mw	0	100	9.90
6.8 ms	0	001	6.75
4.95 ms	0	200, 101	4.95, 4.96
3.56 w	0	201	3.55
3.37 ms	0	002, $30\bar{1}$	3.37, 3.36
3.25 m	0	$20\bar{2}$	3.23
2.92 vvs	2	121, 220	2.95
2.79 mw	0	$30\bar{2}$	2.78
2.68 vw	0	301	2.67
2.48 m	0	202, 400	2.48
	2	022, $32\bar{1}$, 320	2.48, 2.48, 2.46
2.33 vw	0	$10\bar{3}$, $40\bar{2}$	2.33
2.30 ms	0	$20\bar{3}$	2.30
2.25 vw	2	$32\bar{2}$	2.22
2.16 ms	2	321	2.17
2.12 w	2	$42\bar{1}$	2.11
2.09 w	0	302	2.09
2.07 mw	2	222, 420	2.05
1.99 vw	0	500, $50\bar{2}$	1.98, 1.97
1.93 vw	2	$22\bar{3}$, 023	1.95, 1.92
1.86 vvw	2	421, $32\bar{3}$	1.86
1.84 ms	4	040	1.84
1.82 vvw	2	322, 123, $52\bar{1}$	1.81, 1.80, 1.80
1.77 m	0	402, 501	1.77
1.74 vs/b	0	$20\bar{4}$, $50\bar{3}$, $10\bar{4}$	1.75
	2	520	1.74
1.72 vvw	0	$30\bar{4}$, $60\bar{1}$	1.71, 1.72
	2	$52\bar{2}$	1.72
1.66 vw	0	303, 600	1.65
1.63 mw	2	223	1.66
1.59 m	2	422, 521, $22\bar{4}$	1.59, 1.59, 1.58
1.57 vw	0	104, $60\bar{3}$	1.59, 1.55
1.55 vw	2	$62\bar{1}$, $32\bar{4}$	1.55
1.53 w	0	502	1.53
1.52 w	2	024, $62\bar{2}$	1.53
1.51 vw	2	323, 620	1.50

d-spacings (continued)

1.47 mw
1.46 w
1.42 mw
1.40 vw
1.39 vw
1.36 vw
1.35 vvw
1.34 vw
1.32 w
1.29 vw
1.26 mw
1.22 vw
1.18 vw
1.17 vw
1.154 w
1.127 vw
1.115 vvw
1.107 vw/b
1.100 vvw
1.077 vvw
1.057 vw
1.039 mw

OPTICAL AND *X*-RAY RESULTS

The specimen used was from Eakle's collection at the University of California, collected at the type locality and kindly provided by Professor A. Pabst. It consisted of long white fibres. *X*-ray examination showed that even small fibres were composed of crystallites that were well-aligned but rotated at random round the fibre axis, and single-crystal patterns were therefore unobtainable. The fibres have parallel extinction with positive elongation. The refractive index is 1.598 ± 0.002 for light vibrating parallel to the fibre direction and 1.594 ± 0.002 for light vibrating across it. Small crystals of thaumasite, identified optically, are distributed fairly evenly in the material and in places were concentrated in yellowish masses up to a few millimetres in each direction. Occasional crystals of calcite are also present. *X*-ray photographs of fibres taken from different parts of the specimen show that except for one region in which it is intergrown with hillebrandite, the foshagite is free from other known calcium silicate minerals. In all these respects the material agrees closely with Eakle's description, although the latter did not report the presence of hillebrandite.

The *x*-ray powder and oriented fibre data given by Heller and Taylor (1956) were obtained using this specimen and are reproduced in Table 1. The powder data agree substantially with those of McMurdie and Flint, who however reported moderate reflections at 8.0 and 5.67 Å which were not found in the present experiments.

ELECTRON MICROSCOPE INVESTIGATION

A few fibres were lightly crushed in water and drops of the resulting suspension allowed to dry on specimen grids coated with formvar films.

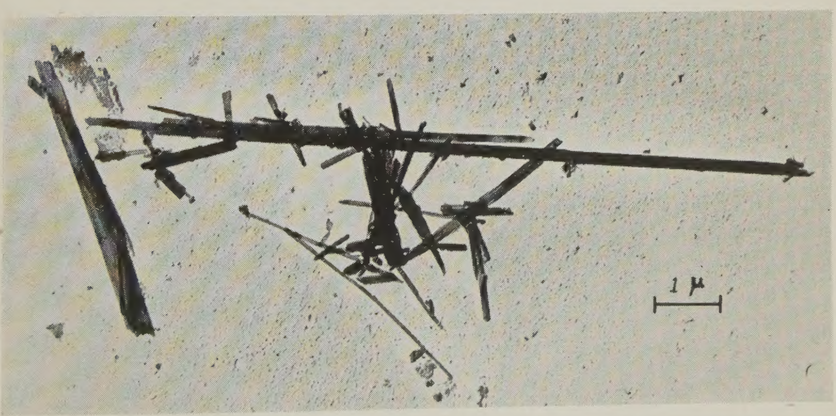

FIG. 1. An electron micrograph of typical fibres of foshagite.

Some of the specimens were shadowcast (Williams and Wyckoff, 1944) with gold palladium alloy at an angle of $\tan^{-1}\frac{1}{4}$. The specimens were examined in a Metropolitan-Vickers EM3 electron microscope. Electron micrographs (Fig. 1) confirmed the fibrous nature of the specimen. Individual fibres had two good cleavages parallel to the fibre axis, and were about 250–4000 Å wide, with thicknesses varying between one-quarter and three-quarters of the width. Electron-diffraction patterns from individual fibres (Fig. 2) showed an orthogonal network of spots with alternate strong and weak layer-lines perpendicular to the fibre axis in accordance with the *x*-ray results. The patterns showed that the fibres were single crystals, of which all but one of those examined lay in the same orientation. The fibre axis will be called *b*, and the principal cleavage, on which most of the crystals lay, will be called (001). The following discussion relates to the pseudo-cell. The weak, intermediate layer-lines with true *k* odd, and their connection with the true cell, are discussed later.

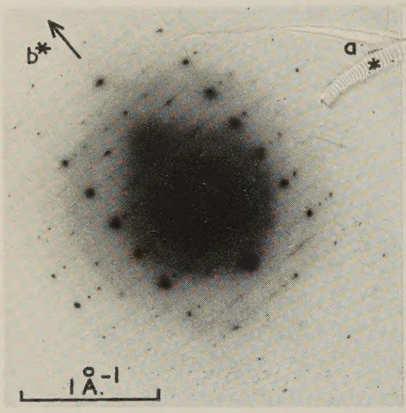

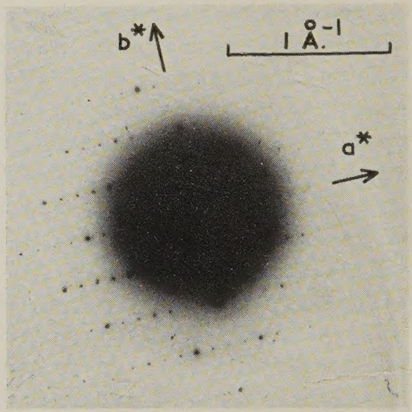

FIG. 2. (left) A typical electron-diffraction pattern from a single fibre of foshagite, with (001) planes normal to the electron beam. There are alternate strong and weak layer lines perpendicular to the fibre direction *b*. Both strong and weak reflections lie on an orthogonal net, which is divided into Laue zones parallel to *b*. The maxima of the odd layer lines are halfway between the Laue zones through the strong reflections of the even layer lines.

FIG. 3. (right) An electron-diffraction pattern from a foshagite fibre with its *c*-axis parallel to the electron beam, so that the *hk*0 Laue zone is almost central. The odd layer lines are very faint streaks, and the spacing of reflections along the even layer lines corresponds to d_{100}. The most intense reflections lie on a slightly distorted hexagonal net with *a* 3.60 Å.

The *a*-axis lies substantially in the plane of the supporting film. As the patterns are orthogonal, it can be chosen normal to *b*, making $\gamma = 90°$. The mean value found for *b* was 3.67 Å. This suggests that the 1.84 Å

x-ray reflection, which has true $k=4$, is 020 on the pseudo-cell, giving 3.68 Å for d_{010}. The agreement between b and d_{010} confirms that $\gamma=90°$ and shows also that $\alpha=90°$. The pseudo-cell is thus geometrically orthorhombic or monoclinic.

Many of the patterns, including that shown in Fig. 2, appeared to be intersected by closely-spaced Laue zones (Brown and Clark, 1952) parallel to the fibre axis. The maximum tilt of the specimen stage (about 7°) was sufficient only in two cases to allow the c-axis to be brought parallel to the electron beam so that the $hk0$ Laue zone was central (Fig. 3).

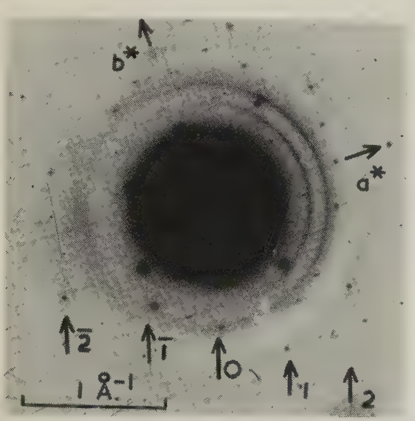

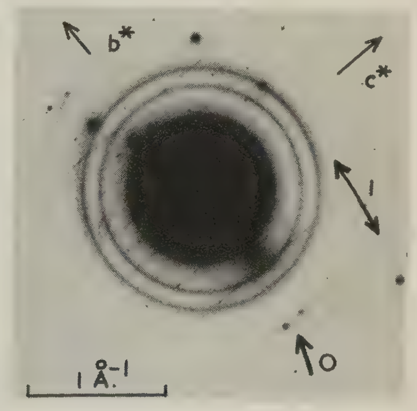

FIG. 4. (left) An electron-diffraction pattern from the foshagite fibre of Fig. 3 after tilting a few degrees from that position. The pattern is now divided into Laue zones arising from the c-axis. The l-values of these zones (indexed on the pseudo-cell) are indicated.

FIG. 5. (right) An electron-diffraction pattern from a foshagite fibre lying on (100), with Laue zones arising from the a-axis; h-values of the zones are indicated. The reflections fall on a face-centred orthogonal net with alternate strong and weak layer lines perpendicular to the b-direction. The reflections on the odd layer lines are joined by streaks, and are not divided into Laue zones. The powder rings are due to the shadow-casting metal.

β therefore probably exceeds 97°. The two exceptional cases presumably occurred with crystals having an initial tilt about the fibre axis, so that their (001) planes were not normal to the electron beam. For both of these patterns with the $hk0$ zone central, d_{100} was 9.95 Å. All other patterns gave higher apparent values of d_{100}, up to a maximum of about 10.6 Å. If it is assumed that this maximum value occurs when (001) is exactly normal to the electron beam, it may be taken as a measure of a; the diffraction conditions are still satisfied because the crystal is necessarily very thin normal to (001). From the relation $d_{100}=a \sin \beta$, β was estimated at about 110°.

Figure 4 shows the effect of tilting the crystal through a few degrees about b on one of the patterns with the $hk0$ zone centred. The pattern is split into clearly-defined Laue zones for different values of l. By tilting through various angles and applying the procedure due to Gard (1956), c was estimated at about 7.3 Å from the Laue zone radii. Comparison of reflections in adjacent zones showed the pseudo-cell was primitive. No space-group absences were observed.

The electron-diffraction pattern from one fibre (Fig. 5) showed that its (100) plane was approximately normal to the beam. Values of 7.0 ± 0.3 Å for c were derived from the spacings of the spots, and of 10.0 ± 0.8 Å for a from the radii of the Laue zones, but the accuracy was poor. These values are in accordance with those already obtained. The electron-diffraction data thus show that the pseudo-cell is monoclinic, with approximate parameters:

a 10.6, b 3.67, c 7.0 Å, β 110°.

The structure of the weak intermediate layer-lines perpendicular to b will now be considered. In the electron-diffraction pattern with the $hk0$ Laue zone central (Fig. 3), the weak layers are continuous, very faint streaks. In the patterns from crystals tilted a few degrees from this position (Fig. 4), the streaks have maxima between adjacent Laue zones through the strong spots, and minima on these zones. Each maximum can be resolved into separate reflections with integral h-indices. In the pattern from a crystal lying on (100) (Fig. 5), the intermediate layers consist of spots with half-integral k- and l-indices in terms of the pseudo-cell. These spots are weak and connected by faint streaks parallel to c^*. There is no apparent division into Laue zones for different values of h. This confirms that the weak reflections are streaked parallel to both a^* and c^*, but principally in the former direction. The true cell is thus A-centred monoclinic with the approximate parameters a 10.6, b 7.34, c 14.0 Å, β 110°, with the a, b, and c axes in the same directions as in the pseudo-cell. The principal cleavage is (001) and the secondary cleavage is (100).

Some of the spots on the pattern shown in Fig. 3 are more intense than others. They may be indexed on the pseudo-cell as $0k0$, $4k0$, $7k0$, $11k0$ where k is even, and $2k0$, $5k0$, $9k0$ where k is odd, and thus lie approximately on a face-centred orthogonal network with a mean spacing of 5.6 Å across the fibre axis. This is a slightly distorted hexagonal network with a about 3.6 Å.

Correlation of Electron Diffraction and X-ray Data

This provided a check on the pseudo-cell determined above and also a means of refining its parameters. The weak superlattice reflections were visible on the x-ray fibre rotation photographs only as continuous streaks corresponding to odd values of true *k*. For convenience, indices were allocated in terms of the primitive monoclinic pseudo-cell, except that, to avoid confusion, the doubled value of *b* was used. All *k*-indices are therefore even.

Consideration of the six longest *x*-ray spacings, all of which have *h*0*l* indices, suggests that the 10.0, 4.95, 6.8, and 3.37 Å spacings correspond respectively to 100, 200, 001, and 002. This gives values of 9.90 Å for d_{100} and 6.74 for d_{001}. The 0a^*c^* face of the reciprocal lattice was drawn, using these values and assuming $\beta^* = 70°$. It was found that the observed *h*0*l* spacing of 3.56 Å could only be 201 and that the one of 3.25 Å could only be $20\bar{2}$. Optimum agreement between calculated and observed values for these spacings was obtained by adjusting β^* to 73.6°. Indices were allotted to all the spacings down to 1.5 Å on the basis of these parameters, taking into account the observed *k*-indices. Agreement was satisfactory (Table 1). The refined values for the parameters of the monoclinic pseudo-cell are thus

$$a\ 10.32, \qquad b\ 3.68, \qquad c\ 7.04\ \text{Å}, \qquad \beta\ 106.4°.$$

The corresponding *A*-centred monoclinic true cell has the parameters

$$a\ 10.32, \qquad b\ 7.36, \qquad c\ 14.07\ \text{Å}, \qquad \beta\ 106.4°.†$$

The *x*-ray fibre data show no systematic absences in the *h*0*l* reflections, and the electron-diffraction data show no absences in the 0*k*0 reflections of the pseudo-cell. The space-group of the latter could therefore be *P*2, *Pm*, or *P*2/*m*. The weak reflections corresponding to the true cell were too indefinite to justify any attempt to determine its space-group.

CHEMICAL ANALYSIS AND UNIT CELL CONTENTS

The results of a new analysis made on the present specimen, by Dr. R. A. Chalmers, are given in Table 2 (column 3) with those of Eakle and Newman for comparison. The specific gravity was determined by suspension in bromoform-benzene mixtures after preliminary evacuation to remove air from the mineral. The material analysed contained a small proportion of thaumasite and possibly also a little calcite. An attempt to purify the material by specific gravity separation was unsuccessful, because of the close admixture of the thaumasite and the difficulty of grinding the highly fibrous material. For the same reason the samples taken for the different parts of the analysis were not perfectly representative, and this may explain the slightly low total (99.3%). It was assumed that

---

† The axes have been chosen in these directions to clarify the relation between the true and pseudo-cells. The conventional true cell would be *C*-centered monoclinic with *a* 14.07, *b* 7.36, *c* 10.32 Å, *β* 106.4°.

TABLE 2. CHEMICAL ANALYSES AND UNIT-CELL CONTENTS

	1	2	3	4	5	6
SiO_2	33.92	36.60	39.8	42.2 Si	12.0	12
Al_2O_3	0.83	0.50	0.6	0.6 Al	0.2	
Fe_2O_3			nil	nil Fe	nil	
MgO	tr	2.61	0.8	0.9 Mg	0.4	
CaO	53.48	48.91	50.7	52.3 Ca	16.1	16
Na_2O	n.d.	n.d.	0.1	0.1 Na	<0.1	
K_2O	n.d.	n.d.	0.1	0.1 K		
H_2O	10.19	8.88	5.7	3.8 H	7.2	8
CO_2	1.83	2.67	0.8	nil O	44.4	44
SO_3	n.d.	n.d.	0.65	nil		
	100.25	100.17	99.3*	(100.0)		
Sp.gr.	2.36		2.73	2.79		

* Also: P_2O_5, nil; MnO, tr.

1. A. S. Eakle, 1925. Analyst, C. A. Gentle.
2. E. S. Newman, 1956.
3. This investigation. Analyst, R. A. Chalmers.
4. Analysis 3 after correction for 5% of thaumasite ($3CaO \cdot SiO_2 \cdot CO_2 \cdot SO_3 \cdot 15\ H_2O$, s.g. 1.9) and 1% of calcite, and normalizing to 100.
5. Atomic cell contents calculated from 4.
6. Theoretical atomic cell contents for $4[Ca_4Si_3O_9(OH)_2]$.

all the SO_3 was present as thaumasite and the remaining CO_2 as calcite; on this basis the analysis and specific gravity were corrected for presence of 5% of thaumasite and 1% of calcite (column 4). Atomic cell contents, calculated using these data, are given in column 5. They approximate to $4[Ca_4Si_3O_{11}H_2]$. The theoretical specific gravity, corresponding to these idealised cell contents, is 2.74.

DEHYDRATION

A dehydration isobar (Fig. 6, curve A) was kindly determined by Mr. J. W. Howison, B.Sc., using a silica-spring balance. A slow stream of air was passed through the apparatus, after adjustment to 6 mm. humidity and passage over caustic soda and soda-lime to remove carbon dioxide. Constant weight was attained at each temperature before proceeding to the next.

The ignited residue from this experiment contained 1.1% SO_3, indicating that the particular sample used contained about 8% of thaumasite. The presence of 1% of calcite was assumed from the analysis. By analogy with the behaviour on dehydration of the related mineral ettringite (Jones, 1938) it was assumed that water from the thaumasite (3.3%)

accounted for all the loss below 600° and for part of the loss above 600°. It was also assumed that the loss above 600° included the CO_2 both from the thaumasite (0.5%) and the calcite (0.4%). A corrected curve was thus obtained for the foshagite and was normalised to 100% foshagite (Fig. 6, curve B). It shows 3.5% of water, lost mainly within the range 650–750°. The discrepancy from the theoretical value of 4.3% is probably not significant in view of the assumptions made and the large effect of any small error in the SO_3 determination.

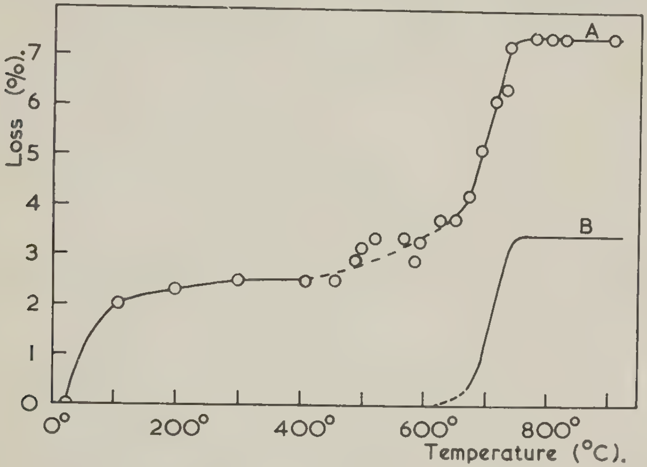

FIG. 6. Curve A. A dehydration isobar for foshagite. Curve B. The dehydration isobar of curve A, after correcting for 8% of thaumasite and 1% of calcite.

Difficulty was encountered in obtaining steady values with the silica-spring balance at 450–600°, and this part of the experimental curve must be considered uncertain. The effect appears due to some aspect of the behaviour of thaumasite on dehydration and has not been further investigated.

An *x*-ray powder pattern of a specimen of the foshagite after heating at 600° showed no change, thus confirming that the water loss below this temperature is probably attributable to the thaumasite. After heating at 800°, the material is still fibrous. *X*-ray examination of these fibres confirmed Heller's view (1952) that they were composed of β-$CaSiO_3$ and β-Ca_2SiO_4, with the *b*-axes in each case parallel to the fibre direction. The β-$CaSiO_3$ was more easily recognized than the β-Ca_2SiO_4. No evidence was found of a CaO-like powder pattern in crystals heated at 550°, as reported in one instance by Heller. It seems possible that this effect also may have been caused by presence of thaumasite.

Electron-micrographs (Fig. 7) of the product obtained by heating at

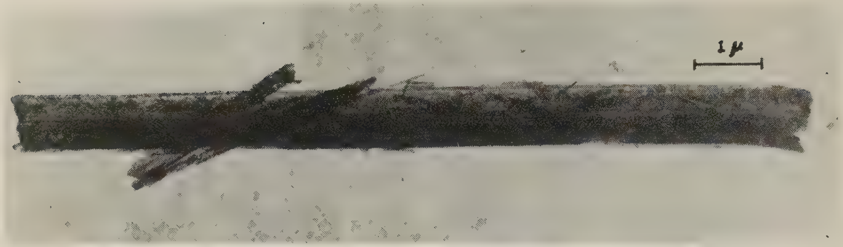

FIG. 7. An electron micrograph of foshagite fibres after heating at 800°. They have split lengthwise into much narrower fibres, and have a fluffy appearance.

800° confirmed that it was a pseudomorph of the foshagite. The fibres had a fluffy appearance and were split lengthwise into much narrower fibres. Electron-diffraction patterns of many of these fibres were those of single crystals (Fig. 8). The spacings and Laue zone radii of the strong reflections indicated a *C*-centred orthorhombic or monoclinic pseudo-cell with *a* 15.40, *b* 3.65, *c* 6.95 Å, γ 90°, elongation *b*, cleavage (001). The h*k*0 reflections were strong for $h=6n$ where k was even and for $h=(6n+3)$ where k was odd. These strong reflections form a distorted hexagonal pattern corresponding to an *a*-axis of about 3.4 Å. These data agree with β-$CaSiO_3$ (Table 3). This name will be used indiscriminately for wollastonite and parawollastonite, which have identical pseudo-cells, where it is undesirable to distinguish the two. Weak odd layer-lines are present in Fig. 8 corresponding to a doubling of *b*. The positions of the spots on these layers indicated a mixture of wollastonite and parawollastonite. There was no direct evidence of β-Ca_2SiO_4.

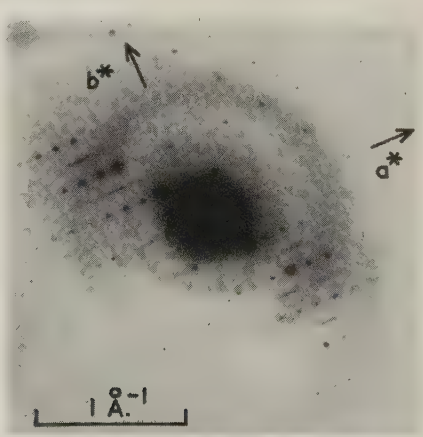

FIG. 8. An electron-diffraction pattern from a foshagite fibre after heating at 800°. The parameters correspond to β-$CaSiO_3$ lying on (001). The *c*-axis is at a small angle to the electron beam, so that the zero- and first-order Laue zones can be seen.

TABLE 3. PARAMETERS, ATOMIC CONTENTS, AND VOLUMES OF THE PSEUDO-CELLS OF FOSHAGITE AND β-$CaSiO_3$ AND OF THE UNIT-CELL OF β-Ca_2SiO_4*

Parameters	Foshagite	β-$CaSiO_3$	β-Ca_2SiO_4
a	10.32 Å	15.33 Å	*c* 9.28 Å
b	3.68	3.64	*b* 6.76
c	7.04	7.03	*a* 5.48
β	106°24′	95°24′	94°33′
$\alpha=\gamma$	90°	90°	90°
Atomic contents.	$Ca_4Si_3O_9(OH)_2$	$Ca_6Si_6O_{18}$	$Ca_8Si_4O_{16}$
Volume (Å^3)	256	390	342
Volume containing 24 Ca^{++} (Å^3).†	1536	1560	1026
% change in volume per 24 Ca^{++}.	—	+1.6	−33.2

* Data for β-$CaSiO_3$ are from Jeffery (1953). Data for β-Ca_2SiO_4 are from Midgley (1952).

† *i.e.*, volume of six pseudo-cells for foshagite, four pseudo-cells for β-$CaSiO_3$, and of three unit-cells for β-Ca_2SiO_4.

Assuming that the fibres of the dehydrated material are pseudomorphs of the original crystals, the electron-diffraction pattern confirms that the foshagite *b*-direction becomes the *b*-direction of the β-$CaSiO_3$. It shows also that the (001) plane of the foshagite becomes, at least approximately, (001) for the β-$CaSiO_3$ pseudo-cell.

SYNTHESIS

Synthesis of foshagite was confirmed by treating synthetic rankinite ($Ca_3Si_2O_7$) with supercritical water at 500° and about 400 atmospheres pressure for 14 days. Apart from some unchanged rankinite, the product consisted mainly of foshagite, which was identified by its *x*-ray powder pattern. The experiment was originally done in an attempt to confirm Flint, McMurdie and Wells' (1938) observation that a different polymorph of $Ca_3Si_2O_7$ was formed under these conditions. No product corresponding to their description was detected.

DISCUSSION

Composition and ionic formula

The present results confirm the status of foshagite as a distinct mineral species, and indicate the composition $4CaO \cdot 3SiO_2 \cdot H_2O$. The $CaO:SiO_2$ ratio 4:3 is also supported by Newman's analysis and it seems certain that Eakle's value of 5:3 is too high. It appears likely that both the earlier analyses, like the present one, were made on material containing thaumasite. Exact interpretation of these analyses is difficult because in neither case was SO_3 determined. It is possible to explain Newman's analysis on the assumption that thaumasite and calcite were present as impurities. The high lime content reported by Eakle cannot be explained in this way; it could possibly have been caused by presence of hillebrandite, which is intergrown with foshagite in parts of the Crestmore specimen, and is hard to distinguish from it by optical methods. The high water contents reported in the earlier analyses could also be attributed to presence of thaumasite. It is significant that synthetic preparations show lower water contents in better agreement with the formula $4CaO \cdot 3SiO_2 \cdot H_2O$; Flint, McMurdie and Wells reported an ignition loss of 5.7% and Jander and Franke considered their product to be $3CaO \cdot 2SiO_2 \cdot H_2O$.

Several lines of evidence suggest the ionic formula $Ca_4(SiO_3)_3(OH)_2$. The material is markedly fibrous, and this could be explained by the presence of metasilicate chains of empirical composition SiO_3^{--}. The number (12) of SiO_3 units in the cell is consistent with the hypothesis that it contains four such chains, kinked as in other calcium silicate minerals such as tobermorite (Megaw and Kelsey, 1956) and wollastonite (Buerger, 1956) so as to give a repeat unit of three linked tetrahedra in the space of the 7.3 Å fibre repeat distance. The ordered transformation at about 700° of part of the material into β-$CaSiO_3$ fits in with this view. Presence of hydroxyl ions not directly linked to silicon appears consistent with the conditions of formation and of dehydration. Those calcium silicates which are known to contain hydrogen in the form of water molecules or in Si-OH groups, or both, such as afwillite or tobermorite, are formed hydrothermally at temperatures usually below 200°. They also tend to suffer dehydration at relatively low temperatures, often below 500°. In contrast, xonotlite, which also shows the 7.3 Å fibre repeat distance and contains hydroxyl groups not attached to silicon (Mamedov and Belov, 1955) is formed hydrothermally at temperatures up to 400° and is only dehydrated at about 750°. This is similar to the behaviour of foshagite.

Dehydration

The stoichiometry of the dehydration process is represented by the equation

$$Ca_4Si_3O_9(OH)_2 \rightarrow 2CaSiO_3 + Ca_2SiO_4 + H_2O$$

Consideration of the respective cell contents (Table 3) shows that twelve pseudo-cells of foshagite yield four pseudo-cells of β-$CaSiO_3$ and three unit-cells of β-Ca_2SiO_4. Assuming tentatively that equal numbers of foshagite pseudo-cells are altered to β-$CaSiO_3$ and to β-Ca_2SiO_4, the process could be represented

$$\begin{array}{lclll}
6[\mathrm{Ca_4Si_3O_{11}H_2}] & \text{(I)} & & 4[\mathrm{Ca_6Si_6O_{18}}] & \text{(II)}\\
\quad\uparrow & & & & \\
6(\mathrm{Si} + \mathrm{O}) \,\Big|\!\rightarrow & & = & \qquad + 12\mathrm{H_2O} & \\
\quad\uparrow & & & & \\
+ 6[\mathrm{Ca_4Si_3O_9(OH)_2}] & \text{(III)} & & + 3[\mathrm{Ca_8Si_4O_{16}}] & \text{(IV)}
\end{array}$$

Formula I represents six pseudo-cells of foshagite which are converted into four pseudo-cells of β-$CaSiO_3$ (II), and formula III represents six pseudo-cells of foshagite which are converted into three unit cells of β-Ca_2SiO_4 (IV). For this to occur, six silicon and six oxygen atoms must be transferred from III to I, as indicated by the arrow, and twelve molecules of water formed by combination of hydrogen from I with hydroxyl from III. Such a conversion of foshagite into β-$CaSiO_3$ would entail negligible change in volume, but the corresponding conversion of foshagite into β-Ca_2SiO_4 would cause a 33% decrease in volume (Table 3). The absence of shrinkage in the β-$CaSiO_3$ would permit some retention of coherence and therefore of orientation, while the considerable shrinkage in the β-Ca_2SiO_4 might cause splitting into very narrow fibres with enough free space to allow random orientation around the fibre axis. The free space might be increased by pressure of escaping steam. Random orientation and small crystal size could explain the failure of electron-diffraction to reveal the β-Ca_2SiO_4. This mechanism would thus explain the experimental findings on the orientations of the products, and is therefore probably correct.

The proposed dehydration mechanism would entail acceptance of silicon and oxygen atoms by the foshagite converted into β-$CaSiO_3$, but no change in the number of calcium ions. It resembles that of xonotlite (Dent and Taylor, 1956), although it is more complex. Xonotlite is dehydrated to β-$CaSiO_3$ at about 750°, and the process seems to involve the breaking of Si-O rather than Ca-O bonds. This suggests that the Ca-O skeleton in foshagite may be closely similar to that in wollastonite. There may also be a more distant structural similarity to β-Ca_2SiO_4.

Structure

The detailed structure remains to be determined but the present results give some strong indications. As already stated, there is evidence that the unit-cell is traversed in the b-direction by four metasilicate chains kinked similarly to those in wollastonite, and that the calcium-oxygen skeletons of the two minerals may be very similar. This is supported by other evidence:

(i) In the electron-diffraction patterns both of foshagite and of β-$CaSiO_3$, the strongest $hk0$ reflections fall on distorted hexagonal nets similar to that of calcium hydroxide. In β-$CaSiO_3$, this is attributable to the arrangement of the relatively heavy calcium ions, which in (001) projection closely resembles that of calcium hydroxide. A similar arrangement may therefore occur in foshagite.

(ii) If only calcium ions are considered, and slight movements of some calcium ions are allowed, β-$CaSiO_3$ can be described in terms of a pseudo-cell almost identical with that of foshagite (Fig. 9), with the (100) planes common to both pseudo-cells. This relation between the pseudo-cells is consistent with the dehydration evidence and appears too marked to be explained by coincidence. It is therefore suggested that the four calcium ions in the pseudo-cell of foshagite are approximately in the positions shown in Fig. 9. This could be compatible with any of the possible space groups ($P2$, Pm, or $P2/m$). The presence evidence is inadequate to locate the metasilicate chains or the hydroxyl groups, though both are probably placed symmetrically relative to two-fold axes. Further work is in progress to complete the structure determination.

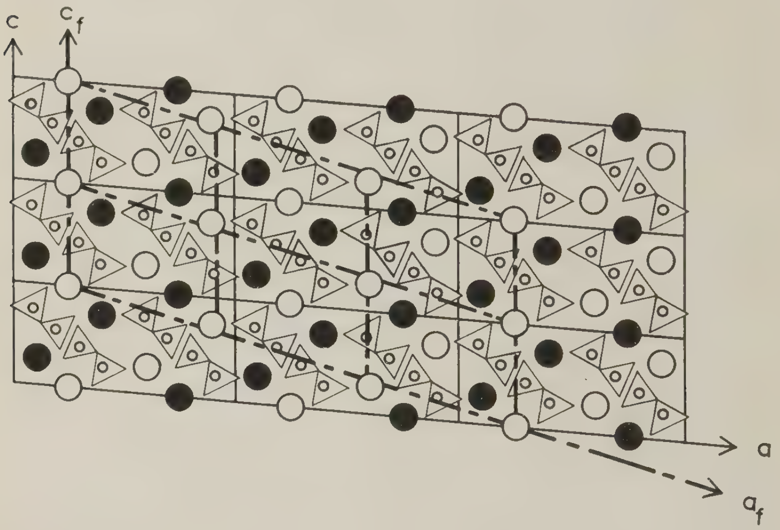

FIG. 9. Nine pseudo-cells of β-$CaSiO_3$, looking down the *b*-axis.

The black and large open circles represent calcium ions at heights 0 and $\frac{1}{2}$ in the pseudo-cell respectively, and the double triangles represent projections of the metasilicate chains. The thick broken lines show the probable outlines of foshagite pseudo-cells before dehydration, with the calcium ions occupying slightly different positions. Three pseudo-cells of foshagite could accept one silicon and one oxygen atom each and change into two pseudo-cells of β-$CaSiO_3$ with negligible volume change, and preservation of the *b*- and *c*-axes. An equal number of adjacent foshagite pseudo-cells could donate silicon and oxygen atoms, and change into β-Ca_2SiO_4 with considerable shrinkage, causing disintegration into very narrow fibres with random orientation round the fibre axis.

A structure of the type suggested would explain the extreme weakness and streaking of reflections with true k odd. The weakness is partly explained by the fact that the pattern of calcium ions repeats at intervals of $b/2$ along the fibre direction. Random displacements of $b/2$ in the placing of the metasilicate chains would enhance the effect and also cause the streaking. This effect is observed with xonotlite (Mamedov and Belov, 1955) and with other fibrous calcium silicates.

REFERENCES

BERMAN, H. (1937), *Am. Mineral.*, **22,** 342.

BROWN, J. F., AND CLARK, D. (1952), *Acta Cryst.*, **5,** 615.

BUERGER, M. J., (1956), *Proc. Nat. Acad. Sci.*, **42,** 113.

DENT, L. S., AND TAYLOR, H. F. W. (1956), *Acta. Cryst.*, **9,** 1002.

EAKLE, A. S. (1925), *Am. Mineral.*, **10,** 97.

FLINT, E. P., MCMURDIE, H. F., AND WELLS, L. S. (1938) *J. Res. Nat. Bur. Stand.*, **21,** 617.

GARD, J. A. (1956) (a) *Brit. J. Appl. Phys.*, **7,** 361.
(b) *J. Sci. Instr.*, **33,** 307.

HELLER, L. (1952), Proc. Third Int. Symposium Chemistry of Cement, London, 1952, p. 237. Cement and Concrete Association, London, 1954, pp. 870.

HELLER, L., AND TAYLOR, H. F. W. (1956), "Crystallographic Data for the Calcium Silicates." p. 53. H.M.S.O., London, pp. 79.

JANDER, W., AND FRANKE B. (1941), *Z. anorg. Chem.*, **247,** 161.

JEFFERY, J. W., (1953). *Acta Cryst.*, **6,** 821.

JONES, F. E. (1938). Proc. Symp. Chem. Cements, Stockholm, 1938, p. 231. Ingeniörsvetenskapsakademien, Stockholm, pp. 578.

MCMURDIE, H. F., AND FLINT, E. P. (1943), *J. Res. Nat. Bur. Stand.*, **31,** 225.

MAMEDOV, KH. S. AND BELOV, N. V. *Doklady Akad Nauk S.S.S.R.*, **104,** 615.

MEGAW, H. D., AND KELSEY, C. H. (1956), *Nature*, **177,** 390.

MIDGLEY, C. M. (1952), *Acta Cryst.*, **5,** 307.

NEWMAN, E. S. (1956), *J. Res. Nat. Bur. Stand.*, **57,** 27.

TAYLOR, H. F. W. (1952), Proc. Int. Symp. Reactivity of Solids, Gothenburg, 1952, 677. Elanders Boktryckeri Aktiebolag, Gothenburg, 1954, pp. 1102.

VIGFUSSON, V. A. (1931), *Amer. J. Sci.*, **21,** 67.

WILLIAMS, R. E., AND WYCKOFF, R. W. G. (1944), *J. Appl. Phys.*, **15,** 712.

Manuscript received April 4, 1957.

THE AMERICAN MINERALOGIST, VOL. 43, JANUARY–FEBRUARY 1958

SIMPLOTITE, A NEW QUADRIVALENT VANADIUM MINERAL FROM THE COLORADO PLATEAU*

M. E. Thompson, C. H. Roach, and Robert Meyrowitz *U. S. Geological Survey, Washington 25, D. C.*

Abstract

Simplotite, $CaV_4O_9 \cdot 5H_2O$, is a new calcium tetravanadite that has been found in five vanadium-uranium mines on the Colorado Plateau. It occurs as dark-green micaceous plates and as hemispherical aggregates of plates, coating fracture surfaces in sandstone impregnated by relatively unoxidized vanadium and uranium minerals. Simplotite represents an early stage in the oxidation sequence of the vanadium ore. It is associated with duttonite, melanovanadite, abundant crystals of hexagonal native selenium, and an undescribed vanadium oxide.

Simplotite is biaxial negative, 2V about 25°, dispersion $r>v$, weak and crossed, $\alpha=1.705\pm0.002$, $\beta=1.767\pm0.002$, $\gamma=1.769\pm0.002$. X$=b$ yellow, Y green, $Z\wedge c\sim-58°$ green. The measured specific gravity is 2.64 ± 0.002.

A chemical analysis of material from the Peanut mine showed, in per cent: CaO, 11.6; V_2O_4, 67.7; V_2O_5, 0.5; H_2O, 18.4; insoluble, 0.5; total, 98.7.

Simplotite is monoclinic, pseudotetragonal; the space group is $A2/m(C_{2h}^3)$, $Am(C_s^3)$ or $A2(C_2^3)$; $a=8.39\pm0.03$ A, $b=17.02\pm0.05$ A, $c=8.37\pm0.03$ A, $\beta=90°25'\pm5'$; a:b:c $=0.4929:1:0.4918$; cell contents $4[CaV_4O_9 \cdot 5H_2O]$; calculated specific gravity 2.65.

The new mineral is named for J. R. Simplot of the J. R. Simplot Mining Company of Boise, Idaho, former owner of the Peanut mine.

Introduction and Acknowledgments

Simplotite was first recognized in a sample from the Sundown Claim, San Miguel County, Colo. The sample was submitted by L. B. Riley to A. D. Weeks (both of the U. S. Geological Survey) for identification in 1952. The mineral was recognized to be new, but there was only enough for determination of optical properties, *x*-ray powder patterns, and qualitative spectrographic analysis.

Early in 1954, simplotite was found in the Peanut mine, Montrose County, Colo., by C. H. Roach, who was making an intensive study of the mineralogy, geology, and geochemistry of the deposit. This study included detailed sampling of the ore and made possible the collection of enough material for determination of the physical properties and chemical composition of the new mineral. A preliminary description of simplotite was published in *Science* (Thompson, Roach, and Meyrowitz, 1956a).

Simplotite has since been found in three other mines: the Shattuck-Denn lease on Club Mesa, Montrose County, Colo., by C. A. Rasor of the U. S. Atomic Energy Commission; the J. J. mine in Paradox Valley, Montrose County, Colo., by D. P. Elston of the U. S. Geological Survey;

---

* Publication authorized by the Director, U. S. Geological Survey.

and the Vanadium Queen mine at La Sal Creek, San Juan County, Utah, by W. D. Carter of the U. S. Geological Survey.

The study of the mineralogy of these samples was made as a part of the U. S. Geological Survey's program on behalf of the Division of Raw Materials of the U. S. Atomic Energy Commission.

Simplotite is named for J. R. Simplot of the J. R. Simplot Mining Company of Boise, Idaho, former owner of the Peanut mine. Mr. Simplot graciously permitted the detailed mine study which resulted in the finding of enough of the mineral for this description.

OCCURRENCE

The five mines in which simplotite has been found are all in vanadium-uranium ore deposits in the Salt Wash sandstone member of the Morrison formation of Late Jurassic age. The locations of these mines are shown on the index map, Fig. 1.

The most detailed study of the occurrence of simplotite was made at the Peanut mine (C. H. Roach and M. E. Thompson, written communication, 1955), which is very near the axis of the Dry Creek Basin syncline between the Paradox Valley and Gypsum Valley salt anticlines (Cater, 1954). The vanadium-uranium ore bodies occur in the upper ore-bearing sandstone of the Salt Wash member. Ore bodies are localized along the flanks of a buried channel by crossbedding structures known as festoon

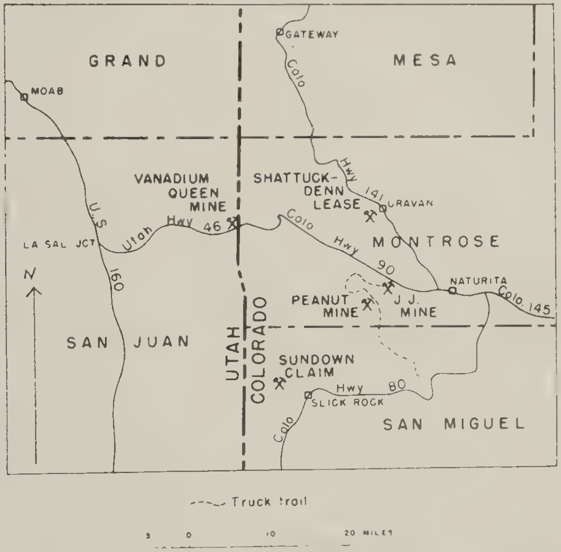

FIG. 1. Index map of parts of Colorado and Utah showing the localities of simplotite.

cross-lamination (Knight, 1930). The main festoon surfaces are relatively impermeable and have caused the formation of perched water tables. Water saturates most of the ore bodies and oxidation of the ore minerals is related to a slowly falling water level.

Simplotite in samples from all five mines occurs as micaceous plates and as hemispherical aggregates of radiating books of platy crystals. It coats fracture surfaces in vanadium-uranium ore-bearing sandstone. The primary ore minerals impregnating the sandstone and replacing coalified wood in the sandstone are montroseite, vanadiferous silicates, uraninite, and coffinite. Montroseite, $VO(OH)$, oxidizes readily to paramontroseite, VO_2 (Evans and Mrose, 1955). Studies of polished sections of samples of fractured ore-bearing sandstone from the Peanut mine show that paramontroseite near the fracture surfaces grades into a thin massive coating of an undescribed vanadium oxide on which crystals of simplotite, duttonite —$VO(OH)_2$—(Thompson, Roach, and Meyrowitz, 1956b), melanovanadite, and hexagonal native selenium formed later.

The original sample of simplotite from the Sundown Claim has recently been re-examined by A. D. Weeks, who reports that the simplotite occurs coating a joint surface of dark sandstone ore with duttonite and native selenium. This marks a second occurrence of duttonite which has previously been recognized only from the Peanut mine.

PHYSICAL AND OPTICAL PROPERTIES

Simplotite is monoclinic, pseudotetragonal. It has a platy habit and a micaceous cleavage on {010}. Aggregates of simplotite are black or greenish black, but thin flakes of the mineral are yellow green. The color of the powdered mineral is brownish black. In color and habit simplotite is very much like sincosite, $CaV_2P_2O_{10} \cdot 5H_2O$, which is structurally related to simplotite.

Simplotite has a vitreous luster. The hardness is about 1, probably because of the very easy cleavage. The specific gravity, measured by immersing a few grains in a mixture of bromoform and acetone, is 2.64 ±0.02.

In immersion simplotite appears as nearly square plates on {010}, commonly with two opposite corners (101) truncated at about 45°. It is biaxial negative, 2V about 25°, dispersion $r > v$, weak and crossed. The optical orientation, pleochroism, and indices of refraction are as follows:

Orientation	*Pleochroism*	*Indices of refraction*
$X = b$	yellow	α 1.705±0.002
Y	green	β 1.767±0.002
$Z \wedge c \sim -58°$	green	γ 1.769±0.002

Mrs. Weeks' recent re-examination of the original sample of simplotite (from the Sundown Claim, 1952) indicates that the mineral apparently dehydrates slowly in a dry atmosphere. The optical properties of the Sundown material, measured in 1952, gave data close to that obtained from the more recently collected material, but in June 1956 the Sundown sample had somewhat higher indices: α (calculated from β, γ, and 2V) is 1.730 ± 0.005, β 1.781 ± 0.003, γ 1.807 ± 0.003, and 2V measured on a universal stage is 40°.

Chemical Analysis

About 150 mg. of simplotite was handpicked from samples collected from the Peanut mine for the chemical analysis. A semiquantitative spectrographic analysis of this material was made by C. S. Annell of the U. S. Geological Survey and showed that Si was the only impurity present in amount over 0.1 per cent. The complete analysis is given in Table 1.

The chemical analysis was made by Robert Meyrowitz; the results, which yield the formula $CaV_4O_9 \cdot 5H_2O$, are shown in Table 2. The $H_2O(-)$ content is equivalent to four of the five water molecules.

Table 1. Semiquantitative Spectrographic Analysis of Simplotite from the Peanut Mine

C. S. Annell, analyst

Per cent	Elements
Over 10	V
5–10	—
1–5	Ca
0.5–1	—
0.1–0.5	Si
0.05–0.1	Al
0.01–0.05	Fe Mg
0.005–0.01	Sr Ti
0.001–0.005	Mo Cr Ba Sc

A sample weighting 36 mg. was used for the determinations of $H_2O(-)$, silica plus insoluble, CaO, and total vanadium. The sample was dried to constant weight at 110° ± 5° C., and silica and insoluble were separated by dehydration in a nitric acid solution. The CaO was determined as the sulfate after separation as the oxalate from the filtrate resulting from the separation of the silica and insoluble. Total vanadium was determined spectrophotometrically using the hydrogen peroxide precedure on an aliquot of the filtrate from the CaO determination after the oxalate had been destroyed by boiling with nitric acid.

The V_2O_4 was determined by dissolving 15 mg. of the mineral in $(1+3)$

TABLE 2. CHEMICAL ANALYSIS OF SIMPLOTITE FROM THE PEANUT MINE

Robert Meyrowitz, analyst

	Analysis of simplotite	Analysis recalculated to 100 per cent[1]	$CaV_4O_9 \cdot 5H_2O$
CaO	11.6	11.8	11.7
V_2O_4	67.7	69.0	69.5
V_2O_5	0.5	0.5	—
SiO_2 plus insoluble	0.5	—	—
$H_2O(+)$	3.9	4.0	3.8
$H_2O(-)$	14.5	14.7	15.0
Total	98.7	100.0	100.0

[1] After subtraction of SiO_2 plus insoluble.

sulfuric acid and titrating with approximately 0.03N standard potassium permanganate, and V_2O_5 was calculated by difference.

Total water was determined in a sample weighting 17 mg. by use of a modified microcombustion train of the type used for the determination of carbon and hydrogen in organic compounds. The sample was decomposed by ignition at 900° C. in a stream of oxygen.

X-RAY DATA

Because of its very easy micaceous cleavage and relatively large unit cell, simplotite does not give very good *x*-ray diffraction patterns. The powder pattern whose *d*-spacings are given in Table 3 was prepared by M. E. Mrose of the U. S. Geological Survey, using a Debye-Scherrer camera of radius 114.59 mm. and nickel-filtered copper radiation. To make a spindle that would produce a powder pattern with this many lines it was necessary to crush the mineral very gently, to make the spindle as dense as possible, and to increase the *x*-ray exposure to about 20 hours.

The intensities given for the diffraction lines in Table 3 were measured by direct comparison with a set of carefully calibrated intensities registered on a strip of film. Such a scale is linear in total *x*-ray energy and not logarithmic as is commonly used. Intensities estimated in terms of apparent density of diffraction lines exaggerate the weaker reflections and would give the three strongest lines as follows:

d (Å)	*I* (density)
8.51	10
3.14	6
2.62	8

Table 3. X-Ray Diffraction Data and Unit-Cell Constants of Simplotite

Indexed on monoclinic unit cell: probable space group, $A2/m$; $a = 8.39 \pm 0.03$ Å, $b = 17.02 \pm 0.05$ Å, $c = 8.37 \pm 0.03$ Å, $\beta = 90°25' \pm 5'$. CuKα radiation, $\lambda = 1.5418$ Å; camera diameter 114.6 mm; d(obs.) cutoff 14.0 Å.

hkl	*d*(calc.) Å	*d*(obs.) Å	I
020	8.51	8.51	100
011	7.51		
120	5.98		
$11\bar{1}$	5.61		
111	5.58		
031	4.70	4.71	3
040	4.26	4.26	9
200	4.19		
002	4.19		
$13\bar{1}$	4.11		
131	4.09	4.10	3
140	3.80		
$10\bar{2}$	3.76		
220	3.76		
022	3.76		
102	3.73		
$21\bar{1}$	3.67		
211	3.65		
$12\bar{2}$	3.44		
122	3.42	3.42	6
051	3.15	3.14	18
$23\bar{1}$	3.13		
231	3.12		
240	2.99		
042	2.98		
$20\bar{2}$	2.97		
$15\bar{1}$	2.95		
151	2.95	2.96	3
202	2.95		
060	2.84	2.84	9
$14\bar{2}$	2.82		
142	2.81		
$22\bar{2}$	2.81		
222	2.79		
013	2.75		
160	2.69		
320	2.66		
$31\bar{1}$	2.63		
311	2.62	2.62	25
$11\bar{3}$	2.62		
113	2.61		
251	2.52	2.52	5
$25\bar{1}$	2.52		
033	2.50		
$24\bar{2}$	2.44		
242	2.43		
$33\bar{1}$	2.41		
331	2.40		
$13\bar{3}$	2.40		
133	2.40		
260	2.35	2.35	3
062	2.35		
340	2.34		
071	2.33		
$30\bar{2}$	2.33		
302	2.32		
$21\bar{3}$	2.31		
213	2.29		
$16\bar{2}$	2.26	2.26	3
162	2.26		
$17\bar{1}$	2.25		
171	2.25		
$32\bar{2}$	2.25		
322	2.24	2.23	1
053	2.16	2.15	1
$23\bar{3}$	2.16		
233	2.14		
080	2.13		
$35\bar{1}$	2.10	2.10	2
400	2.10		
004	2.09		
351	2.09		
$15\bar{3}$	2.09		
153	2.09		
180	2.06		
$26\bar{2}$	2.05	2.05	2
262	2.05		
420	2.04		
$27\bar{1}$	2.04		
024	2.03		
$41\bar{1}$	2.02		
411	2.02		
		1.998	1
		1.882	5
		1.866	5
		1.832	3
		1.696	1
		1.617	1
		1.606	1
		1.567	1
		1.548	1
		1.503	1
		1.439	1
		1.342	2
		1.324	2
		1.308	2
		1.176	2

The powder pattern was indexed using the unit-cell constants measured by H. T. Evans, Jr., and M. E. Mrose from single crystal *x*-ray precession photographs as follows:

Monoclinic, space group $A2/m(C_2^3h)$, $Am(C_s^3)$ or $A2(C_2^3)$
$a = 8.39 \pm 0.03$ Å
$b = 17.02 \pm 0.05$ $\beta = 90°25' \pm 5'$
$c = 8.37 \pm 0.03$
$a:b:c = 0.4929:1:0.4918$
Cell contents: $4[CaV_4O_9 \cdot 5H_2O]$
Specific gravity: calc., 2.65; meas., 2.64 ± 0.02

The pseudotetragonal nature of simplotite is shown clearly by the selected area electron diffraction spot pattern (Fig. 2) taken by Malcolm Ross of the U. S. Geological Survey. The photograph shows the a^*-c^* reciprocal net and the included β angle. The mount was lightly shadowed with aluminum to provide an internal standard for purposes of measure-

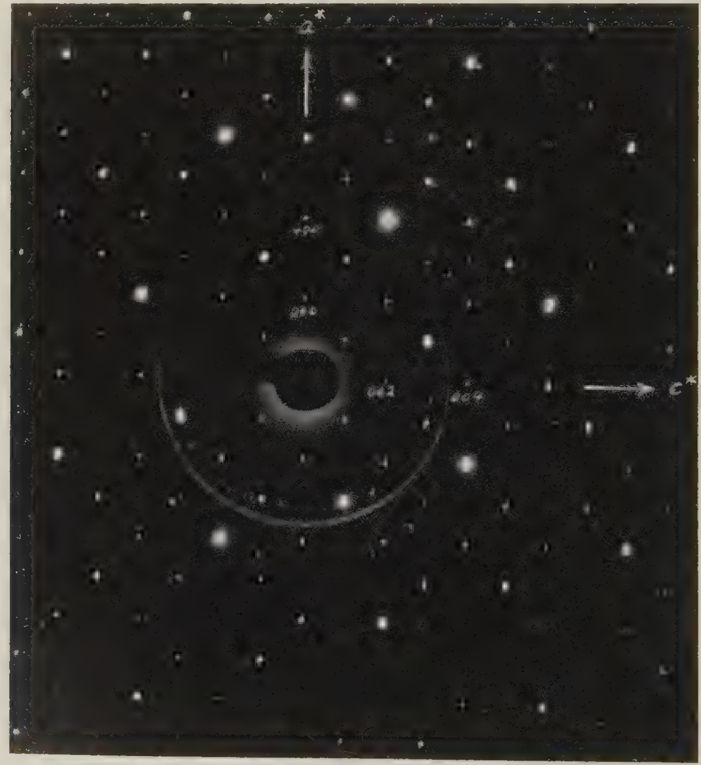

FIG. 2. Electron diffraction spot pattern of simplotite representing the a^*-c^* reciprocal net plane superimposed on an aluminum ring pattern.

ment; the aluminum produced the superimposed ring pattern. Measurements of electron diffraction patterns of simplotite give cell constants in good agreement with those determined by *x*-rays.

To correlate the optical, morphological, and *x*-ray orientations, one crystal was mounted on a goniometer head and studied with the two circle goniometer, polarizing microscope, and Buerger precession camera. The results are shown in Fig. 3. The habit of the crystal is square, with edges parallel to [100] and [001] and beveled by an undetermined prism form. Opposite corners are truncated by (101) in some crystals. In both the electron diffraction and *x*-ray precession photographs of the net normal to [010] the reflections for which $k=0$ and $k=1$ are not easily distinguished. In Fig. 3, the $k=0$ reflections are indicated by circles, the $k=1$ reflections by crosses. The patterns show, in the intensity distribution, a pronounced pseudotetragonal cell of small size inclined to the monoclinic axes. The pseudo-cell is body centered with $a_{ps}=2.6$Å and $c_{ps}=17$Å$=b_m$. The pseudotetragonal *a*-axis is inclined at +18°40′ to the monoclinic *c*-axis. The β angle and the *a* and *c* axial lengths are diffi-

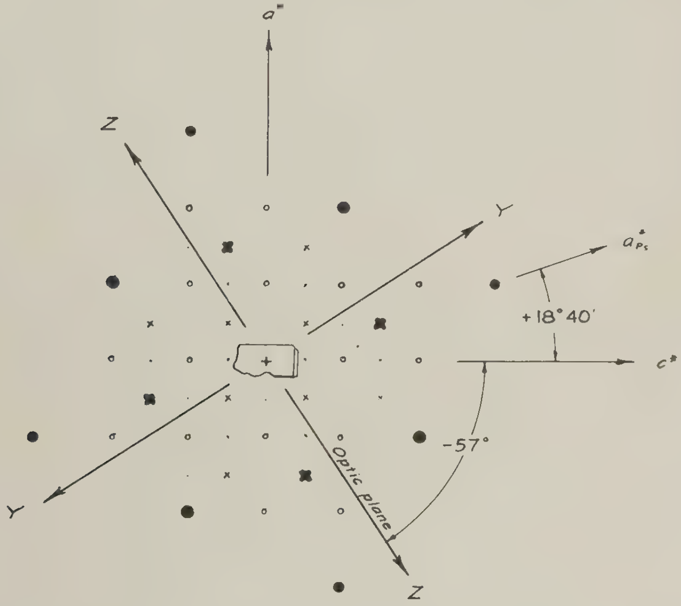

FIG. 3. Schematic drawing showing relation between the reciprocal lattice, optical orientation, and habit of simplotite. Circles represent reciprocal lattice points with $k=0$, crosses those with $k=1$. (See Fig. 2.) Sketch shows approximate appearance of the crystal on which correlative measurements were made (longest dimension 1 mm.).

cult to measure accurately because of the poor quality of the crystals. The best key to the absolute orientation of the simplotite lattice, therefore, is through the relation between the pseudotetragonal lattice and the optic directions to the true monoclinic lattice.

References

Cater, F. W., Jr., (1954) Geology of the Bull Canyon quadrangle, Colorado: U. S. Geol. Survey Geol. Quadrangle Map GQ 33.

Evans, H. T., Jr., and Mrose, M. E. (1955), A crystal chemical study of montroseite and paramontroseite: *Am. Mineral.*, **40,** 861–875.

Knight, S. H. (1930) Festoon cross-lamination (abs.): *Geol. Soc. America Bull.*, **41,** 86.

Thompson, M. E., Roach, C. H., and Meyrowitz, Robert (1956a) Simplotite, new calcium tetravanadite from the Colorado Plateau: *Science*, **123,** 1078.

——— (1956b) Duttonite, new vanadium mineral from Peanut mine, Montrose County, Colorado: *Science*, **123,** 990.

Manuscript received May 20, 1957.

THE AMERICAN MINERALOGIST, VOL. 43, JANUARY–FEBRUARY 1958

A NEW METHOD FOR ORIENTING ELECTRON MICROSCOPE REPLICAS APPLIED TO TWINNED QUARTZ

Robert V. Rice[1] and Alvin J. Cohen,[2] *Mellon Institute, Pittsburgh, Pennsylvania.*

Abstract

A technique which allows successive examination of specific areas of relatively rough surfaces by optical and then electron microscopy has been developed. The method utilizes the focusing action of a meniscus on thin carbon replicas floating on a liquid. The replica is positioned on a grid as the liquid is drawn down through a standard glass ball-and-socket joint. The method is an improvement over older ones since supporting films are not necessary, and therefore maximum resolution is realized. Preliminary studies with shadow-transfer replicas of cleavage surfaces of *d*-*l*-twinned quartz illustrate the method. Very fine striations (lower limit about 35 Å) were found within areas known to contain *d*-*l*-twins. The striations may be growth layers or possibly slip lines.

Introduction

In the course of studies on the morphology of cleavage surfaces of several particular types of quartz it was found desirable to relate specific areas of electron micrographs (up to about 250,000×) to structure on the surface itself visible to the naked eye. A new method for mounting replicas oriented on electron microscope grids was devised to accomplish this. We present here the method illustrated with some preliminary results on the structure of cleaved surfaces of Brazilian amethyst crystals.

Amethyst is characterized by fine *d*-*l*-twinning which extends throughout the crystal. At cleavage surfaces and along internal cracks ridges or lamella can be resolved with the unaided eye. Optical microscopy of such areas is usually sufficient to resolve some cross striations within the larger ridges. Figure 1 (taken with a Leitz "Ultrapak" at 50×) is an optical photomicrograph of the cleavage surface along the *c*-axis of "greened" amethyst from Brazil. From a petrographic microscopical examination it is known that each of the large ridges shown in Fig. 1 is either a *d*- or *l*-member of the alternating twin crystals. After heat bleaching, this amethyst appeared green in color. An optical examination indicated that a portion or perhaps all of the green color is due to another phase oriented between the laminar twins as discussed in an earlier paper (Cohen, 1956).

When we examined replicas of these surfaces in the electron microscope, striations as narrow as 100 Å or less were observed. The problem of relating the microstructure (100 Å striations) to the macrostructure

---

[1] Department of Research in Chemical Physics, Mellon Institute.

[2] Fellowship in Glass Science, Mellon Institute.

(100μ ridges) was solved by use of the electron microscopical specimen mounting device.

Gay and Anderson (1954) have described a method for mounting serial sections on slotted types of electron microscope grids which requires a film of "Formvar" supported by a loop of wire. This works well with sections especially when high resolution is not required in subsequent electron micrographs. However, the supporting plastic film inevitably decreases the resolution attainable. We found it difficult to position *replicas* by picking them up from the surface of water with the "Formvar" covered loop. Various methods for examining identical areas of metallographic specimens by light microscopy and then electron microscopy have been described (McLauchlan, 1953). Since metallographic specimens are smooth and flat, these methods are based on placing an electron microscope grid in a given position on the film covered specimen and subsequently firmly attaching the replica to the grid by a relatively thick coat of plastic. Such methods cannot be used with rougher surfaces,

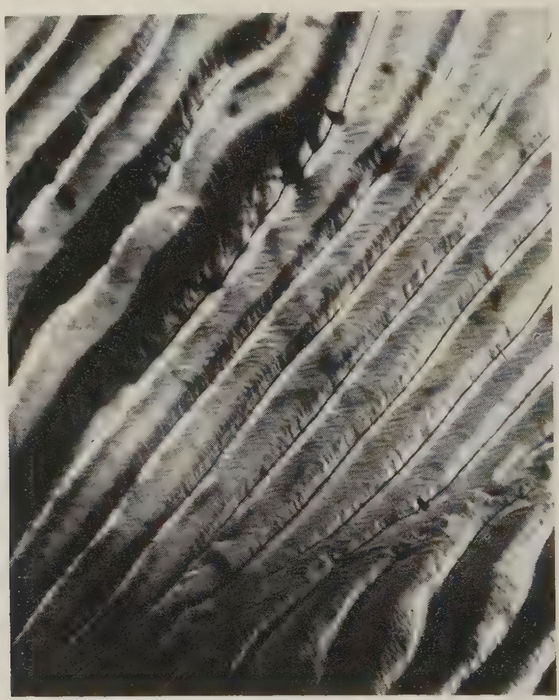

FIG. 1. Photomicrograph of cleavage surface of "greened" amethyst approximately parallel to *c* axis. Magnification 50×.

and high resolution is usually not attempted. Other methods which also protect the replica with thick plastic coatings require that the plastics be dissolved at the end of the process (Page, 1956). We have tried such techniques and found this last step damaged the replica beyond use more often than not. The surface tension of the solvents either breaks the delicate replica or the replica folds and curls while the plastic backing is being dissolved. A method described by Booker (1954) utilizes some of the principles we have used but his technique which was developed for wet stripped replicas requires a rather complicated assembly of apparatus and is useful only on rather smooth surfaces where orienting scratches can be made.

Method and Apparatus

Replicas of cleavage surfaces were prepared by a shadow-transfer technique (Hall, 1953). Platinum wire (0.005 in. diameter) was evaporated in various amounts from 0.025, 0.030 or 0.035 in. diameter tungsten wires bent in the form of a hairpin. A shadow angle of about 3 to 1 was usually used. The direction of shadowing was along the major axis of the ridges. In the same vacuum (10^{-4} to 10^{-5} mm. Hg) carbon was evaporated normal to the specimen surface in the manner of Bradley (1954), except that $\frac{1}{8}$ inch diameter spectroscopically pure carbon rods with one rod end squared off and the other sharpened to a fine point were used. The platinum and carbon film was immediately removed by slowly lowering the specimen at a 45° angle into 48% hydrofluoric acid. The replica usually floated free in one piece. The film was transferred to HCl (1:1 v/v) by picking it up on platinum gauze. After a time sufficient to dissolve any fluorides insoluble in HF or H_2O, the replica was transferred in the same manner to de-ionized water. We found the carbon films to be exceptionally sturdy and all but the very thinnest would withstand several such transfers.

The replica floating on water was then examined through low power (10× to 30×) binocular viewers or an "Ultrapak" microscope using reflected surface lighting. The general areas of interest were cut out of the large replica into pieces about $\frac{1}{8}$ inch diameter by simply touching the film with the edge of wire mesh. These isolated portions were then transferred to the mounting device.

Figure 2 is a diagram of the apparatus we have used for several years to mount replicas and thin sections on electron microscope grids so that macrostructures are oriented with respect to grid wires. Distilled water or water with a wetting agent fills the syringe, rubber bulb, and ball-and-socket joint section as shown. The glass tube is clamped to a ring stand; another clamp holds the syringe. A grid is placed on the 100 mesh platform held in the vertical position shown. In addition to 200 mesh rectangular grids, slotted grids such as Sjöstrand and Anderson types* have been used. The isolated piece of replica is now transferred to the surface of the liquid near the top of the assembly by means of a small appropriately shaped piece of wire mesh held in clamped forceps. The liquid is slowly removed from the column by the syringe until the replica is either just at the constriction of the joint or slightly below. The action of the meniscus during the lowering of the liquid level is that of focusing the floating replica to the center of the column. In the absence of wetting agents the apparatus must be thoroughly clean for focusing action to occur. The rod holding the grid can be moved vertically and horizontally and rotated while further liquid is removed through the syringe.

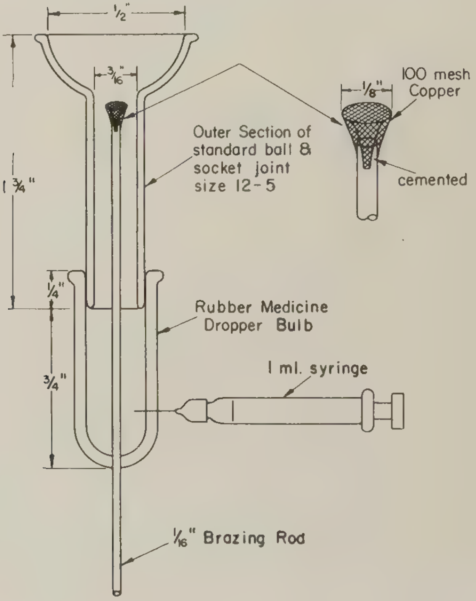
1/2"
3/16"
1/8"
100 mesh Copper
Outer Section of standard ball & socket joint size 12-5
cemented
1 3/4"
1/4"
Rubber Medicine Dropper Bulb
1 ml. syringe
3/4"
1/16" Brazing Rod

FIG. 2. Schematic diagram of replica orienting apparatus.

The operation is observed through a binocular microscope with a large working distance at 10× to 30×. We have used Leitz binocular viewers with which many electron microscopes are now equipped. Surface lighting is used to illuminate the replica. Since the replicas are far too thin to allow any structure to be seen with transmitted light, no provision is made for transmission illumination. It was found helpful to apply black paint to the inside and outside of the glass ball-and-socket joint; this reduces spurious reflections.

---

* Obtained from E. F. Fullam, Inc., P. O. Box 444, Schenectady 1, N. Y.

When the replica and grid are properly aligned so that macrostructure is oriented with the slots of the grid or with grid wires, the rod is gently but quickly pushed up. The replicas stick firmly to the grids and after a minute or two of drying the mounted specimen can be stored or examined immediately in the electron microscope. Cementing of the grid to the copper mesh platform is not necessary or desirable. If the piece of replica is cut large enough to span the gap at the ball-and-socket constriction so that edges of the replica are supported by the glass when the liquid is withdrawn to slightly below this position, the orientation can be accomplished by use of the rod movements alone without withdrawing further amounts of water. Photographs through the "Ultrapak" or binocular viewer serve as a permanent record of the orientation, or sketches may be made for reference when the replica is examined in the electron microscope.

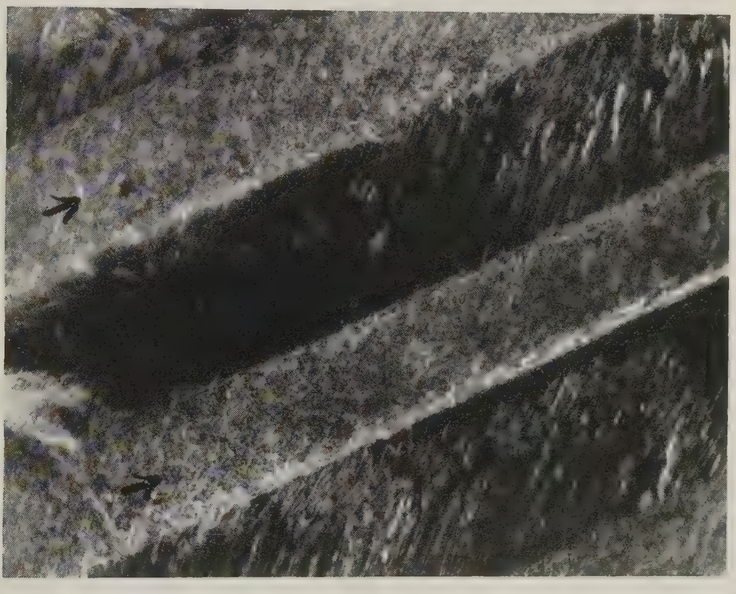

FIG. 3. Photomicrograph of carbon replica of "greened" amethyst cleavage surface mounted on a slotted electron microscope grid. The arrows point to two grid bars. The bands of striations were oriented with respect to the grid slots. Magnification 220×.

Figure 3 is an optical micrograph of a replica of a cleavage surface of "greened" amethyst mounted on a slotted grid so that the major ridges are roughly parallel to the slots. The replica dips between some portions of the grid openings, and this prevents the entire area from being illuminated (with the oblique lighting of the Ultrapak), and being in focus. This is not, of course, a serious difficulty with the electron microscope.

With this method no plastic supporting films are necessary provided the replica is strong enough to support itself on the grid. Most carbon replicas have this strength; the very thinnest films can be mounted on 400 or 1000 mesh grids to give the carbon more support. We prefer to eliminate supporting plastic substrates so that all of the resolution inherent in the replica can be realized.

Results and Discussion

Although the extremely complicated microstructure of amethyst quartz evinced by this study cannot as yet be fully explained, it seems worth while to comment on several features of the electron micrographs of cleavage surfaces prepared as described above. Cleavage was usually effected by heating the quartz above its transition (α to β) temperature and quenching in air at room temperature. This procedure allows a good deal of plastic flow to take place and therefore may complicate the interpretation of the structure. Some samples were cleaved by percussion to see if changes in structure on cleavage surfaces would be obtained. No

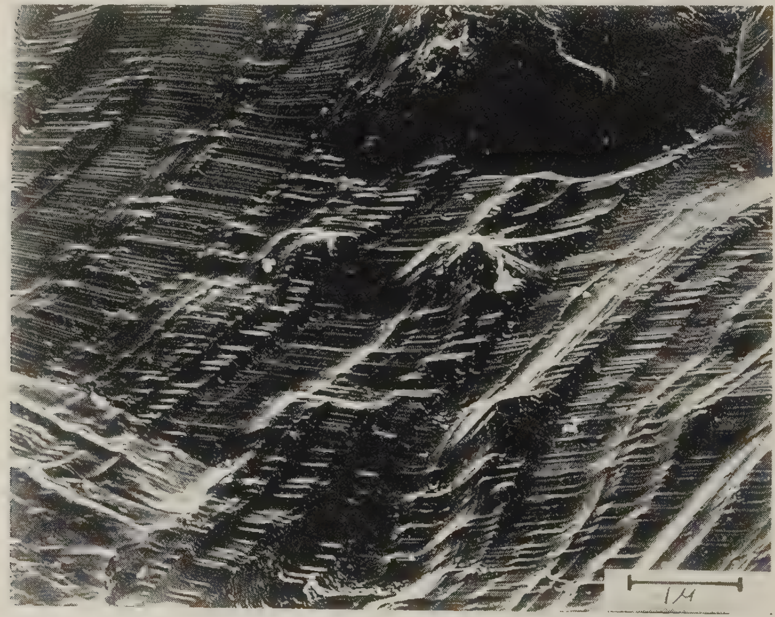

Fig. 4. Electron micrograph of a carbon replica of "greened" amethyst cleavage surface. A portion of the thin replica has been folded over itself at the lower left.

important differences were noted. The "greened" amethyst is imported by the jewelry trade in the form of chips which are prepared by heating. Consequently the samples studied here have a prior history with the complications discussed above.

Figure 4 is an electron micrograph of a replica of the cleavage surface of "greened" amethyst showing very fine striations within bands which cross the figure diagonally. Many such striated bands were seen on surfaces cleaved approximately parallel to the *c* axis of the crystal. The bands run in the same direction as do the major ridges visible in the light microscope such as can be seen in Fig. 1. The bands shown in Fig. 4 are too narrow to be resolved in the "Ultrapak" microscope but they parallel the larger ridges. Since the presence of optical twinning can be shown only by a petrographic microscopical examination (with inherent low resolution), it is not possible to state whether the bands in Fig. 4 are portions of the *d*- or the *l*-components of the laminar twins.

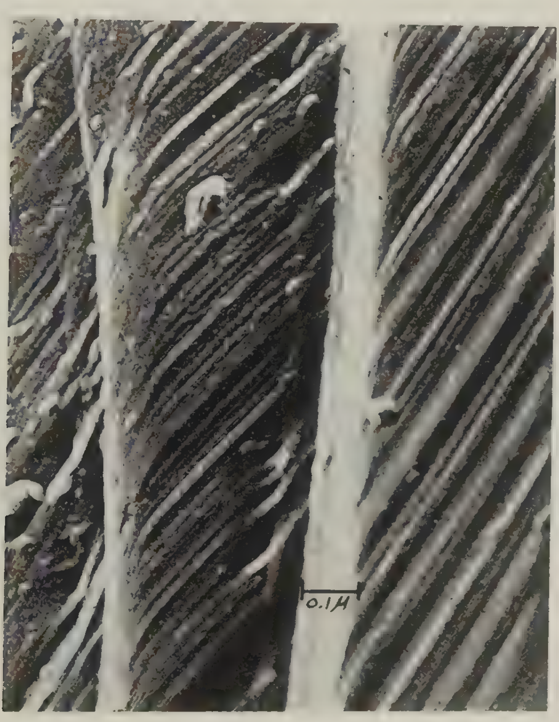

FIG. 5. Electron micrograph of a carbon replica of another area of the same surface shown in Fig. 4.

Figure 5 is an enlargement of another area with similar bands and cross striations. Many areas show the cross striations separated by relatively large distances. For example, some of the most prominent cross striations along a rather narrow band in the lower center of Fig. 4 are separated by as much as 1 μ; in other electron micrographs, distances between striations approach 10μ. In light micrographs such as Fig. 3 the cross striations (of very wide bands) that are just resolved, are most likely the more prominent striations observed in the electron micrographs. At several locations in Fig. 4 the striations cross over to adjacent bands but many areas such as in Fig. 5 give no evidence of the linking of adjacent bands. Figure 6 is a still greater enlargment of the upper right portion of Fig. 5. This electron micrograph shows examples of the very fine striations. Two ridges separated by about 35 Å are indicated by a fork. The ridges appear to be made up of aligned roundish protuberances.

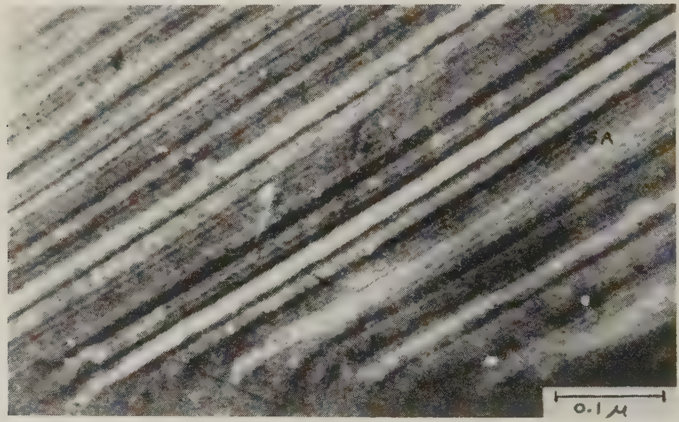

Fig. 6. Electron micrograph of a carbon replica of the upper right area of Fig. 5.

Negatives of several areas similar to Fig. 6 were scanned with a microdensitometer to see if there was any regularity of the striations. None was found.

There are several other features that merit attention. Regular arrays of pits are found at the apparent edges of several bands; however a few pits are also distributed at random over the surface. Conchoidal fractures as might be expected were found in the quartz. These fracture ridges did not have any fine cross striations. None of the various structures seen in these electron micrographs can be definitely assigned to the separate phase found by light microscopy.

A tentative explanation of these cleavage surface structures would be that the striations within the bands are growth layers in one of the twins comprising the amethyst. An alternate explanation is that these are slip lines produced by deformation. Many of the structures seen in Figs. 4, 5 and 6 and in other similar electron micrographs cannot as yet be interpreted. Since the replicas are from *cleavage* surfaces, they may show deformations resulting from cleavage forces. The interplay of these forces with the complex twinned structures of the crystal would be complex itself and difficult to recognize and discuss.

Undoubtedly it would be more fruitful to study natural faces of the "greened" amethyst but we have been unable to procure such specimens. However, further work is contemplated on the $10\bar{1}1$ faces of ordinary amethyst.

ACKNOWLEDGMENTS

We gratefully acknowledge the technical assistance of Mr. Carl Zovko and Mr. Morton Maser in certain phases of this work. We thank Eldot and Co., Inc., New York 23, New York, for gifts of the "greened" amethyst used.

REFERENCES

BOOKER, G. R. (1954) *Brit. J. Appl. Phys.* **5,** 349.
BRADLEY, D. E. (1954) *Brit. J. Appl. Phys.* **5,** 65.
COHEN, A. J. (1956) *Am. Mineral.* **41,** 874.
GAY, H., AND ANDERSON, T. F. (1954) *Science* **120,** 1071.
HALL, C. E. (1953), Introduction to Electron Microscopy. McGraw-Hill Book Co. New York, p. 348.
MCLAUCHLAN, T. A. (1953) Symposium on Techniques for Electron Metallography, Special Tech. Publ. No. **155,** p. 96. American Society for Testing Materials.
PAGE, D. H. (1956) *Research* (*London*) **9,** A1.

Manuscript received March 27, 1957.

THE AMERICAN MINERALOGIST, VOL. 43, JANUARY–FEBRUARY 1958

CHROME MICA-CLAY, TEMPLE MOUNTAIN, UTAH

Paul F. Kerr and P. K. Hamilton, *Columbia University, New York, N. Y.*

Abstract

Chrome mica-clay occurs at Temple Mountain, Utah in association with uranium mineralization. It contains approximately 0.4 to 0.6 per cent Cr_2O_3 and consists of mixed $2M_1$ and 1M mica polymorphs. These mixed polymorphs differ from the well-crystallized single polymorph chrome micas, mariposite and fuchsite. At Placerville, Colorado a similar chrome mica-clay contains as much as 20 per cent interlayered expanding lattice material. Recorded data on synthesis suggest that a likely source of these chrome mica-clays would be hydrothermal chromium-bearing solutions.

Introduction

The rigorous application of *x*-ray diffraction and allied mineralogical techniques to the fine fractions of clays has gained momentum during recent years. As a result, somewhat indefinite clay material long ago recognized as hydromica (Galpin, 1912) and later described as illite (Grim, Bray and Bradley, 1937) is becoming better understood. Grim, Bray and Bradley recognized the uncertain nature of this mineral when they said that illite " . . . is not proposed as a specific mineral name, but as a general term for the clay mineral constituent of argillaceous sediments belonging to the mica group."

The material differs from the other mica minerals in composition, occurrence and origin. Following its introduction, "illite" became widely used as a general term which was applied to the mica clay minerals from argillaceous sediments as well as to those from other environments. However, as long ago as 1928, Mauguin demonstrated by means of *x*-ray diffraction the existence of polymorphism in the mica group. Shortly after the original description of illite, Hendricks and Jefferson (1939) identified 7 crystalline modifications (polymorphs) among 100 specimens of mica, and in 1949 Axelrod and Grimaldi described a 3-layered monoclinic muscovite polymorph which is dimorphous with the more common 2-layered muscovite polymorph. Recently, Smith and Yoder (1956) published the results of an experimental and theoretical study on the structure and relations of the possible mica polymorphs. The simplest polymorphs are classed as 1M, $2M_1$, $2M_2$, 3T, 2O and 6H, but it is noted that more complicated types can be developed. Thus, in the investigation of the mica-clays, the presence of these various polymorphs must be considered. Grim, Bradley and Brown (Brindley, 1951) note that the demonstration of polymorphism in the micas shows that the original characterization of illite as a derivative of 2M muscovite crystallization is not entirely precise. In their investigation of the upper stability limits of muscovite, Yoder and Eugster (1954) synthesized a randomly stacked one-layer monoclinic muscovite (1Md illite) and thus demonstrated that the 2M structure is not unique to the illites. In 1955 Levinson recognized the existence of the 1Md, 1M and 3T mica polymorphs in nature by an *x*-ray diffraction investigation of a number of specimens labeled illite or hydrous mica. Yoder and Eugster (1955) conclude that the material known as "illite" may be ascribed to polymorphs of muscovite, solid solutions close to muscovite or to mixed-layer structures. They summarized the status of the term "illite" by suggesting that it " . . . be used only as a field term as Grim *et al.* originally proposed. When identification is made of the material or materials, the polymorph of the mica should be specified, and note made of the clay mineral with which it may have formed mixed layers."

The terms fuchsite and mariposite have been applied to chromium-bearing micas as defined on the basis of optical and chemical evidence (Kerr, *et al.*, 1951). The varietal names chromium muscovite and chromium phengite were introduced by Whitmore, Berry and Hawley (1946) as a better definition of these chromium-bearing micas. Chrome mica-clay as it occurs at Temple Mountain, Utah and Placerville, Colorado is herein identified as a fine-grained mixture of $2M_1$ and 1M mica polymorphs which may be associated with interlayered expanding material, and in which chromium is an essential constituent. It is less well crystallized than the single polymorph chrome micas. Brindley (1951) uses "clay mica" in referring to this type of material. However, "mica-clay" or "clay-mica" are applied interchangeably (Levinson, 1955). In this investigation and that of Kelley and Kerr (1957) mica-clay is preferred since it emphasizes the essentially micaceous nature of the material.

Recently, Mauguin (1956) reported the results of M. Stangatchilovitch's re-examination of "avalite" from Mt. Avala, Yugoslavia. He concludes that this material, which was originally described by Losanitsch (1884) as an alumino silicate of chromium and potassium and has been placed in the muscovite group or redefined as fuchsite (Ramdohr, 1948), "is neither a particular mineral species nor a fuchsite, but a chrome illite with a small amount of kaolin impurity." Optical examination of a specimen labeled muscovite (avalite), Mt. Avala, Servia from the Egleston Collection, Columbia University shows an impure, fine-grained green aggregate with indices of refraction which lie within the range of Temple Mountain and Placerville chrome mica-clays. It seems likely that this material might be redefined in terms of chrome mica polymorphs rather than "illite." However, a sample sufficiently pure to yield an *x*-ray diffraction pattern free from extraneous lines was not obtained.

OCCURRENCE

Green chrome mica-clay is believed to be a significant alteration product at Temple Mountain, Utah. Field relations suggest precipitation from ascending solutions carrying chromium as an accompaniment of the primary introduction of uranium. The green mineral is localized in the vicinity of collapse areas (Kerr, Bodine and Kelley, 1957). More elevated temperatures probably prevailed near these areas than in the main uranium mining areas some distance away.

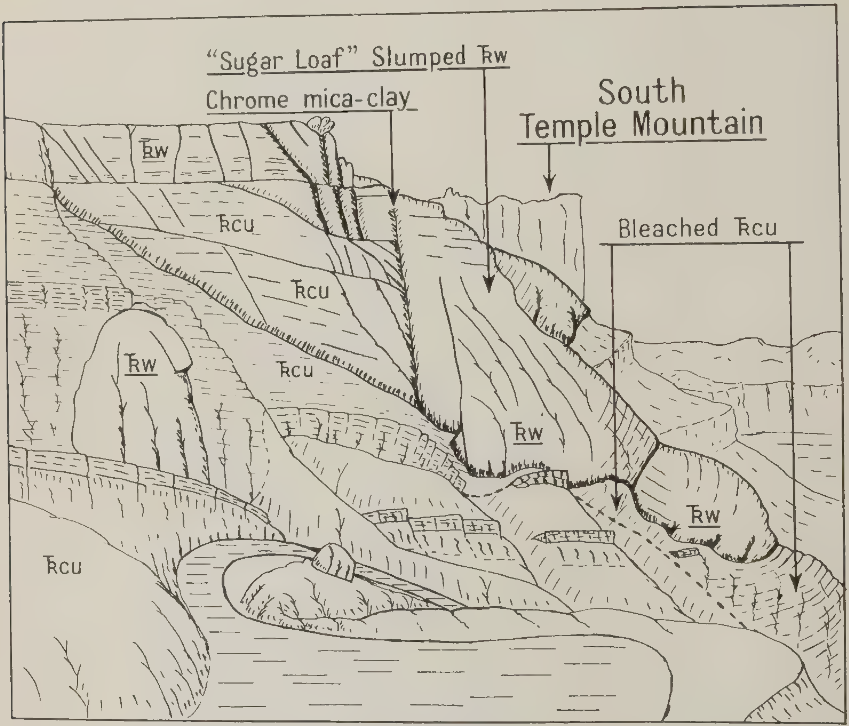

FIG. 1. Chrome mica-clay zone, Temple Mountain, Utah. Mica-clay is distributed in and near fractures in a slumped block of Wingate sandstone (Trw). The block rests upon differentiated Chinle (Trcu).

Surface exposures and drill cores indicate that the mica-clay penetrates strata over a vertical range of 1,200 feet from the upper part of the Wingate formation (Triassic) to the Kaibab formation (Permian). A vertical exposure of nearly 100 feet occurs on the west side of Temple Mountain (Fig. 1), where a collapsed block of Wingate sandstone is stained by the green mica-clay. This material is found in drill cores cut many hundreds of feet below, and also occurs 2.6 miles west in a collapse near Flattop Mesa. It is abundant on the east slope of South Temple Mountain at the base of the Wingate formation, and appears along the eastern margin of the Temple Mountain collapse area. At the Eagle's Nest prospect on the north escarpment of North Temple Mountain, mica-clay shows the greatest depth of color and highest chromium content noted.

The mica-clay occurs in veinlets along bedding planes and dispersed through sediments. Table 1 gives the principal mineral content of these chrome mica-clays. They are found close to areas of dolomitization of the Wingate sandstone, but apparently not within the dolomite. The chromium is an introduced element since the original chromium content of the host rock is negligible. For comparison, chrome mica-clay from Placerville, Colorado—another Plateau uranium locality (Kerr, Rasor and Hamilton, 1951)—has been restudied. In their study of chrome micas from various localities, Whitmore *et al* (1946)conclude that most of the constituents and particularly the chromium, had their origin in solutions derived from some magmatic source. The occurrence of chrome-illite ("avalite") reported by Mauguin (1956) is of interest. This material is present in dolomitic and quartzitic masses in the Mount Avala chromite-bearing serpentine. It is ascribed to hydrothermal action associated with the Tertiary andesitic eruptions which were responsible for the alumina in the mica as well as the alteration of chromite to free the chromium.

TABLE 1. MINERAL CONTENT OF CHROME MICA-CLAYS

Eagle's Nest	*Incline No. 1*
$2M_1>1M$ mica	$2M_1-1M$ mica
quartz	quartz
calcite	feldspar
kaolinite	jarosite
	kaolinite
Drill Hole V-7	*Placerville*
$2M_1$ mica	$2M_1>1M+$montmorillonite
quartz	quartz
apatite	pyrite
calcite	
pyrite	

It is interesting that at the Mi Vida uranium mine in San Juan county, Utah, Gross (1956) notes the occurrence of a vanadium clay as the principal cementing material of the ore samples. The material is described as "a probable mixed-layer montmorillonite-hydromica with substitution of vanadium in one or both lattices." The possible relation of this material to the chrome mica-clay is worthy of further investigation.

TABLE 2. X-RAY DIFFRACTION OF CHROME MICA-CLAY AND MARIPOSITE
(Cu-radiation; Ni-filter)

Eagle's Nest $2M_1>1M$		Drill Hole V-7 $2M_1$		Drill Hole V-7 (leached) $2M_1>1M$		Incline No. 1 $2M_1-1M$		Placerville, Col. $2M_1>1M+$ Mont.		Mariposite Mother Lode Fault, Mariposa Co., Calif. Heinrich and Levinson (1955) 1M		Mariposite Carson Hill, Calveras Co., Calif. Heinrich and Levinson (1955) $2M_1$	
d(Å)	I	d(Å)	I	d(Å)	I	d(Å)	I	d(Å)	I	d(Å)	I	d(Å)	I
10.3	10							10.39[e]	6				
		9.90	10	9.82	10	9.93	10	9.91	10	10.0	s	10.0	s
4.951	5	4.954	4	4.924	1	4.993	5	4.954	3	4.99	m	4.99	m
4.462	3	4.460	5	4.436	8	4.473	6	4.480	5	4.48	s	4.49	s
												4.32	vw
		3.863	1					4.112	1			4.11	vw
3.767[g]	½	3.720	2			3.948	3	3.844	½			3.88 $2M_1$	m
3.608	½			3.705	3	3.736	4	3.705	1			3.73 $2M_1$	m
3.501	3	3.504	3			3.631	4	3.616	½	3.67 1M	m		
3.336	10	3.336*	>10	3.477	2	3.517	4	3.477	2			3.49 $2M_1$	m
3.241	3	3.241	3	3.322*	>10	3.346*	>10	3.336*	>10	3.35	s	3.33	s
3.066	½			3.230	2	3.249[z]	7	3.247	2			3.20 $2M_1$	m
2.985[c]	6	2.976	1			3.076[y]	5	3.076	½	3.08 1M	m		
2.883[g]	4	2.873	1	2.976	2	2.976	3	2.976	1			2.99 $2M_1$	m
2.838	3	2.795[a]	>10	2.838	1			2.847	1			2.86 $2M_1$	m
								2.768	1	2.84	vvw	2.78 $2M_1$	mw
2.562[x]	3	2.561	7	2.550	7	2.568[x]	5	2.696	½	1M			
2.526	2	2.493	½					2.561	4	2.57	s	2.57	s
2.459	2	2.448	3					2.493	1			2.48 $2M_1$	mw
2.377	½	2.383	2			2.371	4	2.383	1	2.39	m	2.39	m
		2.341	1	2.330	3	2.318	3						
2.283[x]	4	2.240[a]	4	2.252	2					2.26	w	2.25	w
		2.204	1					2.199	1			2.20	w
2.130[x]	2	2.125[a]	3	2.111	1			2.120*	4	2.13	w	2.13	m
				2.021	3	2.077	3			2.00	m	1.99	s
1.995	1	1.988[a]	3	1.970	½			1.980*	.7				
		1.651	1			1.645	3			1.72	vw	1.72	vvw
1.631	1	1.637[a]	1	1.639	2			1.648	1	1.66	w	1.65	m
								1.629	1				
												1.60	vvw
												1.56	vvw
1.497	2	1.499[a]	4	1.494	2	1.502	4	1.499	3	1.51	s	1 50	ms

* Mica masked by quartz.
[a] Mica masked by apatite.
Mica masked by calcite.
[e] Expands to 11.62 with ethylene glycol.
[g] Mica line masked by gypsum.
[x] Mica line masked by kaolinite.
[y] Mica line masked by jarosite.
[z] Mica line masked by feldspar.

X-RAY DIFFRACTION

The *x*-ray diffraction spacings for 1M and $2M_1$ mariposite (Heinrich and Levinson, 1955) are given in Table 2 for comparison with the Temple Mountain and Placerville chrome-bearing materials. These reflections, especially of the polymorphs, are sharp and well defined in contrast to the weak, diffuse and asymmetric lines of Temple Mountain mixed polymorphs. The 2.696 Å, 1M reflection which is missing from the mariposite used for comparison, does appear in the Placerville mica-clay.

The separation of the mica-clay fraction for *x*-ray diffraction study was made by collecting material which remained in suspension in distilled water for six to eight hours. *X*-ray patterns were obtained with a Philips diffraction outfit and chemical data with an *x*-ray spectrographic unit. The intensities (Table 2) were recalculated proportional to 10 for the most intense 10.0 Å reflection. Reflections due to impurities are omitted unless they mask or interfere with mica reflections as indicated. The principal polymorph shown by these patterns is based upon the presence and relative intensity of characteristic reflections (Yoder and Eugster, 1955). Three polymorph forms appear which are described as $2M_1 > 1M$, $2M_1 - 1M$. In addition, $2M_1 > 1M +$montmorillonite is found. On the basis of the *x*-ray diffraction data given by Mauguin (1956), this chrome illite does not appear to correlate with any of the polymorphs.

Drill Hole V-7

The *x*-ray difffraction pattern (Table 2) indicates essentially a $2M_1$ polymorph, although the reflections are somewhat diffuse and weak compared with the better crystallized $2M_1$ reference mariposite. The minor development of the 1M polymorph is indicated by the asymmetric 3.72 Å line. It is significant that after leaching with dilute HNO_3 (in order to remove apatite) this line increases in intensity and shifts to 3.705 Å, an approach to the 3.6 Å-1M spacing. However, this may also be caused by the breakdown of the $2M_1$ to 1M polymorph by acid action as the 3.88 Å and 2.48 $2M_1$ spacings disappear. These particular polymorph reflections seem generally weak or missing in the Temple Mountain chrome mica-clays, and the definition of this 3.705 Å reflection may result from purification. The 2.838 Å$-2M_1$ line appears after removal of the apatite in addition to the following mica lines: 2.252 Å, 2.111 Å, 1.970 Å, 1.639 Å and 1.494 Å. The dominance of the $2M_1$ structure is of interest since it occurs at depth and represents a more stable type formed at higher temperatures.

Apatite, quartz and gypsum are fine grained impurities. The gypsum was removed during washing, but apatite is intimately associated and has approximately the same particle size. Hence, it persists unless it is leached out by acid. Before leaching, aggregate fragments which are approximately 100 microns in diameter removed from thin section yield persistent apatite and mica-clay reflections with the *x*-ray micro-camera. The apatite particles yield sharp, well defined reflections compared with those from chrome mica-clay of corresponding size. Thus the diffuseness of the mica-clay is an inherent reflection feature and not due entirely to small particle size.

Eagle's Nest

The *x*-ray diffraction pattern of this material shows contamination by gypsum, calcite and kaolinite. The lines of these impurities are well defined compared with the more diffuse mica-clay lines. The mica-clay consists of mixed $2M_1 > 1M$ polymorphs. The 3.608 Å and 3.066 Å – 1M spacings are equally developed and distinct although definitely weaker than the 3.501 Å and 3.241 Å – $2M_1$ reflections. Since the 3.8 Å – $2M_1$ line is missing and the 3.767 Å – $2M_1$ line is weak (although enhanced by a gypsum reflection), this mixture is believed to contain significant 1M mica-clay. However, it is less abundant than the $2M_1$ polymorph.

It is significant that this material which shows the highest chromium content (3 per cent) among the chrome mica-clays at Temple Mountain also has a relatively prominent 1M structure. This may reflect the most intense hydrothermal activity, although not necessarily the highest temperature of formation, as presumably the 1M polymorph would be less prominent.

Incline No. 1

Quartz, jarosite and feldspar are impurities which interfere with some of the mica-clay reflections. The presence of feldspar explains the intensity of the 3.249 Å spacing which is considerably more intense than would be expected from the $2M_1$ mica reflection only. Since the 3.631 Å and 3.076 Å 1M spacings have the same intensity as the 3.736 Å and 3.517 Å $2M_1$ reflections, the material is interpreted as a more or less equal mixture of $2M_1$ and 1M polymorphs.

The chrome-bearing micaceous clays from Temple Mountain, therefore, are essentially mixed $2M_1$ and 1M polymorphs which show a slight range in proportions. Diamond drill hole V-7 from deep in the collapse shows the best development of the $2M_1$ polymorph, whereas Incline No. 1 and the Eagle's Nest have more 1M. It is also noted that V-7 shows a much stronger tendency to orient when settled from suspension than do the other specimens which contain more of the mixed 1M polymorph. On the other hand, this orientation may result from more rapid settling of the larger and better crystallized $2M_1$ fraction, whereas the finer, possibly 1M particles, remained in suspension.

Placerville, Colorado

A re-examination of the Placerville, Colorado chrome-bearing mica-clay has been made in view of its similarity with the Temple Mountain occurrence. On the basis of chromium content and optical properties, this material was called fuchsite (Kerr *et al.*, 1951). However, recently purified material gives an *x*-ray diffractometer pattern (Table 2, p. 12) which shows the presence of interlayered montmorillonite. The asymmetric (001) reflection has two distinct peaks (10.39 Å and 9.91Å). After orientation and glycolation the 10.39 Å peak shifts to 11.62 Å, and the 9.91 Å remains in the same position. The 3.336 Å peak increases in intensity after glycolation which indicates that the (005) spacing of the expanded layers has moved closer to the (003) reflection of the 10 Å layers. This may signify the presence of as much as 20 per cent expanded layer material (Weaver, 1956). The pattern also shows $2M_1 > 1M$ mixed polymorphs and is therefore similar to the material from Eagle's Nest at Temple Mountain except for the relatively large content of associated interstratified montmorillonite. The 3.616 Å and 3.076 Å 1M lines are of equal intensity, but weaker than the $2M_1$ reflections.

McConnell (1953) has described volkonskoite as a chromium montmorillonite from the Morrison formation near Thompson, Utah which contains about 2 per cent Cr_2O_3. This material is associated with a non-chrome mica, whereas at Placerville an interlayered relation exists. It appears possible that the expanding material in the interlayer position at Placerville also contains chromium.

Glycolated Temple Mountain Chrome Mica-Clay

Due to asymmetry the (001) 9.90 Å reflection exhibits a steep slope on the high angle side and a moderate slope on the low angle side. This suggests interlayered montmorillonite. However, oriented specimens either heated in an ethylene glycol saturated atmosphere (Brunton, 1955), or soaked with the liquid, show no expansion toward the low angle region, and only a slight tendency toward a more symmetrical peak as indicated by a somewhat more gentle slope toward the high angle area. This is confirmed by slowly scanning the peak. There is also a slight increase in the amplitude of the 3.33 Å spacing. If interlayered expanding material is present, it amounts to less than 10 per cent (Weaver, 1956). Yoder (oral communication) suggests that this lack of expansion with ethylene glycol may be explained by the position of this chrome mica-

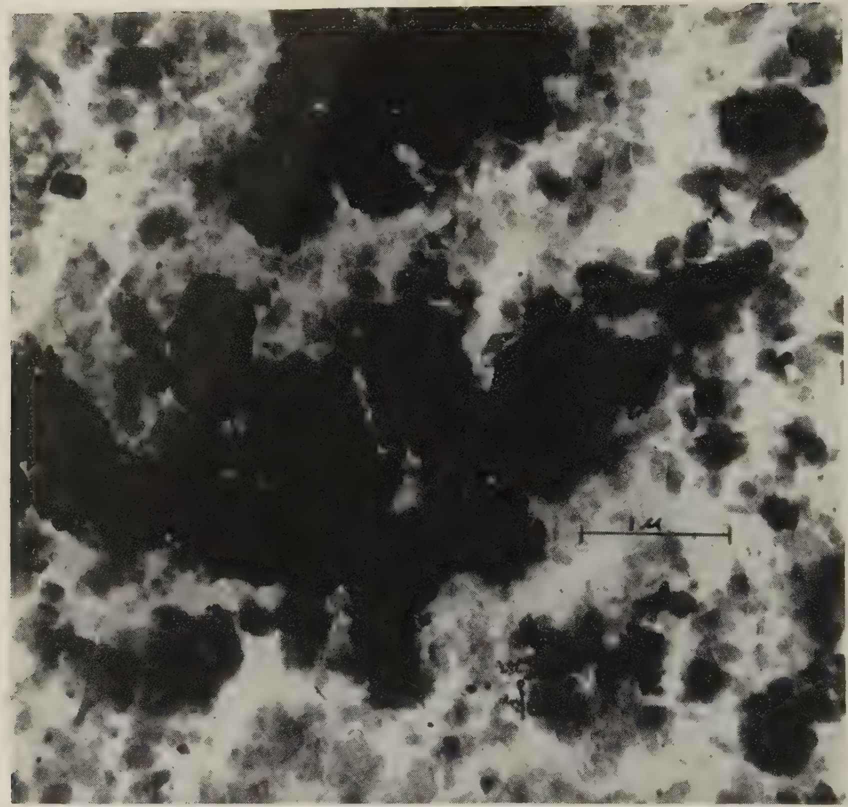

FIG. 2. Electron micrograph of chrome mica-clay from Temple Mountain, Utah. Specimen drill hole V-7 shows a particle size distribution which ranges from approximately 0.1 to 1 micron.

clay near celadonite in the muscovite, celadonite, pyrophyllite series. It is also possible that the association of mixed $2M_1$ and 1M polymorphs as well as the variation (approximately 0.1 to 1 micron) in particle size as seen in the electron micrograph (Fig. 2) may contribute to the asymmetry of this reflection.

X-RAY SPECTROGRAPH

Notwithstanding the presence of fine grained impurities, *x*-ray spectrographic data yield a fair estimate of the Cr_2O_3 content. Three reference mounts containing 1 per cent, 3 per cent and 5 per cent Cr_2O_3 mixed with SiO_2 were prepared and scanned with the Norelco *x*-ray spectrograph. The amplitudes of the $K\alpha$ and $K\beta$ reflections were plotted against per cent Cr_2O_3 and from these the values for the chrome mica-clays were estimated (Table 3). *X*-ray spectrographic examination of bromoform separated fractions indicates that the chromium is concentrated in the lighter micaceous fraction rather than in the heavier pyrite-rich material. Iron is also present and varies inversely with chromium. In the Drill Hole V-7 specimen (leached with dilute HNO_3 to remove the apatite) the Cr_2O_3 content increases with purification which indicates that the chromium is concentrated in the mica-clay.

TABLE 3. Cr_2O_3 IN SOME MICA-CLAYS

	Cr_2O_3 per cent
Drill Hole V-7	0.37–0.68
Drill Hole V-7 (leached)	0.55–0.85
Incline No. 1	0.55–0.85
Eagle's Nest	3.07–3.30
Placerville	3.40–3.60

For comparison, in fuchsite analyses (Whitmore *et al.*, 1946) Cr_2O_3 ranges from 0.27 per cent to 4.81 per cent, whereas in mariposite the Cr_2O_3 ranges between 0 and 0.78 per cent. At Temple Mountain the 1M polymorph suggests the higher chromium content since the Eagle's Nest and Incline No. 1 samples contain more chromium than samples from Drill Hole V-7 where the $2M_1$ polymorph is more prominent. The interlayered expanding material at Placerville is believed to contain chromium as well as the associated mica-clay.

DIFFERENTIAL THERMAL ANALYSIS

Although the published DTA curves of muscovite differ, they exhibit a distinct range at variance with the mica-clays. In his investigation of the decomposition of muscovite, Roy (1949) found that there are no marked changes up to 940° C., but he structure is destroyed within the relatively narrow range between 940° C. and 980° C. However, some vari-

TABLE 4. ENDOTHERMIC PEAKS OF MUSCOVITE

Grim and Bradley (Brindley, 1951) Coarse grained (10–20 microns)	800–900° C.
Grim and Rowland (1942)	750–950° C. 300–400° C.
Grim (1953)	850° C. and 900° C.
Grim (1953)	720° C.

ation probably is due to the time factor. Grim and Rowland (1942) note the variations (Table 4) in the muscovite curves and suggest they may be due to grain size, since the coarse flakes permit only a small amount to be packed loosely in the specimen holder. Grim and Bradley (Brindley, 1951) note that a decrease in the particle size of muscovite is accompanied by a reduction in the temperature of the start of the endothermic reaction, and an increase in the interval during which it occurs.

The typical DTA curve for "illite" (Kerr, Kulp and Hamilton, 1949) shows three endothermic reactions. The first corresponds to the loss of interlayer water between about 120 and 220° C. Grim (1953) says this differs from the well crystallized micas as "a consequence of fewer interlayer actions, less bond between layers, less uniform orientation of successive layers and smaller particle size, and/or a difference in composition within the silicate layer itself."

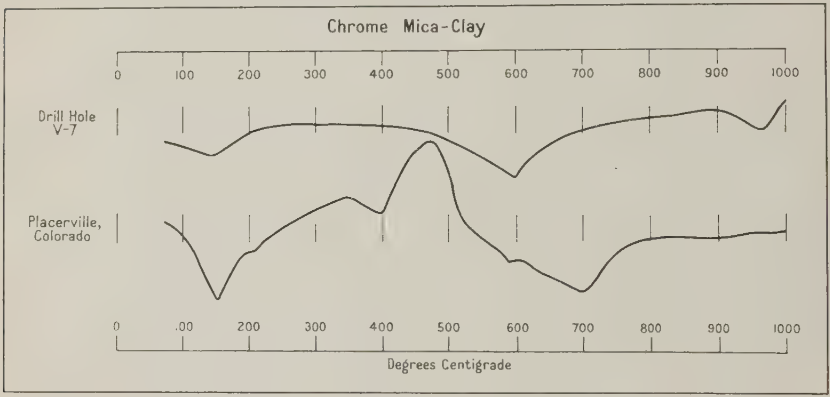

FIG. 3. DTA of chrome mica-clay. In drill hole V-7, the mica-clay is similar to illite with a trace of calcite. The Placerville, Colorado, sample represents an assemblage of mica-clay, montmorillonite, pyrite and quartz.

The second endothermic peak in "illite" is sharp and occurs at about 500° C.–600° C. This is caused by the loss of hydroxyl water. The sharpness of this reaction compared with that in muscovite is attributed by Grim (1953) to differences in particle size. The third endothermic reaction occurs between about 850° C. and 950° C. and represents the complete destruction of the lattice. An exothermic reaction frequently is present between 900° C. and 1000° C., and reflects the crystallization of spinel.

The DTA of the chrome mica-clay shows some of the characteristics of both mica-clay ("illite") and muscovite. V-7 (Fig. 3) has an adsorbed water peak at about 150° C., which corresponds to the loss of adsorbed water in the mica-clays, and a single endothermic peak at about 600° C., which is thought to represent the loss of hydroxyl lattice water, and is also typical of the mica-clays. However, the subsequent endothermic-exothermic effects which are present in "illite" are missing, which is more characteristic of muscovite. The endothermic peak at 960° C. is probably due to some minor associated calcite. Mauguin (1956) gives somewhat similar results for the DTA of "chrome-illite," namely a well defined endothermic peak at 130° C. and another at 570° C. The exothermic effect reported at 830° C. does not appear in the chrome-micas of this investigation, and it is somewhat anomalous for "illite," since it is low in temperature and not preceded by an endothermic effect. Perhaps this is due to an unidentified impurity.

The DTA curve of the Placerville material distinctly shows the presence of the more reactive interlayered montmorillonite. Thus, there are double dehydration peaks between 150° C. and 220° C. rather than the more usual single reactions in the mica-clays as well as an endothermic peak at about 700° C. which corresponds to a similar one in montmorillonite. This peak is particularly broad since the reaction begins at about 500° C. and is believed to include or mask that of the associated mica-clay. However, the usual higher temperature endothermic-exothermic peaks of both "illite" and montmorillonite are missing in the micas. A prominent 470° C. exothermic peak is due to pyrite and the small, sharp endothermic peak at about 580° C. superimposed on the broad endothermic flexure reflects the presence of associated quartz as an impurity.

OPTICAL PROPERTIES

The green chrome mica-clay at Temple Mountain occurs in thin veinlets, layers and streaks disseminated through quartz sand. Although it imparts a general green or gray-green appearance to the rock, in thin section the color is generally tan or pale bluish-green. The darker green bands appear to represent 1M mica-clay derived by later, lower tem-

TABLE 5. OPTICAL DATA ON CHROME MICA-CLAY

	α	β	γ	Birefringence	2V	Optic sign
Eagle's Nest	1.553	1.584	1.587	.034		
V-7 626 feet	1.554	1.585	1.592	.038	ca. 30°	–
Incline No. 1	1.554	1.582	1.589	.035		
Placerville	1.559	1.582	1.590	.031		
Fuchsite (Whitmore, *et al.*)	1.5590–1.5695		1.5973–1.6115	.035–.042	32°–46°	–
Mariposite (Whitmore, *et al.*)	1.56 –1.58		1.60 –1.63	.033–.040	0°–40°	–
Illite (Grim, 1953)	1.545 –1.63		1.57 –1.67	.022–.055	small	–
"Avalite"	1.554	1.582	1.592	.038		
Muscovite (Rogers and Kerr, 1942)	1.556 –1.570	1.587–1.607	1.593 –1.611	.037–.041	30°–40°	

perature chromium-bearing solutions acting on and causing the breakdown of earlier $2M_1$ mica-clay. Micro-camera *x*-ray diffraction patterns of both tan and pale green materials removed from thin section are similar, but the significant polymorph lines may be too weak to register. The optical properties given in Table 5 are compared with reference material. The indices of refraction of the Temple Mountain samples are somewhat lower than those given for fuchsite and mariposite and agree more closely with illite (Grim, 1953). The birefringence of the Placerville specimen is lower than the birefringence of the Temple Mountain material. This is probably due to the presence of interstratified montmorillonite. It appears from the specimens examined that the higher chrome content of Eagle's Nest, Incline No. 1 and Placerville correlates with a lower birefringence. This may be due either to the presence of the 1M polymorph or to interstratified montmorillonite.

TEMPERATURE CONDITIONS

Hydrothermal synthesis by Yoder and Eugster (1955) has indicated that the transition of 1M to $2M_1$ mica polymorphs occurs between 200° C. and 350° C. at 15,000 p.s.i. water pressure. Under natural conditions the effects of catalysts and other variables which include temperature, pressure and ion concentration are not known. If the data of synthesis are applicable, the presence of the $2M_1$ polymorph at Temple Mountain indicates a corresponding temperature of formation.

ACKNOWLEDGMENTS

The study of green chrome mica-clay has been made possible through the aid of the Atomic Energy Commission, Division of Research and the Division of Raw Materials. The cooperation of Dr. Daniel R. Miller, Mr. Robert Nininger, Mr. Ernest Gordon and their associates is gratefully acknowledged.

Discussions of mica polymorphs and mixed-layer clays with Dr. H. D. Glass of the Illinois Geological Survey and Dr. H. S. Yoder of the Geophysical Laboratory have aided this study and are gratefully acknowledged. Also, the writers wish to thank Professor T. I. Taylor and Mr. Samuel R. Kamhi of Columbia University for the electron micrograph.

REFERENCES

AXELROD, J. M., AND GRIMALDI, F. S. (1949), Muscovite with small optic angle: *Am. Mineral.*, **34,** 559–572.

BRINDLEY, G. W., ed. (1951) *X*-ray identification and crystal structures of clay minerals: Min. Soc. Great Britain Monograph, Chap. V, 138–172.

BRUNTON, G. (1955), Vapor pressure glycolation of oriented clay minerals: *Am. Mineral.*, **40,** 124–125.

GALPIN, S. L. (1912), Studies of flint clays and their associates: *Amer. Ceramic Soc. Trans.*, **14,** 301–346.

GRIM. R. E. (1953), Clay mineralogy: McGraw-Hill Book Co., Inc., 384 p.

GRIM, R. E., BRAY, R. H., AND BRADLEY, W. F. (1937), The mica in argillaceous sediments: *Amer. Mineral.*, **22,** 813–829.

GRIM, R. E., AND ROWLAND, R. A. (1942), Differential thermal analyses of clay minerals and other hydrous materials: *Amer. Mineral.*, **27,** 801–818.

GROSS, E. B. (1956), Mineralogy and paragenesis of the uranium ore, Mi Vida mine, San Juan county, Utah: *Econ. Geol.*, **51,** 623–648.

HEINRICH, E. W., AND LEVINSON, A. A. (1955), Studies in the mica group: polymorphism among the high silica sericites: *Amer. Mineral.*, **40,** 983–995.

HENDRICKS, S. B., AND JEFFERSON, M. E. (1939), Polymorphism of the micas: *Amer. Mineral.*, **24,** 729–771.

KELLEY, D. R., AND KERR, P. F. (1957), Clay alteration with uranium mineralization; Moss Back ore member, Temple Mountain, Utah: *Bull. Geol. Soc. Am.* (In press).

KERR, P. F., BODINE, M. W., JR., AND KELLEY, D. R. (1957), Collapse features, Temple Mountain uranium area, Utah: *Bull. Geol. Soc. Amer.* (In press).

KERR, P. F., KULP, J. L., AND HAMILTON, P. K. (1949), Differential thermal analyses of reference clay mineral specimens: *A. P. I. Proj.* **49,** Columbia Univ., New York, N. Y., 48 p.

KERR, P. F., RASOR, C. A., AND HAMILTON, P. K. (1951), Uranium in the Black King prospect, Placerville, Colorado: *Ann. Rep't July 1, 1950–June 30, 1951, U. S. Atomic Energy Comm., RMO-797*, 25–43.

LEVINSON, A. A. (1955), Studies in the mica group: polymorphism among illites and hydrous micas: *Amer. Mineral.*, **40,** 41–49.

LOSANITSCH, S. M. (1884), Die Analyse eines neuen Chrom-minerals (Avalit): *Berichte der deutschen chemischen Gesellschaft*, **17(2),** 1774–1775.

MAUGUIN, M. C. (1928) Étude des micas au moyen des rayons *X*: *Soc. française de mineralogie*, **51,** 285–332.

MAUGUIN, M. C. (1956), Sur la presence d'illite chromifère dans le gisement de cinabre d'Avala, près de Belgrade: (Note de M. Stangatchilovitch présentée par M. C. Mauguin): *Comptes rendus*, **242,** 145–147.

McCONNELL, D. (1953), An American occurrence of volkonskoite: Clays and clay minerals: Proceedings of the Second National Conf. on Clays and Clay Minerals, *Nat'l Academy of Sciences Nat'l Research Council Publication* **327,** 152–157.

RAMDOHR, P. (1942), Klockmann's Lehrbuch der Mineralogie, Stuttgart, 632.

ROGERS, A. F., AND KERR, P. F. (1942), Optical mineralogy, McGraw-Hill Book Co., Inc., New York, 335.

ROY, R. (1949), Decomposition and resynthesis of the micas: *Amer. Ceramic Soc. Jour.*, **32,** 202–209.

SMITH, J. V., AND YODER, H. S. (1956), Experimental and theoretical studies of the mica polymorphs: *Min. Mag.*, **31,** 209–235.

WEAVER, C. E. (1956), The distribution and identification of mixed-layer clays in sedimentary rocks: *Am. Mineral.*, **41,** 202–221.

WHITMORE, D. R. E., BERRY, L. G., AND HAWLEY, J. E. (1946), Chrome micas: *Am. Mineral.*, **31,** 1–21.

YODER, H. S., AND EUGSTER, H. P. (1954), Synthesis and stability of the muscovites: *Am. Mineral.*, **39,** 350–351.

YODER, H. S., AND EUGSTER, H. P. (1955), Synthetic and natural muscovites: *Geochemica et Cosmochimica Acta*, **8,** 225–280.

Manuscript received April 19, 1957

THE AMERICAN MINERALOGIST, VOL. 43, JANUARY–FEBRUARY 1958

HARDNESS OF SINGLE ICE CRYSTALS

T. R. BUTKOVICH, *Snow, Ice & Permafrost Research Establishment, Corps of Engineers, U. S. Army, 1215 Washington Avenue, Wilmette, Illinois.*

ABSTRACT

Brinell and scratch hardness tests were made on single ice crystals. The results of these measurements show that the hardness of single ice crystals increases with decreasing temperature; the Brinell hardness numbers range from about 4 at −5° C. to 17 at −50° C. The greatest increase in the hardness values occurs at the higher temperatures. The temperature dependence of the scratch hardness was similar to that of Brinell hardness. An anisotropism of hardness is evident; the single ice crystal is harder parallel to the *c*-axis than in the direction normal to the *c*-axis. An apparent difference in surface structure with respect to orientation was noticed during the scratch hardness tests. A consistent wavy scratch was produced normal to the *c*-axis, while the scratch parallel to the *c*-axis was always straight.

INTRODUCTION

Two methods for determining the hardness of single ice crystals were used in the measurements discussed in this paper. One series of tests employed the Brinell hardness tester, the other the Microcharacter. The Brinell principle involves forcing a hardened steel ball into the specimen under a definite pressure. The dimensions of the impression thus obtained form the basis for calculating the hardness. With the Microcharacter instrument, the hardness of the material tested is a function of the width of the microcut made on the test surface as it is moved along under a diamond edge which bears down on the surface with a constant pressure.

No detailed work on the Brinell hardness and the microhardness of ice can be found in the literature except for some rather crude experiments by Andrews described in Barnes (1928). Moor (1940) and Blackwelder (1940) conducted experiments on scratch hardness of crystal aggregates using the Moh's scale.

The work described in this paper was undertaken to determine how the hardness of ice varies with temperature, and also to determine whether there is appreciable anisotropism with respect to hardness of single ice crystals. The single ice crystals used in these tests were originally quite large, weighing 2–3 pounds, and were obtained from the Mendenhall Glacier near Juneau, Alaska.

EXPERIMENTAL PROCEDURE

For measuring Brinell hardness of single ice crystals, an Olsen Baby Brinell Hardness Tester was used. This apparatus as delivered by the manufacturer was developed primarily for testing soft metal specimens, which could not be satisfactorily tested by applying the standard Brinell loads under standard Brinell conditions. It operates on the Brinell principle but with light loads and a small ball penetrator. The machine comes equipped with a 1/16-inch ball to be used with a load of 12.61 kg. The load is applied directly from dead weights to the ball stem. Preliminary tests with ice samples showed that this load caused excessive cracking of the ice, so that the machine had to be modified thus: (1) the 12.61 kg. load was replaced by a platform on which different weights could be placed, and (2) the $\frac{1}{16}$-inch ball was replaced by a hardened $\frac{1}{8}$-inch ball. The weight of the ball stem plus platform was 570 g., which was added to the weights placed on the platform to give the total load applied.

The speed of loading, that is, the speed with which the indentor and the specimen approach each other immediately prior to contact, is quite important in order to get satisfactory and consistent readings. Bergsman (1948) states that the loading speed should be kept as constant as possible, and should be given with the hardness number. Therefore, the hardness tester was equipped with a 1800 rpm synchronous motor with suitable gear reductions to provide a loading speed of about 9 mm. per minute.

The test blocks of ice were cut from large single ice crystals into rectangular plates of approximately $7 \times 4 \times 1$ cm, oriented so that the *c*-axis lay parallel to the large face of one plate and normal to the large face of the other. The ice plates were machined plane parallel, polished to a mirror finish on a piece of fine silk stretched across a hard surface, and mounted on a piece of plate glass by heating the glass and allowing the sample to melt slightly and then refreeze onto the glass.

After a series of indentations were made, one of the most obvious physical processes was the piling up of the material around the edge of the imprint. Since this would make the diameter of the penetration appear larger than it actually was, this ridge was polished off on silk before the diameter was measured.

All measurements of diameter were made with a filar micrometer mounted on a microscope with a 32 mm. objective. Temperature measurements were made with a copper-constantan thermocouple placed on the surface of the ice within a few millimeters of the ball penetrator. Temperature varied up to 0.25° C. in any one series of measurements.

Williams (1942) in his book on hardness measurement states that comparative Brinell hardness numbers should be used only as determined by a special table of numbers furnished with the machine. However, since the machine was modified for the purposes already stated, Brinell hardness numbers were computed from the standard Brinell formula:

$$H = \frac{K}{\pi D/2(D - \sqrt{D^2 - d^2})}$$

where

H is the Brinell hardness number
K is the applied load in kilograms
D is the diameter of steel ball in mm.
d is the diameter of the impression in mm.

All the tests were conducted in cold rooms in which any temperature down to −55° C. could be obtained. The actual temperatures were chosen arbitrarily, and enough points were obtained to be able to plot the curves shown in the data section.

The Microcharacter, manufactured by the Spencer Lens Company, was used to determine the microhardness of single ice crystals. A 9 g. weight was used during this series of tests. The formula developed for the instrument is:

$$k = \frac{4 \times 10^4}{\lambda^2} \text{ with the 9 g. weight}$$

where

k is the microhardness number
λ is the width of the cut in microns
4×10^4 is an arbitrary number.

The width of the microcut is given in microns and is measured with a filar micrometer eye-piece of the microscope.

Because the microcuts were made at temperatures as low as −50° and it was necessary to measure the width of the line at a higher temperature (−5° C.), there was considerable fogging due to condenstation on the ice specimens. This condensed vapor quickly obliterated the lines, making it impossible to measure them. Consequently, the following method was developed. The specimen was coated with liquid polystyrene, which was allowed to harden and then peeled off. The exact replicas of the microcuts were thus impressed on the coating. These replicas were then measured for the results obtained.

DATA

Because of the necessity of modifying the Baby Brinell Hardness Tester as described in the previous section, it was necessary to verify that the hardness values obtained, as calculated from the standard Brinell formula, are independent of ball diameter and load. The hardness values, within the limits of accuracy of the apparatus, are nearly identical for the $\frac{1}{16}$-inch ball and the $\frac{1}{8}$-inch ball. A slight general difference in hardness is probably due to the fact that the average temperature was 0.5° C. higher during the time the measurements were made with the $\frac{1}{8}$-inch ball.

Different loads were tried to determine how small a load was necessary to prevent cracking. It was found that a 2 kg. load placed on the platform could be used through the temperature range for the penetrations parallel to the *c*-axis, while it was necessary to reduce the load to 1 kg. for penetration normal to the *c*-axis at temperatures above −20° C. Tests were run to check the independence of calculated Brinell hardness values in relation to the load. This showed that the hardness is independent of the load within the limit of accuracy of the apparatus used.

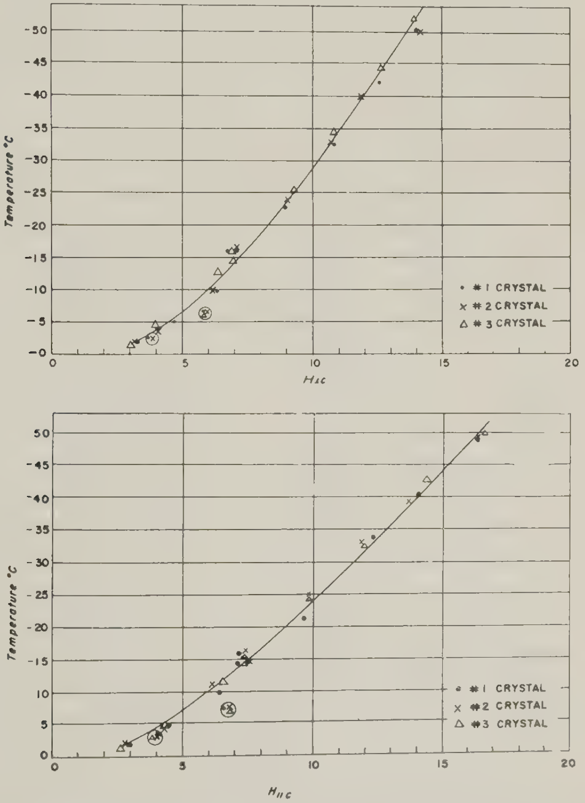

FIG. 1. Brinell hardness of single ice crystals vs. temperature. Twelve second application of load. (Above) Normal to *c*-axis. (Below) Parallel to *c*-axis.

After these preliminary tests were completed experiments were carried out over a temperature range of −5° to −50° C., with 10 impressions at each of six temperatures; and for times of full load applications of 1, 5, 10, 15, and 30 seconds. The load was applied manually. Analysis of the data obtained showed that the hardness is anisotropic in the two direc-

U OF I
LIBRARY

tions, parallel and normal to the *c*-axis. The spread of hardness values was greatest at one-second application of load, as could be expected since this is where the error in measurement is greatest.

Investigation of the possible anisotropism of single ice crystals with respect to parallelism or normality to the secondary crystallographic axis (*a*-axes) was made. No difference in hardness was evident.

At this point during the tests, it was decided to mechanize the hardness tester so that a constant loading speed could be maintained, thereby reducing the spread of the hardness values obtained. Samples were cut normal and parallel to the *c*-axis from three different single ice crystals, in order to be able to compare their hardness. It was found most convenient to use a 12 second application of load. Figure 1 shows the results of these trials, and Fig. 2 shows a definite anisotropism of hardness. Upon examination of Fig. 1 it can be seen that there are two series of hardness values for temperatures above −20°. The first series (circled) yielded values of hardness higher than expected. These points were rechecked to rule out a possibility of error in measurement. It was found that some unexplainable error appeared in the graphs to show the magnitude of the errors.

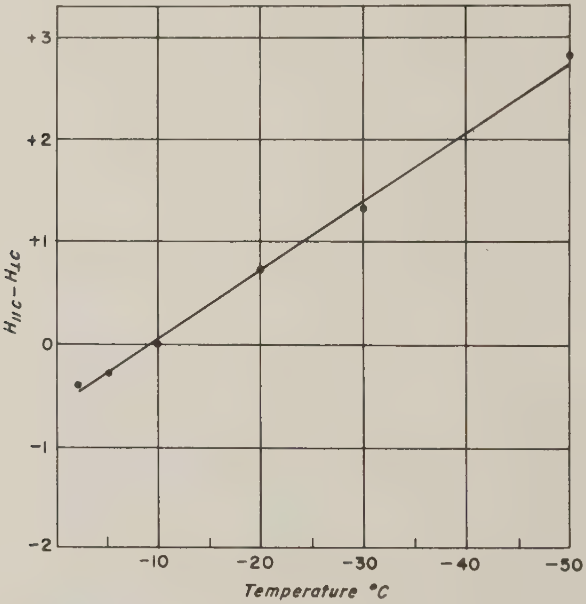

FIG. 2. Difference in Brinell hardness of single ice crystals parallel and normal to *c*-axis.

Figure 2 shows that a crossover of the two curves for hardness normal and parallel to the *c*-axis probably exists at about −10° C. This was also evident in the tests where the load was applied manually. This crossover may indicate that the crystal is harder normal to the main axis below this range and harder parallel to it above this range of temperatures.

Experiments were conducted to check the possible polarity of single ice crystals and the possibility of twinning. No polarity of the main axis was detected in the crystal used. The tests were performed in numerical order, as is shown in Fig. 3. After a series of measurements were made on surfaces 1 and 2, the crystal was planed off about 2 mm. on both sides to new surfaces 3 and 4, on which the next series of measurements were made, and so on.

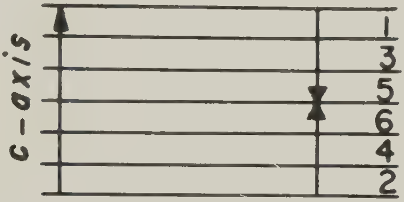

FIG. 3. Order of tests to check possible polarity and twinning.

SCRATCH HARDNESS

The microhardness data were taken on two rectangular plates of approximately 2.5×2.5×1 cm. One of these plates had the *c*-axis oriented normal to its surface so that a scratch in any direction on this surface was normal to the axis. The other plate had the *c*-axis oriented parallel to the surface of the plate so that scratches at different angles to the *c*-axis could be made. Temperatures were chosen arbitrarily but included enough points to draw the curves on Figs. 4 and 5.

A peculiar phenomenon was noticed while measuring the scratches on the plate with the *c*-axis parallel to its surface. A photomicrograph (Fig. 6) shows that the scratches normal to the *c*-axis are wavy, while those parallel to the *c*-axis are quite straight. This phenomenon was particularly evident below −10° C. No apparent mechanical reason for this could be detected, for exactly the same thing happened on several different trials.

In an attempt to observe this phenomenon, a rigidly mounted steel mending needle was substituted for the diamond. The ice specimen with the *c*-axis lying in the plane of the surface was drawn past the needle,

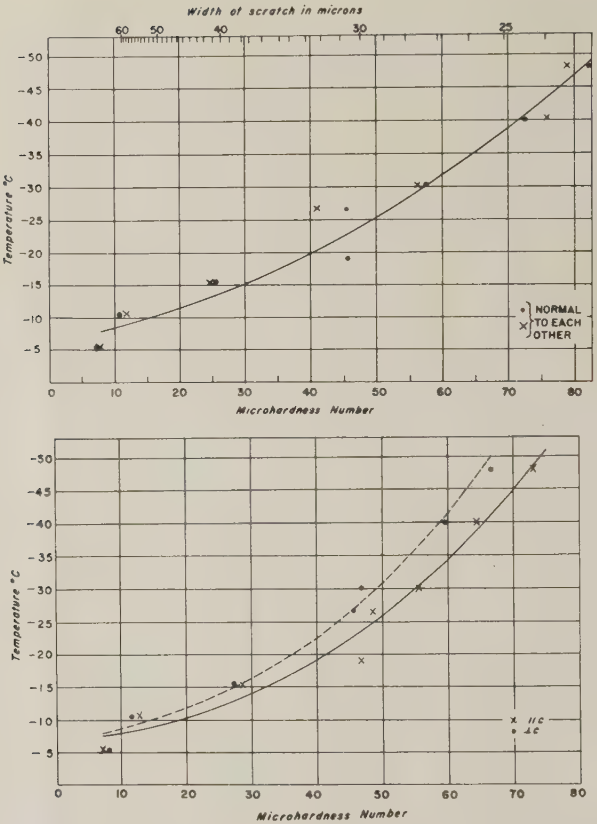

FIG. 4. Microhardness of single ice crystals. (Above) *c*-axis normal to surface. (Below) *c*-axis parallel to surface.

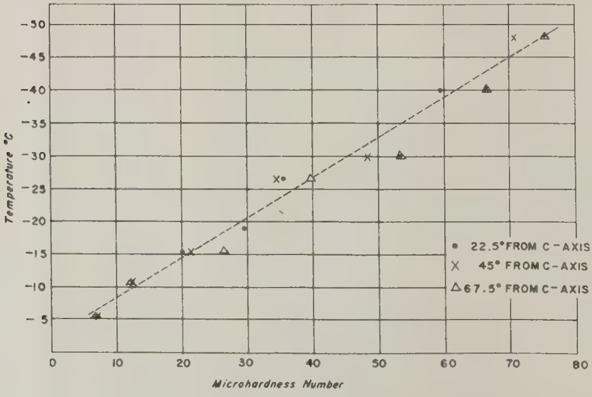

FIG. 5. Microhardness of single ice crystals at various angles to *c*-axis.

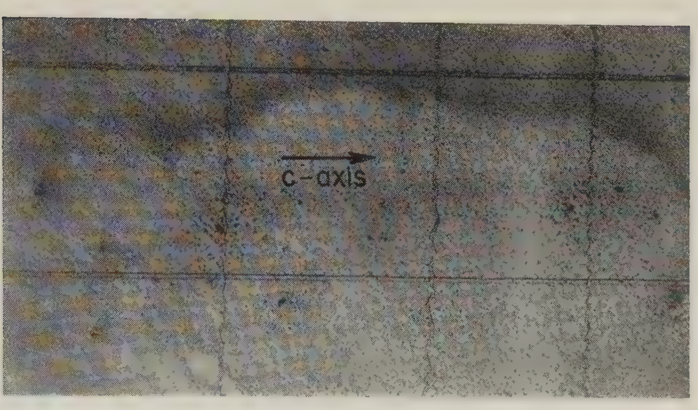

FIG. 6. Scratches made by microcharacter instrument on ice surface parallel and normal to *c*-axis.

first in the direction of the *c*-axis, then normal to this axis, leaving scratches on its surface. When these scratches were observed under the microscope, there was no evidence of the wavy line in either direction. However, all the scratches in these tests were quite irregular, leading to the conclusion that this was not a valid test.

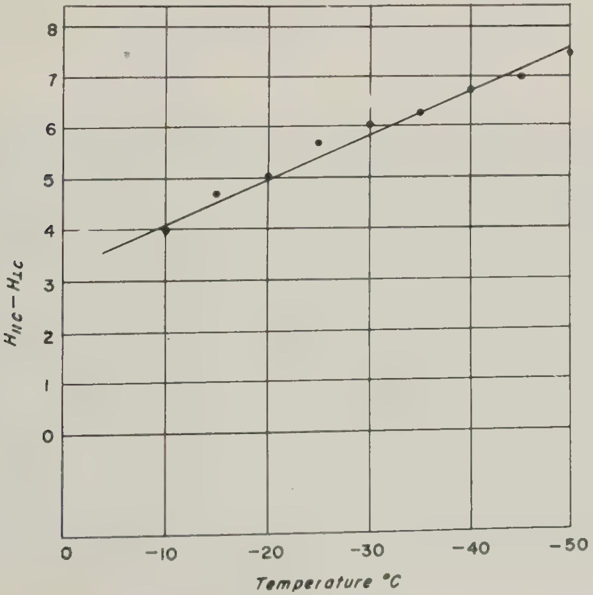

FIG. 7. Difference in microhardness of single ice crystal parallel and normal to *c*-axis.

Discussion of Results

Upon analysis of the data on Brinell and Microcharacter hardness of single ice crystals, the following conclusions were made:

(1) The hardness of ice increases with decreasing temperature. The Brinell hardness test is more reproducible and accurate than the scratch test for measuring the difference in hardness with temperature. The micro-hardness data become less accurate at higher hardness (lower temperature) because a fraction of a micron difference in width of the scratch becomes quite significant. A scale at the top of Fig. 4 gives the difference in hardness values for decreasing width of cut.

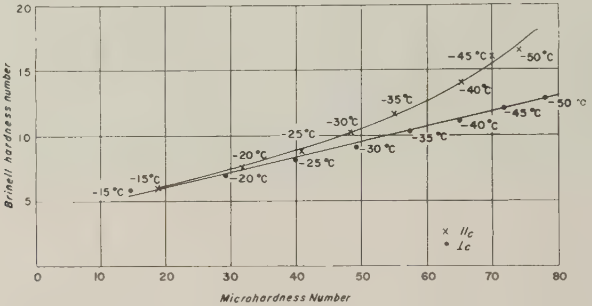

Fig. 8. Empirical relationship between Brinell and micro-hardness numbers, parallel and normal to c-axis.

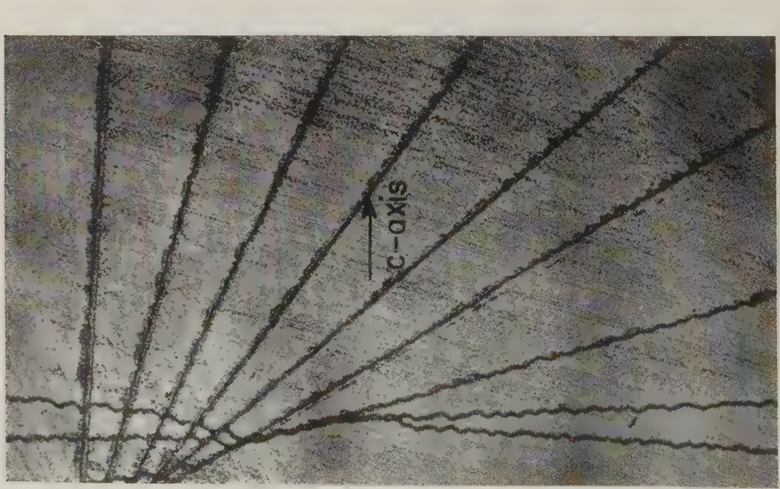

Fig. 9. Scratches made by microcharacter instrument on ice surface. Temperature −30° C. Magnification 15.5×.

(2) There is an anisotropism of hardness with respect to the orientation of the *c*-axis. This is more evident from the Brinell hardness data than from the microhardness data. Brinell hardness $H_{\parallel_c} - H_{\perp_c}$ changes linearly with temperature. The value of $H_{\parallel_c} - H_{\perp_c}$ is negative at high temperatures, zero at approximately −10° C., and positive at lower temperatures (Fig. 2). Anisotropism of hardness is also evident in the microhardness data (Fig. 7), though anisotropy is maximum where the accuracy of determination is least.

(3) A linear empirical relationship exists between the Brinell hardness numbers and the microhardness numbers normal to the *c*-axis, but the relationship between the Brinell and microhardness numbers parallel to the *c*-axis is not linear (Fig. 8).

(4) Apparently, some difference in the structure of the surface with respect to orientation of the single ice crystal consistently causes a wavy scratch normal to the *c*-axis but a straight scratch parallel to it. Figure 9 shows that waviness appears only in the scratches almost normal to *c*. No mechanical or other reason could be found for this phenomenon.

REFERENCES

BARNES, H. T. (1928) Ice Engineering, Montreal, Canada: Renouf Publishing Company, 364 pages.

BERGSMAN, E. (1948) *Metals Progress*, **54,** 183–188.

BLACKWELDER, ELIOT (1940) The hardness of ice: *American Journal of Science*, **238,** 61–62.

MOOR, G. (1940) K voprosu o tverdosti l'da (On ice hardness): *Problemy Arktiki*, No. 5, 119, SIPRE abstract card 2382.

WILLIAMS, S. R. (1942) Hardness and hardness measurements, Cleveland: American Society of Metals, p. 161–162.

Manuscript received April 8, 1957

THE AMERICAN MINERALOGIST, VOL. 43, JANUARY–FEBRUARY 1958

RELATIONSHIPS AMONG IMPURITY CONTENTS, COLOR CENTERS AND LATTICE CONSTANTS IN QUARTZ

ALVIN J. COHEN* AND G. GARDNER SUMNER†, *Mellon Institute, Pittsburgh, Pennsylvania.*

ABSTRACT

The lattice constants of four specimens of synthetic and seven of natural quartz have been measured. The a_0 axis appears the more sensitive to impurity content.

INTRODUCTION

That a color center in α-quartz is impurity related is now well established (1). This anisotropic color center at 460 $m\mu$ (2, 3) is caused by the interaction of an unpaired electron on an oxygen (or possibly in an anion vacancy) with an aluminum ion replacing a tetrahedral silicon in the quartz structure (4).

Although several other color centers have been reported in quartz, none of these has been specifically related to a given impurity in the quartz (5). Frondel and Hurlbut (6) state that unit cell size increases with increasing substitution of aluminum for silicon in the structure and that smoky quartz has smaller cell dimensions than colorless, the content of trace elements of the two samples being about the same. This contradiction will be explained later. Wittels (7) has subjected α-quartz with lattice constants $a_0 = 4.903$ Å and $c_0 = 5.393$ Å to 6.6×10^{19} *nvt* of total integrated neutron flux. The lattice constants were expanded to $a_0 = 5.01 \pm 0.01$ Å and $c_0 = 5.41 \pm 0.02$ Å. The increase in lattice size thus was due within experimental error entirely to anisotropic expansion in the a direction. According to Wittels the most probable positions for dislocated atoms are the interstitial spaces which form long channels parallel to the c axis; and the stuffing of these voids would account for the expansion in the a direction.

Keith and Tuttle (8) have studied the effect of impurities on the inversion temperature of quartz and find that aluminum and lithium tend to be more soluble in the β phase and lower the inversion temperature while the results found for germanium are the opposite.

H. D. Keith (9) in a recent note on the variability of the quartz lattice suggests that impurity atoms or ions would have a larger effect in the plane normal to the optic axis than in the direction parallel to it due to the channels paralleling the latter direction. He suggests that impurities normally found in quartz whether interstitial or substitutional, tend to increase the lattice spacings as the radius of Si^{+4} ion is smaller than that of any other ion likely to replace it.

---

* Fellowship on Glass Science.

† Department of Research in Chemical Physics.

Sabatier and Wyart (10) on the contrary, find that the a_0 parameter is smaller in synthetic quartz to which sodium has been added. They state that the c_0 is unchanged and the transition temperature is raised. These findings conflict with those of the present paper.

Hammond and coworkers (11) have studied the form and width of diffraction lines of synthetic quartz containing controlled impurities. Their method is capable of an accuracy of two parts in 10^7. They find that the defects responsible for blackening smoky quartz (now known to be aluminum) move toward the negative electrode on heating quartz to 530° C. in the presence of a field of 3000 v. across a thickness of 6 mm. Reirradiation indicates that the impurity moves along the Z direction of the crystal. In the region cleared by the field the lattice spacing is decreased toward that associated with a nearly perfect crystal. They find the lattice spacing to expand with increasing concentration of impurities. Their results thus indicate that substitutional aluminum can be moved in quartz under the influence of an electric field.

EXPERIMENTAL

The samples were prepared for the *x*-ray powder diffraction work by grinding to 325 mesh and loading into 0.3 mm. internal diameter, thin-walled capillary tubes. A Buerger-type, Debye-Scherrer camera of 11.46 cm. diameter with 1.0 mm. pinholes was used to obtain the diffraction patterns. Twenty-four hour exposures to CuKα radiation (using a nickel filter only) were made at 25 ± 1° C. The positions of the diffraction lines used were read to the nearest 0.02 mm. using the film measuring device described by Klug and Alexander (12). The effective film circumference was then obtained from these line positions after the method of Straumanis. The cell dimensions were determined by the graphical method of successive approximations (13) using an initially assumed axial ratio (c/a) of 1.10004 (14) and the wide-angle extrapolation function of Taylor and Sinclair (15), viz.

$$f(\theta) = 1/2\left(\frac{\cos^2\theta}{\sin\theta} + \frac{\cos^2\theta}{\theta}\right).$$

Occasionally three extrapolations were required before consistency of the lattice constants was obtained. In general, however two extrapolations were found to be sufficient. The lattice constant determinations for each quartz sample were made with the following diffraction lines, the angular range of which extends from 59.1 to 79.3° θ: CuK$_{\alpha 1}$ lines ($\lambda = 1.53740$ kX or 1.54040 Å (16)) for *hkl* values of 126, 135, 240, 330, 206, 501, 116, 142, 106, and 125; and CuK$_{\alpha 2}$ lines ($\lambda = 1.54124$ kX or

TABLE 1. IMPURITY CONTENTS OF NATURAL AND SYNTHETIC QUARTZ AS DETERMINED BY EMISSION ANALYSES

Impurity	Brush Synthetic[1] %[7]	Bell Synthetic (R-31)[2] %[7]	Dinkey Lakes, Cal. Smoky[3] %[7]	Bell Synthetic (R-537)[2] %[7]	Bell Synthetic (R-27)[2] %[7]	Brazilian Amethyst[4] %[7]	"Greened" Amethyst[4] %[7]	Volcanic[5] %[7]	Rose[6] %[7]	Topaz[6] %[7]
Ag	0.0001	0.0001	N.F.	0.001	0.0001	0.0001	<0.0005	0.0001	0.0001	0.0001
Al	0.003	0.003	0.01	0.01	0.03	>0.01	0.005	>0.01	≫0.01	∼0.01
Bi	N.F.	N.F.	N.F.	0.001(?)	N.F.	N.F.	N.F.	N.F.	N.F.	N.F.
Ca	0.0003	∼0.001	0.003	∼0.001	∼0.001	0.003	>0.0005	∼0.01	0.003	0.003
Cr	0.0003	0.0003	0.0003	0.0003	0.001	N.F.	<0.002	0.003	N.F.	N.F.
Cu	0.001	0.001	0.01	0.003	0.003	>0.0001	<0.0005	∼0.0001	∼0.0001	<0.0001
Fe	0.003	∼0.001	0.001	∼0.001	0.01	∼0.01	>0.005	∼0.01	>0.01	>0.01
Ge	N.F.	0.01	N.F.	N.F.	0.1	N.F.	N.F.	N.F.	N.F.	N.F.
K	N.F.	N.F.	N.F.	N.F.	N.F.	N.S.	N.S.	N.S.	N.S.	N.S.
Li	0.0003	0.0001	0.0003	0.0003	0.01	N.S.	N.S.	N.S.	N.S.	N.S.
Mg	<0.001	<0.001	∼0.003	<0.001	<0.003	∼0.001	<0.0005	∼0.01	∼0.001	∼0.001
Mn	N.F.	N.F.	N.F.	N.F.	N.F.	N.F.	N.F.	N.F.	N.F.	N.F.
Na	0.003	0.003	0.003	0.003	0.003	N.S.	N.S.	N.S.	N.S.	N.S.
Ni	N.F.	N.F.	N.F.	N.F.	N.F.	N.F.	0.001	∼0.001	N.F.	N.F.
Pb	N.F.	N.F.	N.F.	0.003	N.F.	N.F.	<0.05	0.003	N.F.	N.F.
Rb	N.F.	N.F.	N.F.	0.03	N.F.	N.S.	N.S.	N.S.	N.S.	N.S.
Ti	N.F.	N.F.	N.F.	N.F.	N.F.	trace (?)	N.F.	0.003	0.003	trace (?)

[1] Specimen courtesy Signal Corps Engineering Laboratories, Fort Monmouth, New Jersey.

[2] Specimen courtesy Dr. G. T. Kohman, Bell Telephone Laboratories, Murray Hill, New Jersey.

[3] Specimen courtesy Dr. Ronald A. Henry, China Lake, California.

[4] Specimen courtesy Eldot and Company, New York 23, New York. Contains 0.001% Zr in addition to above.

[5] Specimen collected by senior author from pack rat's nest in rock shelter near Little Lake, California. Contains $\sim$0.001% Sn in addition to above.

[6] Specimen courtesy Inter-Ocean Trade Company, New York 36, New York.

[7] Absolute value believed to be between $\frac{1}{3}$ and 3 times the value indicated.

N.F. = not found.

N.S. = not sought.

1.54434 Å) for *hkl* values of 126, 241, 240, 331, 330, 206, 501, 116, 142 and 125. The forms of the Bragg equation used for the calculation of the hexagonal cell dimensions are

$$a_0 = \frac{\lambda}{2 \sin \theta}\sqrt{\frac{4}{3} S + (a/c)^2 l^2} \quad \text{and} \quad c_0 = \frac{\lambda}{2 \sin \theta}\sqrt{\frac{4}{3} (c/a)^2 S + l^2},$$

where $S = h^2 + hk + l^2$.

The samples were prepared for emission analysis by grinding in a boron carbide mortar used exclusively for grinding high purity silica samples.

RESULTS AND DISCUSSION

Table I lists the impurity contents of four specimens of synthetic quartz, a smoky quartz, an amethyst, an amethyst which remains green after heat bleaching (5), a quartz of volcanic origin, a rose quartz and a topaz colored quartz. Emission analyses for alkali content were made for only the first five of the listed specimens. Results presented in this table will be discussed in conjunction with the lattice constants determined for these materials.

Table II lists the lattice constants both in kX units and in angstrom units in order to make comparison with other work easier. The lattice constants of a colorless Herkimer, N. Y., quartz are reported for which no impurity content datum is available. This crystal was about a mm^3. in volume and there was not enough material available for emission

TABLE II. LATTICE CONSTANTS OF NATURAL AND SYNTHETIC QUARTZ AT 25±1° C.

Quartz	a_0(kX)[1]	c_0(kX)[1]	a_0 (Å)[2]	c_0 (Å)[2]	c/a[3]	d calc.
Brush Synthetic	4.9035[4]	5.3940[4]	4.9134	5.4049	1.10003	2.6489
Bell Synthetic (R-31)	4.9034	5.3942	4.9133	5.4051	1.10009	2.6489
Dinkey Lakes, Smoky	4.9033	5.3941	4.9132	5.4050	1.10011	2.6489
Bell Synthetic (R-537)	4.9033	5.3943	4.9132	5.4052	1.10014	2.6489
Bell Synthetic (R-27)	4.9040	5.3943	4.9139	5.4052	1.09997	2.6483
Amethyst, Brazil	4.9035	5.3938	4.9134	5.4047	1.09999	2.6489
Amethyst, "Greened"	4.9032	5.3938	4.9131	5.4047	1.10006	2.6493
Herkimer, Colorless	4.9035[4]	5.3941[4]	4.9134	5.4050	1.10005	2.6487
Volcanic	4.9039	5.3938	4.9138	5.4047	1.09990	2.6485
Rose	4.9042	5.3943	4.9141	5.4052	1.09993	2.6481
Topaz	4.9032[4]	5.3942[4]	4.9131	5.4051	1.10014	2.6491

[1] Error ±0.0002 kX.

[2] kX×1.00202 to give Å.

[3] Calculated from kX values.

[4] Average of measurements by two persons, each of which was within the experimental error.

analysis. This small crystal was discovered on the face of a larger crystal which turned smoky on continued *x*-ray treatment while the smaller crystal developed no visible coloration even after a dosage of many millions of röntgens. This suggests that no aluminum is present substitutionally, as no visible color center giving a resulting smoky color is present. Its measured cell dimensions $a_0 = 4.9035$ kX and $c_0 = 5.3941$ kX both ± 0.0002 kX match the measurements of Frondel and Hurlbut (6) for colorless Herkimer quartz within the experimental errors, their values being $a_0 = 4.9031$ and $c_0 = 5.3938$ kX both ± 0.0003 kX. Comparing these values to the other lattice constants in Table II, one may conclude that the Herkimer quartz contains interstitial impurity (based on expansion of *a* axis) and substitutional impurity other than aluminum (based on expansion of *c* axis). This statement will become clearer as the discussion continues. Keith (14), for example, has reported cell dimensions $a_0 = 4.90309$ kX and $c_0 = 5.39367$ kX (25°) for a Brazilian quartz which presumably has a low impurity content. He claims an accuracy of 1 part in 10^5 for this measurement.

Keith (14, 9) has pointed out that the axial ratio, c/a, decreases as the parameters increase. He states that the elastic anisotropy of quartz suggests that if impurities are present and cause a small *stress* in the lattice which is homogeneous, then this behavior of the axial ratio can be explained. He derives values for the "increment ratio"

$$\left(\frac{\Delta a}{a} \Big/ \frac{\Delta c}{c}\right)$$

for four specimens and finds a mean value of 1.39. This value is then compared to the ratio of adiabatic values of the strain components $S_{11}(1.269 \times 10^{-12})$ parallel to the optic axis and $S_{33}(0.971 \times 10^{-12})$ normal to the optic axis, which is 1.307. Keith then concludes that this agreement indicates that an impurity content in quartz produces a small stress in the lattice and consequent alterations in the parameters. Thus he states that the effect of impurities should be greater in the plane normal to the optic axis than in the plane of the optic axis. A comparison of the cell dimensions reported in the present work are made using Keith's "increment ratio." However, Keith's procedure for obtaining his "increment ratios" by exhaustive cross-comparison was was not employed since it is inappropriate for samples of our series containing interstitial impurities. Instead, the values of Keith's (9) Brazilian quartz are chosen for comparison purposes as being low in impurity content. Nevertheless, some impurity must be present in this sample since Frondel and Hurlbut (6) report $a_0 = 4.90299$ kX and $c_0 = 5.39353$ kX (± 0.0001 kX) for a smoky quartz. Table III gives calculations of the ratio

$$\left(\frac{\Delta a}{a}\Big/\frac{\Delta c}{c}\right)$$

using $a_0 = 4.90309$ kX and $c_0 = 5.39367$ kX (25° C.) as the standard for comparison. The data of this investigation is tabulated with the decrease in c/a ratio. It is seen that the "increment ratio" increases regularly as the c/a ratio decreases with only two exceptions, the Brazilian amethyst and the volcanic quartz. Figure 1 is a plot of c/a vs. the "increment ratio" for the data of Table III. The points for the work from this laboratory fall along a straight line except for the above two samples.

TABLE III

Specimen	"Increment Ratio" $\left(\frac{\Delta a}{a}\Big/\frac{\Delta c}{c}\right)$	c/a
Topaz Quartz	0.220	1.10014
Bell Synthetic (R-537)	0.367	1.10014
Dinkey Lakes (Smoky)	0.550	1.10011
Bell Synthetic (R-31)	0.660	1.10009
"Greened" Amethyst	1.100	1.10006
Herkimer, New York	1.100	1.10005
Brush Synthetic	1.467	1.10003
Brazilian Amethyst	4.400	1.09999
Bell Synthetic (R-27)	1.650	1.09997
Rose Quartz	2.017	1.09993
Volcanic Quartz	8.801	1.09990
Herkimer, New York[1]	0.110	1.10008
Carrara, Italy, Colorless[1]	0.667	1.10008
Synthetic (890°)[1]	1.015	1.10006
Smoky (101)[1]	0.785	1.10005
Rose (111)[1]	1.086	1.10004
Colorless (105)[1]	1.122	1.10004
Rose (102)[1]	1.358	1.10004
Synthetic 800° (Na WO_3 melt)[1]	1.466	1.10003
Synthetic 600° (Al+Li)[1]	1.344	1.10000

[1] Calculated from work of Frondel and Hurlbut, Reference 6.

The distribution of the impurities in the samples of Table III will now be discussed individually. The assignment of impurity to substitutional or interstitial sites will rest mainly on the argument that interstitial impurities should expand only the a directions markedly. Work now in progress in this laboratory is aimed at a more direct demonstration of this plausible assumption.*

---

* Cohen, A. J., Substitutional and Interstitial Aluminum Impurity in Quartz, Structure and Color Center Interrelationships: Symposium on the Defect Structure of Quartz and Glassy Silica, Mellon Institute, May 1957.

The deviation of two quartzes from the straight line in Fig. 1 is most likely due to the predominance of interstitial impurities over substitutional as shown by the greater relative increase in the *a* dimension. The fact that color centers characteristic of substitutional aluminum are not present in amethyst (5) is most likely due to the fact that the aluminum impurity in this quartz is mainly interstitial and not in the proper environment for color center formation.

The quartzes that have a large percentage of their aluminum in substitutional positions as evidenced by the fact that the color center at 460 mμ correlates with the aluminum content (3) are the four synthetic and the Dinkey Lakes Smoky. In the ones having Al content between 0.003 and 0.01 per cent by weight, the "increment ratio" varies from 0.367 to 1.467 and the *c*/*a* ratio between 1.10014 and 1.1003. The Bell Synthetic (R-27) with "increment ratio" of 1.650 and *c*/*a* of 1.09997 has an aluminum impurity content of 0.03 per cent and is higher in germanium and lithium impurity than Bell Synthetic (R-31). One concludes that both the substitutional and interstitial impurity contents of this specimen are high.

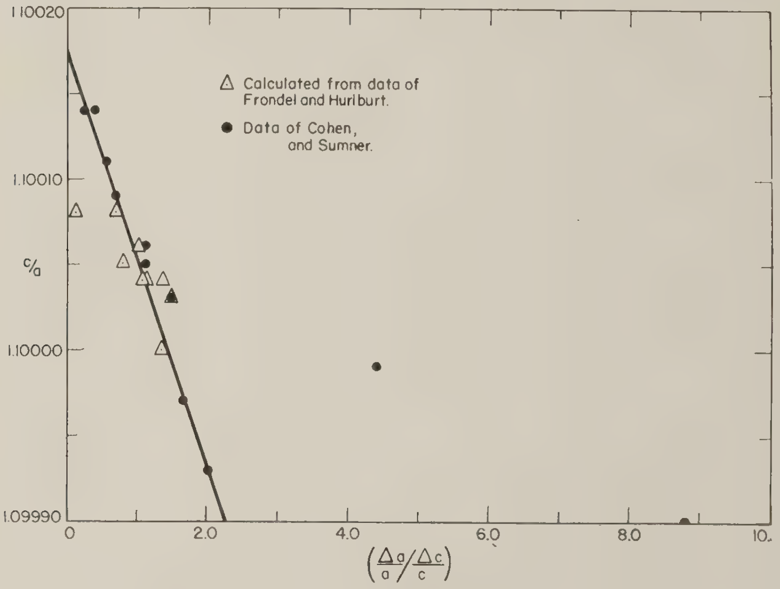

FIG. 1. Plot of "increment ratios" versus axial ratios of α-quartzes.

The rose quartz of this laboratory's series turns smoky upon *x*-irradiation so a portion of its aluminum content at least is substitutional. It contains rutile as a separate phase, as do all other rose quartz specimens that were examined under the microscope in this laboratory. The "increment ratio" of 2.017 and c/a of 1.09993 indicate the expansion in the a-direction, the a_0 being 4.9042 kX which in turn indicates a high content of interstitial impurities. On the other extreme is the topaz quartz from Rio Grande, Brazil with "increment ratio" of 0.220 and c/a of 1.10014; it has the lowest a_0 reported in this paper, 4.9032 kX, along with a c_0 of 4.3942 kX, rather on the high side. This would indicate that the impurity content, largely aluminum and iron, is present substitutionally.

The volcanic quartz with high impurity content and a c_0 on the low side seems definitely to have mainly interstitial impurities as mentioned earlier. The "greened" amethyst with $a_0 = 4.9032$ kX must be low in interstitial impurities compared to its substitutional impurity content. This specimen exhibits the laminar *d*-,*l*-twining associated with amethyst with a separate phase responsible for the green color. This separate phase probably accounts for some of the aluminum, iron and magnesium impurity present. The amethyst discussed earlier with the suggestion that the impurity content was largely interstitial did not exhibit as pronounced laminar twinning as found in the "greened" amethyst.

The calculations of "increment ratios" made on data of Frondel and Hurlbut indicate that their Herkimer quartz is higher in substitutional impurities as is the colorless quartz from Carrara, Italy. The Synthetic 800° ($NaWO_3$ melt), Synthetic 600° (Al+Li) and Rose (102) seem higher in interstitial impurities than the others. In using their lattice constants the same general trend continues with the "increment ratio" increasing with decreasing c/a. As shown in Fig. 1 the plot of "increment ratio" vs. c/a agrees well with data from this laboratory except for the Smoky (101). The cell dimensions of this quartz are smaller than those chosen for comparison purposes. The values given (6) are $a_0 = 4.90299$ and $c_0 = 5.39353$ kX both ± 0.0001 kX. It is on the basis of this result that Frondel and Hurlbut make the statement that smoky quartz has smaller unit cell dimensions than colorless quartz of the same impurity content. An explanation for this finding in view of results presented here is that most of the impurity content of this particular smoky quartz is substitutional. The aluminum must be thus, in order for a smoky color to be produced. The colorless varieties might contain more of their impurity content as interstitials which would cause a greater expansion of the a-axis than of the c-axis and possibly a greater expansion of the a-axis than caused by the same amount of the same substitutional impurity. To compare a smoky quartz to a colorless one properly, the quartz should be x-irradiated to determine whether a smoky color can be developed. Then a colorless region may be compared to a colored region such as actually exists in Y-bar synthetic quartz produced by the Clevite Research Center as shown by work of J. M. Jost (17). No investigation has been made of the effects of color center formation on lattice dimensions; this would presumably lend a smaller effect than that of the impurity content. Hammond *et al.* do mention a small but significant change in the width of the $(12\bar{3}1)$ reflection before and after heat bleaching of a smoky quartz (11).

The color center phenomena in the 320–1000 mμ region has been discussed earlier (3) in detail for the Brush Synthetic, the three Bell Synthetic and the Dinkey Lakes, California quartzes. They all exhibit two anisotropic color centers with maxima at 460 and about 625 mμ related to aluminum present in a substitutional position. These specimens exhibit a relationship between the amount of aluminum found by emission spectral analysis and the saturation absorption coefficient of the color centers that are dependent on substitutional aluminum impurity. Therefore in these synthetic quartzes grown from AT or BT cut seed plates and in the natural smoky quartz studied here the aluminum impurity is mainly substitutional. This may not be the case for all quartz. For example Arnold (18) and Jost (17) find that there is poor agreement in some instances. This is evidence for interstitial aluminum being present in these samples. Work in progress in this laboratory on synthetic quartz (Sample No. 515B) grown on a Z cut seed at General Electric Co. Ltd. (Wembley, England) shows 130 *p.p.m.* of aluminum present although no color centers were developed in the visible region even after $3.8 \times 10^8 r$ of *x*-ray dosage (in air at surface of sample). This indicates that aluminum can occupy an interstitial position as well as a substitutional position in the quartz structure.

The color centers in the "greened" amethyst have been discussed earlier (5).

CONCLUSIONS

By comparing "increment ratio," axial ratio, lattice constants, impurity analysis and color center formation, one may generalize concerning the impurity positions in the quartz structure. Cationic impurities in quartz may be substitutional replacing Si^{+4}, or interstitial. In order to preserve electroneutrality *e.g.* one interstitial Li^{+} per substitutional Al^{+3}, or one interstitial Al^{+3} per three substitutional Al^{+3} ions could be present provided balance is not achieved through oxygen vacancies. In addition quartz containing only interstitial aluminum, as is the case with the G. E. synthetic quartz mentioned, has its interstitial Al^{+3} accompanied by an equivalent amount of interstitial Li^{+} (emission analysis gives 290 Al and 260 Li per 10^6 Si atoms). Another source of impurity that confuses chemical and emission analyses of quartz is that present as a separate microscopic phase as in rose quartz or as a submicroscopic phase as in the laminar twined variety of quartz.

Since interstitial impurities mainly cause expansion of the *a* axis and substitutional impurities cause expansion of both axes, the following generalizations may be used to gain information concerning impurities present where "increment ratio" and axial ratio correlate (as for seventeen of twenty cases in Fig. 1):

(1) a low "increment ratio" ($\sim$1.5 or less) indicates the α-quartz contains mainly substitutional impurities and these impurities have radii larger than Si^{+4}.

(2) an intermediate "increment ratio" ($\sim$1.4–1.7) indicates both substitutional and interstitial impurities are present.

(3) a high "increment ratio" ($>$1.7) or lack of correlation between this and axial ratio indicates that a high percentage of the impurity is interstitial.

ACKNOWLEDGMENTS

The writers wish to thank Dr. L. E. Alexander for making duplicate calculations on three sets of lattice constants. Dr. E. S. Hodge and Mrs. B. S. Milan performed the emission analyses.

Acknowledgments of the gifts of quartz specimens used in this work are made in the footnotes of Table I.

The senior author would like to thank Dr. D. R. Hale (and associates) at the Clevite Research Center, Cleveland, Ohio for discussions and correspondence concerning the synthetic quartz grown under his direction. He would like to thank Dr. G. T. Kohman and associates at the Bell Telephone Laboratories, Murray Hill, New Jersey for discussions concerning synthetic quartz grown in their laboratories. He is grateful to Dr. T. H. Davies for discussions during the progress of this work.

REFERENCES

1. GRIFFITHS, J. H. E., OWEN, J., AND WARD, I. M., Magnetic Resonance in Irradiated Diamond and Quartz: "Defects in Crystalline Solids—Report of 1954 Bristol Conference," Physical Society, London, 81–87.
2. MITCHELL, E. W. J., AND PAIGE, E. G. S., The Anisotropic Absorption of the Visible Bands in Irradiated α-Quartz: *Phil. Mag.* **46,** 1353–1361 (1955).
3. COHEN, A. J., Anisotropic Color Centers in α-Quartz. Part I. Smoky Quartz.: *J. Chem. Phys.* **25,** 908–914 (1956).
4. O'BRIEN, M. C. M., The Structure of the Colour Centres in Smoky Quartz: *Proc. Royal Soc.* (*London*), **231A,** 404–441 (1955).
5. COHEN, A. J. Color Centers in the α-Quartz Called Amethyst: *Am. Mineral.* **41,** 874 (1956).
6. FRONDEL, C. AND HURLBUT, JR., C. S., Investigation into Effects of Radiation on the

Physical Properties of Quartz: PB 111628, U. S. Dept. of Commerce, Office of Technical Services (Released in 1955).

7. Wittels, M., Lattice Expansion of Quartz Due to Fast-Neutron Bombardment: *Phys. Rev.* **89,** 656–657 (1953).
8. Keith, M. L., and Tuttle, O. F., Significance of Variation in the High-Low Inversion of Quartz: *Am. Jour. Sci.*, Bowen Volume, Part 1, 203–252 (1952).
9. Keith, H. D., Lattice Spacings in Clear Crystalline Quartz and Their Variability: *Am. Mineral.* **40,** 530–534 (1955).
10. Sabatier, G. and Wyart, J., Variations of the Cell Parameters and Crystallization Temperatures in the $\alpha \leftrightarrows \beta$ Transformation of Synthetic Quartz: *Comp. rend.* **239,** 1053–1055 (1954).
11. Hammond, D. L., Chi, A. R., and Stanley, J. M., Effects of Impurities on the Resonator and Lattice Properties of Quartz: Engineering Report E-1162, Signal Corps Engineering Laboratories, 3 November, 1955, pp. 1–8.
12. Klug, H. P. and Alexander, L. E., "X-Ray Diffraction Procedures," J. Wiley and Sons, New York, 1954.
13. Lipson, H., and Wilson, A. J. C., The Derivation of Lattice Spacings from Debye-Scherrer Photographs: *J. Sci. Instruments* **18,** 144–148 (1941).
14. Keith, H. D., The Lattice Parameters of Clear Crystalline Quartz: *Proc. Phys. Soc. (London)* **63*B*,** 208–214 (1950).
15. Taylor, A. and Sinclair, H., The Determination of Lattice Parameters by the Debye-Scherrer Method: *Proc. Phys. Soc.* (*London*) **57,** 126–135 (1945).
16. Bragg, W. L., The Conversion Factor for kX Units to Angström Units: *J. Sci. Instruments* **24,** 27 (1947).
17. Jost, J. M., Studies of optimum methods for quartz synthesis. Contract DA-36-939SC64589, U. S. Army Signal Corps Project 142B, 1 March 1955–29 February 1956.
18. Arnold, Jr., G. W., Defects in quartz crystals: Proc. 10th Annual Symposium on Frequency Control, Asbury Park, N.J. (May 1956) 60–74.

Manuscript received May 6, 1957.

THE AMERICAN MINERALOGIST, VOL. 43, JANUARY-FEBRUARY 1958

THE SYSTEM $Fe_3O_4-Mn_3O_4$*

H. J. VAN HOOK AND M. L. KEITH, *Pennsylvania State University, University Park, Pennsylvania.*

ABSTRACT

Investigation of the system $Fe_3O_4-Mn_3O_4$ was carried out on mixtures prepared in evacuated silica glass tubes to ensure the desired stoichiometric proportions. Runs at liquidus temperatures were made on prepared charges sealed in platinum tubes so as to avoid compositional change resulting from reaction with the furnace atmosphere. Subsolidus relationships were determined mainly by *x*-ray diffraction studies of mixtures which had been heated to temperatures between 400° and 1100° C. under conditions which permitted the synthesis and stable coexistence of the cubic and tetragonal phases.

The liquidus exhibits a minimum at 67% Mn_3O_4 and 1543° C. Complete solid solution exists between Fe_3O_4 and Mn_3O_4 above the temperature of the tetragonal to cubic inversion of Mn_3O_4, that is above about 1160° C. Below that temperature there is an immiscibility gap which increases in width at lower temperatures and is consistent with the compositions of the hausmannite and manganiferous magnetite found together in natural intergrowths. Inconsistencies of the interpretations of previous investigators for the intermediate-temperature portion of the diagram are attributed to their failure to allow for the extreme sluggishness of unmixing of the cubic and tetragonal phases.

INTRODUCTION

One of the common oxide structures encountered in minerals and synthetic materials formed at higher temperatures is the spinel structure, which permits substitution of many metallic elements within wide limits. The most abundant natural spinels can be grouped in the magnetite series. Phase equilibria in systems involving Fe_3O_4 and oxides found in natural association with magnetite are important to petrology, to studies of the conditions of formation of iron ores, and to research on steel making processes.

In recent years the study of spinel oxides has received additional impetus from interest in the unusual magnetic properties which certain of these compounds possess. Manganese-iron spinels are particularly interesting in this respect (Economos, 1955: Romeijn, 1953) and have important technical application as ferromagnetic components in electronic devices.

Previous experimental studies of the system $Fe_3O_4-Mn_3O_4$ using materials prepared at high temperatures gave inconsistent interpretations concerning the extent of the region of solid immiscibility (Mason, 1943; McMurdie *et al.*, 1950). In the present study the extent of immiscibility was determined by preparing and quenching oxide compositions at temperatures within the two-phase region.

---

* Contribution No. 56-71 From the College of Mineral Industries, The Pennsylvania State University.

Stability and Structure of $Fe_3O_4-Mn_3O_4$

Fe_3O_4 is stable in air above 1388° C. (Greig *et al.*, 1935); below that temperature α-Fe_2O_3 is the stable form. A cation deficient oxide, γ-Fe_2O_3, having the same structure as Fe_3O_4 can be prepared by various methods (Verwey, 1935).

Verwey and Heilmann (1947) concluded on the basis of a careful *x*-ray diffraction study that Fe_3O_4 is probably an inverse spinel. More recent neutron diffraction studies of Shull *et al.*, (1951) confirm that observation. The structural formula is given as $Fe^{+3}[Fe^{+3}Fe^{+2}]O_4$.

Mn_3O_4 is the stable oxide of manganese in air above about 940° C. (Sidgwick, 1950; Mason, 1943). The structure was first determined by Aminoff (1926); although tetragonal at room temperature, the structure is similar to that of the spinels and may be described as a distorted spinel structure. Cation valencies and distribution have been discussed by Mason (1943), von Eckermann (1943), Verwey (1947), Aminoff (1926), and Montoro (1938). Two possible cation combinations for Mn_3O_4 are: $Mn^{+2}[Mn^{+2}Mn^{+4}]O_4$ and $Mn^{+2}[Mn_2{}^{+3}]O_4$. Mn_3O_4 occurs in nature as the mineral hausmannite. It is not common but in some places occurs in considerable amounts: at Långban, Sweden, it is an important ore of manganese.

The oxide Mn_2O_3 has two established polymorphic forms. The stable form $\alpha-Mn_2O_3$ has a "C" type cubic structure. It occurs naturally as the mineral bixbyite, generally containing considerable iron in solid solution (Mason, 1943). A cation deficient form, $\gamma-Mn_2O_3$ having the same structure as Mn_3O_4 has been reported (Verwey, 1935). Extensive solid solution between Mn_3O_4 and $\gamma-Mn_2O_3$ seems probable, analogous to that reported to take place between Fe_3O_4 and $\gamma-Fe_2O_3$ (Greig *et al.*, 1935).

Previous Experimental Work

An *x*-ray study of synthetic manganese-iron spinels was made by Verwey and von Bruggen (1935). Mixtures of MnO and Fe_2O_3 in equal mole proportions heated in air at 1250° C. were found to have absorbed an amount of oxygen exactly equal to conversion of MnO to Mn_3O_4. The oxide formed was believed to have the composition $Mn_3O_4 \cdot 3Fe_2O_3$ and a spinel-type structure related to $\gamma-Fe_2O_3$. Other mixtures were cooled rapidly from temperatures between 900° and 1300°, a temperature interval considered to be one in which Mn_3O_4 is the stable oxide of manganese (in air) and Fe_2O_3 is the stable oxide of iron. It was apparently assumed that solid solution has no effect on the respective stability ranges of these oxides. The several compositions prepared in this manner were found to exhibit a continuous transition from cubic to tetragonal symmetry. A sample containing 60 mol % Mn_3O_4 and 40 mol % Fe_2O_3 was found to be cubic, whereas a sample with 67 mol % Mn_3O_4 was tetragonal ($c/a=1.05$). Increasing relative amounts of manganese increased the tetragonal character to a maximum axial ratio of $c/a=1.16$ for the end member, Mn_3O_4.

Verwey and von Bruggen described the system as showing solid solution of Mn_3O_4 in $\gamma-Fe_2O_3$. The observed cell dimensions agree very closely, however, with those of more recent workers who considered their preparations as a solid solution series $Fe_3O_4-Mn_3O_4$. In Fig. 1 a graphical comparison of cell variation with composition demonstrates this similarity. Since $\gamma-Mn_2O_3$, which is cation deficient, is an established form of manganese oxide, the assignment of cation deficiency to the Fe component in homogeneous Fe, Mn spinels is artificial, although possible.

Montoro (1938) prepared oxide mixtures in the system $Fe_3O_4-Mn_3O_4$ by co-precipitating manganese and iron hydroxide from solutions of the sulfates. The hydroxides were sintered in air at 1200° C. and quenched. Montoro reported that samples prepared in this manner are cubic up to 67% Mn_3O_4* and tetragonal for higher percentages. He related the change from cubic to tetragonal structure to the formation of a supposed compound $FeO \cdot Mn_2O_3$.

A major contribution to understanding the system $Fe_3O_4-Mn_3O_4$ was made by Brian Mason (1943). Mason had access to specimens of relatively pure $(Mn,Fe)_3O_4$ minerals from the ore districts of central Sweden. Microscopic and x-ray examination revealed the existence of vredenbergite, an intergrowth of Mn-rich magnetite and hausmannite.

In order to determine the compositional limits of the phases in vredenbergites Mason prepared a series of oxide compositions from co-precipitated hydroxides sintered at temperatures ranging from 1100° to 1300°C. Again a continuous variation of cell parameters was observed after quenching. Mason concluded: "Fe_3O_4 and Mn_3O_4 are completely miscible at high temperatures in spite of the difference in symmetry between them. The cubic lattice of Fe_3O_4 changes to a tetragonal lattice at about 60 mol. % Mn_3O_4." He compared the cell dimensions of the synthetic preparations with those of natural vredenbergites and fixed the compositional limits of the two-phase region at low temperatures at 54% and 91% Mn_3O_4.

Mason heated several of his sintered oxide samples in evacuated silica glass tubes at lower temperatures to induce exsolution; the results were generally negative except for a sample with 80% Mn_3O_4 which exsolved into two tetragonal phases at 750° C. but remained unchanged at 900° C.

---

* % Mn_3O_4 indicates calculated mol.% Mn_3O_4. The difference from 100% equals mol.% Fe_3O_4.

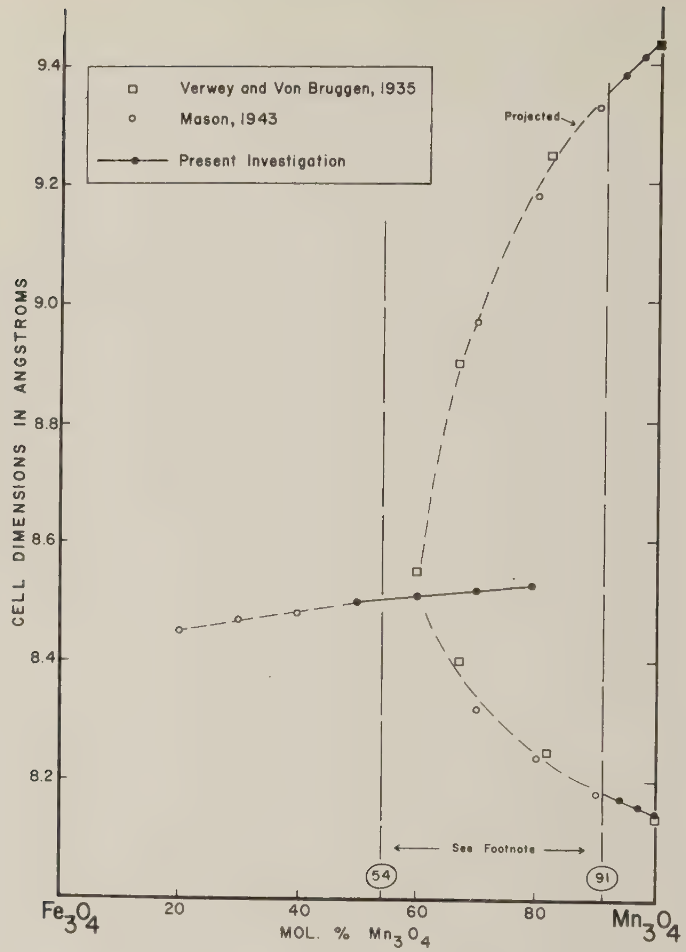

FIG. 1. Variation of cell dimensions with composition.

NOTE: No single crystalline (Fe, Mn)$_3$O$_4$ phase with from 54% to 91% Mn$_3$O$_4$ is stable at room temperature. Cubic solid solutions in that compositional range were obtained only by quenching from higher temperature and are metastable at room temperature. Tetragonal solid solutions which can be prepared in air, probably have a lower cation: oxygen ratio than R$_3$O$_4$ and are to be compared with the R$_3$O$_4$-R$_2$O$_3$ solid solutions of Verwey and Van Bruggen (1935), whose data are projected (open squares) onto the R$_3$O$_4$ plane of Figure 1.

On the basis of this "admittedly meager evidence" for a subsolidus maximum, Mason proposed a tentative phase diagram which is reproduced in Fig. 2, (dashed line).

In 1948 McMurdie and Golovato reported that Mn_3O_4 undergoes a reversible tetragonal to cubic transition at 1170° C. However, they record

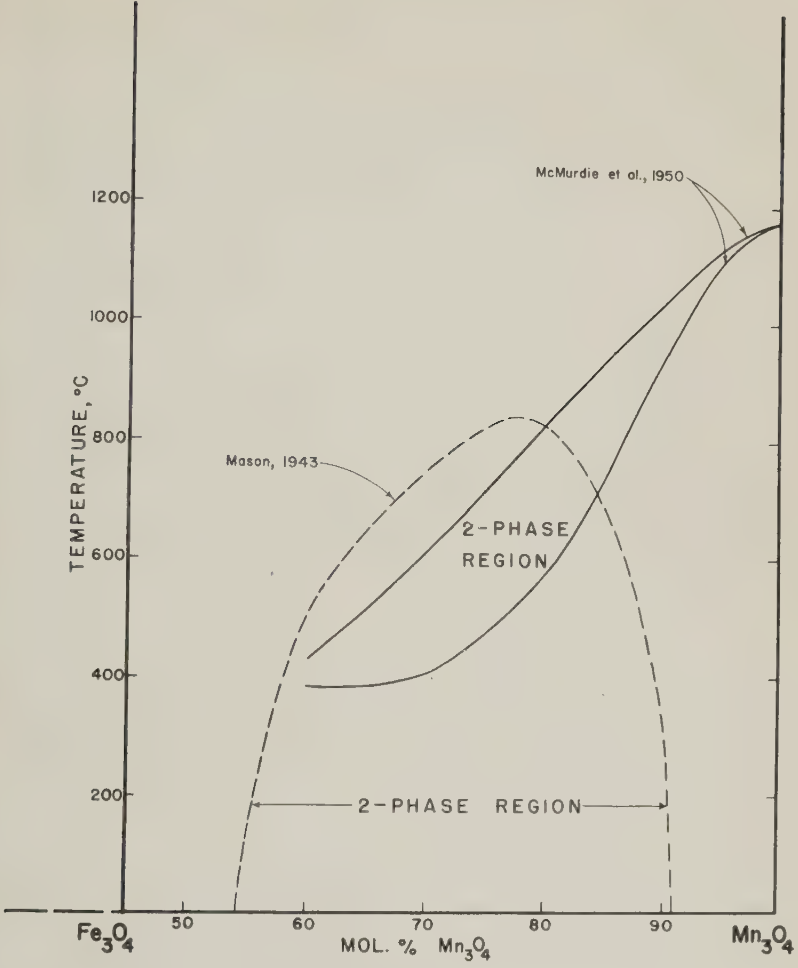

FIG. 2. Previous interpretations of the system $Fe_3O_4-Mn_3O_4$.

(op. cit. p. 597) that on cooling, " . . . an exothermic break took place near 1100° C. with samples of high purity." The transition previously had been estimated from heat content data as 1172° ± 40° C. (Southard and Moore, 1942).

Further high temperature *x*-ray studies were conducted (McMurdie et al., 1950) on the system $Fe_3O_4-Mn_3O_4$. The hydroxides were prepared and sintered by the same methods employed by Mason. A continuous change in symmetry was again observed, the lattice dimensions showing agreement with Mason's results (Fig. 1). X-ray patterns were then recorded at elevated temperatures. It was observed that some compositions showed cubic and tetragonal phases occurring together over a range in temperature. The partial phase diagram of the system according to McMurdie et al. (1950) is reproduced in solid lines in Fig. 2.

The conclusion of McMurdie *et al* that there is no region of immiscibility at low temperatures (below 380° C.) is inconsistent with coexistence (at any temperature) of phases of the compositional limits found in vredenbergites, namely 54% to 91% Mn_3O_4 (Mason, 1943).

EXPERIMENTAL PROCEDURE

SUB-SOLIDUS INVESTIGATION

High Temperature Preparations

In the preliminary investigation MnO_2 and Fe_2O_3 were mixed together and fired in covered platinum crucibles for 2-hour periods in a gas furnace at 1400° C. The crucibles were then removed from the furnace and cooled in air. This treatment yielded homogeneous spinel phases for all compositions from Fe_3O_4 to about 80% Mn_3O_4. *X*-ray diffraction studies showed both tetragonal and cubic reflections in the 90% Mn_3O_4 sample, tetragonal reflections alone in the 100% Mn_3O_4 sample.

The preparation procedure adopted by Mason was repeated with results identical to his. Mixtures co-precipitated as hydroxides and subsequently sintered in air at 1250° C. produced materials which are cubic if the Mn_3O_4 content is less than 60%, tetragonal if the Mn_3O_4 content is higher. All mixtures prepared by this method gave poor *x*-ray patterns, progressively poorer with increasing iron content.

The high temperature preparations described above showed no tendency to exsolve into separate phases Fired oxide and hydroxide preparations remained unaffected after heating in evacuated silica tubes for one month at 750° C. It was therefore evident that in order to confirm or disprove a low temperature two-phase region, an attempt should be made to form the R_3O_4 phase or phases at low temperatures.

Preparations in Vacuo and in Controlled Atmosphere

Manganese dioxide and powdered manganese and iron metals were used as starting materials for preparing $(Fe,Mn)_3O_4$ compositions within the range 67% to 100% Mn_3O_4. This mixture proved particularly suitable for synthesis in evacuated silica glass tubes. MnO_2 decomposes below 500° C. in the presence of the metals and they readily take up the available oxygen. In runs made as low as 500° C., $(Mn,Fe)_3O_4$ phases could be prepared with no other recognizable phases present. At 400° C. some $(Mn,Fe)_2O_3$ reflections were encountered. For compositions with less than 67% Mn_3O_4, Fe_2O_3 was used, of necessity, as one of the component oxides. It is less desirable than MnO_2 as a starting material because it has a higher temperature of decomposition.

An inherent uncertainty in this procedure is in the difficulty of preparing a homogeneous sample. The starting materials were weighed in amounts totaling one gram, then thoroughly mixed and ground together. An aliquot of approximately one-tenth of the total sample was used for each run. The error introduced by any inhomogeneity was apparently small since samples of different compositions heated at the same temperature produced consistent results.

A few runs were made in a controlled-atmosphere furnace. Experimental thermodynamic data delimiting the stability fields of Mn_3O_4 (Ishihara and Kigoshi, 1953) and of Fe_3O_4 (Darken and Gurry, 1945) indicate that any ratio of CO_2/CO from 10 to 10^4 should be in equilibrium with those oxides at the temperatures used. The optimum gas ratio of CO_2/CO for preparing oxides in the desired temperature-composition range was found empirically to be 300/1. This gas ratio was attained by mixing the gases at low pressures in a tank. The gas mixture was passed slowly through a vertical tube furnace designed for controlled atmosphere experiments.

Determination of Two-Phase Region

With the exception of confirmatory runs at 800° C., 900° C., and 1000° C. in a controlled atmosphere, all subsolidus data are based on runs made in evacuated silica glass tubes. The determination of the existing phases and their respective cell dimensions was made after quenching to room temperature. The boundary curves limiting the two-phase region were determined by two methods.

1) The compositions of co-existing cubic and tetragonal phases were determined from their cell dimensions by using extrapolated curves giving cell variation versus composition.
2) Each boundary curve was bracketed by runs made at different compositions and temperatures. This method was used in particular to check the boundary between the two-phase area and the cubic-phase area because the variation of the cubic parameter with composition is small.

Determination of Mn_3O_4 Inversion

Mn_3O_4 previously prepared from MnO_2 was packed in a platinum sample holder and mounted within a heating unit* in air on a G. E. -XRD 3 geiger counter spectrometer. A Pt vs 10% Rh Pt reading couple and Pt Rh vs. Au Pd control couple were used. *X*-ray diffraction patterns were taken at room temperature and at successive temperature intervals up to 1270° C. In each case, the *x*-ray pattern was taken after the temperature had reached a steady state. The *x*-ray furnace thermocouple was calibrated with barite from Stoneham, Colorado, heating inversion 1180° C. (Gruver, 1951).

---

* Heating unit designed by H. McKinstry, Pennsylvania State University.

The Mn_3O_4 inversion was also investigated by differential thermal analysis, using a heating rate of 2° to 3° per minute and a cooling rate of about 1.5° per minute. D.T.A. runs were made on initially stoichiometric Mn_3O_4 in air and in evacuated silica glass. The temperature standard used was $Na_2O \cdot 3\ TiO_2$, melting point 1128° C. (Shafer and Roy 1956). The inversion on cooling could not be determined using the sodium titanate standard due to an overlap of its freezing-point thermal effect with that due to the Mn_3O_4 inversion. Therefore granular alumina was subsituted for sodium titanate for the cooling run.

Liquidus Investigation:

Charges for investigation of equilibria at liquidus temperatures were prepared from metal plus oxide mixtures heated in platinum foil envelopes in evacuated silica glass tubes for four days at 650° C., then 17 hours at 950° C. Sintered charges prepared in this manner at 10 mol% intervals were ground, and portions of each were packed in platinum tubes which were then sealed by welding. The sealed charges were heated for 10 hours or longer, in a vertical tube furnace and then quenched in mercury. Quenched charges were polished and examined microscopically under reflected light for the presence of primary crystals, well-formed octahedra easily distinguished from the fine-grained mass representing quenched liquid. Temperatures were measured with a Pt vs. 10% Rh Pt thermocouple calibrated at the melting point of pseudowollastonite, $CaSiO_3$ (1544°).

Controlled atmosphere runs and runs at liquidus temperatures were quenched by dropping the envelopes or tubes directly into a mercury container connected to the bottom of the vertical tube furnace.

Experimental Results

Tables 1, 2 and 3 below summarize the critical runs and experimental data and the results are shown in diagrammatic form in Figure 3.

Sub-Solidus Equilibria

The inversion of Mn_3O_4 from the tetragonal hausmannite form to a cubic high-temperature form with spinel structure was confirmed; we propose that the cubic form be called high hausmannite and the tetragonal form, low hausmannite.

Determination of the inversion temperature of Mn_3O_4 was found to be complicated by the fact that *H*, (the beginning of inversion on heating) is at a higher temperature than *C*, (the beginning of inversion on cooling). The inversion has been described as a readily reversible inversion at 1170° C., (McMurdie and Golovato 1948). However our results lead us to suspect that the "exothermic break" which they obtained at a temperature near 1100° C. on cooling, probably is due to the inversion on cooling.

TABLE 1. LATTICE DIMENSIONS OF Mn_3O_4 IN AIR

	Temp., °C.	a_0	c_0
Tetragonal Form	20	8.136 Å	9.422 Å
	250	8.14	9.45
	450	8.15	9.47
	625	8.16	9.49
	800	8.175	9.50
	1000	8.20	9.49
	1160	8.22	9.46
	1162—(first cubic reflections on heating)		
Cubic Form	1270	8.57	
	1220	8.56	
	1144—(first tetragonal reflections on cooling)		
	1140	8.54	

Our results by two different methods are summarized below and compared with the data of McMurdie and Golovato.

Inversion Break, Degrees C.			*Method*
Heating	*Cooling*	*H−C*	
1170	(1100±)	(70±)	D.T.A. in air at 8°/min. (McMurdie and Golovato)
1167	1130	37	D.T.A. in air at 2°/min.
1162	1144	18	*x*-ray diffraction and slow step-wise heating in air.

It is apparent that the Mn_3O_4 inversion can be inhibited or delayed and that the measured inversion break is a function of the rate of heating or cooling. If *H-C* is plotted against *H* and separately against *C*, extrapolation yields a temperature of about 1160° C. at *H-C* = zero. We propose to use 1160° C. as an estimate of the equilibrium inversion temperature of Mn_3O_4 in air.

Differential thermal analysis at about 2° per minute, of a sample of Mn_3O_4 contained in an evacuated silica glass tube* showed at 26° hys-

---

* The calculated amount of oxygen in the silica glass tube at 1160° is less than 1 part per million of the oxygen in the sample.

TABLE 2. CRITICAL SUBSOLIDUS RUNS

Mn:Fe Ratio	Starting Materials	Time	Temp. °C.	Atmos-phere	Product, and Cell Dimensions		
100:0	MnO_2	2 hrs.	1400	gas furn.	Mn_3O_4, tetragonal		
90:10	$MnO_2+Fe_2O_3$	2 hrs.	1400	gas furn.	Essentially cubic (some splitting of cubic reflections)		
80:20	$MnO_2+Fe_2O_3$	2 hrs.	1400	gas furn.	Cubic		
				Ratio CO_2/CO	Cubic a_0	Tetragonal a_0	c_0
90:10	$MnO_2+Mn^0+Fe^0$	48 hrs.	1000	300	8.525	8.17	9.39
80:20	$MnO_2+Mn^0+Fe^0$	48 hrs.	1000	300	8.53	8.17	9.40
70:30	$MnO_2+Mn^0+Fe^0$	48 hrs.	1000	300	8.52	8.16	9.40
90:10	$MnO_2+Mn^0+Fe^0$	54 hrs.	900	300	8.52	8.17	9.38
80:20	$MnO_2+Mn^0+Fe^0$	54 hrs.	900	300	8.52	8.17	9.38
70:30	$MnO_2+Mn^0+Fe^0$	72 hrs.	900	300	8.52	8.17	9.38
60:40	$MnO_2+Mn^0+Fe^0$ $+Fe_2O_3$	72 hrs.	900	300	*8.51**		
94:6	$MnO_2+Mn^0+Fe^0$	48 hrs.	800	300		*8.17*	*9.38*
90:10	$MnO_2+Mn^0+Fe^0$	48 hrs.	800	300	8.51	8.17	9.38
70:30	$MnO_2+Mn^0+Fe^0$	55 hrs.	800	300	8.515	8.17	9.38
60:40	$MnO_2+Mn^0+Fe^0$ $+Fe_2O_3$	55 hrs.	800	300	*8.51*		
90:10	$MnO_2+Mn^0+Fe^0$	24 hrs.	1100	in vacuo	8.535	8.16	9.40
80:20	$MnO_2+Mn^0+Fe^0$	24 hrs.	1100	in vacuo	*8.53*		
100:0	$MnO_2+Mn^0+Fe^0$	40 hrs.	1000	in vacuo		*8.15*	*9.43*
97:3	$MnO_2+Mn^0+Fe^0$	40 hrs.	1000	in vacuo		*8.16*	*9.41*
94:6	$MnO_2+Mn^0+Fe^0$	40 hrs.	1000	in vacuo		*8.17*	*9.38*
70:30	$MnO_2+Mn^0+Fe^0$	45 hrs.	950	in vacuo	*8.52*		
90:10	$MnO_2+Mn^0+Fe^0$	36 hrs.	900	in vacuo	8.52	8.17	9.39
80:20	$MnO_2+Mn^0+Fe^0$	36 hrs.	900	in vacuo	8.52	8.17	9.40
70:30	$MnO_2+Mn^0+Fe^0$	36 hrs.	900	in vacuo	8.52	8.17	9.39
90:10	$MnO_2+Mn^0+Fe^0$	1 week	730	in vacuo	8.51	8.17	9.38
80:20	$MnO_2+Mn^0+Fe^0$	1 week	730	in vacuo	8.51	8.16	9.38
60:40†	$MnO_2+Mn^0+Fe^0$	1 week	730	in vacuo	*8.51*		
90:10	$MnO_2+Mn^0+Fe^0$	17 days	664	in vacuo	8.51	8.17	9.36
80:20	$MnO_2+Mn^0+Fe^0$	17 days	664	in vacuo	8.51	8.17	9.37
70:30	$MnO_2+Mn^0+Fe^0$	17 days	664	in vacuo	8.515	8.17	9.37
100:0	$MnO_2+Mn^0+Fe^0$	30 days	610	in vacuo		*8.16*	*9.43*
97:3	$MnO_2+Mn^0+Fe^0$	30 days	610	in vacuo		*8.16*	*9.41*
94:6	$MnO_2+Mn^0+Fe^0$	30 days	610	in vacuo		*8.17*	*9.39*
90:10	$MnO_2+Mn^0+Fe^0$	32 days	600	in vacuo	8.51	8.17	9.36
80:20	$MnO_2+Mn^0+Fe^0$	32 days	600	in vacuo	8.51	8.18	9.36
60:40†	$MnO_2+Mn^0+Fe^0$	32 days	600	in vacuo	8.51	8.17	9.37
94:6	$MnO_2+Mn^0+Fe^0$	25 days	600	in vacuo		*8.17*	*9.39*
90:10	$MnO_2+Mn^0+Fe^0$	60 days	500	in vacuo	8.51	8.17	9.36
80:20	$MnO_2+Mn^0+Fe^0$	60 days	500	in vacuo	8.51	8.18	9.36
60:40	$MnO_2+Mn^0+Fe^0$	60 days	500	in vacuo	*8.51*		
90:10	$MnO_2+Mn^0+Fe^0$	85 days	400	in vacuo	8.5	8.18	9.35
80:20	$MnO_2+Mn^0+Fe^0$	85 days	400	in vacuo	cubic+tetragonal‡		
70:30	$MnO_2+Mn^0+Fe^0$	85 days	400	in vacuo	cubic+tetragonal‡		

* Italicized figures indicate cubic only or tetragonal only.

† Plus Fe_2O_3.

‡ Some R_2O_3 present.

TABLE 3. HIGH TEMPERATURE RUNS IN Pt TUBES

Mn:Fe Ratio	Time	Temp.	Product
50:50	10 hrs.	1556	crystals & liquid*
60:40	10 hrs.	1556	all liquid*
50:50	19.5 hrs.	1561	liquid>crystals
80:20	19.5 hrs.	1561	all liquid
50:50	14 hrs.	1566	all liquid*
90:10	14 hrs.	1566	all liquid*
100:0	14 hrs.	1566	all liquid*
60:40	10 hrs.	1545	crystals (80%+) & liquid
80:20	10 hrs.	1545	crystals (90%+) & liquid
60:40	16 hrs.	1550	crystals & liquid
70:30	16 hrs.	1550	all liquid
70:30	12 hrs.	1544	liquid>crystals
90:10	12 hrs.	1560	liquid>crystals
90:10	15 hrs.	1562	all liquid
100:0	15 hrs.	1562	liquid plus very rare crystals

* Sample tubes quenched in air (quench less rapid than mercury quench).

teresis between the thermal break on heating and on cooling, i.e., appreciably less than the 37° hysteresis indicated by D.T.A. in air at the same rate of heating and cooling. This suggests that part of the retardation, (superheating or undercooling) of the inversion in air may be due to an accompanying compositional change which requires diffusion of oxygen into or from the sample.

The low hausmannite structure tolerates a maximum of about 9 mole % of Fe_3O_4 in solid solution at room temperature (Mason, 1948); this decreases to 8% at 400° C., and continues to decrease with rising temperature, to zero Fe_3O_4 at 1160° C., the inversion temperature of Mn_3O_4 (See Fig. 3).

On the other hand, the magnetite-high hausmannite solid solution series contains a maximum of 54% Mn_3O_4, at low temperatures and the maximum amount of Mn_3O_4 increases progessively with increasing temperature, to 100% Mn_3O_4 at 1160° C. (See Fig. 3). There are no binary compounds, and intermediate members of the series can simply be described by giving the molecular percentage of Mn_3O_4.

Single-phase tetragonal products with Mn:Fe ratio in the range of the 2-phase region can be prepared by heating in air; the compositions of such preparations apparently are off the join $Fe_3O_4-Mn_3O_4$ in the direction of excess oxygen. The basis of this conclusion is the experimental evidence that stoichiometric metal+oxide mixtures in the range from Mn:Fe approximately 60:40 to 90:10 yield cubic phases upon heating to 1200° C. in evacuated silica glass tubes or in the slightly reducing

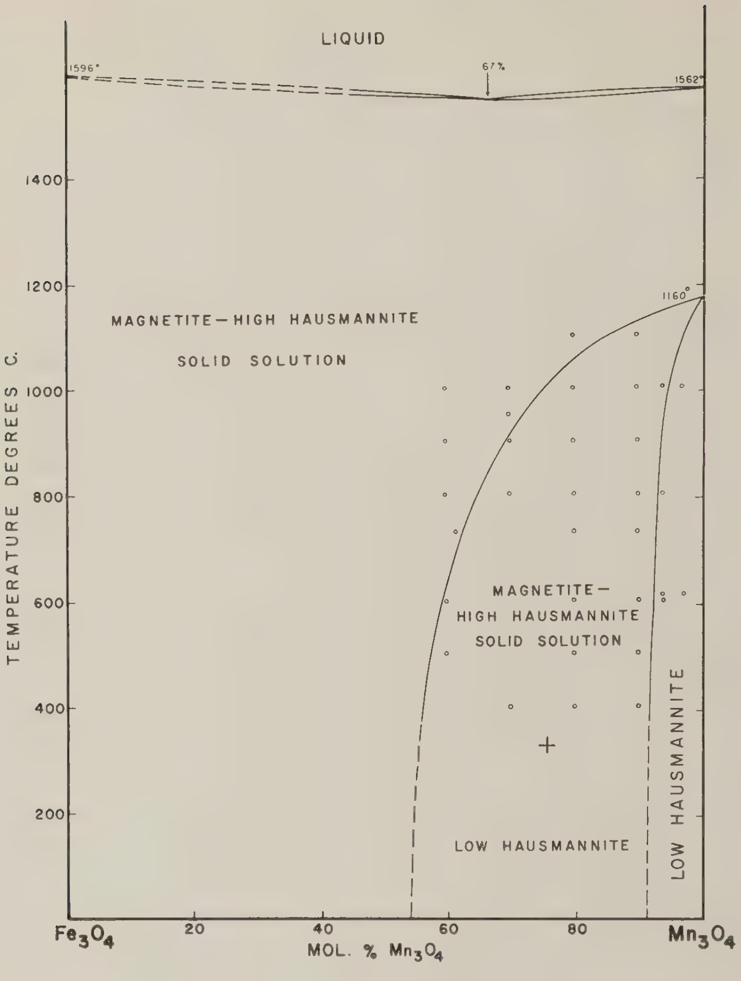

FIG. 3. Phase equilibria in the system $Fe_3O_4-Mn_3O_4$.

atmosphere of a gas furnace, while similar materials fired at equivalent temperatures in air have a poorly developed tetragonal structure. Coprecipitated hydroxide starting materials promote formation of the tetragonal structure.

A tetragonal 80 Mn:20 Fe oxide composition prepared at 1200° C. from an hydroxide starting mixture, and a cubic 80:20 sample prepared at 1400° C. (gas furnace) from a metal+oxide starting mixture, were both heated above the liquidus temperature in air on a strip resistance furnace and quenched. Each sample recrystallized with the same structure it had before being melted, indicating that the difference in structure probably is due to a compositional difference.

Liquidus Temperatures

The melting point of Fe_3O_4 is taken as 1596° C. (Darken and Gurry, 1946), the melting point of Mn_3O_4 as 1562° C., (present investigation), in good agreement with the melting temperature, 1565° C., given by Wartenburg and Reusch (1932). Intermediate compositions exhibit solid solution with a liquidus minimum at about 67% Mn_3O_4 and 1543° C., (See Fig. 3).

CONCLUSIONS

The temperature of inversion of Mn_3O_4 from the tetragonal hausmannite form to the cubic high temperature form (here designated high hausmannite) is determined to be 1160° ± 5° C.

Above 1160° C. there is complete solid solution between magnetite and high hausmannite. At lower temperatures there is a progressively widening region of solid immiscibility in which a cubic phase and a tetragonal phase can coexist in equilibrium. Compositional limits of the phases present at 400° C. are 57% Mn_3O_4:43% Fe_3O_4 and 92% Mn_3O_4:8% Fe_3O_4. Extrapolation of the boundary curves (Figure 3) to room temperature gives composition limits in agreement with the results of Mason's work (op. cit., 1943) on natural intergrowths, namely 54% Mn_3O_4 and 91% Mn_3O_4.

The name *jacobsite* has been used to refer to spinel-structure minerals with intermediate compositions in the system $Fe_3O_4-Mn_3O_4$ (Mason 1943, p. 158), and use of that name for the complete high temperature series could be defended, on the basis that the present work shows that the compositional range of jacobsite increases with increasing temperature. However, the upper limit of 54% Mn_3O_4 in the cubic series is a logical and useful point of subdivision for minerals, and we therefore propose to follow Mason for the most part, and to use the following definitions of minerals whose compositions fall in the system Fe_3O_4-Mn_3O_4:

Mineral Name	*Molecular % Mn_3O_4*
magnetite	0 to 10*
jacobsite (magnetite-high hausmannite solid solution)	10 to 54
vredenbergite (intergrowths of jacobsite and low hausmannite)	54 to 91
hausmannite	91 to 100

Results of the present investigation show that the compositional range of the tetragonal structure is much greater for cation deficient compositions, which may be written $(Mn,Fe)_{3-x}O_4$, than for stoichiometric

---

* Mason (op. cit. 1943a) set the boundary between magnetite and jacobsite at 16.7% Mn_3O_4, a composition half-way between Fe_3O_4 and the hypothetical compound $MnFe_2O_4$. There is no evidence that such a compound exists and therefore it seems preferable to set the division arbitrarily at 10% Mn_3O_4.

$(Mn,Fe)_3O_4$ preparations. Synthesis of stoichiometric $(Mn, Fe)_3O_4$ oxides requires that the partial pressure of oxygen be controlled or that the effect of furnace atmosphere be eliminated by use of sealed sample tubes.

It seems likely that the tetragonal mineral described by Mason (1943b) as alpha-vredenbergite is cation deficient. This would be consistent with its reported mode of origin, by alteration of bixbyite $(Mn,Fe)_2O_3$ and would explain the existence of the mineral as a single phase rather than as an intergrowth of cubic and tetragonal phases, as would be expected from its Mn:Fe ratio. The existence of single phase metastable minerals in the compositional range of vredenbergite is possible but we would expect them to be cubic rather than tetragonal if the cation:oxygen ratio is stoichiometric.

Fine-grained vredenbergite (oriented intergrowths of jacobsite and iron-bearing hausmannite) may have originated by unmixing of a homogeneous magnetite-high hausmannite solid solution formed at temperatures above the two-phase region, as suggested by Mason. If an origin by unmixing could be proven to be the only means of producing such intergrowths, then it would be possible, for a vredenbergite sample of known composition, to estimate a minimum temperature of formation of the homogeneous solid solution by use of the equilibrium diagram (Fig. 3). However, there is no evident way of proving that such intergrowths do not originate from sedimentary iron-manganese deposits by thermal metamorphism at maximum temperatures *within* the two-phase region.

Unmixing of the cubic and tetragonal phases is so sluggish that it is practically useless in laboratory investigations of the system Fe_3O_4-Mn_3O_4 and that sluggishness, together with the difficulty of maintaining the stoichiometric proportions of preparations, probably is a principal reason for the inconsistencies of previous interpretations of the intermediate temperature portion of the system.

ACKNOWLEDGMENT

Part of the investigation was carried out under a research grant from the American Iron and Steel Institute, whose support is gratefully acknowledged.

REFERENCES

AMINOFF, G. (1926), Uber die Kristallstruktur von Hausmannit ($MnMn_2O_4$): *Z. Krist.*, **64**, 475–90.

DARKEN, L. S., AND GURRY, R. W. ,(1945), The system iron-oxygen, I. The Wustite field and related equilibria: *J. Am. Chem. Soc.*, **67**, 1398–1412.

ECONOMOS, G., (1955), Methods of Ferrite preparation: *J. Am. Cer. Soc.*, **38**(7) 241–44.

FYFE, W. W., (1949), The state of Mn in Mn Oxides: *Nature*, **164**, 790.

Goodenough, J. B., and Loeb, A. L., (1955), Theory of ionic ordering, crystal distortion and magnetic exchange due to covalent forces in spinels: *Phys. Rev.*, **98**, 391–408.

Greig, J. W., Posnjak, E., Merwin, H. E., and Sosman, R. B., (1935), Equilibrium relationships of Fe_3O_4, Fe_2O_3 and oxygen: *Am. J. Sci.*, **30**, 239–316.

Gruver, R. J., (1951), Differential thermal-analysis studies of ceramic materials: *J. Am. Cer. Soc.*, **34**, 353–57.

Ishihara, T., and Kigoshi, A., (1953), On equilibrium in the reduction of Mn_3O_4 with CO: *Sendai Japan, Tohoku Univ. Sci. Reports of the Research Institutes, Sec. A***5**, 172–78.

Mason B.; (1943a), Mineralogical aspects of the system FeO-Fe_2O_3-MnO-Mn_2O_3: *Geol. Foren. Forhandl.*, **65**, 95–180.

Mason, B., (1943b), Alpha-Vredenbergite: *Geol. Foren. Forhandl.*, **65**, 263–272.

McMurdie, H. F., and Golovato, Ester, (1948), A study of the modifications of MnO_2: *J. Res. N. B. S.*, **41**, 589–600.

———, Sullivan, Barbara M., and Maur, F. A., (1950), High temperature *x*-ray study of the system Fe_3O_4-Mn_3O_4: *J. Res. N. B. S.*, **45**, 35–41.

Montoro, V., (1938), Miscibilita frai Sesquiossidi di Ferro e di Manganese: *Gazz. Chim. Ital.*, **68**, 728–33.

Romeijn, F. C., (1953), Physical properties and cation arrangement of some spinels: *Philips Res. Res. Rep.*, **8**, 304–20.

Shafer, M., and Roy, R., (in press), Phase equilibria in the system Na_2O-Nb_2O_5: *J. Am. Cer. Soc.*

Shull, C. G., Wollan, E. O., and Koehler, W. C., (1951), Neutron scattering and polarization by ferromagnetic materials: *Phys. Rev.*, **84**, 912–21.

Sidgwick, N. V., (1951), Chemical Elements and their compounds: Oxford Univ. Press.

Southard, J. C., and Moore, G. E., (1942), High temperature heat content of Mn_3O_4, $MnSiO_3$, and Mn_3C: *J. Am. Chem. Soc.*, **64**, 1769–71.

Verwey, E. J. W., and Von Bruggen, M. G., (1935), Structures of solid solutions of Fe_2O_3 in Mn_3O_4: *Z. Krist.*, **92**, 136–38.

———, (1935), The crystal structure of Fe_2O_3 and Al_2O_3: *Z. Krist.*, **91**, 65–69.

———, and Heilmann, E. L., (1947), Physical properties and cation arrangements of oxides with the spinel structure: *J. Chem. Phys.*, **15**, 174–87.

Von Eckermann, H., (1943), Some remarks on the Fe_3O_4-Mn_3O_4 system: *Geol. Foren. Forhandl.*, **65**, 258–62.

Wartenburg, H. and Reusch, H. J., (1932), Schmeltzdiagramme hochstfeuerfester Oxyde. VI Berichtigung: *Z. anorg. allgem. Chem.*, **208**, 380–381.

Manuscript received May 27, 1957

THE AMERICAN MINERALOGIST, VOL. 43, JANUARY-FEBRUARY 1958

RELATION BETWEEN LATTICE CONSTANTS AND COMPOSITION OF THE Ca-Mg CARBONATES

Julian R. Goldsmith* and Donald L. Graf† with additional analytical determinations by A. A. Chodos,‡ O. I. Joensuu§ and L. D. McVicker†

Abstract

Synthetic magnesian calcites containing 4.94, 9.89, 14.83, and 19.78 mol per cent $MgCO_3$ in solid solution were prepared by solid-state reaction of pelletized mixtures of $CaCO_3$ and basic Mg carbonate at temperatures between 800° and 860° C. Spectrographic analyses of the Mg content of these solid solutions, using copper spark and *d.c.* arc methods, gave results which were, with one exception, within ±7 per cent of the true values.

Dolomite crystals from five localities were analyzed by wet chemical methods, and gave molar compositions ranging from $Ca_{0.4940}$ (Mg, Fe, Mn)$_{0.5060}$ to $Ca_{0.5063}$ (Mg, Fe, Mn)$_{0.4937}$.

Values of a_0 and c_0 for magnesian calcites, the dolomites, and a synthetic magnesite were obtained from x-ray diffractometer and film measurements. The spacings of $d_{633(30\cdot12)}$, the third order of the strongest reflection, measured on the diffractometer agree with those computed from measured values of a_0 and c_0. The synthetic magnesite has $a_0=4.6330$ Å, $c_0=15.016$ Å, $a_{rh}=5.6752$ Å, $\alpha=48°\ 10.9'$.

The average a_0 for the dolomites studied is 0.092 per cent less than one-half the sum of a_0 values for calcite and magnesite, and the average c_0 value, 0.21 per cent less than the analogous hypothetical c_0 value. If the magnesian calcite curves are extrapolated to 50 mol per cent $MgCO_3$, the comparable numbers are 0.98 per cent for a_0 and 0.44 per cent for c_0. The implied smaller mole volume for the hypothetical disordered equivalent of dolomite must be viewed with skepticism, however, because of the length of the extrapolation and the fact that cell constants of the magnesian calcites were measured at room temperature, from 500° to 800° C. below the minimum temperature at which they are stable.

Compositions of single-phase materials between calcite and dolomite can be determined from c_0 values to within about 2 mol per cent $MgCO_3$ if mixed-layer effects do not occur.

Introduction

In an earlier paper (Goldsmith, Graf, and Joensuu, 1955) x-ray and compositional data were used to prepare several curves showing spacing versus composition for a number of naturally occurring magnesian calcites. Wet chemical analyses consistently gave higher magnesium values than did spectrochemical analyses. The spectrochemical analyses were used, largely because the homogeneous single-phase samples available were frequently quite small. The validity of determinations of composition from x-ray spacing, given later in that paper, were thus dependent upon the spectrochemical data.

In order to examine further the validity of our curves showing spacing

---

* Department of Geology, The University of Chicago.

† Illinois State Geological Survey, Urbana.

‡ Division of Geological Sciences, California Institute of Technology, Pasadena.

§ Department of Geology, The University of Chicago. Present address: Heavy Minerals Company, Chattanooga 8, Tennessee.

versus composition, several synthetic magnesian calcites have been prepared and examined by spectrochemical analysis and powder x-ray diffraction. In addition, compositions and spacings of synthetic magnesite and five carefully selected dolomites have been obtained in order to evaluate more accurately the composition-unit cell relationships in the Ca-Mg carbonates.

PREPARATION OF MAGNESIAN CALCITES

The synthetic magnesian calcites were prepared by reacting pelletized mixtures of C. P. basic magnesium carbonate and Johnson and Mathey's "Specpure" $CaCO_3$ in cold-seal pressure vessels using the apparatus decribed by Graf and Goldsmith (1955). The runs were held one or two days at temperatures of 800° to 860° C. under CO_2 pressures sufficient to prevent decomposition of dolomite, typically 20,000 to 24,000 lbs./in.^{2} The temperatures chosen for individual runs were sufficiently high to insure complete solid solution of the mixture (Graf and Goldsmith, 1955).

Initially runs were made using mixtures of calcium carbonate with MgO and with magnesite. Ca-Mg carbonate solid solutions could be obtained with both these mixtures, but equilibrium was much more readily established and results were more consistent when basic Mg carbonate was used instead. Only those materials prepared with basic Mg carbonate as a source of Mg were used for analytical determinations. The MgO content of the basic carbonate was determined by dead-burning a portion of the material.

Mixtures equivalent to 4.94, 9.89, 14.83, and 19.78 mol per cent $MgCO_3$ were weighed out, hand-mixed under alcohol in an agate mortar, and pressed into cylindrical pellets 3/16 inch in diameter by $\frac{1}{8}$ inch long. Several runs were made of each composition in order to obtain the desired amount of material. At the completion of a run the furnace was quickly removed and an air blast applied to the hot end of the bomb. Powder x-ray diagrams were taken of each batch of pellets, and in a few cases it was found that a small but detectable amount of dolomite had formed by exsolution during cooling. Pellets containing dolomite were not used for measurement of x-ray spacings.

SPECTROCHEMICAL METHODS

The spectrochemical method used by one of us (Joensuu) for determining Ca and Mg is essentially that described in Goldsmith, Graf, and Joensuu (1955). The beads from the 900° C. fusions were ground with graphite (1:2), and placed in $\frac{1}{8}$ inch O. D. graphite elec-trodes which had been drilled to a depth of 8 mm. with a #46 drill. The electrodes were arced at 6 amperes using the gas jet (Stallwood arc) with carbon dioxide (Stallwood, 1954), and the following lines used for analysis:

Element	*Wavelength, Å*	*Internal Standard*	*Concentration range wt. per cent*
Mg	2782.9	Co 3072.3	0.1– 5
Mg	3096.9	Co 3072.3	0.5–20
Mg	3336.1	Co 3334.1	2 –25
Ca	2997.3	Ba 3071.6	20 –50

The samples were also analyzed spectrochemically for Mg using the copper spark method (Chodos). A sample weighing 25 mg. was dissolved in 1 per cent HCl and 10 ml. of an internal standard solution containing 0.25 g. ammonium molybdate/liter was added. The volume of the solution was adjusted to 25 ml. with 1 per cent HCl, and 0.1 ml. of the solution was then transferred to the top of a copper electrode and evaporated under an infrared lamp. The residue was sparked for 30 seconds using a low resistance, low inductance, and low capacitance spark from the Jarrell-Ash Varisource, and the spectrum was photographed on III-O plates. The line pair Mg 3838.3/Mo 3903.0 was used. Standards were made from National Bureau of Standards Dolomite (#88) diluted with high-purity calcium carbonate.

MAGNESIAN CALCITE ANALYSES

The results of spectrochemical analysis of the synthetic magnesian calcites are given in Table 1. With only one exception, the average value for $MgCO_3$ obtained from multiple analyses differs less than ±7 per cent from the actual amount present. The accuracy of these results would appear to be somewhat better than that usually attributed to spectrochemical analyses.

TABLE 1. SPECTROCHEMICAL ANALYSES OF SYNTHETIC MAGNESIAN CALCITES

Mol % $MgCO_3$ (by synthesis)	Wt. % $MgCO_3$ (by synthesis)		Wt. % $MgCO_3$[*]	Av.	Error (% of amount present)	Wt. % $MgCO_3$[†]	Av.	Error (% of amount present)	Wt. % $CaCO_3$[‡]
4.94	4.50		5.10, 4.61, 4.51, 4.50	4.72	+4.9	4.8, 4.6, 4.5	4.6	+2.2	95, 96, 96
9.89	8.99	§(*a*)	7.28, 8.39, 8.08, 6.87	7.66	−14.8	10.0, 9.4, 9.4	9.6	+6.8	93, 86, 88
		§(*b*)	8.08, 8.84, 8.29, 8.95	8.53	−5.1				
14.83	13.48	(*a*)	13.70, 12.83, 13.00, 12.66	13.04	−3.3	13.6, 13.7, 13.8	13.7	+1.6	82, 84, 86
		(*b*)	14.22, 13.70, 13.18, 13.70	13.63	+1.1				
19.78	17.98	(*a*)	17.34, 19.76, 18.72, 20.63	19.10	+6.2	17.6, 18.2, 18.2	18.0	+0.1	80, 82, 85
		(*b*)	18.20, 19.07, 19.42, 17.34	18.52	+3.0				

[*] Reported as wt. per cent Mg. Analysis by A. A. Chodos.

[†] Reported as wt. per cent MgO. Analysis by O. I. Joensuu.

[‡] Reported as wt. per cent CaO. Analysis by O. I. Joensuu.

[§] The (*a*) (*b*) pairs for each composition represent different batches of pills prepared from the same original mixture.

Chemical Composition of Selected Dolomites

Five dolomites, from Serra das Eguas, Brazil, Hammondsville, Vermont, Gabbs, Nevada, Monroe County, New York, and Binnental, Switzerland, were selected for correlation of composition with unit cell dimensions. The criteria used in selecting these materials were the absence of extraneous phases, which would affect chemical analyses, relative freedom from cations in solid solution (especially Fe^{++} and Mn^{++}), which would affect unit cell size, and homogeneity throughout. The Hammondsville and Serra das Eguas materials were single cleavage pieces of water-clear material. The Binnental sample was made up of several water-clear crystals taken from the same cavity. The Gabbs material was obtained from a single somewhat milky cleavage piece, and the Monroe County sample was made up of a number of somewhat milky crystals taken from the same cavity.

In order to check the wet chemical procedures for Ca and Mg against an absolute standard, 1:1 and 4:1 molar mixtures of Illinois Geological Survey Spectrographic Standard $CaCO_3$ and Johnson and Mathey's "Specpure" MgO were prepared. The analytical results for these mixtures are shown in Table 2. The weight of material found gravimetrically (Column 2) was corrected for MgO in the CaO product and for $Ca_3(PO_4)_2$ in the $Mg_2P_2O_7$ to obtain the corresponding value in column 4.

Table 2. Analytical Data on Synthetic $CaCO_3$-MgO Mixtures

		1:1 molar Ca:Mg mixture		
gms. $CaCO_3$ taken‡	gms. $CaCO_3$ found‡	wt. % MgO in CaO§	corrected gms. $CaCO_3$ found (average)	average % error
1.0027*	1.0076	0.60	1.0045	+0.18
1.0027*	1.0063	0.62		
gms. MgO taken	gms. MgO found	wt. % CaO† in $Mg_2P_2O_7$	corrected gms. MgO found (average)	average % error
0.4032	0.4005	0.20	0.4025	−0.17
0.4032	0.4003	0.15		
		4:1 molar Ca:Mg mixture		
gms. $CaCO_3$ taken	gms. $CaCO_3$ found	wt. % MgO in CaO	corrected gms. $CaCO_3$ found (average)	average % error
1.0027*	1.0058	0.04		
1.0027*	1.0062	0.04	1.0075	+0.48
gms. MgO taken	gms. MgO found	wt. % CaO† in $Mg_2P_2O_7$	corrected gms. MgO found (average)	average % error
0.1008	0.1013	0.35		
0.1008	0.1011	0.45	0.1007	−0.11

* Samples of 1.008 gm. $CaCO_3$ were weighed out. The figure 1.0027 is a corrected value which takes into account the actual CaO content of the material as determined by calcining a sample at 1200° C. and weighing as CaO.

† The CaO reported in these analyses was assumed to be present as $Ca_3(PO_4)_2$.

‡ Analysis by L. D. McVicker.

§ Analysis by O. I. Joensuu.

TABLE 3. CHEMICAL ANALYSES OF SELECTED DOLOMITES

	Wt. % CaO found[2]	Wt. % MgO found	Wt. % FeO found	Wt. % MnO found	Wt. % CO_2 found	Wt. % SiO_2 found	Wt. % Al_2O_3 found	Wt. % impurities in CaO				Wt. % impurities in $Mg_2P_2O_7$			Cations/100 Cations: Corrected for impurities in precipitates				Cations/100 Cations: Further corrected against standard mixtures, Table 2			
								Total[1]	MnO[4]	MgO	Fe_2O_3	MnO[8]	CaO[9]	Fe_2O_3[10]	Ca	Mg	Fe	Mn	Ca	Mg	Fe	Mn
Gabbs	30.50	22.24	.07	.004	47.46			100.41	<.01	.05	<.04	<.01	.10	.015	49.53	50.30	0.09	0.08	49.40	50.43	0.09	0.08
	30.46	22.25	.08		47.63				<.01	.06	.035	<.01	.10	<.01								
			.06[11]	.06[11]		.05[11]	.009[11]															
Hammondsville	30.11	20.70	2.50	.12	47.11			100.67	.07	.065	.025	.19	.15	.02	49.56	47.03	3.23	0.18	49.43	47.16	3.23	0.18
	30.00	20.73	2.52		47.24				.065	.05	.025	.18	.18	.01								
			3.07[11]	.16[11]		.08[11]	.013[11]															
Binnental	30.71	22.20[5]			47.45			100.62	.03	.04	<.01	.06	.11	.015	49.80	50.02	0.10	0.08	49.67	50.15	0.10	0.08
	30.72	22.24[5]			47.53				.04	.06	.015	.09	.12	.01								
			.08[11]	.06[11]		.05[11]	.013[11]															
	30.78[7]	21.79[5]			47.26																	
	30.73	21.85[5]			47.30			99.98[6]	.06	.08	<.01	.13	.14	.01	50.41	49.45	0.01	0.13				
			.01[11]	.10[11]		.02[11]	<.01[11]															
Serra das Eguas[3]	30.37	22.18	.27	.08	47.62			100.79	.04	.09	.01	.10	.20	<.01	49.55	50.00	0.33	0.12	49.42	50.13	0.33	0.12
	30.54	22.33	.25		47.74				.035	.07	.015	.10	.25	.01								
			.26[11]	.11[11]		.05[11]	.015[11]															
	30.45	21.95	.26	(.08)	47.36	.08	.17	100.51														
	30.46	21.99	.23		47.47	.09	.24															
Monroe County[3]	30.90	21.41[5]							.03	.05	.015											
	30.98	21.41[5]							.03	.05	.015	.09	.22	<.01	50.76	48.56	0.58	0.10	50.63	48.69	0.58	0.10
			.45[11]	.08[11]		.06[11]	.38[11]															
	30.94	21.29[5]	.46		47.44	.07	.17	100.59														
	30.96	21.32[5]	.44		47.49	.12	.17															
				(.08)[11]																		

---

[1] Includes spectrochemical values in instances where gravimetric determinations were not made.

[2] SrO was shown spectrochemically to be <0.01 wt. per cent in all of the samples, except for the second Binnental analysis where the CaO figure includes 0.02 wt. per cent SrO.

[3] Independent analyses of the same Serra das Eguas and Monroe County samples, made several years ago, are shown for comparison.

[4] Assumed to be present as Mn_2O_3.

[5] Value given has been corrected for wt. per cent MnO, determined spectrographically. Other wt. per cent MgO figures have been corrected on the basis of the colorimetric MnO determinations.

[6] This analysis, as used by Richard Robie in his Ph.D. thesis at the University of Chicago (1957) has MgO finally corrected to 21.54 wt. per cent and CO_2 corrected to 47.38 wt. per cent. The additional corrections are the amounts by which the analyst failed to duplicate the wt. per cent MgO reported for U. S. Bureau of Standards dolomite #88, and the wt. per cent CO_2 reported for U. S. Bureau of Standards Na_2CO_3.

[7] CaO, MgO and CO_2 for the second Binnental analysis by M. C. Batchelder, other non-spectrochemical determinations by L.D.M.

[8] Assumed to be present as $Mn_2P_2O_7$.

[9] Assumed to be present as $Ca_3(PO_4)_2$.

[10] Assumed to be present as $Fe_4(P_2O_7)_3$.

[11] Spectrochemical determinations for the second Binnental analysis by A. J. Leoni, for SiO_2 and Al_2O_3 in the other analyses by Kozo Nagashima, others by O.I.J.

The dolomites were similarly analyzed in duplicate for Ca and Mg by McVicker using the standard Ca oxalate and Mg ammonium phosphate precipitations, the latter in triplicate. The CaO and Mg pyrophosphate obtained after heating were analyzed spectrochemically by Joensuu for extraneous ions carried down with the precipitate. Spectrochemical determinations of MnO, FeO, and SrO in the dolomites were made. Where sufficient samples were available MnO was also determined colorimetrically and FeO gravimetrically. The results are summarized in Table 3. The differences in Ca and Mg content obtained with and without corrections based upon Table 2,

$$\left(\frac{0.48 + 0.18}{2} = 0.33 \text{ per cent for Ca}, \frac{0.17 + 0.11}{2} = 0.14 \text{ per cent for Mg}\right)$$

are less than 0.15/100 cations. The final $CaCO_3$ figures for four of the five samples are approximately 0.5 mole per cent below the ideal 50 per cent, but the Monroe County dolomite has about 0.5 per cent $CaCO_3$ in excess of that figure.

Some further information on the reliability of the various analytical determinations is furnished in Table 3 by analyses of the same Serra das Eguas and Monroe County samples made several years ago by McVicker, and by an independent analysis of the same Binnental sample for another purpose made by M. G. Batchelder of the Institute of Metals, University of Chicago, with spectrographic analyses of precipitates by A. J. Leoni. The three pairs of CaO determinations differ by a maximum of only 0.05 wt. per cent; the two pairs of CO_2 determinations, by 0.20 and 0.26 wt. per cent. The pairs of MgO determinations differ by 0.10, 0.29, and 0.44 wt. per cent. The discrepancy between MgO determinations is the reason for the difference in values (cations/100 cations) computed for the two Binnental analyses, a difference which is half the maximum difference observed among the several dolomites.

It may be noted that most of the analyses total somewhat high, and that moles of CaO+MgO+MnO+FeO exceed moles of CO_2 by from 0.009 (Monroe County) to 0.022 (Binnental, L. D. M.). This difference corresponds to a range of 0.37 to 0.87 wt. per cent MgO, for example, and is greater than the amount of material that could be combined with the small amounts of SiO_2 and Al_2O_3 present. The last two materials, furthermore, are at least partly derived from reagents, laboratory glassware, and the mullite mortar in which the samples were ground. The anomalies could be most easily resolved if MgO determinations were slightly high, but the analyses summarized in Table 2 indicate that correction for spectrographic analysis of precipitates seems to yield quite accurate results for MgO.

X-RAY METHODS

Spectrographically pure $CaCO_3$, the synthetic magnesian calcites, the five chemically analyzed dolomites as well as U. S. Bureau of Standards dolomite #88, and a synthetic magnesite* were run on the General Electric XRD-3 *x*-ray diffractometer using Cu radiation. Because only small amounts of some of the materials were available, all mounts were prepared by spreading the finely ground powder evenly in *n*-butyl alcohol on a glass slide and then allowing the alcohol to evaporate. A similar mount of high-purity silicon having $a_0=5.4306_2$ Å was used to prepare a graph of 2θ versus errors in *d*-values calculated from the observed maxima. This graph was then used to correct observed carbonate *d*-values. At moderate to low values of 2θ the correction incorporates not only instrumental error but also the effect of partial $\alpha_1\alpha_2$ overlap.

The reflections used were $21\bar{3}$ (140)† which ranged from $2\theta=109°$ to 123° for the carbonates studied and from which a_0 can readily be obtained, 444 (00·12) at $2\theta=65°$ to 76°, the highest angle basal reflection available, and 633 (30·12) at $2\theta=99°$ to 115°, the third order of the strong 211 (104) reflection which lies at about 45° to *a* and *c*. The $30\bar{3}$ (330) reflection at $2\theta=136°$ could also be detected for calcite, and was used to obtain a_0 values. Diffraction angles were obtained from charts recorded at a rate of 1°/5 min. with a time constant of 1.0 second for 444 (00·12) and 633 (30·12), 3 seconds for the other two reflections.

The complete set of samples examined with the diffractometer was also run using standard 114.59 cm. Philips Straumanis-mount powder cameras and suitable radiations, in order to obtain an independent check. The Straumanis method of film shrinkage correction was used, and $\cos^2\theta$ extrapolations to $2\theta=180°$ were carried out to obtain a_0 and c_0, except where otherwise noted. The various radiations and *x*-ray reflections used in determining a_0 and c_0 are summarized in Table 4. An upper limit to the accuracy of the extrapolations is set by the sharpness of the back reflections which can be obtained. The dolomites examined, even though macroscopically good single crystals, typically have somewhat more diffuse back reflections than do well crystallized single-cation carbonates such as calcite and magnesite. Attempts to obtain structurally more perfect dolomites by recrystallization in the presence of water and CO_2 at 700° C. yielded materials which were not significantly improved.

---

* The magnesite was prepared by heating C.P. basic Mg carbonate to 300° C. for 15 hours in a Morey bomb in the presence of CO_2 and H_2O. Spectrographic analysis of this material by Juanita Witters of the Illinois State Geological Survey shows Ca equivalent to 0.38 mol per cent $CaCO_3$ and Fe equivalent to 0.013 mol per cent $FeCO_3$.

† Rhombohedral indices $h_rk_rl_r$ are followed by the equivalent hexagonal indices $hk\cdot l$ throughout the paper.

TABLE 4. BACK REFLECTIONS USED TO DETERMINE a_0 AND c_0 FROM PHILIPS POWDER *X*-RAY FILMS OF Ca-Mg CARBONATES

Materials	Radiation	Constant desired	Reflections used†
Calcites and Mg-calcites	Co	a_0	$21\bar{3}(140)$, $440(048)$, $41\bar{1}(324)$, $31\bar{2}(232)$, $400(404)$, $521(318)$
Calcites and Mg-calcites	Co	c_0	$642(22\cdot 12)$, $664(02\cdot 16)$, $653(12\cdot 14)$, $633(30\cdot 12)$, $644(20\cdot 14)$
Calcites, 4.84 mol% and 9.89 mol% Mg-calcites	Fe	a_0	$31\bar{2}(232)$, $521(318)$, $400(404)$, $420(226)$, $32\bar{1}(134)$
14.83 mol% Mg-calcite	Fe	a_0	$31\bar{2}(232)$, $30\bar{2}(321)$, $521(318)$, $400(404)$, $420(226)$, $32\bar{1}(134)$
19.78 mol% Mg-calcite	Fe	a_0	$400(404)$, $420(226)$, $32\bar{1}(134)$
Dolomites	Co	a_0	$21\bar{3}(140)$, $41\bar{1}(324)$, $31\bar{2}(232)$, $30\bar{2}(321)$
Dolomites	Co	c_0	$664(02\cdot 16)$, $653(12\cdot 14)$, $633(30\cdot 12)$, $655(10\cdot 16)$,* $654(11\cdot 15)$*
Dolomites	Cr	c_0	Average c_0 extrapolation slope run through ${c_0}'_{543(11\cdot 12)}$
Magnesite	Cu	a_0	$540(149)$, $33\bar{2}(054)$, $11\bar{4}(05\bar{2})$, $520(327)$, $440(048)$
Magnesite	Co	c_0	Coincidences of $654(11\cdot 15)$—$30\bar{2}(321)$ and $655(10\cdot 16)$—$633(30\cdot 12)$—$312(232)$; fit of ${a_0}'_{540(149)}$ to a_0 extrapolation (see text)

† Tables of indexed *d*-spacings for the rhombohedral carbonates will be given in a separate publication (Graf, ms. in preearation).

* The $654(11\cdot 15)$ and $655(10\cdot 16)$ reflections of calcite and the magnesian calcites are too nearly coincident to be measured, but are resolved for dolomite.

Reflections with a strong *c*-axis component are more often broadened than are those from planes having a strong *a*-axis component, both for the dolomites and for the magnesian calcites.

It will be noted from Table 4 that the accuracy of $\cos^2\theta$ extrapolation is also restricted by the fact there are no basal reflections in the back reflection region, at least for the radiations commonly available. This has made it necessary first of all to carry out an a_0 extrapolation using the relation,

$$a_0' = d\sqrt{4/3(h^2+hk+k^2)+\left(\frac{a_0}{c_0}\right)l^2} \qquad (1)$$

where the prime indicates that a_0' is in general not equal to a_0 except at $2\,\theta = 180°$. Greater reliance is placed upon the reflections from planes having no *c*-axis component, and those having a relatively small *c*-axis component so that a_0/c_0 in (1) need not be known too accurately.

With a_0 known, a series of c_0 extrapolations can be made using

$$c_0' = d\sqrt{4/3\left(\frac{c_0}{a_0}\right)^2(h^2+hk+k^2)+l^2} \qquad (2)$$

and a range of assumed c_0 values in order to determine which one best fits the several c_0' values to a straight line and which one most nearly gives an extrapolated c_0 equivalent to that assumed. Inasmuch as the several reflections used in making the c_0 extrapolation have varying a-axis components and thus varying contributions from the $(c_0/a_0)^2$ term in (2), an error in assumed c_0 will affect them unequally and tend to destroy the linearity of the plot. The extrapolated c_0 value obtained can be tested by using it in computing a_0' values for reflections containing small to moderate c-axis components, and seeing whether these a_0' values fall close to the line in the a_0 extrapolation.

The suggested c_0 extrapolation for dolomite in Table 4 using Co radiation is not possible for most of the dolomites studied because the reflections are too weak and diffuse to measure. Instead, $d_{543(11\cdot 12)}$ at $2\theta = 158°$ can be measured quite accurately using Cr radiation, and c_0 then computed using equation (2) and a known value of a_0. Inasmuch as c_0' and c_0 in (2) are not identical for $2\theta < 180°$, it is necessary to establish the relationship between them. By determining the average of c_0 extrapolation slopes for some 20 carbonates which had been run previously, it was found that $c_0' \cong c_0 + 0.0009$ at $2\,\theta \cong 158°$, for the particular Philips camera used. Thus the c_0 value for dolomite is changed by about 0.001 Å relative to that obtained if c_0' is assumed equal to c_0.

The determination of c_0 for magnesite by $\cos^2\theta$ extrapolation is made difficult by the near-coincidence* of 654 (11·15) − 30$\bar{2}$ (321) and of 655 (10·16) − 633 (30·12) − 31$\bar{2}$ (232). However, the synthetic material available is very well crystallized, and these multiple reflections can be observed in the back reflection region at $2\theta \cong 155°$ using Co radiation. They do not appear broader than other back reflections of comparable intensity, indicating that coincidence is very closely approached. Using the accurately determined value $a_0 = 4.6330$ Å for magnesite, pairs of (2) can be solved simultaneously to eliminate c_0' and obtain c_0. For the three pairs 654 (11·15) − 30$\bar{2}$ (321), 655 (10·16) − 31$\bar{2}$ (232), and 633 (30·12)—312 (232) the same c_0 value, 15.013 Å, results. The two reflections with no c-axis component, 31$\bar{2}$ (232) and 30$\bar{2}$ (321), are weaker for calcite and dolomite than the reflections listed which have strong c-axis components but have appreciable intensity. Thus noticeable broadening of the multiple reflections would surely result if pairs of reflections from magnesite were separated by a fifth of the $\alpha_1\alpha_2$ separation in this 2θ region, and might be detectable at half this value. By leaving the reflections with no c-axis component fixed, and moving those with strong a-axis components these distances, it is possible to place limits of ±0.008 and ±0.004 Å respectively on the 15.013 value.

A probable value for c_0 within the ranges mentioned may be obtained in at least two ways. Using the rather accurately measured reflection 540 (149), which lies at $2\theta = 165°$ for Cu radiation and has about 75 per cent a-axis component, it is found that an assumed c_0 of 15.016_5 Å is required in (1) in order to make a_0' for 540 (149) fall on the line in the a_0 extrapolation. Values of c_0 of 15.013 and 15.019 Å (average 15.016) were obtained by running average c_0 extrapolation slopes through c_0' values derived from measurements of $d_{542(12\cdot 11)\alpha_1}$ and $d_{542(12\cdot 11)\alpha_2}$ at $2\theta = 145°$ using Fe radiation. A probable c_0 value of 15.016 Å is therefore chosen for magnesite.

The x-ray measurements were made in laboratories whose temperatures varied from 23° to 29° C. Thus if one ignores the possible heating-up inside the Philips cameras during long exposures, the measurements are valid for 26±3° C. The correction in a_0 for these materials resulting from a temperature difference of 5° C., based upon available thermal expansion data for calcite, dolomite, and magnesite, is about 0.0001 Å, which is much less than error from other sources and is ignored. The value for c_0 is about 0.002 Å, which is comparable to the experimental error from other sources in the more favorable cases. Correction of individual c_0 values to 26° C. does not change any of the conclusions reached in the remainder of the paper.

---

* The indexing of x-ray reflections in this paper is based upon tables of calculated d-values which are presented in a separate paper (Graf, ms. in preparation).

X-RAY MEASUREMENTS

The *x*-ray measurements are summarized in Table 5 and shown graphically in Figs. 1–4. Figure 1 gives a complete picture of the results, and Figs. 2, 3, and 4 are more detailed plots of the a_0, c_0 and $d_{211(104)}$ data, respectively. The relationships shown in these figures supplant the preliminary ones suggested in Fig. 6 of Goldsmith, Graf, and Joensuu (1955). The values given are the most probable in each instance, but no attempt is made to specify probable error because of the difficulty of taking into

TABLE 5. MEASURED VALUES OF c_0, a_0, AND $d_{211(104)}$ FOR THE Ca-Mg CARBONATES

Sample Number	Materials	$d_{211(104)}$ from $d_{633(30\cdot 12)}$ Spectrometer Cu rad.	c_0 from $d_{444(00\cdot 12)}$ Spectrometer Cu rad.	c_0 from $\cos^2\theta$ Extrapolation Co rad.	a_0 from $d_{213(140)}$ Spectrometer Cu rad.	a_0 from $\cos^2\theta$ Extrapolation Co rad.	a_0 from $\cos^2\theta$ Extrapolation Fe rad.
	Illinois Geological Survey Spectr. Standard $CaCO_3$	3.0356	17.059	17.065	4.9894 4.9898*		
	Johnson-Mathey "Specpure" $CaCO_3$				4.9903 4.9899*	4.9900	4.9896
G-680	(4.94 mol% $MgCO_3$)	3.0196	16.951	16.955	4.9676	4.9697	4.9691
G-684		3.0197	16.952		4.9679		4.9693
G-694		3.0198	16.950	16.956	4.9679	4.9682	4.9693
G-698	(9.89 mol% $MgCO_3$)	3.0018	16.852	16.852	4.9428	4.9430	4.9440
G-700		3.0030	16.845	16.855	4.9448	4.9443	4.9449
G-714		3.0021	16.850	16.852	4.9435	4.9430	4.9443
G-696	(14.83 mol% $MgCO_3$	2.9854	16.735	16.734	4.9216	4.9220	4.9219
G-661		2.9857	16.736	16.738	4.9213	4.9226	4.9223
G-663		2.9864	16.735	16.741	4.9219	4.9215	4.9218
G-672	(19.78 mol% $MgCO_3$)	2.9712	16.636	16.638	4.9022	4.9025	4.9019
	Dolomite, Gabbs	2.8842	16.004	16.002† 15.997	4.8056	4.8064	
	Dolomite, U.S.B.S. #88	2.8850	16.004	16.007†	4.8073	4.8068	
	Dolomite, Monroe County	2.8857	16.014	16.013†	4.8084	4.8080	
	Dolomite, Serra das Eguas	2.8843	16.004	16.000†	4.8065	4.8054	
	Dolomite, Hammondsville	2.8862	16.008	16.009† 16.011	4.8078	4.8070	
	Dolomite, Binnental	2.8857	16.015	16.014†	4.8070	4.8082	
	Synthetic magnesite	Interf.¶	15.013	15.016§	4.6333	4.6330‡	

* a_0 from $d_{30\bar{3}(330)}$ at $2\theta = 136°$.

† c_0 from extrapolation through $c_0'_{643(11\cdot 12)}$, Cr rad.

‡ a_0 from $\cos^2\theta$ extrapolation, Cu radiation.

§ See text.

¶ Computed from $a_0 = 4.6630$ Å and $c_0 = 15.016$ Å to be 2.7412 Å.

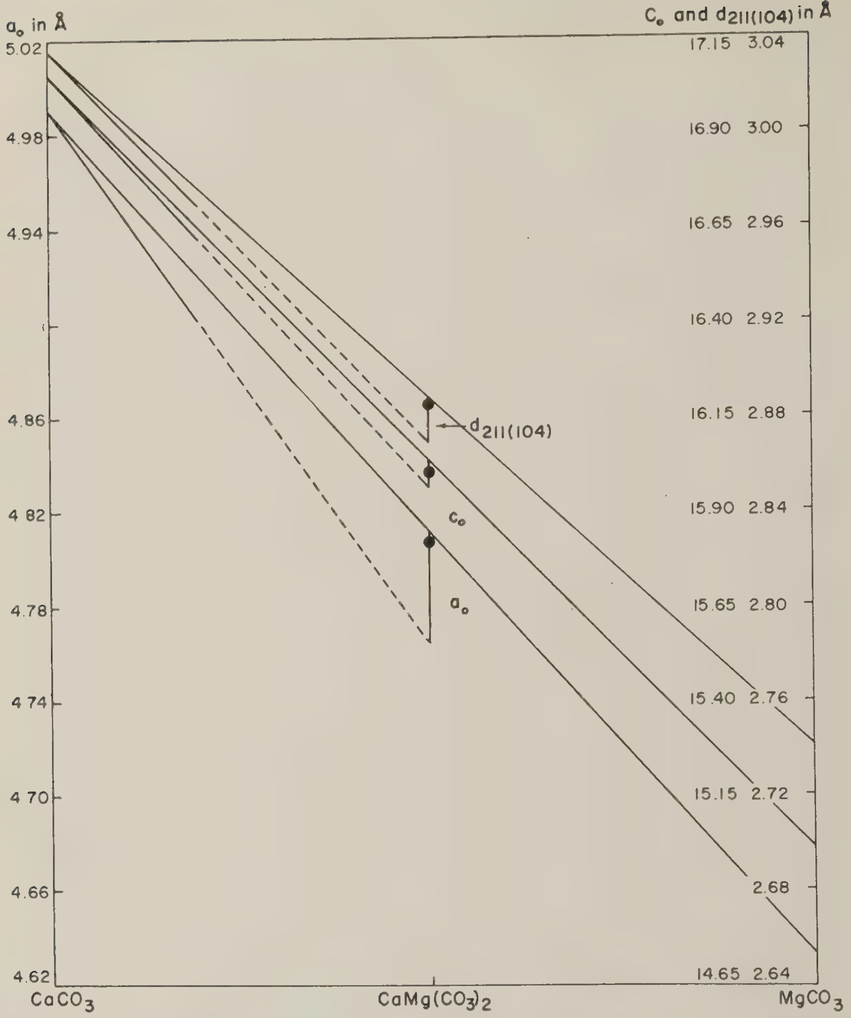

FIG. 1. Variation of a_0, c_0, and $d_{211(104)}$ for the Ca-Mg carbonates. The dots indicate the range of measured spacings for the several dolomites studied. Individual measurements for the dolomites and magnesian calcites are shown in Figs. 2, 3, and 4.

account such factors as variable line broadening and consequent variable $\alpha_1\alpha_2$ interaction.

The cell constants of calcite have been accurately determined by a number of workers (see discussion by Graf and Lamar, 1955, p. 643). At 20° C. $d_{211(104)} = 3.0357$ Å and α(cleavage rhomb) $= 101° 54'3''$, from which one obtains $a_0 = 4.9900$ Å, and $c_0 = 17.061_5$ Å. Using the thermal expansion data of Austin et al. (1940), the comparable values at 26° C.

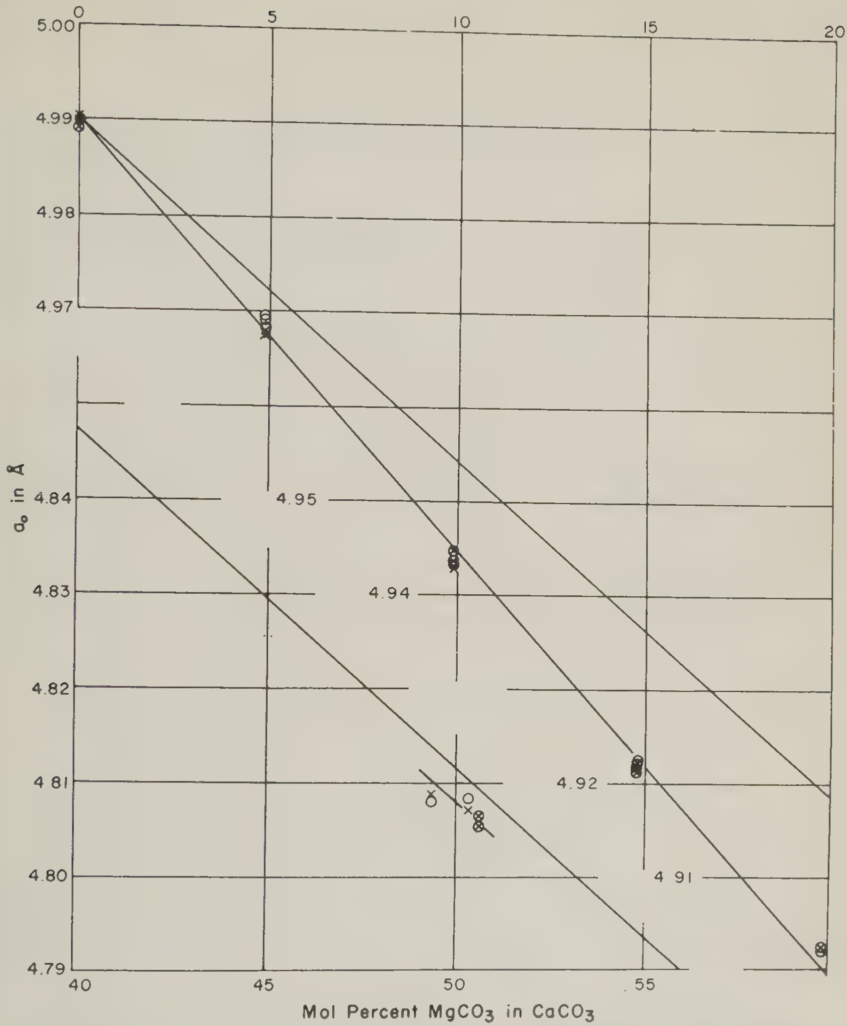

FIG. 2. Variation of a_0 for the Ca-Mg carbonates. Circles represent measurements obtained with Philips powder cameras; crosses show *x*-ray diffractometer results. The small dot is the literature value for calcite. The extension of the magnesian calcite line through the dolomite region has been inadvertently omitted, but passes through points 4.8085 Å, 40 mol % $MgCO_3$, and 4.7900 Å, 44.08 mol % $MgCO_3$.

are $a_0 = 4.9899$ Å and $c_0 = 17.064$ Å, from which $d_{211(104)}$ is computed to be 3.0359 Å. These literature values are plotted at the left-hand sides of Figs. 1–4 for comparison with our experimental determinations (Table 5).

Diffractometer and Philips camera determinations of a_0 and c_0 for the magnesian calcites are plotted in Figs. 2 and 3 respectively. The lower

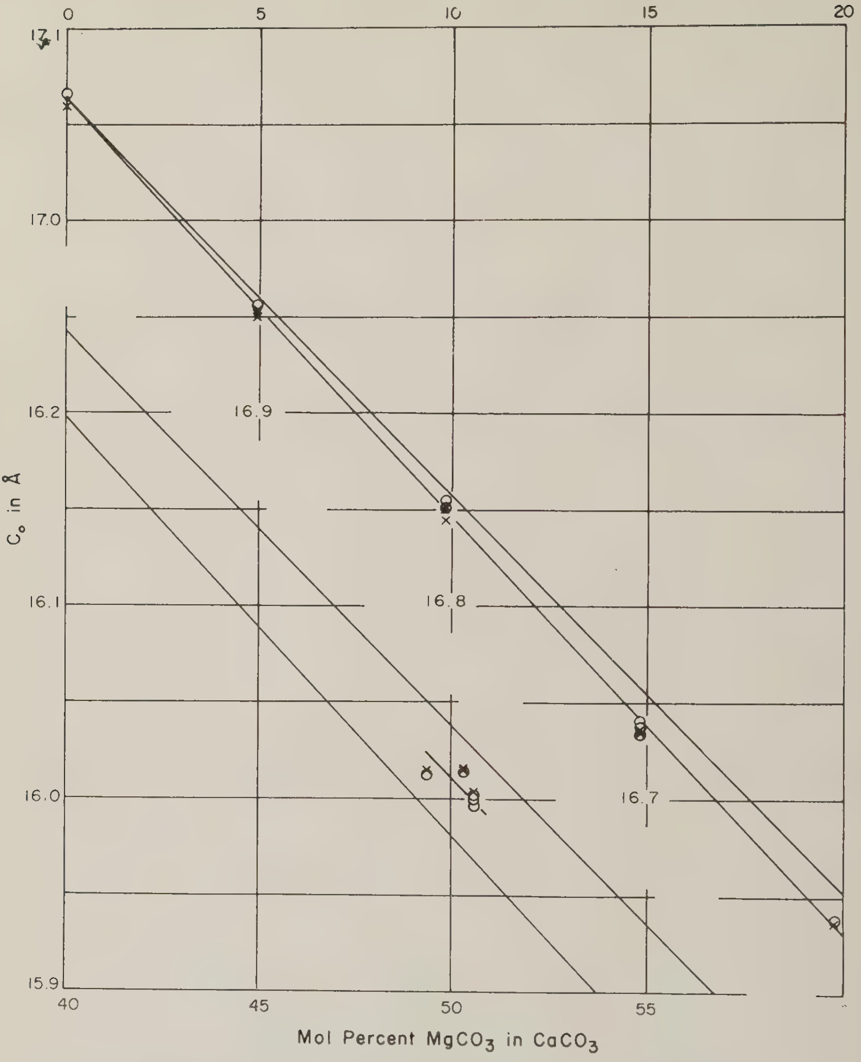

FIG. 3. Variation of c_0 for the Ca-Mg carbonates. Circles represent measurements obtained with Philips powder cameras; crosses show x-ray diffractometer results. The small dot is the literature value for calcite.

of the two straight lines in each figure is drawn through these values. The values of a_0 and c_0 for a calcite containing 20 mol per cent $MgCO_3$, as determined by the straight lines through the plotted points, have been used to compute $d_{211(104)}$ for this composition. The calculated $d_{211(104)}$ has been used to determine the slope of the lower of the two lines in Fig. 4,

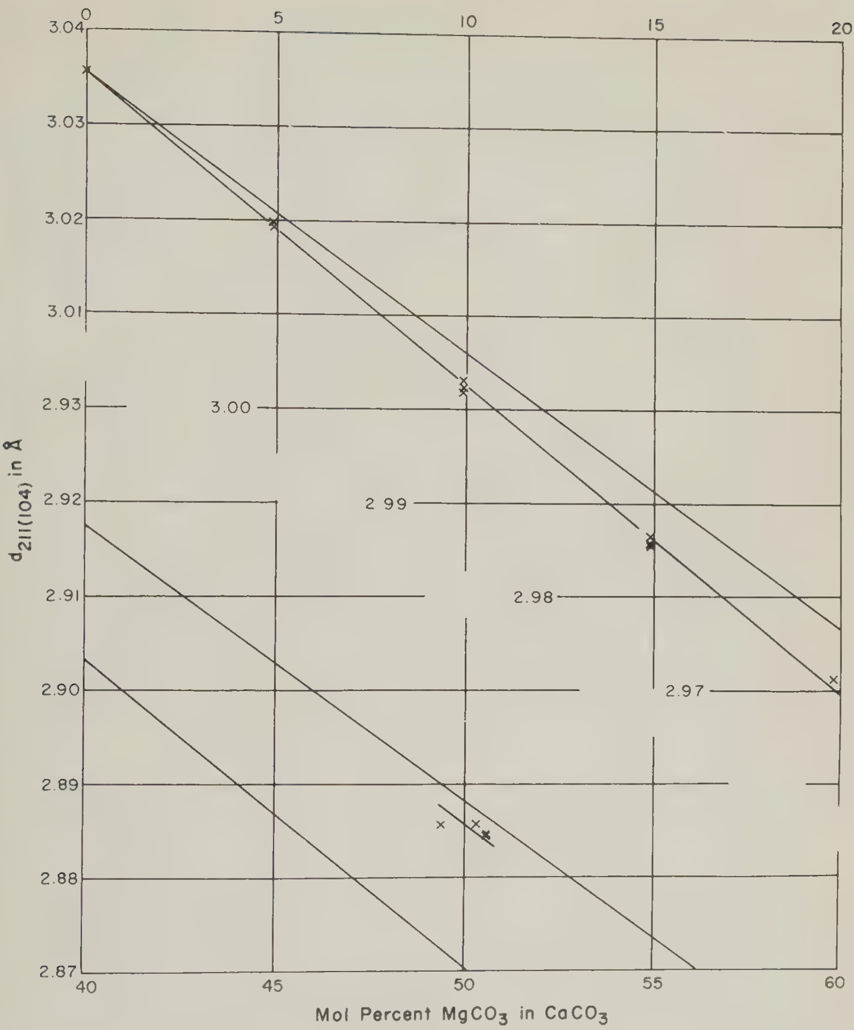

FIG. 4. Variation of $d_{211(10\bar{1})}$ for the Ca-Mg carbonates. Crosses indicate measurements made with the x-ray diffractometer. The small dot is the literature value for calcite. The straight line through the plotted points was computed from the analogous a_0 and c_0 lines in Figs. 2 and 3.

which is seen to pass satisfactorily through the plotted experimental points. The curvature suggested in the a_0 and $d_{211(104)}$ plots is less convincing if one ignores the single point at 19.78 mol per cent $MgCO_3$, and with the amount of information available does not justify drawing anything but straight lines.

The a_0, c_0 and $d_{211(104)}$ values for the Gabbs, Serra das Eguas, Binnental, and Monroe County dolomites are also plotted using McVicker's analyses together with the calcite-magnesite and extended magnesian calcite lines indicated in the dolomite region for reference. For these plots Mn^{++} and Fe^{++} are totalled with Mg^{++}. The short lines through these points in Figs. 2, 3, and 4 have been drawn so that they connect with the measured values for calcite if extended. This construction assumes that the contraction in a_0 and c_0 of dolomite relative to the averages of these values for calcite and magnesite results from the segregation of Ca and Mg into separate cation layers, as required by the dolomite structure. Ordered near-dolomites with some extra Ca in solid solution in Mg layers would have cation layers somewhat more alike, and would correspondingly retain only a proportionate part of the added packing efficiency gained by segregating cations. The fit of the plotted points to the short lines is a possible one, in view of the uncertainty in chemical analysis discussed earlier, but the points are too few and too close to 50 mol per cent to prove or disprove the assumption made in drawing the lines.

The a_0 and c_0 values obtained for ideal dolomite by noting where the short lines cross the 50 mol per cent composition are 4.8079 Å and 16.010 Å respectively. The $d_{211(104)}$ value computed from these values, 2.8855 Å, is in good agreement with that read from Fig. 4, 2.8857 Å. The accuracy of these constants is principally dependent upon the chemical analyses. To the extent that Mg values are high, for example, these constants will be high.

Values for U. S. Bureau of Standards dolomite #88 and a dolomite from Hammondsville, Vermont, are also reported in Table 5. Sample #88 was studied because of the wide use of this material as a chemical standard, even though it is, strictly speaking, not a single-phase material. Its cell dimensions fall within the range of those for the other dolomites. The Hammondsville dolomite contains some $3\frac{1}{4}$ mol per cent $FeCO_3$ which might be expected to increase the dolomite cell size because of the larger cell of siderite relative to that of magnesite (Graf, ms. in preparation). The fact that the Hammondsville material has cell dimensions only slightly larger than those of the Gabbs and Serra das Eguas dolomites, which have the same $CaCO_3$ content, indicates how little the substitution of Fe^{++} changes the unit cell size of dolomite.

DISCUSSION

The a_0/c_0 ratios of calcite, dolomite, and magnesite differ significantly. The a_0 of magnesite is 7.15 per cent less than that of calcite, but c_0 is 12.00 per cent less than the calcite c_0. For dolomite having $a_0 = 4.8079$ Å and $c_0 = 16.010$ Å, the comparable figures are 3.65 per cent and 6.18 per cent. It is thus not surprising that substitution of Mg into calcite occasions an anisotropic contraction, e.g., a 1.82 per cent smaller a_0 but a 2.54 per cent smaller c_0 for calcite containing 20 mol per cent $MgCO_3$ in solid solution than for pure calcite. In all three of these cases the percentage c_0 contraction relative to calcite is greater than the decrease in a_0. Comparisons between the data for magnesian calcite and dolomite can best be made by referring them to joins connecting c_0 and a_0 values for calcite and magnesite.

The data of Table 5 and Figs. 2 and 3 show that a_0 and c_0 of dolomite are quite close to one-half the sum of the corresponding values for calcite and magnesite. However, there remains a measurable contraction of both axes in dolomite. The graphically derived a_0 value for dolomite, 4.8079 Å, is 0.074 per cent less than the a_0, 4.8114_5 Å, of an hypothetical material halfway between calcite and magnesite. Similarly, the c_0 for dolomite, 16.010 Å, is 0.18 per cent less than the hypothetical 16.039_5 Å.

If one extrapolates the a_0 and c_0 magnesian calcite curves to 50 mol per cent $MgCO_3$, for comparison with dolomite, the a_0 and c_0 values obtained are 0.98 per cent and 0.36 per cent less than the hypothetical values. On the basis of the extrapolation, the a_0 and c_0 contractions for this magnesian calcite referred to the hypothetical values on the calcite-magnesite join are both greater than the corresponding contractions for dolomite. This would imply that the diordered equivalent of dolomite would have a smaller molar volume than dolomite itself, as measured at room temperature.

The extrapolation of the magnesian calcite curves must, however, be viewed with considerable skepticism. First of all, there may be no real physical significance in an extrapolation to the dolomite composition. Although increasingly high temperatures are needed to accommodate larger amounts of Mg in the calcite structure (Graf and Goldsmith, 1955; Harker and Tuttle, 1955), the composition and degree of Ca-Mg order of the equilibrium high-temperature phase or phases having a total composition of $Ca_{50}Mg_{50}$ are not known. It has not been established that the disordered equivalent of dolomite exists at any temperature below that at which melting or some other phase change occurs. Secondly, the lines through the a_0 and c_0 points for the magnesian calcities may actually be curved rather than straight, and of course may deviate even more in the extrapolated region. Furthermore, the mganesian calcite cell constants are measured on quenched samples, metastable at room temperature.* In view of the unknown thermal expansions of these materials, especially over a temperature range in excess of 800° C., comparison of molar volumes at other than the equilibrium temperatures could lead to erroneous conclusions.

---

* For example, 20 mol per cent $MgCO_3$ in calcite is stable only at temperatures greater than approximately 825° C.

The percentage contraction figures derived above also indicate that, with increasing substitution of Mg, a_0 values for the magnesian calcites deviate more rapidly percentagewise from the calcite-magnesite a_0 join than do c_0 values from the c_0 join. Yet the a_0 value for dolomite is percentagewise closer to the a_0 join than is the c_0 value to its join. This apparent reversal presumably results from the fact that Mg^{++} ions are accommodated in two different ways in these materials, by random cation subsitution in the magnesian calcites and as separate cation layers in dolomite.

One practical consequence is that c_0 values may be used to define the composition of single-phase materials between calcite and dolomite, regardless of whether cations occur in random solid solution or in the ordered dolomite arrangment, with a maximum error of about 2 mol per cent $MgCO_3$ at 50 mol per cent $MgCO_3$† and lesser errors toward $CaCO_3$. This statement is contingent upon retaining the assumption made earlier that the relation between $CaCO_3$ content and cell size of dolomites may be satisfactorily approximated by a line on the c_0 plot connecting calcite and the value for dolomite of 1:1 composition, and that this line may be used to determine composition of materials near dolomite which show order reflections of proper intensity. Materials with cation disorder would be referred to the extrapolated magnesian calcite line, which lies about 2 mol per cent $MgCO_3$ away for a given c_0 near the dolomite composition. The probable maximum errors using a_0 and the spacing of the strongest reflection, 211(104), or its higher orders, can be shown by similar reasoning to be 9 and 5 mol per cent $MgCO_3$ respectively.

ACKNOWLEDGMENT

We are grateful to Dr. W. F. Bradley for a critical reading of the manuscript.

REFERENCES

AUSTIN, J. B., SAINI, H., WEIGLE, J., AND PIERCE, R. H. H. (1940) Direct comparison on a crystal of calcite of the x-ray and optical interferometer methods of determining linear thermal expansion: *Phys. Rev.*, **57**, 931–933.

---

† Materials between calcite and dolomite in composition with hypothetical mixed layer effects, in which relatively Ca-rich and relatively Mg-rich cation planes occur in other than perfect alternation, would in some cases have c_0 values larger than those predicted from a join connecting the spacings for calcite and magnesite, and might even have bimodal intensity maxima for the basal reflections. Additional x-ray diffraction criteria are needed to describe these materials (Graf, Blyth, and Stemmler, ms. in preparation), and they are not considered in this discussion.

Goldsmith, J. R., Graf, D. L., and Joensuu, O. I. (1955) The ocurrence of magnesian calcites in nature: *Geochim. et Cosmoch. Acta*, **7**, 212–230.

Graf, D. L., Blyth, C. R., and Stemmler, R. S. (In preparation) Mixed-layer effects in the rhombohedral carbonates.

Graf, D. L., and Goldsmith, J. R. (1955) Dolomite-magnesian calcite relations at elevated temperatures and CO_2 pressures: *Geochim. et Cosmoch. Acta*, **7**, 109–128.

Graf, D. L. (In preparation) Unit-cell dimensions and *d*-spacings for the rhombohedral carbonates.

Graf, D. L., and Lamar, J. E. (1955) Properties of calcium and magnesium carbonates and their bearing on some uses of carbonate rocks: *Econ. Geol.*, **50th Anniv. Vol.**, 639–713.

Harker, R. I., and Tuttle, O. F. (1955) Studies in the system CaO-MgO-CO_2: Part 2. Limits of solid solution along the binary join, $CaCO_3$-$MgCO_3$: *Amer. Jour. Sci.*, **253,** 274–282.

Stallwood, B. J. (1954) Air-cooled electrodes for the spectrochemical analysis of powders: *Jour. Opt. Soc. Amer.*, **44,** 171–176.

Manuscript received May 27, 1957

THE AMERICAN MINERALOGIST, VOL. 43, JANUARY–FEBRUARY 1958

SOME PROPERTIES OF DIAMOND*

E. N. BUNTING AND A. VAN VALKENBURG, *National Bureau of Standards, Washington 25, D. C.*

ABSTRACT

Measurements have been made of some of the optical, electrical, and other physical properties of more than eleven hundred gem diamonds. Tests included infrared transmission, spectrographic analyses, fluorescence under ultraviolet light, and conductivity measurements.

INTRODUCTION

Many of the differences found in the properties of natural diamonds could be understood if it were possible to prepare diamonds with no impurity or with controlled amounts uniformly dispersed throughout the crystal. As many as thirteen elements have been found in small amounts in diamonds although any one diamond is not likely to contain traces of more than seven elements. It has often been suspected that the nonuniformity in the impurity content was associated with some of the differences in properties.

One of these differences is in the ultraviolet and infrared absorption spectra (1). All diamonds show an absorption band in the five micron region and all but a few per cent also have considerable absorption over the 8 to 10 micron region and have been designated type I; only about one per cent have low absorption in this region and have been known as type II. This absorption band is not temperature sensitive, but the five micron band is sensitive to temperature and is connected with the thermal vibrations of the atoms (2). In the ultraviolet the type II is opaque at wavelengths less than about 2250 angstroms but type I is opaque below about 3000 angstroms. The opacity is lowered somewhat by long exposures (3). Those with values in between might be considered a modified type.

EXPERIMENTAL DATA

Out of eleven hundred gem-cut diamonds which were tested here recently for infrared transmission it was found that about seventy-four per cent were type I with very high absorption in the 8 to 10 micron region; twenty per cent were type I, modified, with moderate to high absorption; and only five per cent with moderate to low absorption which might be called type I, highly modified. Just ten gems were "pure" type II. Typical infrared patterns from a single beam spectrometer are shown in Figs. 1, 2, and 3, and contain the air bands present when a single

---

* This work was done under ONR Contract NAonr-123-52 NRO 32402.

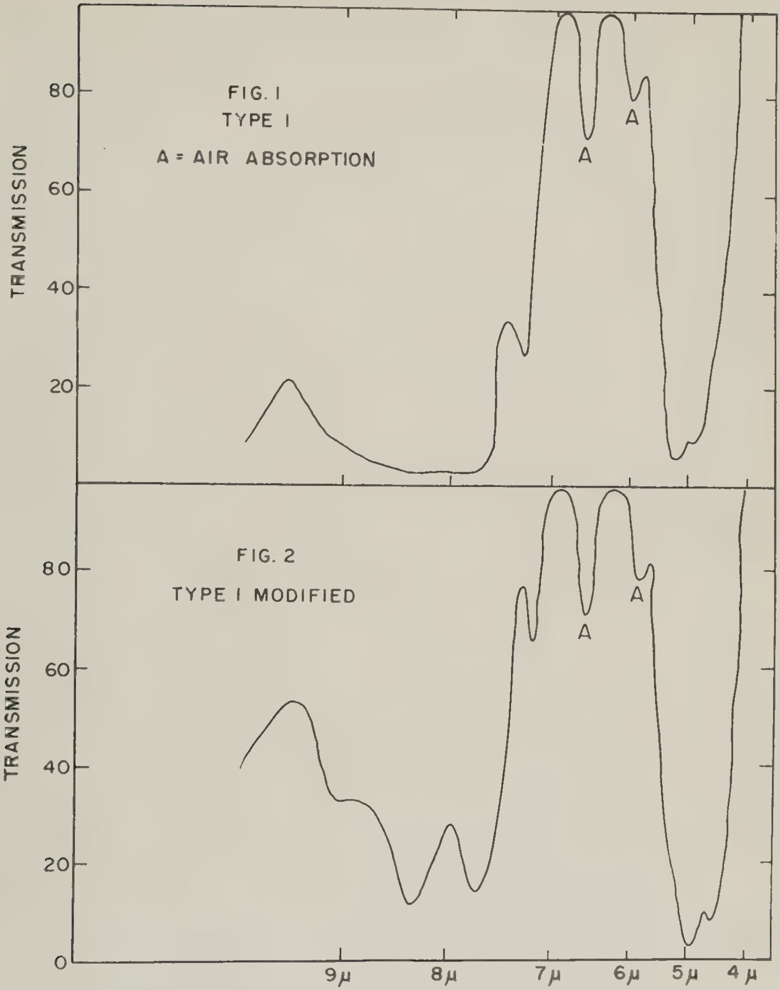

FIGS. 1 and 2. Infrared transmission in type 1 diamonds.

beam instrument is used. The resolution was not sharp because a wide 1 mm. slit was needed to obtain a suitable pattern for the gems without reducing them to a powder. Since most of the diamonds were between 0.2 and 0.5 carat and were not as long as the slit in the spectrometer, a platform had to be used in front of the slit to block off part of it and fix the gem so that the thin end just covered the top of the slit. When the gem was turned into the proper position, with two facets opposite one another, enough energy was admitted to give an acceptable pattern.

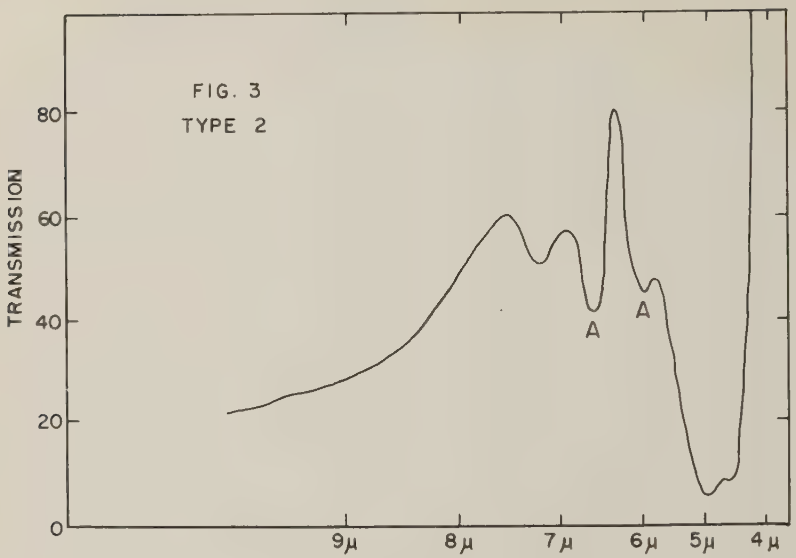

FIG. 3. Infrared transmission in type 2 diamonds.

It is apparent that this procedure does not give a quantitative measure of the transmission but is sufficient to indicate the type of gem being measured.

It is well-known that traces of impurities can change the color of some materials and it has been thought that the 8 to 10 micron absorption was an illustration of this fact. Some substantiation of this view has been reported by Chesley who found that the purest diamond among thirty-three was the only one which was a type II (4).

Three of each type were analyzed by spectrographic methods in our laboratories. The surfaces of the gems were cleaned with alcohol, aqua-regia, and distilled water before being analyzed. The results are given in Table 1. Thirty-six other elements were tested for but not found. No test was made for cesium, lithium, potassium, rubidium, or the rare-earth elements. There appears to be no evident correlation between the amount of impurity and the type of diamond, as one type I was as low as the type II in contaminants. To confirm further this conclusion, five additional diamonds, all type II, were analyzed and most of them were found to have as much impurity as any of the type I in the first group. These tests indicate that differences in impurity content cannot account for the variations in the absorption spectra. There is still the possibility that the presence of traces of the elements not tested for may be connected with the differences in absorption. Among others, Brophy (5) and Bishui (6) are of the opinion that the absorption differences between the two types are due to impurities, while Raman (7) believes these differences are connected with crystal structure variations.

Another variable property is the intensity and color of fluorescence under ultraviolet light. None of the ten type II, or of the type I highly modified gems showed any fluorescence. Those of type I which fluoresced always gave a blue or blue-green color. Several of the type I, slightly modified, and some of the type I, modified, also gave this color. No other color was noted in any of the gems tested, but one of the modified type which had a yellow-green fluorescence was reported by Rendall (8). This phenomenon has been thought to be connected either with structural differences or with the presence of the right impurities in the proper proportions. From ten to fifteen per cent of any batch of fifty or more gems showed fluorescence under a commercial ultraviolet lamp, emitting radiations between 2400 and 4000 Å, with peak emission at 3200 Å, and with about 700 microwatts per cm^2 of U-V energy.

Table 1. Results of Spectrographic Analyses

Element	Type I			Type II		
	No. 1	No. 2	No. 3	No. 4	No. 5	No. 6
Al	T	—?	T	FT	—?	—?
B	T	—?	T	—	VW	—
Ca	W	—	W	VW	T	—
Cu	VW	FT	T	VW	FT	FT
Fe	T	—?	T	VW	T	FT
Mg	T	FT	T	VW	T	FT
Na	W	—	W	W	—	—
Si	VW	FT	T	VW	T	FT

In general the symbols indicate the following concentration ranges as parts per millon of metal in the diamonds: W, 100–1000 ppm; VW, 10 to 100 ppm; T, 1 to 10 ppm; FT, less than 1 ppm; and dash (—), not detected. The gems weighed from 25 to 50 mg. each.

Although the diamond crystallizes in the cubic system and would be expected to be isotropic, the type I often shows birefringence. The type II is isotropic, or nearly so. It might seem plausible to attribute any anisotropy to the presence of impurities which could be expected to cause internal strain. Variations in the distribution of the contaminants might account for the various birefringence patterns that have been observed. We made no tests for birefringence.

Some diamonds have been found with a graphite coating which could have been formed while hot under diminished pressure, as the change always begins at the surface. Although diamond is not stable under ordinary conditions, its rate of transformation to graphite is practically zero and only above about 1300° C. does the rate become perceptible (9). When the thermal vibrations of its atoms become large enough to exceed 0.14 Å, the change to graphite can occur only under very high pressure. At 1500° C. this pressure must be greater than about 40,000 atmospheres and becomes higher with increasing temperature (10). One of the values used in calculating the graphite-diamond equilibrium is the thermal expansion. Previous measurements had not been made above 1000° C., but recently the thermal expansion has been determined here by x-ray methods to temperatures as high as 1400° C. (11). From 0° to 1400° C. the linear thermal expansion was found to be 0.58 per cent, with the coefficient changing from 1.3×10^{-6} at 25° C. to 7.0×10^{-6} at 1400° C.

Nearly all diamonds are good electrical insulators but a new rare type which is a semi-conductor was reported by Custers and designated type IIb (12). All blue diamonds are type IIb but not all of this type are blue. Their conductivity is attributed to the presence of many lattice defects probably produced by radiations from radioactive substances at one time in the vicinity of the crystal. This type will act as a crystal rectifier for small alternating currents. Types I and II do not conduct appreciably except at elevated temperatures. In measurements we made it was found that the conductivity versus temperature curve for these types showed a marked inflection at 750° to 800° C. which was present on both heating and cooling in helium from a maximum of 1250° C. Above 800° C. the conductivity increased much faster than at lower temperatures. No difference between the two types was shown by this test.

We are indebted to B. F. Scribner and Mrs. M. M. Darr of this Bureau for the spectrographic analyses, and to C. D. Smithson, of the General Services Administration, who obtained the diamonds for the Bureau of Standards.

REFERENCES

1. R. Robertson, J. J. Fox, and A. E. Martin. *Phil. Trans. of the Royal Soc. (London)* **232,** 463–535 (1933–34).
2. R. J. Collins and H. Y. Fan. *Phys. Rev.* **93,** 674–678 (1954).
3. K. G. Ramanathan. *Proc. Indian Acad. Sci.* **24A,** 130–44 (1946).
4. F. G. Chelsey. *Am. Mineral.* **27,** 20–36 (1942).
5. J. J. Brophy. *Physica* **22,** 156–158 (1956).
6. B. M. Bishui. *Indian J. Physics* **26,** 347–356 (1952).
7. C. V. Raman. *Proc. Indian Acad. Sci.* **19A,** 189 (1944).
8. G. R. Rendall. *Proc. Indian Acad. Sci.* **24A,** 168–175 (1946).
9. F. S. Phinney. *Science* **120,** 393–394 (1954).
10. R. Berman and Sir Francis Simon. *Z. Elektrochem.* **59,** 333–338 (1955).
11. F. A. Mauer and L. H. Bolz. Personal communication.
12. J. F. H. Custers. *Physica* **18,** 489 (1952); *Nature* **176,** 173 (1955).

Manuscript received May 3, 1957.

THE AMERICAN MINERALOGIST, VOL. 43, JANUARY-FEBRUARY 1958

A CHLORINE-RICH BIOTITE FROM LEMHI COUNTY, IDAHO

Donald E. Lee, *Stanford University, California.*

Abstract

A metamorphic biotite from Lemhi County, Idaho, has a chlorine content of 1.11 per cent and a fluorine content of 0.23 per cent. The biotite occurs in schist, associated with garnet, muscovite and quartz, smaller amounts of tourmaline and zircon, and a few rare grains of sphene. A complete analysis is given for the biotite, the mineralogy of the schist is described, and the features of its field occurrence are outlined.

Geologic Occurrence

A reconnaissance survey of the area was made in August, 1955. Biotite-garnet schist crops out for a distance of several hundred feet at about 45°07′ N, 114°18′ W, in Lemhi County, about 23 miles west of Salmon City, Idaho. The exposure is on a steep face along the north side of Big Deer Creek, about two miles east of its junction with Indian Creek.

The biotite-garnet schist occurs as irreglar pods, as much as six feet across, along the entire exposed length of a narrow shear zone that strikes northeast and dips about 30° NW. The shear zone is developed in a folded quartz-biotite schist of pre-Cambrian age. Acidic dikes, striking north-south, cut the quartz-biotite schist within 200 yards east of the shear zone; beyond the northern end of the shear zone the strike of these dikes swings toward the northwest. Granite has intruded the quartz-biotite schist within 500 yards of the shear zone both to the north and to the east, forming an arcuate contact concave toward the southwest. The acidic dikes were not observed to cut the granite.

Basic dikes also are exposed in the area, and the biotite-garnet schist may be a metamorphosed basic dike. Whether the rock is a metamorphosed dike or a rock developed in place out of sheared material, metasomatism has certainly played a role in its formation. The chlorine and fluorine contents of the biotite and the presence of tourmaline (boron) in the biotite-garnet schist are evidence of metasomatism; moreover the quartz-biotite schist "country rock" bordering the shear zone is locally impregnated with sulphides. Erythrite (cobalt bloom) and secondary copper minerals are present here and there immediately adjacent to the pods of biotite-garnet schist, and the shear zone along which this schist occurs probably has exerted a structural control on the sulphide mineralization. (Cobalt and copper have been known in this area since 1901. See for example Umpleby, 1913, pp. 71, 72 and 160.)

MINERALOGY

Biotite

This mineral makes up about 60 per cent of the rock. In thin section some garnet grains are seen to be partly rimmed by a thin coating of chlorite, formed mostly at the expense of biotite and suggesting incipient retrograde metamorphism. Also, a few biotite grains contain inclusions of zircon, some of which are surrounded by dark (not pleochroic) halos. But on the whole the biotite is remarkably fresh and free of inclusions, and the preparation of a clean fraction for analysis was acually a simple matter, certainly an unusual circumstance in the case of metamorphic biotite.

The following physical properties were determined on the material analyzed: Specific gravity $3.21 \pm .01$; $\alpha = 1.605 \pm .003$, $\beta = \gamma = 1.668 \pm .003$; $\gamma - \alpha = .063$; $2V = 0°$, or practically 0°, and pleochroism pronounced, with X = light olive green, and Y = Z = very dark olive green. The chemical analysis is given in Table 1.

The composition of this metamorphic biotite combines some of the

TABLE 1. BIOTITE, LEMHI COUNTY, IDAHO
Analyst: Eileen H. Oslund

	Weight per cent	Metal Atoms/12 Oxygens		
SiO_2	33.09	2.69		4.00
			1.31	
Al_2O_3	17.65	1.69		
			.38	2.93
TiO_2	1.30	.08		
Fe_2O_3	2.42	.15		
FeO	29.22	1.98		
MnO	.04	.003		
MgO	2.83	.34		
CaO	.10	.01		.98
Na_2O	.13	.02		
Rb_2O	.10	.005		
K_2O	9.04	.94		
BaO	.09	.003		
H_2O^+	2.92	1.58		1.79
F	.23	.06		
Cl	1.11	.15		
H_2O^-	.04			
Total	101.31			
Less O≡F & Cl	.34			
	99.97			

distinctive features of igneous biotites of several different parageneses (Heinrich, 1946, and Nockolds, 1947). For example, the high FeO content is what one might expect to find in biotite from granitic pegmatites or from alkalic igneous rocks, while the extremely low MnO is more typical of biotite associated with pyroxene and/or olivine.

But it is the chlorine content of this biotite that is most noteworthy. The highest chlorine content previously reported for the mineral is 0.24 per cent, in siderophyllite from Brooks Mountain, Alaska (Gower, 1957, p. 154). Other chlorine contents reported for the mineral are: 0.20 per cent, in biotite from a quartz monzonite at Butte, Montana (Weed, 1899, pp. 742–743); 0.18 per cent, in biotite from a quartz monzonite at Rockville, Minnesota and 0.11 per cent, in biotite from St. Lawrence County, New York (Kuroda and Sandell, 1953, pp. 889, 891). Kuroda and Sandell (1953, p. 889) state: "Determinations of chlorine in biotite are scarce, but the data available indicate that as much as 0.2 per cent is not uncommon." Correns (1956, p. 192) also points out the lack of information on chlorine in biotites.

The high chlorine content has no apparent effect on the optical propertities of the Idaho biotite. Hall (1941) has related the color of biotites to their contents of FeO, MgO, and TiO_2. The color of the Idaho biotite is in accord with Hall's findings. Heinrich (1946, p. 347) has graphed the relationship between index of refraction (γ) and chemical composition in the biotite-phlogopite series. Values for the Idaho biotite cross at a point almost exactly on his curve.

Garnet

Garnet, present almost exclusively as discrete euhedral grains 1–3 mm. across, makes up about 30 per cent of the rock. In impressive contrast to the biotite, the garnet is dirty with tiny inclusions. These are tourmaline, zircon, possibly rutile, and grains of unidentified material.

In grains of 0.07 mm. size the garnet has a pale mauve or lilac color in reflected light. In transmitted light these are pale pink to colorless, but grains of 0.15 mm. size exhibit a definite reddish hue. In addition, the following properties were determined: Specific gravity maximum $4.24 \pm .01$, minimum 4.20 ± 0.1, average 4.22; index of refraction maximum $1.818 \pm .003$, minimum $1.814 \pm .003$, average 1.816; and unit cell size 11.550 Å ± .003. The MnO content was determined by C. O. Ingamells of the University of Minnesota Rock Analysis Laboratory, to be 1.64 per cent, which is equivalent to a spessartite content of 3.8 molecular per cent.

Fleischer (1937), in a statistical study of 57 garnet analyses, confirmed Ford's (1915) thesis that there is a direct relationship between chemical composition and physical properties in the garnet group. The specific gravity, index of refraction and unit cells size values determined for this mineral suggest that other end member garnets (along with spessartite) are present in molecular per cents about as follow: almandine, 81–83; pyrope, 8–10, and grossularite and andradite, 5.

Tourmaline

Tourmaline is estimated to make up less than .05 per cent of the rock. It occurs as unzoned euhedral to subhedral grains, generally with biotite, but in some instances included in garnet. In both cases the *c* axis of the tourmaline tends to parallel the general schistosity of the rock. The tourmaline crystals associated with biotite are fairly uniform in size, with an average length of about 0.06 0.07 mm.; the grains included in garnet are somewhat smaller.

The following physical properties were determined: Specific gravity = 3.18±.02; uniaxial, with $o=1.665$, $e=1.635$; both ±.003; $o-e=.030$, and pleochroism intense, from dark bluish green or black (o) to pale reddish violet (e). Therefore the mineral must contain a high molecular per cent of the iron tourmaline, schorlite, which one would expect in view of the compositions of the associated minerals.

Zircon

This mineral probably comprises less than 0.1 per cent of the rock, but the small portion recovered during fractionation work is worthy of special note. In reflected light the mineral has an ash-gray color. Under the microscope most grains are 0.05–0.15 mm. long, and although zircon is noted for its resistance to attack and alteration, these grains have suffered severe corrosion and pitting; crystal faces have been completely obliterated. Perhaps these zircons were originally detrital in the quartz-biotite schist "country rock," only to be mixed with the basic dike during the time of shearing. Thus incorporated into the original materials of the biotite-garnet schist, they would be exposed for a time to the rigors of a pneumatolytic environment.

Other Minerals

Muscovite, intergrown with the biotite, probably amounts to more than five per cent of the rock. Quartz is only about a third as abundant as muscovite. A few rare grains of fresh-looking sphene were encountered during the fractionation process, but this mineral is not apparent in thin section. Minor quantities of an unidentified yellow secondary mineral are forming along fractures in the garnets.

CONCLUSIONS

As mentioned above, Kuroda and Sandell (1953, p. 889) and Correns (1956, p. 192) have pointed up the need for further determinations of chlorine in micas. To this one might add that the presence of chlorine is especially to be suspected when careful analysis of a mica gives a low total for the oxides and fluorine, and calculations show the deficiency to be in the (OH) group.

ACKNOWLEDGMENTS

The chemical analysis of the biotite presented here was made possible by the Shell Oil Company through the Shell Grant for Fundamental Research.

It is a pleasure to acknowledge the help received during this study from Dr. Samuel S. Goldich and Mrs. Eileen H. Oslund of the University of Minnesota Rock Analysis Laboratory. The chlorine content of the biotite described was detected and determined by Dr. Goldich and Mrs. Oslund solely on their own initiative, when the oxide and fluorine determinations requested gave a low total, and their calculations showed the deficiency to be in the (OH) group. Thus the discovery of the most remarkable feature of the biotite described in this paper is largely a result of their research.

BIBLIOGRAPHY

1. CORRENS, CARL W. (1956), The geochemistry of the halogens: in *Physics and Chemistry of the Earth,* Edited by Ahrens, L. H., Rankama, Kalervo and Runcorn, S. K., McGraw-Hill, pp. 181–233.
2. FLEISCHER, M. (1937), The relation between chemical and physical properties in the garnet group: *Am. Min.*, **22,** pp. 751–759.
3. FORD, W. E. (1915), A study of the relations existing between the chemical, optical and other physical properties of the members of the garnet group: *Am. Jour. Sci.*, Ser. 4, **40,** pp. 33–49.
4. GOWER, JOHN ARTHUR (1957), X-ray measurement of the iron-magnesium ratio in biotites: *Am. Jour. Sci.*, **255,** No. 2, pp. 142–156.
5. HALL, A. JEAN (1941), The relation between color and chemical composition in the biotites: *Am. Min.*, **26,** pp. 29–33.
6. HEINRICH, E. WM. (1946), Studies in the mica group; the biotite-phlogopite series: *Am. Jour. Sci.*, **244,** No. 12, pp. 836–848.
7. KURODA, P. K. AND SANDELL, E. B. (1953), Chlorine in igneous rocks: *Bull. Geol. Soc. Am.*, **64,** pp. 879–896.
8. NOCKOLDS, S. R. (1947), The relation between chemical composition and paragenesis in the biotite micas of igneous rocks: *Am. Jour. Sci.*, **245,** No. 7, pp. 401–420.
9. UMPLEBY, JOSEPH B. (1913), Geology and ore deposits of Lemhi County, Idaho: *USGS. Bull.* **528,** 182 pp., esp. pp. 71, 72, 160.
10. WEED, WALTER HARVEY (1899), Granite rocks of Butte, Montana, and vicinity: *Jour. Geol.*, **7,** No. 8, pp. 737–750, esp. pp. 742–743.

Manuscript received May 17, 1957.

THE AMERICAN MINERALOGIST, VOL. 43, JANUARY-FEBRUARY 1958

NOTES ON TAPIOLITE, WITH SPECIAL REFERENCE TO TAPIOLITE FROM SOUTHERN WESTLAND, NEW ZEALAND

C. OSBORNE HUTTON, *Stanford University, California.*

ABSTRACT

An occurrence of rare particles of the multiple oxide tapiolite in beach sands near Otorokua Point, southern Westland, New Zealand, is recorded. For this mineral the following data have been determined: $O_{Na}=2.33\pm0.01$, $E_{Na}=2.53\pm0.04$. $E-O=0.20$. O=pale brown, E=reddish-brown to opaque. $E>O$. $S.G._{21°C.}=7.65$. *X*-ray diffraction powder patterns show that the mineral has a true trirutile structure with unit cell dimensions of $a_0=4.750$ Å, $c_0=9.208$ Å, and with *d*-spacings and intensities that are comparable to those recorded for analyzed tapiolite from Brazil and Morocco, but distinct from the pattern yielded by unheated tapiolite from Skogsbole, Finland. The latter occurrence is shown to have a rutile structure but, after appropriate heat-treatment, a trirutile structure is developed with resultant denser packing of the atoms. Unit cell dimensions for ordered and disordered Skogsbole tapiolite, determined from quartz-calibrated Weissenberg films, are $a_0=4.752$ Å, $c_0=9.204$ Å, and $a_0=4.753$ Å, and $c_0=3.092$ Å respectively.

INTRODUCTION

A recent examination of some specimens that were collected in southern Westland, New Zealand in the early part of 1954, led to the recognition of kobeite as a constituent of a granite boulder from the gravels of the Paringa River. In order to determine if this or other tantalum-niobium-titanium-bearing minerals might be represented in the heavy mineral assemblages of the local sands and silts, a careful study was made of a number of concentrates also obtained at that time. Kobeite has not been detected so far in any of these samples, but rare particles of tapiolite were isolated from two concentrates obtained by panning blacksand paystreaks on the beach just north-east of Otorokua Point, north-east of the mouth of Cook River (latitude 43°25′ South, longitude 169°48′ East).

Consequently this is the second tantalum-rich mineral that has been recorded from southern Westland but, unfortunately, neither mineral has been found in situ and both appear to be distinct rarities.[1] The only other tantalum-bearing minerals recognized and recorded from New Zealand are cassiterite and monazite (Hutton, 1950, pp. 656–658; 667–669) from southern Nelson and northern Westland, and yttrotantalite from Collingwood, Nelson (Morgan, 1927, p. 107); furthermore Morgan (1927, pp. 99) has stated that concentrates from Addison's, near Westport, Nelson, have been found to contain considerable amounts of Ta_2O_5, but in this instance the specific tantalum-bearing mineral or minerals have not been recognized.

---

[1] An occurrence of kobeite in boulders from Paringa River has been described recently (Hutton, 1957).

MINERALOGY

After removal of ferromagnetic material, 9.6% and 10.2% respectively, from two 3 kg. samples the concentrates were screened[2] to give the following fractions: +32: 3.0%, 3.4%; −32+60: 30.8%, 32.6%; −60+115: 55.7%, 52.9%; −115+250: 0.8%, 0.5%; −250: 0.1%, 0.4% respectively. These fractions, the two finest grade sizes excepted, were carefully fractionated in Clerici solution that had been adjusted to a density of 4.0, and the heavy fraction of each grade-size was subsequently split electromagnetically into several fractions. The resultant material was then studied in oblique illumination with a binocular microscope.

Rare particles of tapiolite were found in the small concentrates attracted at 0.45 amps. and rejected at 0.3 amps.[3] in both −16+32 and −32+60 mesh material. Garnet and monazite were the chief associates of tapiolite in these fractions, whereas, in the same size-fractions untreated in Clerici solution but electromagnetically separated, clinozoisite-epidote, clear brown and intensely dichroic tourmaline, non-metamict allanite, pale pink garnet, sphene, monazite, and composite fragments were recognized.

Tapiolite forms highly irregular conchoidally bounded particles with vitreous luster, that are opaque in oblique illumination except at the thinnest edges. In transmitted light very fine fragments of the mineral are translucent and deep brown to red-brown in color. All fragments appeared to be devoid of inclusions and free from any alteration phenomena. The refractive index of the ordinary ray was determined to be 2.33 ±0.01 in sodium light, but a value for E is reported with considerable reservations, *viz.* 2.53_{Na}, because the intensity of absorption for the extraordinary ray only permitted one to obtain results reproducible within a range of ±0.04. Dichroism is intense with O = pale brown, E = deep reddish brown; opaque in thicker fragments; $E > O$. The specific gravity, determined for a collection of particles that had a total weight of 11.9 mgm., is 7.65 at 21° C., a figure that definitely points to a highly tantalian variety rather than to mossite. Isolated fragments of tapiolite were found to have a narrow range of magnetic susceptibility, since they were rejected at 0.40 amps. but attracted at 0.45 amps., with the Frantz separator set as for the main fractionation reported above.

Excellent *x*-ray diffraction powder patterns of the trirutile type were obtained and the *d*-spacings and relative intensities (Table 1) are, except for quite minor points, closely comparable to those recorded by Tavora and Peixoto (1951, p. 451) and Permingeat (1955, p. 137) for tapiolite from Mecejana, Brazil, and Iguerda and Tazenakht, French Morocco, respectively. A number of very faint lines and the rather weak (505) reflection yielded by southern Westland tapiolite are not recorded by Permingeat (1955, p. 137, Table 1), although they may be seen in the author's own film yielded by Angarf, Plaine de Tazenakht tapiolite. Tavora and Peixoto (1951, p. 451, Table 1) do not record very weak reflections at 1.930 Å, 1.134 Å, .978 Å, although Tavora (1955, Fig. 6B) does indicate the presence of the (226) reflection, that is the second of the lines just noted, in his photograph of a tapiolite powder pattern. It

---

[2] Tyler standard screen scale.

[3] The Frantz separator was set as follows: tilt 10°, slope 15°.

TABLE 1. *X*-RAY DIFFRACTION DATA FOR TAPIOLITE FROM WESTLAND, NEW ZEALAND AND SKOGSBOLE, FINLAND

Radiation: CuKα ($\lambda = 1.5418$ Å). Camera Diameter: 114.59 mm.

New Zealand				Skogsbole, Finland						
	Unheated			Heated			Unheated			
hkl	*d*. meas. Å	*d*. calc. Å	I	*d*. meas. Å	*d*. calc. Å	I.	*d*. meas. Å	*d*. calc. Å	I.	*hkl*
002	4.62	4.60	2	4.58	4.60	2				
101	4.22	4.23	3	4.22	4.22	3				
110	3.37	3.36	10	3.35	3.36	10	3.35	3.36	10	110
112	2.71	2.716	2	2.712	2.715	2				
103	2.58	2.58	9	2.572	2.578	9	2.58	2.59	9	101
200	2.375	2.374	5	2.371	2.375	5	2.37	2.37	5	200
004				2.300	2.301	<1				
113	2.265	2.267	2	2.265	2.265	2	2.27	2.27	2	111
210	2.125	2.125	1	2.125	2.126	1	2.12	2.12	1	210
202	2.114	2.111	1	2.112	2.112	1D				
211	2.067	2.070	2	2.069	2.071	2				
212	1.930	1.930	<1							
114	1.900	1.899	<1	1.900	1.899	1				
213	1.747	1.748	9	1.745	1.746	9	1.75	1.753	9	211
105	1.716	1.718	<1	1.714	1.717	1				
220	1.677	1.679	5	1.679	1.680	5	1.678	1.681	5	220
204	1.652	1.653	<1	1.651	1.653	1				
222	1.5775	1.577	1	1.577	1.579	1				
301	1.560	1.560	<1	1.562	1.562	<1				
006	1.534	1.535	2	1.533	1.534	2	1.546	1.546	2	002
310	1.501	1.503	5	1.502	1.504	5	1.503	1.505	5	310
312	1.429	1.429	1	1.428	1.430	1				
303	1.407	1.407	5	1.408	1.408	5	1.411	1.411	5	301
116	1.395	1.396	5	1.397	1.396	5	1.405	1.405	5	112
215		1.392			1.392					
224	1.357	1.357	<1	1.357	1.357	<1				
321	1.302	1.303	<1	1.304	1.305	<1				

I: Intensity, determined visually
D: Diffuse line.
B: Broad line.

TABLE 1. (*continued*)

	New Zealand			Skogsbole, Finland						
	Unheated			Heated			Unheated			
hkl	*d*. meas. Å	*d*. calc. Å	I.	*d*. meas. Å	*d*. calc. Å	I.	*d*. meas. Å	*d*. calc. Å	I.	*hkl*
206	1.289	1.289	3	1.290	1.290	2	1.2985	1.296	2	202
107		1.268			1.267					
314	1.256	1.257	<1	1.258	1.258	<1				
323	1.212	1.211	4	1.210	1.210	4	1.212	1.213	4	321
305		1.200			1.201					
400	1.188	1.188	1	1.188	1.188	1	1.189	1.189	1	400
410	1.1525	1.152	<1		1.153		1.154	1.154	<1	410
402, 008	1.150	1.150	<1	1.151	1.151	<1				
411	1.144	1.1435	<1	1.145	1.144	<1				
226	1.134	1.133	3	1.134	1.133	2	1.139	1.139	2	222
330	1.120	1.120	2	1.120	1.121	1	1.121	1.1205	2	330
217		1.119			1.119					
118, 332	1.0895	1.089	<1	1.090	1.089	1				
413	1.0785	1.081	3	1.079	1.079	3	1.080	1.081	3D	411
316	1.075	1.074	3	1.074	1.074	2	1.079	1.079	3D	312
325		1.072			1.072					
420	1.063	1.062	2	1.063	1.063	<1	1.063	1.064	1	420
404		1.055			1.056					
208, 422	1.036	1.036	<1	1.036	1.036	<1				
307		1.012			1.012					
334		1.007			1.0075					
109	1.001	1.000	2	1.001	1.000	1	1.008	1.008	1	103
415	.978	.977	<1	.977	.977	<1				
424	.965	.965	<1	.965	.965	<1D				
228	.951	.950	<1	.950	.950	<1				
431, 501	.946	.945	<1	.946	.946	<1				
406	.940	.940	2	.9405	.940	2	.9435	.942	1	402
327, 510	.932	.932	2	.932	.932	2	.933	.932	1	510
416, 219	.923	.922	3	.922	.922	3	.929	.927	2	412, 213
318, 512	.915	.914	<1	.9145	.914	<1				
433, 503	.9085	.907	4	.908	.908	4	.910	.9085	4BD	431, 501
336	.906	.905	4	.905	.905	4	.9065	.9065	4D	332
1·1·10		.889			.888					
521		.878			.879					
426	.874	.874	3	.874	.874	3	.877	.8765	3	422
417		.866			.8665					
514		.863			.864					
309	.8605	.860	2	.859	.8595	2	.864	.863	1	303
2·0·10		.859			.8585					
523	.849	.848	4	.849	.849	4	.8495	.849	3	521
505	.845	.845	2	.846	.845	1				
440	.840	.840	1	.8405	.840	1	.841	.840	1	440
408, 442	.827	.8265	<1	.827	.827	<1				
530	.815	.815	2	.815	.815	2	.8155	.815	1	530
329	.8095	.809	4	.809	.809	4				
532	.8035	.803	<1	.803	.803	1				
516	.7975	.797	5	.797	.797	5	.800	.799		512
525		.796			.796					
600	.793	.792	1	.7925	.7925	1	.7925	.792	<1D	600
444		.789			.790					
3·1·10		.785			.785					
602, 428	.782	.780	<1	.781	.781	<1				
611	.779	.7785	<1	.779	.779	2				

might be noted here that Tavora (1955, Fig. 6B) incorrectly labels the reflection at 1.001 Å in his film as (104) instead of (109).

Employing powder patterns of southern Westland tapiolite, tentative values for a_0 and c_0 were subsequently refined to give $a_0=4.750$ Å and $c_0=9.208$ Å; this leads to a ratio $a_0:c_0$ of 1:1.9385, that is intermediate in value to those recorded by Palache, Berman, and Frondel (1944, p. 775) for the tapiolite-mossite series, *viz.* 1:1.941 to 1:1.936, yet larger than the ratio of 1:1.942 reported by Tavora and Peixoto (1951, p. 451). Furthermore, the close relationship between the structures of tapiolite and rutile is clearly brought out if the value $c_0/3a_0$ for southern Westland tapiolite is compared with the ratio $a_0:c_0$ for rutile, *viz.* 0.646 and 0.644 respectively (cf. Goldschmidt, 1926, p. 18).

For comparative purposes a powder pattern was obtained with tapiolite from Skogsbole, Finland and, while the latter is comparable in a general way with the pattern yielded by southern Westland tapiolite, a considerable number of lines present in the film yielded by the latter mineral are absent from the former, but the relative intensities of the lines common to the two films are quite similar. Furthermore, there are significant shifts in the relative positions of several of the stronger lines; reflections at 1.411 Å, 1.405 Å, 1.139 Å, 1.080 Å, 1.079 Å, and .929 Å are especially noteworthy in this connection. If fragments of Skogsbole tapiolite are now heated in vacuo at 600° C. for $\frac{3}{4}$ hour a pattern is obtained that is identical to that yielded by southern Westland tapiolite, except for a very slight shift in the positions of lines due to somewhat different cell dimensions in the two cases, and a slight diffuseness in the reflections at high 2θ values in the film of the former mineral. However, if Skogsbole tapiolite is heated in vacuo at 1200° C. for one hour, the lines in the back-reflection region of the pattern are quite clearly and precisely resolved.

This situation is clearly indicative of an order-disorder relationship for the tetragonal compound $Fe(Ta,Nb)_2O_6$, a condition that has already been noted for tapiolite from Ross Lake, Northwest Territories (Hutchinson, 1955, p. 443), and for a number of AB_2X_6 compounds in general Byström, Hök, and Mason, 1941, pp. 1–8). In most of the films yielded by unheated or disordered Skogsbole tapiolite traces of a number of weak lines, normally found in the ordered phase, were detected. This would seem to suggest that, in unheated tapiolite, domains exist in the crystals in which some degree of order is apparent, and others that are in a state of disorder. In an attempt to verify this situation a number of very small particles of unheated Skogsbole tapiolite, 0.1 mm. in diameter, were hand-picked, crushed in gum tragacanth, and *x*-rayed. The films yielded by these preparations appear to support the suggestion just offered since a number of the lines due to the trirutile structure are present although faint in some films, but only barely detectable in others.

After a number of attempts, a fragment of Skogsbole tapiolite was obtained that yielded a rotation photograph that was strictly of the rutile type. Measurements of rotation and quartz-calibrated Weissenberg films led to cell dimensions of $a_0 = 4.753$ Å and $c_0 = 3.092$ Å, both values ±0.002 Å. This identical crystal fragment when heated in vacuo at 1200° C. for one hour yielded *a*- (or *b*-) axis rotation films with the same number of layer-lines as found for similar orientations of unheated tapiolite, but with many more reflections present than in similar films of the unheated mineral. The recrystallized mineral yielded *c*-axis photographs with six layer-lines compared with only two in the unheated mineral, and the 3rd layer of the former corresponds to the 1st layer of the latter. Furthermore, the reflections of the zero and 3rd layers are very much more intense than those in the 1st, 2nd, 4th and 5th layers, all of which are relatively weak. Accordingly a marked superlattice is evident in the trirutile or ordered form.

Measurements of the rotation and quartz-calibrated Weissenberg films yielded by heated Skogsbole tapiolite, give unit cell dimension of $a_0 = 4.752$ Å and $c_0 = 9.204$ Å, ±0.002 Å. Now if we compare these data with the unit cell dimensions, $a_0 = 4.753$ Å and $3 \times c_0 = 9.278$ Å, determined for the unheated or disordered Skogsbole tapiolite it is clear that the ordered form, with a trirutile structure, has a cell volume that is distinctly less than that of the disordered phase, namely 207.840 Å^3 and 209.599 Å^3 respectively. The specific gravities of unheated and heated Skogsbole tapiolite are interesting in this connection. For three fragments the following specific gravities were measured[4] before and after heating to 1200° C. for one hour in vacuo; the weights of the particles used are recorded in parentheses in each case: 7.50, 7.51 (9.70 mgm.); 7.50, 7.51 (10.95 mgm.); 7.502, 7.508 (18.46 mgm.).

In Table 1 the measured and calculated *d*-spacings for unheated, but ordered, tapiolite from south Westland are set out and are compared with the data obtained for both the ordered and disordered phases of the Skogsbole mineral. In the ordered forms it should be noted that a number of weak reflections were found on Weissenberg films, which have not been detected in the powder patterns.

An attempt has been made to determine the amount of heat-treatment required to cause an approach to a state of order in Skogsbole tapiolite, and a summary of this work is set out in Table 2. In every case samples were sealed in vacuo in silica or high-silica glass capillaries; then each

---

[4] These figures represent the average of five determinations in each instance.

TABLE 2. SUMMARY OF RESULTS OBTAINED BY HEAT-TREATMENT OF SKOGSBOLE TAPIOLITE

Temp. in °C.	Period of heating	Result
300	1, 2, 4, 8, 12, 24 hrs.	Disorder maintained.
	168 hrs.	Disorder maintained.
450	24 hrs.	Disorder maintained.
	48 hrs.	Slight amount of ordering.
500	1, 2, 3, 4, 5, 7 hrs.	Disorder maintained.
	15½ hrs.	Almost completely ordered.
	24 hrs.	Complete order.
600	5, 10, 15, 20 mins.	Disorder maintained.
	25, 30 mins.	Slight degree of order.
	35 mins.	Almost completely ordered.
	45 mins.	Ordered.
1200	1 hr.	Ordered.
1360	30 mins.	Slight amount of disorder.

tube was inserted in turn into an already heated furnace, and after the correct period of heating, the tube was withdrawn, and cooled rapidly to room temperature.

In films yielded by fragments heated at 1360° C., a marked diffuseness was evident in reflections at high 2θ values, and this effect may result from either of two situations: (*a*) the disordering temperature may have been reached, or (*b*) decomposition has commenced, but since no sintering together of fragments or dulling of the sharp edges of conchoidally fractured particles occurred as a result of heating, the first alternative is tentatively believed to be the more acceptable.

ACKNOWLEDGMENTS

I wish to acknowledge the opportunities provided for this research by the award of a John Simon Guggenheim Foundation Fellowship. I am indebted to Professor C. Alvarez-Tostado who very kindly heated one specimen to 1360° C. My appreciation is extended also to Mr. Jules Agard of the Sérvice géologique du Maroc, Rabat, for his kindness in providing me with a fine specimen of tapiolite from Morocco.

REFERENCES

BYSTRÖM, A., HÖK, B., AND MASON, B. (1941), The crystal structure of zinc metantimonate and similar compounds: *Arkiv för kemi, min. o. geol.*, **15**, 4, 1–8.

GOLDSCHMIDT, V. M. (1926), Geochemische Verteilungsgesetze der Elemente. VI. Über die Krystallstructuren vom Rutiltypus mit bermerkungen zur Geochemie Zweiwertiger und Vierwiertiger Elemente: *Vidensk.-Akad. i. Oslo I, Mat.-Nat. Kl., Skr.* **1**, paper 1, 5–21.

HUTCHINSON, R. W. (1955), Preliminary report on investigations of minerals of columbium and tantalum and of certain associated minerals: *Am. Mineral.*, **40,** 5/6, 432–452.

Hutton, C. Osborne (1950), Studies of heavy detrital minerals: *Bull. Geol. Soc. Amer.*, **61,** 635–716.

——— (1957), Kobeite from Paringa River, south Westland, New Zealand; *Am. Mineral.*, **42,** 342–353.

Morgan, P. G. (1927), Minerals and mineral substances of New Zealand: *N. Z. Geol. Surv.*, Bull. **32,** 1–110.

Palache, C., Berman, H., and Frondel, C. (1944), *Dana's System of Mineralogy, 7th. Ed.*, vol. 1, John Wiley and Sons, Inc., New York.

Permingeat, F. (1955), Sur les niobo-tantalates de l'Anti-Atlas, Maroc: Tapiolite et columbite: *Bull. Soc. Franç. Mineral. Crist.*, **78,** 123–156.

Tavora, E. (1955), X-ray diffraction powder data for some minerals from Brazilian localities: *Anais da Acad. Brazil de Ciênc.*, **27,** 1, 7–27.

Tavora, E., and Peixoto, F. (1951), Lattice constants of tapiolite from Mecejana, Fortaleza County, Ceará: *Anais da Acad. Brazil de Ciênc.*, **23,** 4, 449–454.

Manuscript received May 31, 1957.

THE AMERICAN MINERALOGIST, VOL. 43, JANUARY–FEBRUARY 1958

ALTERATION OF OLIVINE AND ORTHOPYROXENE IN BASIC LAVAS AND SHALLOW INTRUSIONS

H. G. Wilshire, *University of Sydney, Sydney, Australia.*

Abstract

Alteration products of olivine and orthopyroxene, previously identified as iddingsite, bowlingite, and serpentine among other minerals, have been found to consist predominantly of mixed layer smectite-chlorite with a variety of accessory minerals. Alteration products from shallow basic intrusions may contain antigorite or chrysotile as well as smectite-chlorite, and are much richer in MgO than those from basic lavas. Optically isotropic varieties (chlorophaeite) are closely associated with smectite-chlorite minerals and sometimes have a poorly developed chlorite (?) structure.

It is probable that all of these secondary minerals can form by deuteric alteration, but evidence is presented which suggests that oxidized varieties (commonly containing goethite) may also form by weathering of green varieties. Implications of chemical and physical properties are discussed and it is concluded that equal volume replacement of Mg-rich olivine or orthopyroxene in basic lavas results in selective leaching of Mg which may be removed from the altered rock and recombined in the same secondary minerals in joints. Quantitative data for the effects of alteration on bulk composition of the enclosing rock are presented. In shallow intrusions, where there is little evidence of Fe-enrichment in residual solutions, complete solution of olivine is possible. Application of these results to some problems in soil clay mineralogy is briefly considered.

Introduction

Although many optical, chemical and *x*-ray data are now available for alteration products of olivine and orthopyroxene in igneous rocks, little attempt has been made to organize these data, with the consequence that relations among alteration products are not clearly understood and misidentifications based on inadequate data are common. The object of this study is to identify typical alteration products by *x*-ray techniques, to attempt an integration of ideas concerning their mode of origin and relationships, and to discuss possible implications of these relationships. A sampling problem is recognized in view of the widespread occurrence of these minerals and has been accounted for to some extent by selection of material from widely separated localities.

Previous Work

It is impossible to be exhaustive in the treatment of previous work, for the literature on these minerals is very large. Among the more important contributions are those of Ross and Shannon (1926) whose chemical formula of iddingsite is quoted in most textbooks, Peacock and Fuller (1928) who have presented the most comprehensive study of the occurrence and mode of origin of chlorophaeite, and Caillere (1935) and Caillere and Henin (1951) whose *x*-ray and thermal studies of bowlingite have led to redesignation of this mineral as saponite.

METHODS OF INVESTIGATION

X-ray powder photography using a Philips *X*-ray Diffraction unit was the principal method used in identification. Filtered copper radiation was found adequate except with optically isotropic material. Some basal spacing expansions were obtained from oriented aggregates using a Philips Geiger Counter Spectrometer with filtered copper radiation.

Refractive index measurements were made with standard immersion oils which were checked with a Leitz-Jelley refractometer. Olivine compositions were determined from n_y using Kennedy's curves (Troeger, 1951, p. 37). Refractive indices of the alteration products are quoted only to the nearest second decimal place because the index varies with the type of immersion oil used.

Plagioclase compositions were determined with the universal stage microscope using Turner's (1947) method and van der Kaaden's (1951) data. All measurements of 2V were also made with the universal stage microscope. All other mineral identifications and fabric descriptions were made with a standard petrographic microscope.

MODE OF OCCURRENCE AND IDENTIFICATION

In basic lavas olivine and orthopyroxene are commonly altered to a reddish-brown substance with high birefringence and refractive indices ranging from approximately 1.61 to 1.86. This is usually identified as iddingsite if it is pseudomorphic after olivine, and is assigned the chemical formula, $MgO \cdot Fe_2O_3 \cdot 3SiO_2 \cdot 4H_2O$ (Ross and Shannon, 1926). Average chemical analyses of iddingsite are given in Table 4A. Optically identical material in amygdules and joints is sometimes called chlorite. A recent *x*-ray investigation of iddingsite (Ming-Shan Sun, 1957) revealed the presence of goethite mixed with amorphous substances.

A green substance with moderate birefringence and refractive indices ranging from approximately 1.48–1.62 is also a common alteration product of olivine and orthopyroxene and is exceptionally abundant in shallow basic intrusions. Optically identical material occurs in amygdules and joints. This material has been assigned a wide variety of mineral names including bowlingite, serpentine, chlorite, nontronite, saponite, and vermiculite. Average chemical analyses, all of saponite from shallow intrusions, are given in Table 4A. *X*-ray and thermal studies by Caillere and Henin (1951) indicated a montmorillonite-type structure and this, combined with the chemical composition, led them to redefine bowlingite as saponite. Other *x*-ray powder studies of minerals fitting the optical

TABLE 1. *X*-RAY DATA: SAMPLES UNTREATED

Group 1											
1			2			3			4		
d	I*	Id†	*d*	I	Id	*d*	I	Id	*d*	I	Id
14.0 Å	m	S	14.0 Å	m	S	15.49 Å	ms	S	7.3 Å		
4.80	vw	S	4.92	vw	G; S	4.52	s	S	7.0	mw	K
4.46	m	S	4.49	ms	S	4.30	vw	F?	4.47	s	K
4.18	s	G	4.15	vs	G	3.37	vw	Q?	4.19	vs	G; Q
3.70	vw	F	3.71	vw	F	3.26	vw	F?	3.35	vs	G; Q; K
3.35	vw	Q	3.33	w	Q	2.59 —			3.22	vw	K
3.21	m	F	3.20	m	F	2.52	m	S	2.72	vw	K
2.94	vw	F	2.70	m	G; S	1.71	w	S	2.66	vw	G
2.69	m	G; S	2.59	m	S	1.513	mw	S	2.55	m	K
2.59	w	S	2.50	vw	S				2.43	ms	G; Q
2.52	vw	S	2.44	s	G				2.28	vw	G; K
2.44	ms	G	2.25	vw	S				2.24	vw	G; Q; K
2.22	vw	S	2.15	vw	S				2.19	vw	G; K
1.71	m	G; S	1.96	vw	S				2.12	vw	Q; K
1.56	vw	S	1.79	vw	S				1.82	vw	Q; K
1.509	w	S	1.72	s	G; S				1.71	w	G; K
1.455	vw	S	1.60	vw	S				1.67	w	Q; K
			1.563	vw	S				1.544	mw	Q; K
			1.510	mw	S				1.495	mw	G; K
			1.460	vw	S				1.459	vw	G; K
									1.377	w	Q

* I =intensity, visually estimated.

† Id =identification. S =smectite-chlorite; F =feldspar; G =goethite; Mg =magnetite; Ca =calcite; Q = quartz; Mi =mica; T =talc; Se =sepiolite; Sp =serpentine; K =kaolinite.

1. Carmel Bay, California. Pseudomorphs after olivine.
2. Carmel Bay, California. Pseudomorphs after olivine.
3. Santa Rosa, California. Pseudomorphs after olivine.
4. Orange, New South Wales. Joint-filling.

Group 2									Group 3		
5			6			7			8		
d	I	Id	*d*	I	Id	*d*	I	Id	*d*	I	Id
14.0 Å	vs	S	16.0 Å			15.4 Å			15.0 Å		
7.13	vvw	S	14.5	vs	S	14.0	vs	S	14.0	s	S
4.60	m	S	7.8 —			4.55	m	S	7.4 —		
4.25	vw	Q	7.0	vvw	S	4.25	mw	Q	7.0	s	S; Sp
4.02	vw	F	5.0	vw	S	3.70	vw	F	4.83	m	S
3.33	w	Q	4.52	s	S	3.34	s	Q	4.57	m	S
3.17	s	F	4.26	vw		3.19	w	F	3.84	w	Ca
3.03	w	Ca	3.21	m	F	2.96	m	Mg; F	3.61	m	S; Sp
2.95	w	F	2.59	s	S	2.70	w	S	3.03	vs	Ca
2.88	m	F	2.47	mw	S	2.59	vw	S	2.89	vw	S
2.83	w	S	2.28	vw	S	2.52	vs	Mg; S	2.65 —		
2.71	w	S	2.20	vw	S	2.44	vw	S	2.41	w	S
2.54	w	S	1.90	vvw	S	2.29	vw	S	2.50	mw	Ca; S; Sp
2.50	w	S	1.72	w	S	2.12	vw	S	2.28	m	Ca; S
2.47	w	S	1.533 —			2.09	m	Mg; S	2.09	m	Ca
2.12	vw	S	1.512	s	S	1.82	vw	Q; S	1.91	ms	Ca
2.09	vw	S	1.314	w	S	1.71	w	Mg; S	1.87	ms	Ca
2.05	vw	S				1.66	vw	S	1.74	vw	S
1.99	vw	S				1.61	m	Mg; S	1.63	vw	Ca
1.96	vw	S				1.535	w	Q; S	1.60	w	Ca
1.74	vw	S				1.515	vw	S	1.540	s	S
1.546	vvw	S				1.480	ms	Mg; S	1.506	mw	S
1.531	m	S				1.453	vw	S	1.443	w	Ca
1.487	w	S				1.379	w	Q; S	1.418	w	Ca
1.472	w	S							1.326	vw	S
1.387	vw	S							1.299	vw	S
									1.230	vw	S

5. Ebbetts Pass, California. Pseudomorphs after hypersthene.
6. Orange, New South Wales. Joint-filling.
7. Carmel Bay, California. Pseudomorphs after olivine.
8. Prospect Hill, Sydney, New South Wales. Joint-filling.

TABLE 1. (*continued*)

Group 3											
9			10			11			12		
d	I	Id	*d*	I	Id	*d*	I	Id	*d*	I	Id
14.5 A	vs	S	14.0 Å	w	S	15.0 Å	s	S	15.0— A		
12.10	vw	Se?	9.35	w	T	10.0	vvw	Mi	14.0	vs	S
9.50	w	T	7.5—			7.4—			7.30	s	S; Sp
7.5—			7.0	vs	S; Sp	7.0	s	S; Sp	4.87	vw	S
7.0	s	S; Sp	4.57	s	S	5.0	vvw	Mi	4.58	mw	S
5.88	vw	Se?	3.89	w		4.55	s	S	4.32	vw	Q
4.90	m	S	3.62	s	S; Sp	3.60	m	S; Sp	3.61	m	S; Sp
4.57	s	S; Se?	3.13	w	T	3.35	mw	Mi	3.33	m	Q
3.66	s	S; Sp	3.03	w	Ca	3.19	w	F	3.03	w	Ca
3.25	m	T	2.85	vw	S	2.99	m	F	2.66	vw	S
2.90	ms	S	2.66—			2.90	w	S	2.48	vw	S; Sp
2.65	w	S	2.41	w	S	2.62	w	S	1.545	s	S
2.58	2	S; Sp	2.50	vs	S; Sp	2.51	s	S; Sp	1.514	vw	S
2.43	s	S	2.33	vw	S	2.45	w	S			
2.27	m	S	2.28	vw	S; Ca	2.20	vw	S			
2.08—			2.15	m	S	2.13	vw	S			
2.00	w	S	2.09	vw	Ca; S	2.05	vw	S			
1.88	vw	S	1.96	w	S	1.83	vw	S			
1.74	w	S	1.91	vw	Ca; S	1.76	vw	S			
1.71	vw	S	1.87	vw	Ca; S	1.62	vw	S			
1.576	vw	S	1.79	mw	S	1.540—					
1.540	s	S	1.74	w	S	1.520	s	S			
1.508	mw	S	1.64	vw	S	1.425	vw	S			
1.401	vw	S	1.56	vw	S	1.315	vw	S			
1.324	w	S	1.573	s	S						
1.299	vw	S	1.503	s	S						
			1.412	w	S						
			1.329	w	S						
			1.307	m	S						
			1.278	w	S						
			1.252	vw	S						
			1.167	w	S						

9. Prospect Hill, Sydney, New South Wales. Joint-filling.
10. Prospect Hill, Sydney, New South Wales. Joint-filling.
11. Prospect Hill, Sydney, New South Wales. Pseudomorphs after olivine.
12. Dumbuck Quarry, Milton, Scotland. Joint-filling.

Group 3						Group 4					
13			14			15			16		
d	I	Id	*d*	I	Id	*d*	I	Id	*d*	I	Id
14.5 Å	vs	S	14.5— Å			15.0— Å			15.0— Å		
7.2	s	Sp; S	14.0	s	S	14.0	s		14.0	s	
4.84	vw	S	7.1	s	S; Sp	4.45	s		4.5	vvw	
4.59	w	S	5.37	w		2.60	s		4.48	vw	
4.26	vw	Q	4.57	vw	S	1.535	vw		2.59	vw	
3.62	m	Sp; S	4.26	m					1.55	vvw	
3.33	m	Q	3.58	vs	S; Sp						
1.73—			3.14	w							
1.71	vw	S	3.05	w	Ca						
1.541	s	S	2.74	vw	S						
			2.65	vw	S						
			2.51	vw	S; Sp						
			2.25	vw	S; Ca						
			1.83	m	S						
			1.63	vw	S						
			1.58	vw	S						
			1.539	vw	S						
			1.430	vw	S						

13. Bowling Quarry, Dumbartonshire, Scotland. Joint-filling.
14. Bowling Quarry, Dumbartonshire, Scotland. Joint-filling.
15. Locality unknown. Vesicle-filling.
16. Walla Walla, Washington, Vesicle-filling.

description or mode of occurrence of this material are those of Bradley (1945), (vermiculite), Prider and Cole (1942), (nontronite), and Earley and Milne (1956), (regularly interstratified montmorillonite-chlorite).

When the alteration product, whether it occurs as pseudomorphs after mafic minerals, joint-filling or in amygdules, is optically isotropic it is usually called chlorophaeite (Peacock and Fuller, 1928). It is characterized by a refractive index ranging from 1.50 to 1.62, optical isotropy, and a bright orange to deep green color. Average chemical analyses are given in Table 4A.

INTERPRETATION OF THE *X*-RAY POWDER PHOTOGRAPHS

The data presented in Tables 1, 2, and 3 are representative of 170 powder photographs of 60 specimens. Sample numbers are arranged so that the same number refers to material from the same bulk sample. These are divided into four groups, nos. 1–4, which represent red, oxidized alteration products usually called iddingsite; nos. 5–7, which represent green alteration products in lavas; nos. 8-14, which represent green alteration products in shallow intrusions; and nos. 15–16, which represent optically isotropic alteration products.

Group 1

Photographs of untreated material (Table 1) are characterized by a broad but strong reflection near 14 Å. Rarely very weak second and third order reflections from the basal spacing occur. A few specimens have a reflection near 7 Å with no 14 Å reflection. A weak 060 reflection typically occurs between 1.49–1.51 Å, although two lines are frequently present in the region (1.49–1.54 Å) in which the 060 reflection for dioctahedral

TABLE 2. *X*-RAY DATA: BASAL SPACINGS OF GLYCOLATED SAMPLES

Sample Number	*d*	I
1	15.38 Å	m
2	15.8	mw
3	16.35	s
6	16.05	vs
7	16.5	s
8	15.22	vs
9	15.1	vs
10	14.5	w
11	15.5	vs
12	15.5	s
13	15.5	s
14	15.77	ms

and trioctahedral structures occurs. With ethylene glycol treatment (Table 2) the basal spacing expanded to 15–16 Å. Upon heating to 500° C., a new line appeared between 9.5–10 Å in specimens having a 14 Å spacing (untreated). Heating to 700° C. (Table 3) produced no additional results. Higher order reflections from the basal spacing and the 7 Å structure disappear with heating to these temperatures.

The usual expansion of the 14 Å spacing with glycol solvation and collapse with heating indicate the presence of vermiculite or smectite.* A possible means of distinguishing these by Mg-saturation and glycerol expansion was suggested by G. F. Walker (Pers. comm.). No change in expansion was observed after a 24 hour treatment with saturated $MgCl_2$ solution indicating that the structure is a smectite. Since the expansion is rarely to the full limit (17 Å) expected of glycol solvation, it is possible that the smectite is randomly interlayered with chlorite. Absence of higher order reflections, which render this interpretation difficult to evaluate, may be due to auto-oxidation. As will be shown later, alteration takes place before consolidation of the magma is complete so that high temperatures and, in lava flows, oxidizing conditions may be expected. It is concluded, therefore, that oxidized alteration products are composed predominantly of smectite-chlorite. Goethite is almost always present, quartz and calcite are common constituents and talc and mica rare constituents.

Group 2

These powder photographs (Tables 1–3) are nearly identical with those of group 1 and are interpreted in the same way. The more common occurrence of higher order reflections from the basal spacing is attributed to incomplete oxidation of iron (which also accounts for optical differences). Evidence presented in a later section suggests that weathering of green alteration products can result in extraction and oxidation of iron, producing aggregates which are optically identical with oxidized varieties, this process possibly accounting for differences in position of the 060 reflection between the two. Calcite is common in these aggregates, while magnetite, quartz and feldspar sometimes occur. Talc is a rare constituent.

Group 3

Powder patterns of untreated material (Table 1) from shallow intrusions are characterized by a strong reflection between 14 Å and 15 Å with nonintegral higher order reflections from this spacing of comparable intensity. The 060 reflection is usually strong and near 1.54 Å, although it is usually accompanied by a weaker line near 1.50 Å. With ethylene glycol treatment (Table 2), the 14 Å spacing expanded to 15–16 Å and gave rise to a nonintegral series of higher order lines. Upon heating to 500° C. a new line appeared between 9.4–10 Å in most specimens, at 11.78 Å in one specimen. Heating also resulted in a considerable reduction in intensity of higher order reflections from the basal spacing so that these patterns are, with the exception of differences in intensity and position of the 060 reflection, identical with most heated specimens of Group 1. Since heating was done in air, oxidation of iron produces from the green alteration products an aggregate which is optically identical with natural oxidized types. Heating to 700° C. (Table 3) produced no additional results.

---

* The term smectite (Brown, 1955) denotes members of the montmorillonite group.

TABLE 3. *X*-RAY DATA: BASAL SPACINGS OF HEATED SAMPLES

23 hr. 700° C.		23 hr. 700° C.		21 hr. 525° C.		23 hr. 700° C.		25 hr. 700° C.		2 hr. 710° C.	
1		2		3		6		7		8	
d	I	*d*	I	*d*	I	*d*	I	*d*	I	*d*	I
9.82	m	9.77	mw	9.5	vs	9.60	vs	9.93	s	9.5	vvw
23 hr. 700° C.		23 hr. 525° C.		23 hr. 700° C.		2 hr. 710° C.		1 hr. 480° C.			
9		10		12		13		14			
d	I	*d*	I	*d*	I	*d*	I	*d*	I		
11.78	vs	9.45	m	9.6	s	9.40	vvw	10.4	w		

This behavior again indicates that an expanding 14 Å structure is present. That this is probably interlayered with a non-expanding 14 Å structure is indicated by the nonintegral series of higher order reflections. It is also possible that variable amounts of smectite-chlorite are mechanically mixed with a kaolin-type structure (antigorite or chrysotile), the latter giving rise to strong reflections near 7.2 Å and 3.6 Å. In specimens showing large expansion with glycol solvation, the second order reflection split, one line being roughly half the spacing of the expanded spacing, the other occurring at about 7.2 Å, which strongly suggests a mechanical mixture of a serpentine mineral with the smectite-chlorite. An attempt was made to separate the two, but without success. Although

Hargreaves and Taylor (1946) found that conversion of chrysotile and antigorite to olivine takes place at about 600° C., no reflections belonging to olivine were found in photographs of material heated to and above this temperature.

Material from shallow intrusions is therefore composed at least in part of smectite-chlorite with possibly one or both of the serpentine minerals. Considerable variation in proportions of these components occurs among different samples. Minor amounts of talc, mica, quartz and possibly sepiolite are sometimes present.

Group 4

Optically isotropic alteration products are closely associated with anisotropic material which is optically identical with members of Group 1. In addition, optically isotropic material is itself sometimes submicroscopically crystalline, giving diffuse reflections corresponding to the strongest lines in powder photographs of Group 1. No change in position of the basal reflection was observed with heat and glycol treatment, so that it is probable that the incipient structure is chlorite. Absence of higher order reflections may again be due to auto-oxidation of iron. Goethite and calcite (optically detectable) are sometimes present.

Differential Thermal Analysis

With the exception of specimen no. 14, thermograms (Fig. 1) of specimens from shallow intrusions all have endothermic peaks between 100–200° C. which are attributed to loss of adsorbed water from the smectite component. Absence of this peak in no. 14, which also has a smectite component, is not explained. The second endothermic peak, representing loss of structural water, is typically broad and occurs anywhere between 535°-700° C. It is likely that this behavior reflects variation in the proportions of chlorite and smectite. In most specimens this peak is followed by another, relatively sharp endothermic peak, representing decomposition of the aggregate, between 780–840° C. In specimens 13 and 14, this peak is followed by another endothermic peak at 865° C. and 820° C., respectively. Doubling of the last endothermic peak probably indicates decomposition of different components of the aggregate at different temperatures. Most samples show a final exothermic peak between 820°–860° C. indicating the formation of new mineral phases.

The thermogram of no. 6 (from a lava) is very similar to that of nontronite. No. 4 is the weathered equivalent of no. 6. The endothermic peak at 305° C. in the latter is due to decomposition of goethite, while the peak at 545° C. may be due to kaolinite.

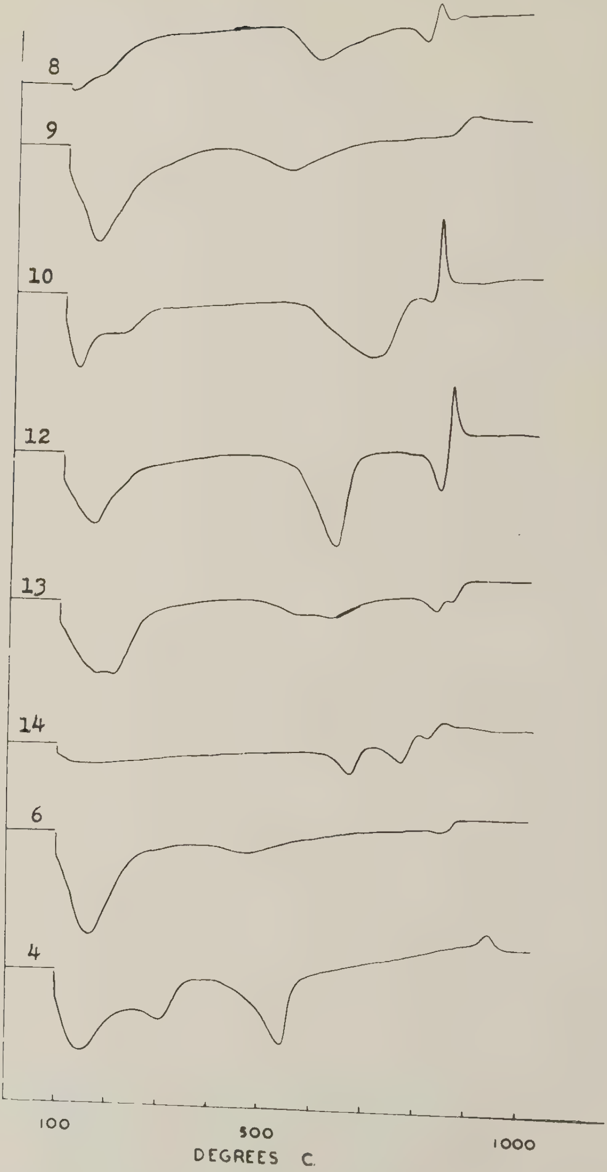

FIG. 1. Differential thermal analyses.

PETROLOGY

Specimens of basalt flows containing both red and green varieties of alteration products were obtained from Carmel Bay, California (type locality for iddingsite; Lawson, 1893), from near Santa Rosa, California, Hawaii, Orange, New South Wales, and from Tertiary lavas near Ebbetts Pass, California.

Carmel Bay, California

At Sunium Point a series of basalt flows outcrop with an exposed thickness exceeding 75 feet. Weathering to a depth of approximately 20 feet has resulted in bleaching of the groundmass and alteration of pyroxene and plagioclase phenocrysts. The only obvious mafic mineral is red pseudomorphs after olivine. In very deeply weathered material pseudomorphs after olivine may be detected only with a hand lens. Below the weathered zone the groundmass is black, fresh pyroxene phenocrysts may be seen with a hand lens, and, at the base of the exposure, the alteration product of olivine is green.

Weathered rocks are characterized microscopically by an abundance of smectite-chlorite and goethite pseudomorphs after olivine, plagioclase and pyroxene phenocrysts completely replaced by a colorless to pale green fibrous material with moderate birefringence, set in an intergranular groundmass of altered plagioclase microlites, granular and euhedral pyroxenes, iron oxides and unaltered apatite. Small amounts of pale green to brown interstitial material is often present, while biotite occurs rarely.

Almost all of the specimens show a distinct flow banding in the plagioclase microlites. There is commonly a concentration of very finely crystalline green to brown material and iron oxides in bands parallel to the flow banding, appearing as a distinct macroscopic lineation on cut surfaces. Pseudomorphs after olivine within these bands are distorted (Figs. 2 and 3).

In unweathered specimens the same textural relations hold, but olivine is usually the only altered mineral. Augite (2V 45°–48°) and plagioclase (An_{53-62}) aggregates are common. In some specimens the groundmass pyroxenes consist in part of colorless euhedra of orthopyroxene which are partly altered to green smectite-chlorite (?). Iron oxides occasionally predominate over clay minerals in pseudomorphs after olivine, while in several specimens green and red alteration products occur side by side in the same pseudomorphic aggregate (Fig. 4). Pseudomorphs are usually connected by delicate stringers, which appear to be thin films coating plagioclase and pyroxene microlites, of material optically identical with that in the pseudomorphs, and sometimes have halos of the same secondary minerals.

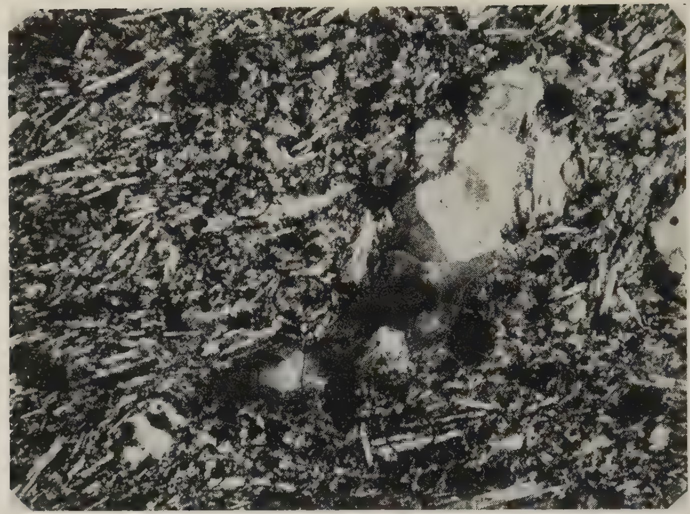

FIG. 2. Pseudomorph after olivine distorted by flow of the enclosing lava. Plane polarized light. ×45.

Rocks from another locality about a mile east of Sunium Point show nearly identical textural and mineralogical relations, except that augite (2V 46°–54°)-plagioclase (An_{54-68}) aggregates are usually larger than those in the Sunium Point flows, and, although often very deeply weathered, colorless clay pseudomorphs after these aggregates are obvious in

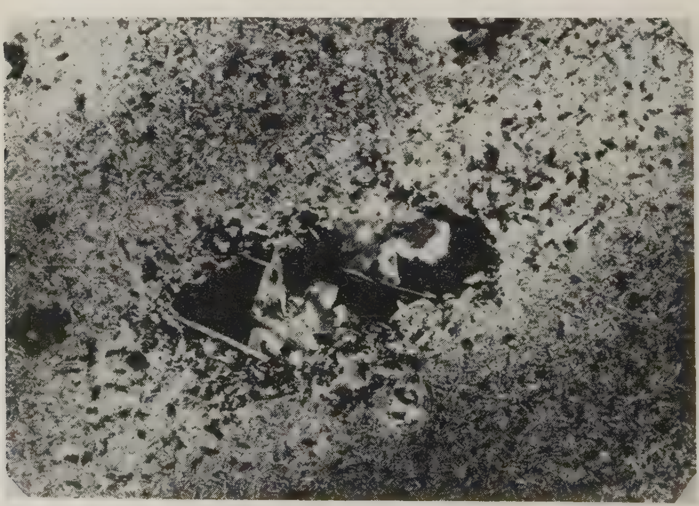

FIG. 3. Smectite-chlorite, iron oxide, biotite pseudomorph after olivine distorted by flow. Color banding is opposite from usual. Plane polarized light. ×30.

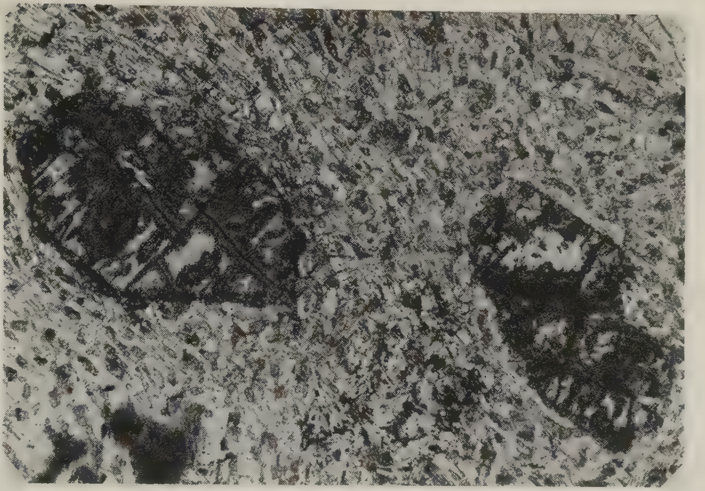

FIG. 4. Oxidized and green smectite-chlorite pseudomorphs after olivine. Plane polarized light. ×70.

hand specimen. Pseudomorphs after olivine are dull brown to nearly colorless and, when nearly colorless, are distinguished from weathered pyroxene and plagioclase only by their form.

In thin section, the material replacing pyroxene-plagioclase aggregates is colorless to pale green, has a moderate birefringence and occurs as randomly oriented fibers in the pseudomorphs.

Santa Rosa, California

All of these specimens are weathered and in some all the major minerals are altered and pseudomorphs after olivine are bleached. Most specimens are characterized by olivine phenocrysts (Fo_{85-95}) partly altered to iron oxides and smectite-chlorite, plagioclase (An_{60-69}) and some augite (2V 53°-57°) phenocrysts set in an intergranular groundmass composed of plagioclase, iron oxide and clinopyroxene microlites with accessory apatite. A small amount of optically isotropic pale green or brown mesostasis is usually present. Flow banding in plagioclase microlites is conspicuous and parallel to this are bands in which the clay minerals and iron oxides are concentrated. The bands are often connected by stringers of the same minerals resulting in a crudely rectangular or polygonal pattern. Pseudomorphs after olivine within these bands are distorted and alteration of olivine is complete. Within the polygonal areas olivine is incompletely altered to green smectite-chlorite. Identical secondary minerals, including optically isotropic varieties, also occur in microscopic amygdules in the bands (Fig. 5). Weathering has produced the same

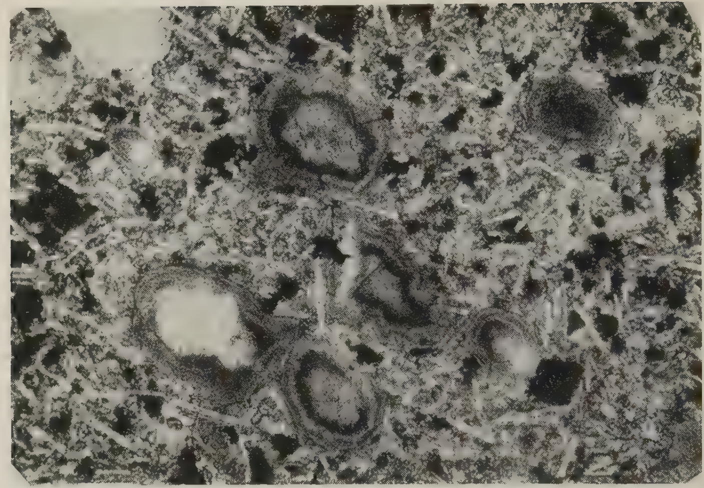

FIG. 5. Smectite-chlorite vesicle-filling. Plane polarized light. ×45.

effect as in the Carmel Bay specimens. Cores of altered olivines are occupied by a colorless, fibrous material which is randomly oriented.

Hawaiian basalts

Specimens, from the museum collection, University of California, consist of olivine phenocrysts (Fo_{75-80}) partly or completely altered to oxidized smectite-chlorite, iron oxide aggregates, augite (2V 52°) or titanaugite and plagioclase (An_{20-49}) phenocrysts in an intergranular groundmass composed of plagioclase, granular clinopyroxene and iron oxide microlites with accessory apatite. Olivine microlites are present in some specimens.

Orange, New South Wales

These specimens were obtained from a small quarry in a single basalt flow, the surface of which has been severely weathered. Part of the flow has well developed columnar jointing and adjacent to each joint plane the basalt has a dark rim approximately 0.5″ wide in which olivine has been altered to smectite-chlorite and iron oxides. The same minerals also occur as thin films coating the joint surfaces. For a distance of about 10 feet below the surface both the joint-filling and the altered rims are bright orange red.

The unaltered rock consists in part of augite (2V 48°–50°) phenocrysts and aggregates which ophitically or subophitically enclose plagioclase laths (An_{50-55}) and often enclose rounded grains of olivine. In areas between the evenly distributed pyroxene-plagioclase intergrowths, the rock consists of plagioclase laths and olivine phenocrysts (Fo_{85-95}), some of which are highly resorbed, set in a glassy groundmass. Some iron oxides, rounded olivine grains, rod-shaped clinopyroxenes and skeletal plagioclase crystals are distributed through the glass. In the altered rims below the weathered zone, olivine has been partly or wholly converted to green smectite-chlorite; in a few cases (Fig. 6) red cores are surrounded by green rims, but the opposite relations may be seen in the same thin section. Green smectite-chlorite also occurs as thin films along cleavages and fractures in plagioclase and clinopyroxene grains and along grain boundaries (Fig. 7). Such veinlets disappear at crystal-glass boundaries and the glass is locally altered, the veinlet reappearing in crystals on the opposite side of the altered glass. In a few places these veinlets occupy micro-shear zones (Fig. 8). Within the weathered zone joint-filling and alteration products of olivine and glass are red aggregates of kaolinite and goethite. With a few mineralogical and textural differences, this occurrence is nearly identical with that recorded by Smedes and Lang (1955).

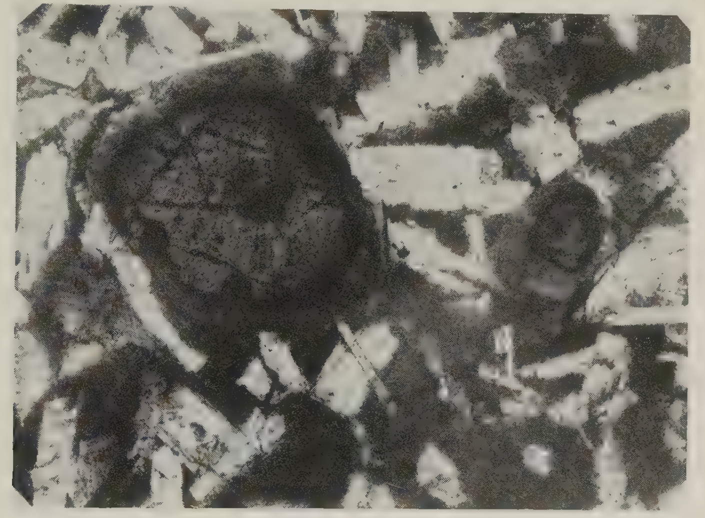

FIG. 6. Pseudomorphs after olivine consisting of oxidized smectite-chlorite cores and green smectite-chlorite rims. Plane polarized light. ×115.

Ebbetts Pass, California

Green smectite-chlorite is very widespread in the Tertiary lavas of the Mehrten Formation as an alteration product of olivine in basalts and of hypersthene in andesites. It is also present in amygdules and as coatings on joint surfaces. In many places it occurs in isolated patches several inches to several feet across within flows, and in these occurrences its dis-

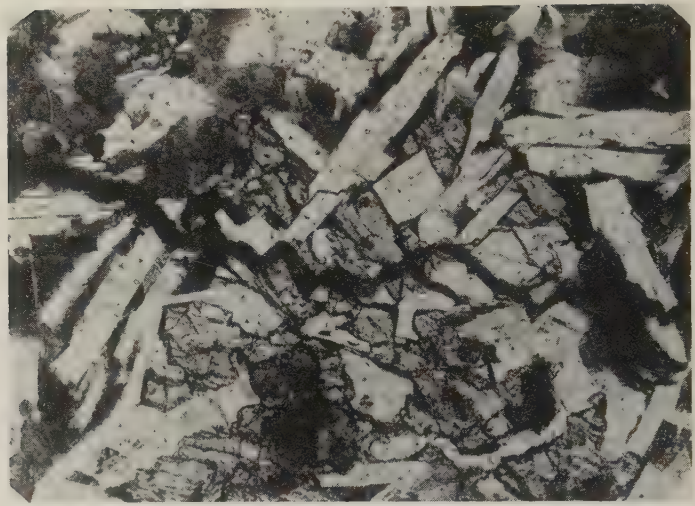

FIG. 7. Smectite-chlorite veinlet. Note control of grain boundaries and fractures on position of the veinlet. Plane polarized light. ×105.

tribution shows no relation to weathered surfaces. Coats (1940) mentioned some of these occurrences and referred to the alteration product as bastite. In view of the common retention of hypersthene cores, there is no doubt that this mineral alters to a product optically identical with that which replaces olivine. The andesitic lavas also commonly have ortho-

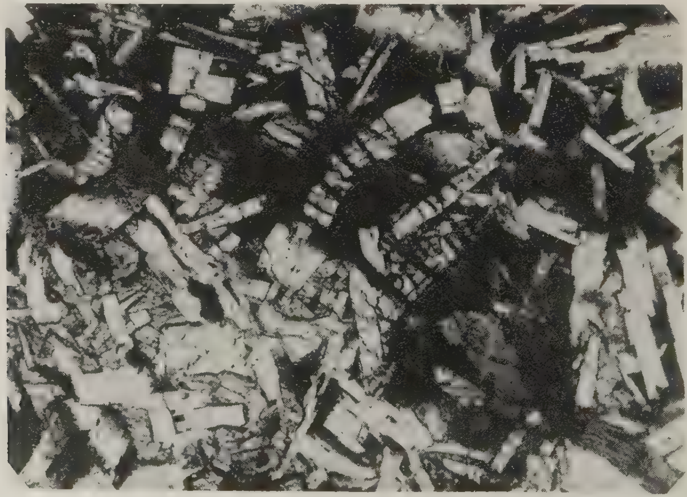

FIG. 8. Smectite-chlorite veinlets occupying micro-shear zone. Glass is locally altered to smectite-chlorite. Plane polarized light. ×55.

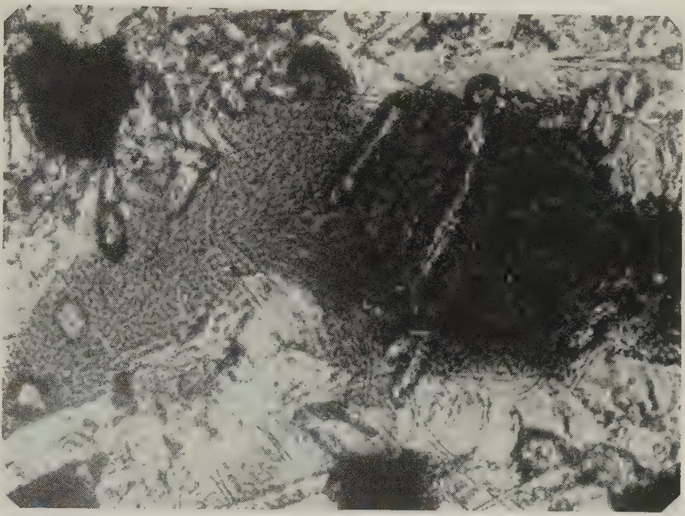

FIG. 9. Pseudomorph after olivine and material extracted during alteration. Plane polarized light. ×345.

pyroxene microlites partly or completely altered to the same mineral, while the clinopyroxene microlites have remained unaltered. Aggregates pseudomorphic after hypersthene commonly contain calcite and sometimes contain cristobalite.

Specimens of altered shallow basalt intrusions were obtained from Bowling Quarry, Dumbartonshire, Scotland (type locality of "bowlingite"; Hannay, 1877); from Dumback Quarry, Milton near Bowling; and from Prospect Hill near Sydney, New South Wales.

Bowling Quarry, Scotland

Material from this locality was all taken from joints where it occurs as veins $\frac{1}{2}''$–$1\frac{1}{2}''$ thick. According to Hannay (1877) it also occurs as vesicle-filling and as pseudomorphs after olivine in the dolerite. Other constituents of the rock are unaltered.

Dumbuck Quarry, Scotland

This material has the same mode of occurrence as that from Bowling Quarry. In thin section green smectite-chlorite pseudomorphs olivine microphenocrysts and occurs as interstitial filling and as thin films coating other minerals (Fig. 9). It is commonly intergrown with a colorless, micaceous material. A few plagioclase phenocrysts (An_{50-57}) which enclose clinopyroxene grains occur along with the altered olivine in an intergranular groundmass composed of plagioclase, clinopyroxene and iron oxide microlites with accessory apatite.

Prospect Hill, New South Wales

Green smectite-chlorite is abundant in this dolerite intrusion, occurring as joint-filling, fibrous aggregates pseudomorphic after olivine and as interstitial filling. In the dolerite phases it is commonly associated with green and brown mica while in pegmatitic phases it occurs as interstitial filling and rarely as pseudomorphs after olivine. In the chilled margin olivine phenocrysts (Fo_{70-85}) are fresh or partly altered, altered phenocrysts being connected by veinlets of optically identical material.

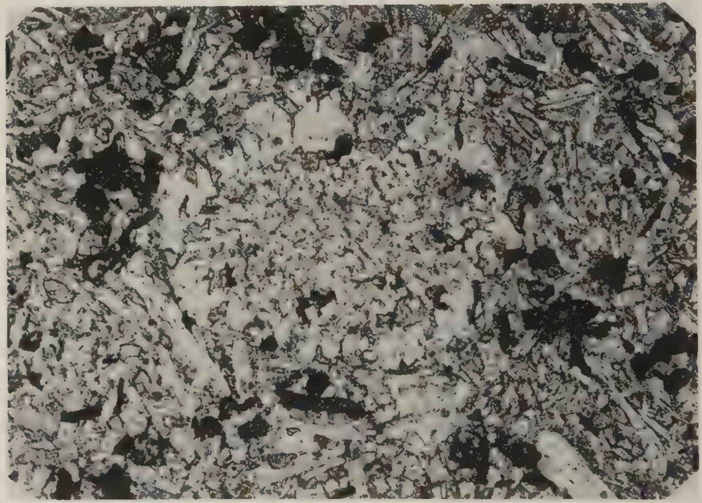

FIG. 10. Resorbed plagioclase with sieve structure due to enclosed clinopyroxene and iron oxide. Plane polarized light. ×95.

Weathered parts of the chilled margin show partial oxidation of alteration products, grading away from exposed surfaces into green alteration products. Such relations may be seen in a single thin section. Specimens used in this study were selected from joints and pseudomorphs after olivine.

Specimens of basalt flows containing optically isotropic alteration products (chlorophaeite) were obtained from the Grande Ronde dike, Oregon (Peacock and Fuller, 1928) and from several Tertiary lavas in eastern Washington and Oregon near Walla Walla, Washington.

Grande Ronde dike

In view of some discrepancies between the author's observations and those of Peacock and Fuller, specimens from this locality will be described in detail.

In the chilled margin a few olivine phenocrysts (Fo_{87}) partly altered to chlorophaeite and anisotropic smectite-chlorite, a few plagioclase aggregates which are corroded and have a sieve structure enclosing clinopyroxene and iron oxide grains (Fig. 10), and rare quartz grains with clinopyroxene halos are set in an intergranular groundmass composed of olivine partly or completely altered to both red and green smectite-chlorite and chlorophaeite, plagioclase, clinopyroxene and iron oxide microlites with accessory apatite. There are a number of chlorophaeite amygdules some of which contain carbonate. Amygdules in which the chlorophaeite is bright orange are connected by a delicate network of veinlets which consist of chlorophaeite films coating the groundmass minerals. These stringers form a crudely polygonal or rectangular pattern. Amygdules which are not so connected contain green chlorophaeite.

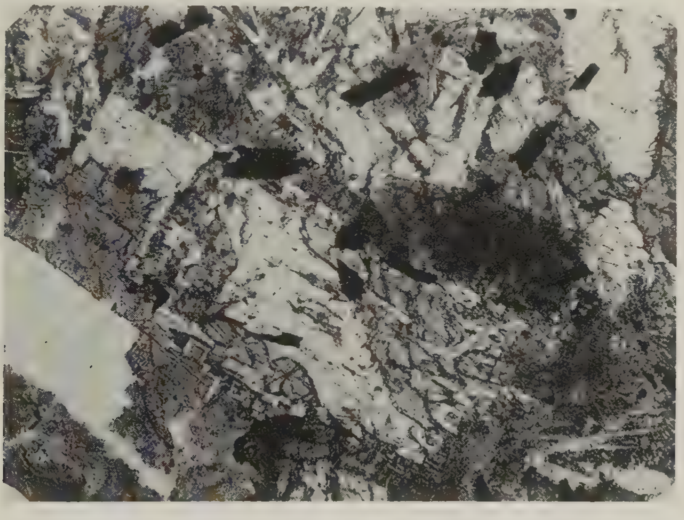

FIG. 11. Peripheral alteration of plagioclase resulting in formation of skeletal plagioclase grains. Areas of high relief within the plagioclase are clinopyroxene. Plane polarized light. ×55.

The center of the dike consists of plagioclase phenocrysts and aggregates (An_{12-44}) and olivine phenocrysts which are partly or completely altered, set in an intersertal groundmass composed of skeletal plagioclase grains, iron oxide microlites and glass or chlorophaeite with accessory apatite. Plagioclase is commonly intergrown with clinopyroxene and is peripherally altered, the alteration being controlled by cleavage planes resulting in skeletal plagioclase grains (Fig. 11). Chlorophaeite amygdules have a halo extending into the groundmass in which plagioclase has been partly altered to chlorophaeite (Fig. 12).

MODE OF ORIGIN

When the oxidized alteration product (iddingsite) was first named (Lawson, 1893) it was considered to be a primary mineral precipitated directly from basaltic magma. Other investigations showed that residual olivine is commonly present within pseudomorphs and this hypothesis was abandoned in favor of Iddings' (1892) suggestion that it formed by weathering of iron-rich olivine. Since the work of Ross and Shannon (1926) on iddingsite and that of Peacock and Fuller (1928) on chlorophaeite, both of these have been generally accepted as products of deuteric alteration of primary mafic minerals in basaltic lavas, iddingsite being a distinct mineral species, chlorophaeite being an amorphous substance of variable composition. Green alteration products, whether they are called bowlingite or any of their other names, are also widely thought to arise by the same process.

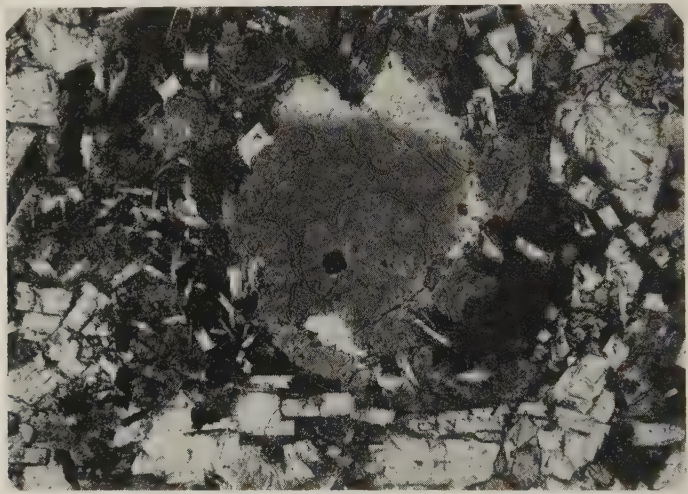

FIG. 12. Chlorophaeite amygdule with alteration halo. Plane polarized light. ×40.

Ross and Shannon presented convincing arguments favoring a deuteric origin which have been substantiated by subsequent investigations (e.g., Edwards, 1938; Fuller, 1938). However, Ming-Shan Sun (1957) has suggested that identical alteration may be continued in weathering. This conclusion is based on the identity of deuteric alteration products (only goethite was identified) with weathering products and similarity of chemical changes involved in both processes. The occurrence of both green and red varieties of alteration products at Carmel Bay, California, Orange, New South Wales, and Prospect Hill, New South Wales where oxidized material is present only in the weathered horizon clearly indicates that weathering may change the original deuteric alteration products rather than simply continue the same process. It was shown from x-ray data that both alteration products from Carmel Bay are composed of the same structural types except that the oxidized variety contains goethite. Conversion of green smectite-chlorite (sometimes mixed with magnetite) to red smectite-chlorite plus goethite can be effected either by leaching iron and recombination as goethite or by weathering of included magnetite, in either case the goethite acting as a pigment. Weathering of the Orange, New South Wales material resulted in formation of goethite, but the smectite-chlorite did not survive and in its place kaolinite is present. As will be shown later, the additional constituent, smectite-chlorite, of "iddingsite" identified in this study may also form by weathering of mafic minerals. However, the weathering products differ in being dioctahedral while oxidized smectite-chlorite in the same rocks is usually intermediate.

TIME OF ALTERATION

Edwards (1938) and Ross and Shannon (1926) presented textural evidence which suggests that alteration takes place after the enclosing lava ceased to flow, but sometimes prior to completion of crystallization of primary minerals. Fresh olivine rims surrounding altered olivine cores suggested to Edwards a sequence in which crystallization of olivine was followed by hydration-oxidation alteration, which in turn was followed by renewed crystallization of olivine. To Ross and Shannon, the same relationships suggested zonal replacement of olivine which had completed crystallization before alteration commenced.

Ross and Shannon further state that "The magma must have come to rest before iddingsite formed for though it is a very brittle mineral it is never fractured, or distorted by flow." Descriptions of the Carmel Bay, California and Santa Rosa, California basalts showed that, in these rocks, distortion of pseudomorphs is common, but restricted to narrow bands parallel to the flow banding (Figs. 2 and 3). These data are interpreted as indicating at least partial alteration of olivine prior to cessation of flow, followed by distortion in shear zones developed when laminar flow is interrupted by consolidation.

CHEMICAL AND PHYSICAL PROPERTIES AND THEIR IMPLICATIONS

It is evident from the x-ray data that the formula of "iddingsite" represents at least two minerals and possibly as many as three or four, and that, in general, none of these are optically distinguishable.

Notwithstanding mineralogical difficulties, bulk chemical compositions are important, for they represent alteration products of primary minerals whose composition can often be determined from relicts. It is, however, still a matter of conjecture whether or not relicts are representative of the entire original crystal. Most of the chemical data now available are of "iddingsite," chlorophaeite, and associated olivine. By comparison of these analyses it is seen that, although a broad range of compositions occurs, they are characterized by high Fe/Mg ratios, the lowest being about 2/1 while the average is about 8/1. Of all associated olivines reported in the literature, the highest Fe/Mg ratio is 1/2 and most are lower. It was by similar interpretation of data that Ross and Shannon (1926) were led to state, "the proportion of silica has remained nearly constant . . . , the iron has all been changed from the ferrous to the ferric state and its proportion has greatly increased, water has been added in large amount, and magnesium has been largely abstracted. It is clear that in the change of olivine to iddingsite there has been a metasomatic replacement . . . ," In addition Ross and Shannon, noting the occurrence of fresh olivine rims surrounding altered olivine cores and fresh olivine microlites with altered olivine phenocrysts, state that alteration is partly dependent on composition of the olivine. Although these relations indicate selective replacement of magnesian olivine (assuming normal zoning), some authors (e.g., Tomkeieff, 1934) have interpreted this ambiguous statement to mean selective alteration of fayalitic olivine. Typically the initial stages of alteration are characterized not by zonal replacement of olivine, but by replacement along fractures randomly cutting the phenocrysts. Since textural relationships indicate either no zonal preference or preference for magnesian zones, composition differences between olivine and its alteration products are best explained by Ross' and Shannon's conclusion that Mg is leached. The common occurrence of iron oxides with the clay minerals and the not rare complete replacement of olivine by iron oxides indicates addition of iron as well as removal of magnesium. It is of course clear that the alteration cannot be simply a process of hydration and oxidation, for the proportions of FeO (recalculated from Fe_2O_3), MgO and SiO_2 do not approach those of olivine. It is not, therefore, unreasonable to suppose that compositions of relicts are representative of the entire original phenocryst subject to zoning fluctuations no more severe than found in unaltered olivine.

These changes in bulk composition and structure have resulted in alteration products which are considerably less dense (see Table 4A) than the minerals they replace. Since the alteration is pseudomorphic, volume relations require removal of material, which, according to the above arguments, involves selective leaching of Mg. Ross and Shannon do not consider the ultimate disposition of the extracted material, but Peacock and Fuller (1928) clearly state their belief that chlorophaeite

TABLE 4A. CHEMICAL ANALYSES*

	A		B		C	
	Average	Range	Average	Range	Average	Range
SiO_2	41.20	22.08–48.36	44.79	42.68–46.32	45.11	43.42–48.17
TiO_2	0.14	0.12–0.26	0.22	0.00–0.46	0.29	0.00–0.82
Al_2O_3	3.81	0.00–5.09	8.24	5.87–10.62	3.91	1.37–7.12
Fe_2O_3	35.42	25.48–60.13	8.90	6.33–12.30	22.13	12.37–30.02
FeO	0.38	0.00–1.97	4.77	2.70–7.98	6.66	2.36–12.10
MnO	0.05	0.00–0.11			0.47	0.35–0.62
MgO	6.85	0.60–12.71	22.50	21.71–23.29	8.16	6.26–11.73
CaO	2.35	1.72–3.26	1.96	0.32–3.29	3.13	1.97–4.02
Na_2O	0.12	0.12–0.13			0.55	0.00–2.21
K_2O	0.10	0.09–0.10			0.14	tr – 0.47
H_2O^+	9.30	5.74–11.00	8.84	7.47–10.00	8.39	6.83–10.97
Total	99.54		100.22		98.94	
H_2O^-	9.84	4.76–22.85	10.72	7.69–13.52	20.78	12.54–27.44
Density		2.5 – 2.8		2.24–2.30		1.81–2.23

* Column A (iddingsite) represents 10 analyses, 2 from Tomkeieff (1934), 8 from Ross and Shannon (1926). Column B (saponite) represents 4 analyses from Caillere and Henin (1951). Column C (chlorophaeite) represents 4 analyses from Peacock and Fuller (1928).

All analyses were recalculated to 100% excluding H_2O^- before averages were computed.

vesicle-filling and veinlets result from an alteration of mafic minerals. In the same manner, it is believed that material extracted from mafic minerals during alteration to anisotropic varieties is recombined in the same structural types (principally smectite-chlorite) in joints and vesicles.

The limited chemical data presented in Table 4 may now be divided into two groups: 1) those representing extracted material in motion at the time of consolidation (columns B and C, Table 4A; specimens 6, 8, and 10, Table 4B), and 2) those representing alteration residues (column A, Table 4A). It is clear by comparison of these groups that, in basalt lavas, both are characterized by high Fe/Mg ratios. It is reasonable to ask, then, why pseudomorphs are retained at all if the material which precipitates from the final solutions is of the same composition as that in pseudomorphs. This is probably largely due to concentration of iron in the altering solutions; as the mafic minerals break down, Mg passes into solution over a concentration gradient while iron is recombined in place in a solid phase appropriate to the environment. It is presumed that Mg

TABLE 4B. CHEMICAL ANALYSES

	8*	10	6
SiO_2			49.48
Al_2O_3	12.80	7.14	5.85
Fe_2O_3	0.43	0.80	18.86
FeO	6.67	6.09	3.90
MgO	25.24	31.80	12.66
CaO			2.13
TiO_2	nd	0.37	0.35

Rock Analyses†

	Unaltered	Altered	gms/m³ Unaltered	gms/m³ Altered
SiO_2	51.66	51.51	140.0	134.5
Al_2O_3	15.88	16.98	43.0	44.4
Fe_2O_3	0.76	5.49	2.1	14.4
FeO	9.70	4.82	26.3	12.7
MgO	7.35	5.26	19.9	13.7
CaO	8.07	8.56	21.9	22.4
Na_2O	2.81	2.17	7.6	5.7
K_2O	1.52	1.05	4.1	2.7
TiO_2	1.60	1.68	4.3	4.0
CO_2	nd	nd	0.0	0.0
H_2O^+	0.65	2.48	1.8	6.5
Total	100.00	100.00		
H_2O^-	0.09	3.08		
Density	2.71	2.61		

* Numbers correspond to same samples in other tables. See Table 1 for descriptions.

† Olivine basalt near Orange, New South Wales. See text for description. Analyses recalculated to 100% excluding H_2O^-.

Analysts: Avery and Anderson, Melbourne.

added to the solutions is outweighed by Fe, the final crystalline product still being Fe-rich. Since the structural groups represented by the alteration products can accommodate any variation in Fe, Mg and Al, the presence of these minerals in joints and vesicles does not imply alteration of mafic minerals, but the two usually occur together. When this material is accommodated interstitially, its composition can have only an indirect bearing on the nature of liquid residues formed by fractional crystallization.

The data on alteration products from shallow intrusions indicate that the material in motion is rich in Mg and relatively poor in Fe. Since associated Fe-bearing minerals are rare in joint-filling, this is taken to indicate a lack of iron enrichment in the residual solutions. Since neither Mg nor Al can be expected to be concentrated in the altering solutions, complete solution of mafic minerals susceptible to the alteration is possible. Where pseudomorphs are retained, duration of alteration may be more important than composition of solutions, but additional factors of structural inheritance in alteration products and heat supply provide problems for which there are no quantitative data. The markedly higher alumina may be attributed to contributions from altered Al-bearing minerals such as plagioclase which is much more extensively altered in these rocks than in typical altered basalt lavas.

Mechanisms of Movement of Extracted Material

Since there is good evidence that alteration takes place, at least in some lava flows, at a late stage of consolidation, some mechanism for rapid removal of material extracted during alteration is required. Occurrence of alteration products as delicate networks of veinlets connecting pseudomorphs and vesicles, as veinlets parallel to flow banding, and, principally, along major joints all suggest operation of a pressure gradient. Smedes and Lang (1955) appealed to jointing to provide low pressure areas towards which altering solutions moved. If alteration precedes jointing, extracted material could be removed in this manner. Polygonal networks of veinlets may be interpreted as micro-joints and may have served the important function of cleaning out on a small scale. Veinlets parallel to flow banding could be caused by shearing along irregular flow planes resulting in dilated areas of low pressure. Curtis (1954) utilized the last proposal in interpreting autobrecciation of lavas. Whatever the mechanism of cleaning out on a small scale, the major joint system acts as a permanent low pressure area until pressures are equalized, and it is towards these that the altering fluids tend to move. In shallow intrusions, low pressure areas are probably created chiefly by jointing, the location of much of the smectite-chlorite, but this will depend greatly on the nature of the wall rock.

Effects of the Alteration on Bulk Chemical Composition of Some Basaltic Rocks

It is clear from the conclusions drawn above that alteration of mafic minerals results in selective leaching of Mg which, in lavas, is later combined with iron and silica presumably derived from the altering solutions. If these components are not recombined within the rock, but escape into joints or wall rock, the composition of the rock no longer represents the composition of the magma from which it crystallized. The quantitative effects of the alteration can be assessed only where fresh and altered equivalents occur. The effects of loss of Fe, silica and other components concentrated in solution prior to alteration cannot be quantitatively assessed.

In Table 4B are given chemical analyses of altered and unaltered portions of the Orange, New South Wales basalt. These differ only in nearly complete alteration of olivine and minor alteration of glass in the altered phase. Since density changes have taken place, comparison of weight per cents does not give a true picture of composition changes and these have been recalculated to gms./m^3. Specimens were collected from several columns and combined to reduce sampling error. The most significant changes are loss of MgO and SiO_2, addition of H_2O and change of ferrous to ferric iron in the altered rock. Total iron and alkalis show a small loss and alumina a small gain in the altered phase, but, in view of sampling and analytical error, these cannot be safely interpreted. The analysis of smectite-chlorite joint-filling from this locality (no. 6, Table 4B) clearly indicates the final disposition of Mg leached from olivine. It also shows that the Fe content of the fresh rock is not representative of the magma.

Data presented by Fuller (1938) indicate that opposite changes in bulk composition can take place under certain conditions. In the basalt flows described by Fuller, alteration of olivine is confined to cores of columns, residues of the alteration being accommodated interstitially. Although direct comparison of analyses shows little change between altered cores and unaltered sheaths, Fuller (Pers. comm.) believes that the porous texture of the sheaths is explained by loss of the mesostasis (formed as a crystallization residue, not by alteration). Under these conditions recalculation of weight per cent analyses to gms./$m.^3$ would probably show changes in the opposite direction from those described above.

It is necessary to bear in mind that these minerals are only a small part of a much more complex association. This is particularly true of shallow intrusions where carbonates and zeolites are invariable associates of the clay minerals and the total secondary mineral assemblage extremely varied. Since these too are usually less dense than the primary minerals from which they are derived, their escape into joints may be expected to have a similar effect on bulk chemical composition of the altered rocks.

Application to Some Problems in Soil Clay Mineralogy

It is apparent from the results of this investigation that chlorites and smectites occurring in soils derived from basic volcanic rocks cannot be assumed to have originated by weathering. The possibility that these minerals remain as relicts, although probably modified depending on conditions of weathering, is strengthened by a detailed study of the

Carmel Bay, California basalts which lie in a temperate climate zone, and which are structurally disposed to allow through drainage. A section is accessible at this locality which contains rocks ranging from those whose only altered constituent is olivine to those so deeply weathered that all of the primary minerals are altered and the rock is very porous. The freshest rocks contain green alteration products which are trioctahedral smectite-chlorite aggregates, while the most highly weathered rocks contain oxidized smectite-chlorite and goethite aggregates, the smectite-chlorite of these rocks being predominantly intermediate to dioctahedral. By plotting the position of the 060 reflection against a qualitative estimate of degree of weathering of the enclosing rock it was found that the higher the degree of weathering the more closely the smectite-chlorite approached a dioctahedral structure. *X*-ray powder photographs of a colorless clay pseudomorphing clinopyroxene-plagioclase aggregates (presumed to have formed by weathering because such alteration occurs only in the weathered zone) show that it is also composed in part of smectite-chlorite aggregates, but differs in having kaolinite (?) as part of the aggregate. It might be expected, since the structural types represented by deuteric alteration products are stable in the weathering environment while pyroxene and plagioclase undergo a complete structural change, that conversion of these to dioctahedral structures will lag behind alteration of plagioclase and pyroxene. This was found to be true since pseudomorphs after olivine, even in the most deeply weathered rocks, are still composed in part of a trioctahedral structure. In addition, the occurrence of lightly pigmented (goethite) smectite-chlorite in deeply weathered, almost colorless rocks attests to continued leaching of iron. Although weathering of these rocks took place in a temperate climate with through drainage, it is obvious that weathering conditions which favor formation of trioctahedral chlorites and smectites will also favor preservation of the original trioctahedral products of deuteric alteration. It should be noted, however, that weathering of smectite-chlorite in the Orange, New South Wales basalt resulted in an aggregate of goethite, quartz and kaolinite without preservation of the smectite-chlorite.

It is believed that recognition of the abundance and character of these minerals as pre-weathering constituents of basic igneous rocks will aid in solution of some problems in soil-clay mineralogy which have heretofore been explained by complicated chemical or physical histories such as those described by Allen and Scheid (1946) and Ross and Hendricks (1945). In no case will it be a simple problem to evaluate residual contributions to the clay fraction, for these minerals are not evenly distributed through the parent rock. This is particularly true of differentiated shallow intrusions such as that at Prospect, New South Wales, where the smectite-chlorite content of different specimens ranges from practically nil to more than half by volume.

ACKNOWLEDGMENT

The author is indebted to Drs. C. D. Campbell, A. B. Edwards, B. C. King, R. L. Rose, A. C. Waters, L. Weiss and H. Williams for specimens used in the study. Members of the Geology and Physics Departments, Univ. of Technology, Sydney, are gratefully acknowledged for making equipment available for the author's use. Special thanks are due Profs. Howel Williams and Charles Meyer of the University of California for having critically read the manuscript, and to Drs. R. E. Fuller and G. F. Walker for their helpful discussion of some of the problems. Professor Pabst of the University of California kindly supplied powder photographs of iron oxides for comparison. Financial assistance was received from the University Research Grants Committee, Sydney University.

REFERENCES

ALLEN, V. T., AND SCHEID, V. E. (1946), Nontronite in the Columbia River region: *Am. Mineral.*, **31,** 294–312.

BRADLEY, W. F. (1945), Glycol-montmorillonite: *Am. Mineral.*, **30,** 704–713.

BRINDLEY, G. W. (ed.) (1951), *X*-ray identification and crystal structures of clay minerals: The Mineralogical Society, London.

BROWN, G. (1955), Report of the clay minerals group sub-committee on nomenclature of clay minerals: *Clay Mins. Bull.*, **2,** 296.

CAILLERE, S. (1935), Sur les caracteres specifiques de la bowlingite: *Compt. Rend. Acad. Sci. Paris*, **200,** 1483–1485.

CAILLERE, S. AND HENIN, S. (1951), The properties and identification of saponite (bowlingite): *Clay Mins. Bull.*, **1,** 138–144.

COATS, R. R. (1940), Propylitization and related types of alteration on the Comstock Lode, Nevada: *Econ. Geol.*, **35,** 1–16.

CURTIS, G. H. (1954), Mode of origin of pyroclastic debris in the Mehrten Formation of the Sierra Nevada: *Univ. of Calif. Pub. in Geol. Sci.*, **29,** 453–502.

EARLEY, J. W. AND MILNE, I. H. (1956), Regularly interstratified montmorillonite-chlorite in basalt: *Proc. 4th Nat'l. Conf. on Clays and Clay Mins.*, pub. **456,** 381–384.

EDWARDS, A. B. (1938), The formation of iddingsite: *Am. Mineral.*, **23,** 277–281.

FULLER, R. E. (1938), Deuteric alteration controlled by the jointing of lavas: *Am. Jour. Sci.*, **35,** 161–171.

HANNAY, J. B. (1877), On bowlingite, a new Scottish Mineral: *Min. Mag.*, **1,** 154–157.

HARGREAVES, A., AND TAYLOR, W. H. (1946), An *x*-ray examination of decomposition products of chrysotile (asbestos) and serpentine: *Min. Mag.*, **27,** 204–216.

IDDINGS, J. P. (1892), *U. S. Geol. Survey.*, Mono. **20,** Append. **B,** 388–390.

KAADEN, G. VAN DER (1951), Optical studies on natural plagioclase feldspars with high- and low-temperature optics: *Pub. van het Min. Geol. Inst. Ryks.*, Univ., Utrecht, Holland.

LAWSON, A. C. (1893), The geology of Carmelo Bay: *Univ. of Calif. Pub. in Geol. Sci.*, **1,** 1–59.

MING-SHAN SUN (1957), The nature of iddingsite in some basaltic rocks of New Mexico: *Am. Mineral.*, **42,** 525–533.

PEACOCK, M. A., AND FULLER, R. E. (1928), Chlorophaeite, sideromelane and palagonite from the Columbia River Plateau: *Am. Mineral.*, **13,** 360–382.

PRIDER, R. T., AND COLE, W. F. (1942), The alteration products of olivine and leucite in the leucite-lamproites from the west Kimberly area, Western Australia: *Am. Mineral.*, **27,** 373–384.

ROSS, C. S., AND HENDRICKS, S. B. (1945), Minerals of the montmorillonite group: their origin and relation to soils and clays: *U. S. Geol. Surv. Prof. Paper* no. **205-B,** 23–79.

ROSS, C. S., AND SHANNON, E. V. (1926), The origin, occurrence, composition and physical properties of the mineral iddingsite: *Proc. U. S. Nat'l. Museum,* **67,** Art. 7, 1–19.

SMEDES, H. W., AND LANG, A. J., JR. (1955), Basalt column rinds caused by deuteric alteration: *Am. Jour. Sci.*, **253,** 173–181.

TOMKEIEFF, S. I. (1934), Differentiation in basalt lava, Island Magee, Co. Antrim: *Geol. Mag.*, **71,** 501–512.

TROEGER, W. E. (1952), Tabellen zur optischen Bestimmung der gesteinsbildenden Minerale: E. Schweizerbartsche Verlagsbuchhandlung, Stuttgart.

TURNER, F. J. (1947), Determination of plagioclase with the four-axis universal stage: *Am. Mineral.*, **32,** 389–410.

Manuscript received June 4, 1957.

THE AMERICAN MINERALOGIST, VOL. 43, JANUARY–FEBRUARY 1958

ON CHLORINE IN SERPENTINIZED DUNITE*

J. W. EARLEY, *Gulf Research & Development Company. Pittsburgh, Pennsylvania.*

ABSTRACT

Serpentinized Precambrian dunites from Ontario, Canada, contain several tenths of a per cent chlorine while peridotites and pyroxenites, which are associated, show a nearly normal amount of chlorine, about 0.04 per cent. The chlorine in dunite is fairly soluble in hot water and readily soluble in cold sulphuric acid, except for a few hundredths of a per cent. It is suggested that the readily soluble chlorine was introduced into the rock during serpentinization by chloride-rich solutions from adjacent sediments and tuffs. The difficultly soluble chlorine is probably entrapped in silicate crystals.

INTRODUCTION

The chlorine content of igneous rocks including grabbo, basalt and diabase averages about 0.02 per cent and varies only a few hundredths of a per cent. In contrast the ultramafic rocks, particularly dunite and serpentinized dunite, are quite variable in chlorine content, the amount ranging from a few thousandths of a per cent to several tenths of a per cent.

Although the reason for the variability of chlorine content in serpentinized dunite is controversial, it is believed generally that most of the chlorine is introduced by deuteric or hydrothermal solutions which permeated the rock after primary crystallization. A small amount is undoubtedly introduced as a part of the parent material. If this origin of chlorine in dunites is correct, one would expect the primary chlorine to be more or less uniformly distributed while chlorine introduced by solution would be distributed somewhat unevenly. The present study was undertaken to provide additional analyses of chlorine in serpentinized Precambrian rocks and to determine the distribution of this element in such rock masses.

ANALYTICAL METHOD

Diamond drill core samples[1] from serpentinized ultrabasic rocks in Ontario, Canada, Fig. 1, were used in all of the determinations except for one sample of olivine from a bomb in Hawaiian basalt. Grab samples of clean core which weighed approximately 25 grams were taken at approximately 50 or 100 foot intervals through the rock mass. These samples were crushed and ground to minus 120 mesh in a porcelain mortar.

All of the chlorine determinations were made by a potentiometric method in which one gram of the sample is fused with six grams of sodium carbonate. The fused product is leached on a steam bath for one hour, and the leachate filtered and washed. The filtrate is neutralized with dilute sulphuric acid and excess acid is added to make the solution 7.5 normal. The sample is titrated potentiometrically with standard silver nitrate using silver/silver chloride and glass electrodes.

---

* Publication authorized by Executive Vice President, Gulf Research & Development Company.

[1] Courtesy Dominion Gulf Company, Toronto, Canada.

Care was taken to avoid possible chlorine contamination although it is recognized that some contamination may have occurred during the drilling operation. Owing to the substantially impermeable nature of the rock, it is believed that this source of chlorine contamination does not introduce a serious error in the analyses. Blank determinations were made through the whole procedure. Deionized and triple distilled water was used in all of the determinations.

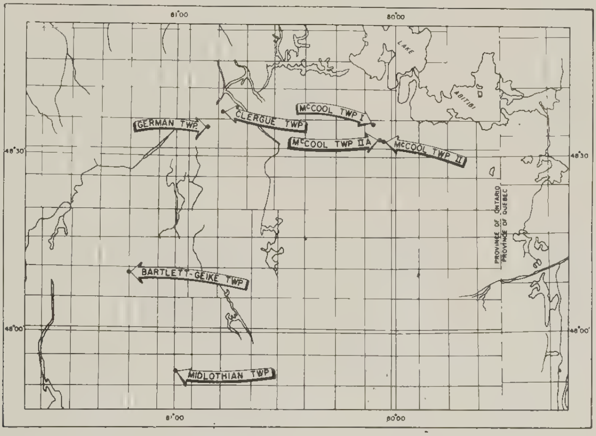

Fig. 1. Location of drill holes.

Data and Results

The chlorine contents of samples from eight diamond drill holes are given in Table 1. The analyses show that the amount of chlorine in dunite[2] varies from about 0.1 to 0.7 per cent and averages 0.23 per cent for all of the samples. In contrast the next most common rock type in this suite of samples, peridotite,[2] averages 0.049 per cent chlorine. The metamorphosed sediments in the lower portion of the German Township drill hole average 0.048 per cent chlorine with the suggestion of a slightly higher chlorine content near the contact with the pyroxene bearing periodotite. The tuff which is in contact with the dunite in the Clergue Township drill hole shows 0.19 per cent chlorine while the dunite immediately adjacent to the contact contains 0.70 per cent chlorine. Where dunite is in contact with peridotite the chlorine content of the dunite is greater by approximately one order of magnitude. Table 1 and Fig. 2 show that the chlorine content of the peridotite is significantly less than that of the dunite. The contact zone may grade over one hundred feet or more. There is also a suggestion that within the dunite mass the chlorine content decreases away from the contact with the peridotite. Dunite from the McCool II drill hole does not show a decrease in chlorine content similar to the other sections but rather remains substantially constant over the length of the section examined. The Clergue dunite, which is in contact with metamorphosed sediments, shows a sharp increase in chlorine content near the contact.

---

[2] Highly serpentinized.

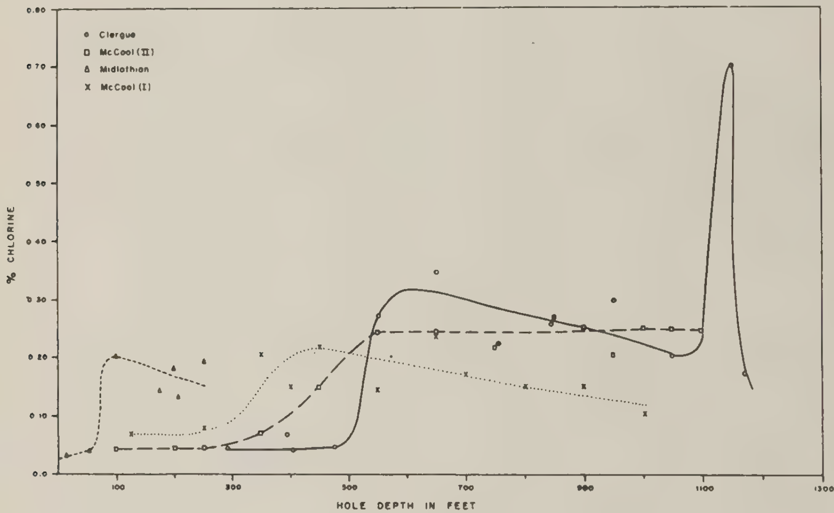

FIG. 2. Per cent of chlorine as a function of depth.

Fluorine determinations were carried out on samples from the McCool II drill hole at 450 feet, the McCool IIA drill hole at 950 feet and the Clergue Township drill hole at 753 feet. None of these samples showed more than 0.01 per cent fluorine, using the method wherein distilled fluosilicic acid at pH 3.0 is titrated with thorium nitrate using sodium alizarin sulfonate as an indicator. Time would not permit fluorine determinations on all of the samples and as a result it can only be assumed that the other high chlorine samples had a low fluorine content.

Table 1. Chlorine Contents of Drill Cores*

German Township			Bartlett-Geike Township			Clergue Township		
Depth	Rock	% Cl	Depth	Rock	% Cl	Depth	Rock	% Cl
170	Perid.	0.098	86	Perid.	0.076	296	Perid.	0.043
225	Perid.	0.077	141	Basalt	0.015	396	Pyrox.	0.070
275	Perid.	0.060	238	Lamp.	0.023	404	Pyrox.	0.038
375	Perid.	0.017	404	Perid.	0.034	471	Perid.	0.046
475	Perid.	0.090	515	Perid.	0.023	551	Dunite	0.27
625	Perid.	0.039	614	Basalt	0.015	651	Dunite	0.37
725	Perid.	0.036	720	Perid.	0.015	753	Dunite	0.22
830	Perid.	0.090				842	Dunite	0.26
925	Pyrox.	0.028				949	Dunite	0.30
1095	Seds.	0.078				1050	Dunite	0.21
1150	Seds.	0.057				1150	Dunite	0.70
1190	Seds.	0.021				1170	Tuff	0.19
1250	Seds.	0.036						

Midlothian Township			McCool Township I			McCool Township II		
Depth	Rock	% Cl	Depth	Rock	% Cl	Depth	Rock	% Cl
5	Perid.	0.03	130	Perid.	0.07	100	Gabbro	0.04
50	Perid.	0.04	250	Perid.	0.08	200	Perid.	0.04
100	Dunite	0.20	350	Dunite	0.21	250	Perid.	0.04
175	Dunite	0.14	400	Dunite	0.15	350	Perid.	0.07
200	Dunite	0.18	450	Dunite	0.22	450	Perid.	0.15
202	Dunite	0.13	550	Dunite	0.14	550	Dunite	0.24
250	Dunite	0.19	650	Perid.	0.24	650	Dunite	0.24
			700	Dunite	0.17	750	Dunite	0.22
			800	Dunite	0.15	850	Dunite	0.27
			900	Dunite	0.15	900	Dunite	0.25
			1000	Dunite	0.11	950	Dunite	0.21
						1000	Dunite	0.25
						1050	Dunite	0.25
						1100	Dunite	0.24

Note: Perid.—Serpentinized peridotite; Pyrox.—Serpentinized Pyroxenite; Lamp.—Lamprophyre; Seds.—metamorphosed graywacke and argillite; Basalt—Olivine basalt dike.

* Analysts—B. B. Osthaus and J. A. Solomon

Relationship of Chlorine to Water Content

It seems reasonable to suggest that there may be a relationship between the high chlorine content of ultramafic rocks and their water content. Analyses of composite samples of anorthosite, altered peridotite and altered dunite which are given in Table 2 show that although the water content of the anorthosite is approximately one-quarter of the water content of the peridotite which underlies it, the chlorine contents of both rocks are approximately the same. On the other hand the water contents of the peridotite and dunite are similar but the chlorine content of the dunite is several times greater.

Further, the determination of chlorine in a fresh olivine bomb in recent basalt from Hawaii shows 0.01 per cent chlorine in the olivine and 0.04 per cent chlorine in the basalt. The water content of the volcanic material was not determined but in view of the fresh nature of the rock and the lack of alteration of the olivine it is reasonable to suppose that the total water content of either the olivine or basalt was less than one per cent.

TABLE 2. ANALYSES OF McCOOL TOWNSHIP IIA COMPOSITE CORE SAMPLES†

Depth, Feet	Rock Type	Per Cent Cl	Per Cent Total H_2O
92– 112	Anorthosite	0.01	4.18
225– 296	Peridotite*	.01	12.54
332	Peridotite*	.07	11.82
463– 493	Dunite*	.26	13.70
585– 607	Dunite*	.23	13.15
756– 760	Dunite*	.23	13.80
962– 995	Dunite*	.21	13.00
1126–1226	Dunite*	.21	12.59

* Highly serpentinized.

† Analysts—B. B. Osthaus and J. A. Solomon.

Analyses of a variety of ultramafic rocks reported by Kuroda and Sandell (1953) suggest that high chlorine content is associated with high water content, although there are notable exceptions as evidenced, for example, by Harzburgite from Lewis Hill, Newfoundland, which shows 0.06 per cent chlorine and 10.05 per cent water. However, none of the ultramafic rocks reported by Kuroda and Sandell or by the author shows a high chlorine content and a low water content. In contrast, the water content of alkaline lavas reported by Bowen (1937) is low while the chlorine and fluorine contents are relatively large. From published data and the data given in this report, one can suggest that a high chlorine content in dunite is associated with a high water content but a high water content does not necessarily indicate a high chlorine content.

DISTRIBUTION OF CHLORINE IN ALTERED DUNITE

Since all of the dunites were highly serpentinized with the development of chrysotile veinlets, samples at depths of 651 and 753 feet in the

Clergue Township hole which contained chrysotile fiber and massive serpentinized dunite were separated and each fraction was analyzed for chlorine. The chlorine contents of the chrysotile fiber and serpentinized dunite were 0.46 per cent and 0.36 per cent, respectively, for the sample at 651 feet and 0.27 and 0.19 per cent, respectively, for the sample at 753 feet. Although the chlorine content of the chrysotile fiber fraction is larger in each sample the difference is not great and one must conclude that chlorine is more or less evenly distributed throughout the whole rock mass.

TABLE 3. SOLUBILITY OF CHLORINE IN DUNITE AT 1150 FEET IN CLERGUE TOWNSHIP DRILL HOLE

Solvent	Digestion Time	Temperature	Per Cent Cl
H_2O	1 hour	85° C.	0.20
7.5N H_2SO_4	5 mins.	25° C.	0.62
7.5N H_2SO_4	1 hour	85° C.	0.65
Total chlorine as determined by fusion procedure			0.70

An attempt was made to determine the location of the chlorine in the rock mass by carefully hand-picking the various mineral components for study. Although the Clergue Township sample at 1150 feet showed 0.70 per cent chlorine, suggesting the presence of one or more per cent of a chlorine bearing mineral and possibly isomorphous substitution of chloride ions for hydroxyl ions, no *x*-ray diffraction evidence could be found for either of these conditions. One must, therefore, suspect that the chlorine is present in an amorphous phase and/or that it occurs in minute fluid inclusions. Small and undetectable amounts of crystalline chlorides may be present as discrete particles located along grain boundaries.

The solubility of the chlorine bearing component was determined in water and in 7.5N sulphuric acid as shown in Table 3. These results indicate that a portion of the chlorine is soluble in water and this may be derived from soluble metal chlorides which are intergranular or present as minute particles along grain boundaries. The amount of chlorine dissolved in cold acid in five minutes is substantially the same as that dissolved in hot acid for one hour indicating that the chlorine bearing component is readily soluble in acid. The difference between the amount of chlorine which is soluble in hot acid and the total chlorine as determined by sodium carbonate fusion, 0.05 per cent, may be accounted for in part by analytical error, sample variation or actual chlorine which is held tightly by the less soluble part of the rock. Some combination of these possibilities seems to be the most likely explanation.

Although the samples were studied by *x*-ray and chemical methods, the location of chlorine in serpentinized dunite remains unknown. However, as one would suspect, the bulk of the chlorine does not occur as chloride ions in isomorphous substitution for hydroxyl ions in chrysotile or antigorite or for that matter in any of the common hydrous silicates found in serpentinized dunite.

DISCUSSION

Dunite is a nearly pure forsteritic rock, and by virtue of its composition, formation by simple magmatic processes is practically precluded. From a geochemical viewpoint, Bowen and Tuttle (1949) concluded that ultramafic rocks can be intruded only in a solid state. This condition can be met by crystallization of olivine from a basic magma with subsequent filter pressing and intrusion of the olivine as a crystal mush. Subsequently dunite may be altered by metamorphic and/or hydrothermal processes to serpentinized dunite. Alternatively, serpentinized dunite may be formed by metasomatic processes involving desilication of basic rocks by water vapor which is undersaturated with SiO_2.

The real problem at hand is one of accounting for several tenths of a per cent chlorine. Several explanations can be offered for the high chlorine content of these serpentinized Precambrian dunites but it must be remembered that there is no proof for any.

Firstly, one can propose that the parent olivine crystals formed in a closed system, a magma, at high temperature and pressure and as a result a portion of the volatiles in the system was trapped during primary crystallization. Inclusion of trace amounts of various elements can be accounted for by this means. Normally gaseous elements such as chlorine seldom amount to more than a few hundredths of a per cent of the rock. Furthermore, appreciable amounts of fluorine are generally present in magmas and as a result entrapped magmatic gases should contain comparable amounts of fluorine and chlorine. However, the dunites included in this study do not show unusual amounts of fluorine. For these reasons it seems impossible to account for the high chlorine content of the rocks on a basis of entrapped magmatic volatiles, although it is quite reasonable to suggest that the few hundredths of a per cent chlorine which is difficultly soluble and the fluorine can be attributed to such an origin.

Secondly, if the chlorine in the dunite was not introduced as entrapped material, it must have been introduced later by dueteric or hydrothermal solutions or by imbibition of fluids from adjacent rocks. Any of these fluids or solutions must have had a high concentration of chlorine but a low concentration of fluorine. Without entering into a long discourse on the character of hydrothermal solutions it is probably sufficient to point out that hydrothermal solutions usually follow channel ways. However, it must be remembered that metasomatism affects large rock masses and it is entirely possible that serpentinization in these rocks is the result of metasomatic processes involving chloride-rich fluids.

Since dunites are frequently associated with orogenic belts and are found associated with sedimentary rocks, is it possible that these Precambrian dunites were formed in zones containing sediments saturated with a high chloride brine? Cores from only two of the basic rock masses studied showed that there were sediments in contact with altered peridotite in German Township and with altered dunite in Clergue Township. The altered peridotite in contact with graywacke and argillite in German Township shows a slightly higher chlorine content than most peridotites, approximately 0.060 per cent as compared with an overall average of 0.049 per cent. Here the metamorphosed sediments show a high chlorine content near the contact with the ultrabasic rocks. The relationship between the chlorine content of the Clergue Township dunite and the tuff is more striking in that the dunite immediately adjacent to the contact contained 0.70 per cent chlorine while the tuff adjacent to the contact contained 0.19 per cent chlorine. Away from the contact the chlorine content of the dunite is only about half of that near the contact. Although this is rather scant evidence on which to base a hypothesis, there is a suggestion that the water necessary for serpentinization of the dunite was derived from adjacent sediments which were saturated with a chloride brine. It is conceivable that such a brine permeated the rock mass either during or shortly after formation. Water was used up in the formation of serpentine and the resultant fluid was concentrated to a point where chlorides were precipitated either along grain boundaries or in interstices of the rock. If metal chlorides or oxychlorides were precipitated it is difficult to see why there is no evidence for such compounds in the rock. One would expect these compounds to be readily soluble and this is consistent with the observations. Further, one would expect the chlorine content of the rock to increase away from the contact with the sediment since the fluids would be concentrated as they migrated through the rock. There is evidence of this in the Clergue, Midlothian and McCool rock masses.

Other interpretations may be equally valid. It is the author's sincere hope to interest someone in undertaking a comprehensive study of chlorine rich ultrabasic rocks including processes of serpentinization.

REFERENCES

KURODA, P. K., AND SANDELL, E. B. (1953); Chlorine in Igneous Rocks, *Bull. Geol. Soc. of Amer.*, **64,** 879–896.

BOWEN, N. L. (1937); Recent high-temperature research on silicates and its significance in igneous geology, *Amer. Jour. Sci.* **33,** 1–21.

BOWEN, N. L., AND TUTTLE, O. F. (1949); The system MgO-SiO_2-H_2O, *Bull. Geol. Soc. of Amer.*, **60,** 439–460.

Manuscript received June 8, 1957.

THE AMERICAN MINERALOGIST, VOL. 43, JANUARY–FEBRUARY 1958

NOTES AND NEWS

AN OCCURRENCE OF MOLYBDENIAN STOLZITE IN ARIZONA*

JOHN N. FAICK, *U. S. Geological Survey, Tucson, Arizona* AND FRED A. HILDEBRAND, *U. S. Geological Survey, Washington, D. C.*

Stolzite containing about 9 per cent MoO_3 occurs near Miami, Gila County, Arizona. This tungsten-bearing mineral, which is considered to be an intermediate member of the isomorphous wulfenite-stolzite series, was noted by Faick and J. A. MacKallor,† in a prospect that was examined on behalf of the Defense Minerals Exploration Administration in November 1951. This prospect is situated low on the east slope of Day Peaks in the Lost Gulch area of the Inspiration quadrangle, and is about $1\frac{3}{4}$ miles southwest of the Copper Cities open-pit mine. The locality is in the Globe-Miami district, the geology of which has been described by Ransome (1903, 1904, 1919) and Peterson (1954).

The prospect in which the molybdenian stolzite was found consists of an adit about 100 feet long in a mineralized zone along a nearly vertical, easterly trending fault that cuts diabasic rocks. The principal constituents in the zone are altered host rock, limonite, and minor amounts of quartz. Scheelite, which was identified by its pale-bluish fluorescence under an ultraviolet light, was observed in the altered zone as a few isolated grains and as a single small pod about one inch wide and 4 inches long. The molybdenian stolzite occurs in cavities in quartz and disseminated in limonite. The thin, tabular, imperfectly formed white, lemon-yellow and orange crystals of the stolzite are megascopically indistinguishable from wulfenite.

From specimens collected by Faick, L. G. Evans‡ prepared a heavy-liquid concentrate of mineral grains using acetylene tetrabromide, and further purified the concentrate by handpicking out impurities with the aid of a microscope. Evans identified the mineral by its specific gravity (7.5), optically negative character, high indices of refraction like other members of the series, and by visual arc spectroscopic tests for W, Mo, and Pb. Examination of grains in thin section indicated that the mineral is altered along fracture planes to an unidentified isotropic material. Chemical analyses of the concentrate are given in Table 1.

Material submitted to the U. S. Geological Survey laboratories for *x*-ray confirmation of the molybdenian stolzite was found to contain minute amounts of an unidentified mineral and some brownish and

---

* Publication authorized by the Director, U. S. Geological Survey.

† Geologist, U. S. Geological Survey.

‡ Mineralogist, U. S. Bureau of Mines, Tucson, Arizona.

Table 1. Chemical Analyses of Molybdenian Stolzite from the Lost Gulch Locality, Miami, Arizona

Analyses by F. G. Hawley*

	(1)	(2)
PbO	56.27	56.3
WO_3	25.40	23.9
MoO_3	8.62	9.3
As_2O_5	4.56	4.2
P_2O_5	2.14	0.73
CaO	0.80	0.8
Fe_2O_3	0.28	—
SiO_2	—	0.4
R_2O_3	—	1.4
Total	98.07	97.03
Ratio W:Mo	3.5:1	3.06:1

* Chemist, retired, U. S. Bureau of Mines; Tucson, Arizona. During the 1930's Mr. Hawley analyzed two other samples of physically similar material from unidentified prospects in the Lost Gulch area, with results as follows: (1) PbO 51.2, WO_3 20.4, MoO_3 5.5; (2) PbO 52.4, WO_3 30.8, MoO_3 6.27.

greenish-brown grains that were proved by *x*-ray powder diffraction to belong to the mimetite-pyromorphite group of minerals. The presence of these minerals probably accounts for the high content of As_2O_5 and P_2O_5 in the analyses, and also for the high content of PbO, which is in excess of that needed to satisfy the formulas of intermediate members of the wulfenite-stolzite series. Apparently the material used in the chemical analyses contained admixtures of these associated minerals although reasonable precautions were taken to obtain a pure sample.

In order to compare the mineral from Arizona with other wulfenites and stolzites, Hildebrand used *x*-ray patterns of wulfenite from Copiapo, Chile, and from Inyo County, California, and prepared *x*-ray patterns of stolzite from Broken Hill, New South Wales, Australia; tungstenian wulfenite (chillagite) from the Chillagoe and Christmas Gift mines, Chillagoe, Queensland, Australia, and wulfenite from Cairo, Egypt. A few analyses of the minerals from these localities have been published, but there is no assurance that the minerals acquired for *x*-ray exactly represent those used for the original analyses. A recent spectrographic examination of the wulfenite-stolzite group mineral from Cairo, Egypt by Janet Fletcher§ shows that it contains major amounts of lead and molybdenum and no detectable tungsten. Hence, it is a true wulfenite representing an end member of the wulfenite-stolzite series. It is noteworthy that *x*-ray examinations revealed that the two samples from Chillagoe, Queensland, Australia are dissimilar and neither of them corresponds to the tungstenian wulfenite reported by Palache and others (1951, pp. 1083–1085).

---

§ Spectroscopist, U. S. Geological Survey.

Comparison of the *x*-ray powder patterns of the minerals studied permits them to be grouped as follows:

Stolzite from Broken Hill (film 11468) and the mineral referred to as chillagite from the Chillagoe mine (film 11469) were found to be nearly identical and were accepted as standard patterns representing stolzite.

Wulfenites from Copiapo, Chile (film 5695), Inyo County, California (film 6544), Cairo, Egypt (film 11482) and the tungstenian wulfenite (chillagite) from the Christmas Gift mine (film 11483) were found to be nearly identical with each other but appreciably different from the two stolzites cited above, and were, therefore, accepted as standard patterns representing wulfenite.

The molybdenian stolzite from Arizona (films 11428, 11429, 11480 and 11481) gives an *x*-ray pattern that is intermediate between the stolzites and wulfenites cited above and it should probably be placed toward the stolzite end of the series.

Tungstenian wulfenite (chillagite) from Santa Rosa, province of San Luis, Argentina, is described by Ahlfeld and Angelelli (1948, pp. 204–205) and two analyses are given. These analyses and analyses of the tungstenian wulfenites from Chillagoe, Australia are reproduced in Table 2 for comparison with the analyses of the molybdenian stolzite from Arizona as given in Table 1.

Table 2. Chemical Analyses of Tungstenian Wulfenites

	Christmas Gift Mine Chillagoe, Australia	Santa Rosa, Province of San Luis, Argentina	
	1	2	3
PbO	53.9 to 54.7	47.80	49.50
WO_3	21.1 to 29.5	19.60	18.40
MoO_3	16.3 to 22.2	19.30	20.40

1—Analyses from Palache and others (1951, p. 1085).
2 & 3—Analyses from Ahlfeld and Angelelli (1948, p. 205).

According to Palache and others (1951, pp. 1083, 1087–1088), at least a partial isostructural series exists between wulfenite ($PbMoO_4$) and stolzite ($PbWO_4$) and W may substitute for Mo in intermediate members of the series; those authors state, however, that the few reported analyses of stolzite do not reveal the substitution of Mo for W. As shown by chemical analyses the mineral collected at the Lost Gulch locality in Arizona probably is an example in which Mo takes the place of some of the W in the stolzite formula. The mineral is properly termed molybdenian stolzite because the ratio of W:Mo exceeds 1:1.

Insofar as the writers know, intermediate members of the wulfenite-stolzite series have been identified only from the above mentioned areas in Australia and Argentina. The scarcity of reported occurrences of intermediate members of this isostructural series is surprising inasmuch as neither wulfenite nor stolzite is very rare. The intermediate members of the series probably have been overlooked because of their similarity in appearance to wulfenite.

The writers gratefully acknowledge the assistance of L. G. Evans, F. G. Hawley and others whose efforts have made this report possible.

REFERENCES

Ahlfeld, F., and Angelelli, V., Las Especes Minerales de la Republica Argentina, *Univ. Tucumen, Inst. Geol. Pub.* **458,** 204–205 (1948).

Palache, C., Berman, H., and Frondel, C., Dana's System of Mineralogy, Vol. II, 1081–1088 (1951).

Peterson, N. P., Copper Cities Copper deposit, Globe-Miami district, Arizona, *Econ. Geol.,* **49,** 362–377 (1954).

Ransome, F. L., Geology of the Globe copper district, Arizona, *U. S. Geol. Survey, Prof. Paper* **12,** 168 pp. (1903).

———, Description of the Globe Quadrangle, Arizona, *U. S. Geol. Survey,* Folio **111,** 17 pp. (1904).

———, The copper deposits of Ray and Miami, Arizona, *U. S. Geol. Survey,* Prof. Paper **115,** 192 pp. (1919).

THE AMERICAN MINERALOGIST, VOL. 43, JANUARY–FEBRUARY 1958

HUNTITE FROM TEA TREE GULLY, SOUTH AUSTRALIA

Brian J. Skinner, *University of Adelaide, Adelaide, Australia.*

Huntite, $Mg_3Ca(CO_3)_4$, occurs as a weathering product in the Proterozoic, Torrens Dolomite, near Tea Tree Gully, South Australia.

The Torrens Dolomite is fine-grained and compact, with minor interbedded shale and quartzite bands. Folding, minor faulting and jointing are present throughout the horizon. Around fold noses the shales and quartzites are often brecciated, though the dolomite itself is unbroken. Minor faults and a brecciated shale band are well-exposed to a depth of 50 feet in two small quarries in the Torrens Dolomite, 1 mile east of Tea Tree Gully.

Huntite occurs as sporadic nodules in the fault zones and in the brecciated shale. The distribution of the huntite strongly suggests a close relation to the present surface. In the fault zones huntite has not been observed more than 30 feet below the surface, and in the brecciated shale band, not more than 10 feet.

The present soil cover is 3 to 4 feet deep and appears to be derived by weathering of the underlying dolomite and shale beds. The predominant carbonate in the soil is calcite. Examination of surficial weathering products in the area shows that the compact dolomite breaks down to a fine powdery calcite. The calcite remains in the soil or, commonly, fills joints and cracks in the rock. The magnesium is apparently removed in solution, for magnesite is only found in isolated nodules at the base of the soil layer.

Faults and breccia zones localize deep weathering processes below the soil level and provide obvious channel-ways for descending surface waters. It is in these deep weathering zones that the huntite occurs. The huntite nodules are always found in the most porous zones, and generally in channel-ways that can be visually followed to the surface. The fault zones and breccias are filled with fragments of rock and huntite nodules up to 6 inches in diameter, set in a fine clay matrix. *X*-ray powder diffraction studies have shown the clay matrix to consist of kaolin, muscovite, quartz, chlorite, minor talc, goethite and magnesite.

In this deposit, huntite does not appear to form at depths greater than 30 feet below the surface. Suitable water channels persist below this depth, but the only carbonates present are dolomite and nodular magnesite.

No evidence has been found which suggests that huntite forms by interaction of dolomite and descending surface waters. Huntite has not been observed crusting either dolomite fragments or magnesite nodules. Since it is always nodular and is found in brecciated shales, the evidence

TABLE 1. ANALYSIS OF HUNTITE, TEA TREE GULLY, SOUTH AUSTRALIA

	(1)	(2)
MgO	34.4	33.2
CaO	16.0	15.6
CO_2	50.4	48.9
Cl_2	Tr.	N.D.
Insol.	Nil.	N.D.
Total	100.8	97.7

(1) Analysed in Geology Department, University of Adelaide.

(2) Analysed by J. T. Hutton, Soils Division, C.S.I.R.O.

strongly suggests that the huntite is formed by direct precipitation from descending surface waters. However, the possibility that huntite may form by interaction between descending surface water and previously formed magnesite nodules cannot be ignored.

In appearance and physical properties the huntite is identical with that reported from Currant Creek, Nevada, by Faust (1953). The grain size is less than two microns.

Two nodules have been analysed (see Table 1). One analysis was made in the Geology Department, University of Adelaide, the other by J. T. Hutton, Soils Division, C.S.I.R.O. The C.S.I.R.O. sample contained some insoluble clay material, which accounts for the numerical differences between the two analyses. The two analyses are in excellent agree-

TABLE 2. *X*-RAY POWDER DIFFRACTION DATA FOR HUNTITE*

d Å	I	*d* Å	I	*d* Å	I
5.64	W	1.515	VVW	1.111	VVVW
4.73	VW	1.479	M	1.102	VVW
3.63	W	1.462	VVW	1.095	VVW
3.12	VVW	1.450	VW	1.080	VVW
2.89	M	1.443	W	1.074	VVW
2.830	VVS	1.415	VW	1.055	VVW
2.74	VW	1.395	W	1.044	VW
2.598	M	1.382	VW	1.037	VVVW
2.443	M	1.370	W	1.006	M (Doublet)
2.372	M	1.354	W	0.9957	VVVW
2.279	W	1.333	VW	0.9865	VVVW
2.188	M	1.318	W	0.9785	VW
1.988	W	1.302	M	0.9735	W
1.966	VS	1.291	VVVW	0.9625	VVVW
1.895	VVW	1.277	VW	0.9554	VVVW
1.888	VW	1.259	VW	0.9508	W
1.832	W	1.244	VW	0.9444	VW
1.818	VW	1.239	W	0.9395	W
1.793	W	1.218	W	0.9322	VVVW
1.762	VS	1.205	VW	0.9264	W
1.752	VS	1.195	VVW	0.9199	VVW
1.696	M	1.178	W	0.9174	VVW
1.651	VW	1.161	W	0.9143	VW
1.608	VVW	1.142	W	0.9071	VVVVW
1.581	M	1.133	VVW	0.8983	VVW
1.523	VW	1.125	M		

* These data were obtained from 5 *x*-ray powder diffraction photographs taken with a Philips 114.83 mm. diameter camera, using cobalt radiation with an iron filter. The necessary corrections for film shrinkage were applied.

ment, and in both cases the formula is obviously $Mg_3Ca(CO_3)_4$.

X-ray powder diffraction data (Table 2) are in agreement with those of Faust (1953) and Koblencz and Nemecz (1953). More diffraction lines have been recorded than reported by the previous workers, and not all can be indexed on the unit cell proposed by Faust. A spacing of 2.74 Å, not previously reported, has been persistently recorded and does not vary in intensity from sample to sample which would be expected if it were due to an impurity. This diffraction line has now been recorded in Currant Creek, Nevada material (Personal communication, Dr. George T. Faust, Feb. 1957).

Attempts to refine the unit cell proposed by Faust, to fit the observed *x*-ray diffraction data, have been unsuccessful.

REFERENCES

FAUST, G. T., (1953) "Huntite, $Mg_3Ca(CO_3)_4$, a new mineral." *Am. Mineral.* **38,** 4–24.

KOBLENCZ, V., AND NEMECZ, E., (1953) "Huntite from the Dorog Mine, Dorog, Hungary." *Foldtani Közlöny* **83,** 391–395.

THE AMERICAN MINERALOGIST, VOL. 43, JANUARY–FEBRUARY 1958

CHROMIAN MUSCOVITE FROM BAKER MOUNTAIN, VIRGINIA

R. V. DIETRICH, *Virginia Polytechnic Institute, Blacksburg, Virginia.*

Further research concerned with possible correlation between type and color of mica and intensity of color of associated kyanite, as previously outlined by the writer (Dietrich, 1956), has been postponed indefinitely because of a shift in research objectives. The following data derived from already completed studies of chromium-bearing muscovite ("fuchsite") from Baker Mountain, Prince Edward County, Virginia, are presented here because it is believed that possibly other workers may find them of value.

1. *X*-ray investigations: The mica is of the 2M type. As compared to "pure K-muscovite" this chromian muscovite has a slightly larger $c \sin \beta$ value (10.00 Å and 10.10 Å, respectively, for 002 reflection). Partial substitution of Cr^{+3} (radius .63 Å), Fe^{+3} (radius .64 Å), and perhaps Fe^{+2} (radius .74 Å) and $V^{+5,+4,+3}$ (radii .59 Å, .63 Å, and .74 Å, respectively) for Al^{+3} (radius .57) probably accounts for this.

2. Optical properties:

Pleochroism—slight in thick cleavage fragments
Indices of refraction—$\alpha - 1.553$ (calc.)
$\beta - 1.591$
$\gamma - 1.596$
Biaxial (−)
$2V = 37° \pm 3°$
Slight dispersion $r > v$.

3. Specific Gravity: 24.8 ± .01
4. Chemical data:

Analysis (*a*) and analysis reduced to atomic proportions on the basis of O = 48 atoms (*b*):

	(*a*)		(*b*)	
SiO_2	47.00	Si	12.57	16.00
TiO_2	.55*			
Al_2O_3	34.58	Al	10.99	
Cr_2O_3	.17	Cr	.035	8.40
V_2O_5	.07	V	.01	
Fe_2O_3	1.02	Fe'''	.21	
FeO	.29	Fe''	.065	
Mn	tr.			
Li_2O	tr.			
MgO	1.30	Mg	.52	
CaO	.14	Ca	.04	3.98
Na_2O	1.99	Na	1.23	
BaO	.12	Ba	.01	
K_2O	7.90	K	2.70	
Rb_2O	.01	Rb		
Cl	tr.			
F	1.27	F	1.27	48.00
H_2O^+	3.60	OH	6.78	
H_2O^-	.19	O	39.95	
	100.20			

(Analyst: C. O. Ingamells, Rock Analysis Laboratory, University of Minnesota.)

* The titanium oxide was not included in the calculations made to reduce the analysis to atomic proportions because it is believed to represent contamination by rutile. Possibly a small amount of the ferric iron, vanadium, and even chromium also are carried by the rutile.

The analysis expressed as a formula is $4[(K, Na, Ca, Ba, Rb)\,(Al, Cr, Fe''', Fe'', Mg, V)_{2.10}\,(Al_{.86}\,Si_{3.14})\,O_{9.99}(OH, F)_{2.01}]$ which is remarkably similar to the formula that would represent the "average numbers of atoms" of the 9 analyses presented by Whitmore, *et al.* (1946, Table 3, p. 9), *i.e.*, $4[(K, etc.)_{.91}(Al, etc.)_{1.98}(Al\,Si_3)O_{9.65}(OH, F)_{2.35}]$ and also to the "ideal muscovite" formula, $4[KAl_2(AlSi_3)O_{10}(OH, F)_2]$.

The chromium content of this "chromian muscovite" is less than that reported for any muscovite termed "chromian muscovite," "fuchsite," or the like. That the indices of refraction also are lower than those of any of the previously studied specimens corroborates the suggestion (Szadeczky-Kardoss, 1937) that the indices increase with the chromium content. On the other hand, if the calculated value of α is correct, on the basis of formula

$$V_{(-)} = \frac{\frac{1}{\beta^2} - \frac{1}{\gamma^2}}{\frac{1}{\alpha^2} - \frac{1}{\gamma^2}},$$

the suggestion (*ibid.*) that the birefringence also increases with chromium content is not substantiated. The data presented by Whitmore, *et al.* (1946, Table 4, p. 11) also point out the lack of agreement between observed values and the suggested relationship between birefringence and chromium content.

Actually, the chromium content is so low that perhaps the mineral is nearer "pure muscovite" chemically than are many "muscovites" which are impure because of other elemental contaminations. Here, for example, despite the fact that this muscovite contains more than nine times as much iron as chromium, it probably would be referred to by no one as ferri- (or ferro-) muscovite. However, the perhaps less significant, though more readily apparent, fact that the muscovite is definitely abnormally greenish in color has led nearly all previous workers to use some connotation related to its chromium content. Further, it is not impossible that some of the greenish color is dependent upon, or at least contributed to by, the vanadium content. In any case, here is another fine example of the fact that certain elements are strong pigmenting agents even in extremely small amounts.

It is of at least passing interest that the Baker Mountain material contains lithium and barium. Partridge (1937, p. 458) noted that these elements are characteristic of the Mashishimala, Northeast Transvaal, material. Perhaps, instead, they are characteristic of chromium- and/or vanadium-bearing muscovite.

The chromium-bearing muscovite, herein described, occurs with kyanite, rutile, quartz, and minor zircon. Its distribution ranges from a role of the predominant mineral (up to nearly 100 per cent) of schistose segregates through a major constituent of a kyanite schist to a relatively minor constituent of a kyanite-bearing quartzite. The rutile occurs in nearly all cases as small (less than 1×1×1 mm.) grains intimately associated with the mica. Zircon is present in microscopically distinguishable grains, as inclusions in the mica, only. In some specimens kyanite and the mica are associated in such an intimate manner that the mica occurs along cleavage planes of individual kyanite laths. It was because of these relationships that the material had to be hand-sorted and checked microscopically prior to chemical analysis. Despite this care, the analyst reported that at one stage he detected a small residue containing kyanite, rutile, and zircon.

Although no corundum occurs with this suite, the paragenesis appears to fit best "Type 3" of Whitmore *et al.* (1946, p. 18), of which it is suggested that it represents formation at high temperature and high pressure with the chromium likely having " . . . origin in solutions derived from some magmatic source." Jonas (1932) who has made the most complete study of the deposit suggested essentially the same conditions but, although she did not mention the chromium separately, appeared to favor the derivation of constituent elements from the original sediment. She thought the suggestion of Taber (1913) that the kyanite-bearing rock might have been formed as a result of contact metamorphism associated with intrusion of the "Columbia granite" to be an unlikely answer.

The writer wishes to acknowledge the fact that J. J. Glass checked some of the optical determinations. The chemical analysis was paid for by the Kyanite Mining Corporation, through a grant to the Virginia Engineering Experiment Station of the Virginia Polytechnic Institute.

REFERENCES

DIETRICH, R. V. (1956), Trigonal paragonite from Campbell and Franklin counties, Virginia: *Am. Mineral.*, **41,** 940.

JONAS, A. I. (1932), Geology of the kyanite belt of Virginia: *Va. Geol. Sur. Bull.*, **33,** 12–13.

PARTRIDGE, F. C. (1937), Note on the green micas of north-eastern Transvaal: *Trans. Geol. Soc. S. Africa*, **39,** 457–460.

SZADECZKY-KARDOSS, ELEMER (1937), The optical properties of fuchsites: *Math. Naturw. Anz. ungar Akad. Wiss.*, **56,** 346–351.

TABER, STEPHEN (1913), Geology of the gold belt in the James River Basin, Virginia: *Va. Geol. Sur. Bull.*, **7,** 27.

WHITMORE, D. R. E., BERRY, L. G., AND HAWLEY, J. E. (1946), Chrome micas: *Am. Mineral.*, **31,** 1–21.

THE AMERICAN MINERALOGIST, VOL. 43, JANUARY–FEBRUARY 1958

A COMPLEX FORM OF NATURAL NEPHELINE FROM IIVAARA, FINLAND

TH. G. SAHAMA, *Institute of Geology, University of Helsinki, Finland.*

In a paper dealing with the petrology of the cancrinite-ijolite from the alkaline massif of Iivaara in northern Finland, Lehijärvi (1956) described a nepheline with 19.8 atomic $\%K/(K+Na+Ca)$. The same nepheline sample was also used by Smith and Sahama (1954) in developing an x-ray method for determining the composition of natural nephelines. Another sample of nepheline that, according to a personal communication of Mr. Lehijärvi, originates from an exactly similar rock specimen (this Institute collection No. 9341) from the same locality, was investigated by single crystal x-ray methods. The result of this study is briefly summarized in the following.

In addition to the strong reflections that correspond to the ordinary nepheline structure with $a_0=10$ Å and $c_0=8.4$ Å, a series of rotation and Weissenberg photographs revealed a pattern of weak extra reflections which are observable only on strongly exposed photographs. These weak reflections indicate that the ordinary nepheline cell is only a pseudo cell and that the true cell is considerably larger. Like the pseudo cell, the true cell is also hexagonal. The *a*-axes of the cells are at an angle of 30°. The dimensions of the true cell are: $a_0=17.4$ Å; $c_0=76$ Å±1 or 2%. A rotation photograph about the *c*-axis shows the presence or absence of the following layer lines:

Layer lines with $l=9n$..................strong.
Layer lines with $l=9n\pm 2$................very weak.
Layer lines with $l\not\equiv 9n$ or $9n\pm 2$..........absent.

As revealed by the Weissenberg photographs, the rules limiting possible reflections are:

For $(hk\bar{i}l)$ reflections: if $l=9n$ then $l-h$ and $l-k=3n$.
if $l=9n\pm 2$ then there are no restrictions.
For $(000l)$ reflections: $l=18n$.

The extra reflections of the true cell are too weak to allow a determination of the space group to be made with any certainty.

The author is indebted to Dr. J. V. Smith, of the Pennsylvania State University, for checking the measurements of the *x*-ray films.

REFERENCES

Lehijärvi, Mauno (1956), Cancrinite-ijolite from Iivaara, Kuusamo, Finland: *C. R. Soc. geol. Finlande,* **XXIX,** 9–12.

Smith, J. V., and Sahama, Th. G. (1954), Determination of the composition of natural nephelines by an *x*-ray method: *Ming. Mag.,* **XXX,** 439–449.

THE AMERICAN MINERALOGIST, VOL. 43, JANUARY–FEBRUARY 1958

A CHART SHOWING THE SPHERE OF INFLUENCE OF ATOMS AND IONS IN MINERALS

Jerome H. Remick, *Mineralogical Laboratory, University of Michigan, Ann Arbor, Michigan*

A chart showing both the radii and valences of the atoms and ions which enter into minerals can easily be constructed by pressing transparent colored Zip-a-tone circles onto a large size (76″×52″) periodic chart of the elements (Fig. 1). The chart is entirely visual and at a glance one can tell the valence of the ion and its relative size. It has proven to be particularly useful in teaching mineralogy and geology courses dealing with mineral formation. The chart is easily amenable to changes as the colored Zip-a-tone circles are easily replaceable.

The data for the selection of valences found in minerals were taken from Goldschmidt (1954), Green (1953) and Rankama and Sahama (1950). Only the valences found in minerals were used. Circles representing the radii of elements formed only from radioactive disintegration processes and those of the inert gases are not shown.

Atomic and ionic radii as given by Green (1953) were used for this chart. The values in angstrom units were multiplied by 2×10^8 so as to give the radii in centimeters of the circles. For example, the ionic radius for O^{-2} (1.40 Å) when multiplied by 2×10^8 cm./Å gives a radius of 2.80 cm. This was found to be the best scale for the chart as the large ions such as Br^{-1} and I^{-1} just fit in their respective squares. Some overlap occurs with the circles in the squares for Hg, Se, Te, and I. Since the value for the ionic radius for H^{+1} is too small to show to scale, its size is exaggerated so that it is visible. It is the only circle on the chart that is not to scale.

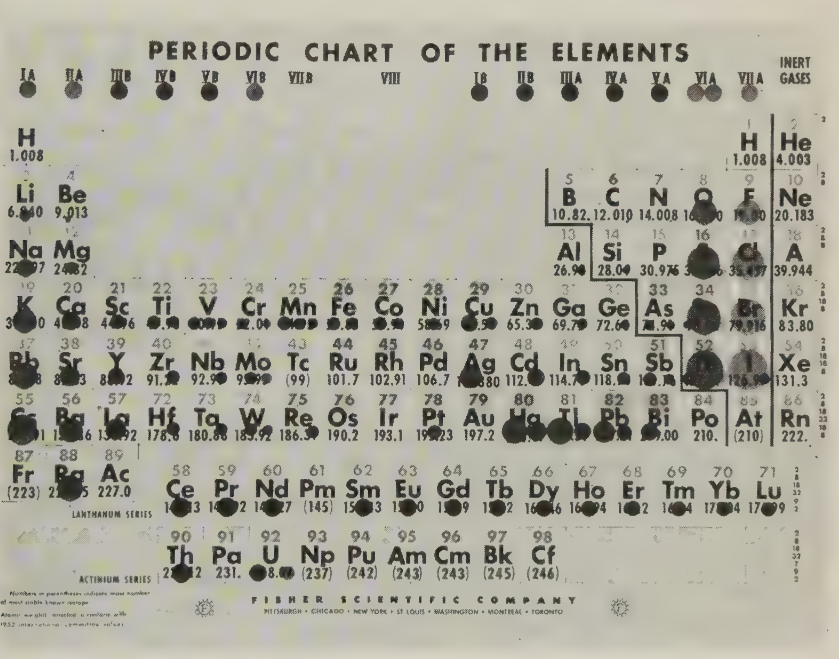

FIG. 1. A chart showing the sphere of influence of atoms and ions in minerals. (Although in the photograph some of the circles appear opaque, they actually are transparent.)

Each valence is designated by a specific color, the colors being used in the order in which they appear in the spectrum. A valence of +1 is represented by red circles, +2 by yellow circles, +3 by green circles, +4 by blue circles, +5 by purple circles, and +6 by gray circles. Elements having a valence of −1 are represented by lighter red circles and those of −2 by lighter yellow circles.

Colored circles showing valence are at the top of the chart just under the sub-group numbers. These have radii of 2 cm. which represents a value of 1 Å, so a rough idea of the size of any radius on the chart can be had by comparison with these unit circles.

Atomic radii are shown by a transparent black and white ruled pattern and are located in the upper part of the square over the atomic number.

Colored circles showing the relative size of the ionic radius or radii for each element, with appropriate color for different valences, are located in the lower part of each square over the value for the atomic weight. If more than one ionic radius of positive valence is given for an element, the radius with the lowest valence is placed to the left. Valences of the same value and so of the same color are aligned so that their centers are in a straight vertical line as for instance Ti^{+4}, Zr^{+4} and Hf^{+4}. The circles representing the positive ionic radii for each period are aligned horizontally so that their centers are on a straight line across the chart.

The Zip-a-tone circles were cut out with a compass with a small piece of sharpened steel in place of the usual pencil point.

The writer wishes to thank the Fisher Scientific Company for permission to use a photograph of their chart. Thanks are also rendered to Professors R. M. Denning and E. Wm. Henirich of the Mineralogical Laboratory, University of Michigan and to Drs. E. Ingerson and C. L. Christ of the U. S. Geological Survey for their suggestions, comments, and criticisms of this chart. If perchance the writer has repeated another's idea, he has done so unknowingly and unintentionally.

BIBLIOGRAPHY

GOLDSCHMIDT, V. M., 1954, Geochemistry, 730 p., Oxford, Clarendon Press.

GREEN, J., 1953, Geochemical table of the elements for 1953: *Bull. Geol. Soc. Amer.*, **64**, 1001–1012.

RANKAMA, K., AND SAHAMA, TH. D., 1950, Geochemistry, 910 p., Chicago, University of Chicago Press.

THE AMERICAN MINERALOGIST, VOL. 43, JANUARY–FEBRUARY 1958

NONFIBROUS ULEXITE FROM THE KRAMER DISTRICT, CALIFORNIA*

ROBERT D. ALLEN, *Jet Propulsion Laboratory, California Institute of Technology, Pasadena, California*

AND

HY ALMOND, *U. S. Geological Survey, Claremont, California*†

Veinlets of a vitreous nonfibrous transparent mineral were observed on a specimen of bedded euhedral borax and clay from the Jenifer mine by Siegfried Muessig, U. S. Geological Survey. The vitreous mineral, first recognized after the enclosing vitreous borax had dehydrated to white tincalconite, was subsequently identified as strontium-bearing ulexite by chemical analysis and verified as ulexite by *x*-ray examination. The ulexite veins, which occur in a zone up to 10 mm. wide, are from less than 1 mm. to 4 or 5 mm. wide and irregularly separated by borax—now altered on exposed surfaces to tincalconite. Clay and disseminated realgar are associated with both borax and the ulexite.

The ulexite occurs in irregular or crudely radiating columnar to bladed masses and in prismatic crystals. Individual columns or blades are striated parallel to their length and are up to 5 mm. long and 1 mm. wide; they exhibit prominent cleavages parallel to their length—presumably the $\{010\}$ and $\{1\bar{1}0\}$ cleavages of ulexite. Discrete crystals, some of which are doubly terminated, are usually not longer than 0.5 mm. or wider than 0.2 mm.

Microscopically, the ulexite grains are short prismatic crystals or nearly equant cleavage fragments (in crushed material). Some of the crystals exhibit a single twin plane. Neither the long prismatic habit nor polysynthetic twinning, both so characteristic of most ulexites, were observed. The optical properties of non-fibrous ulexite are as follows: α_{Na} 1.493 ± 0.001, β_{Na} 1.505 ± 0.001, γ_{Na} 1.526 ± 0.001, birefringence $(\gamma-\alpha)$ 0.033 ± 0.002, 2V (calculated) 75°.‡

---

* Publication authorized by the Director, U. S. Geological Survey.

† Present address, Autonetics Division of North American Aviation, Inc., Compton, Calif.

‡ According to W. T. Schaller (private communication) the published γ index of ulexite, 1.519 or 1.520, is in error and γ is actually near 1.530. He mentions various nonfibrous ulexites from the Kramer district whose indices lie in the following ranges: α, 1.490 to 1.493; β, 1.505 to 1.507; γ, 1.528 to 1.531.

The chemical analysis of nonfibrous ulexite is compared with the theoretical oxide percentages for ulexite in the columns below.

	Nonfibrous Ulexite	Theoretical Ulexite
Na_2O	7.85%	7.65%
CaO	13.51	13.85
SrO	1.06	—
B_2O_3	41.31	42.95
H_2O (+ and −)	36.41	35.55
Total	100.14	100.00

Two fibrous ulexite samples from the Kramer district were analyzed for strontium oxide with a spectrophotometer to evaluate the significance of the strontium oxide content found in nonfibrous ulexite. One contained 0.118 per cent, the other, 0.056 per cent—each considerably less than the 1.06 per cent found by the same method in nonfibrous ulexite.

X-ray powder patterns of nonfibrous and fibrous ulexites from the Kramer district are practically identical with respect to interplanar spacings and relative intensities.

The presence of strontium in the ulexite described may account for its nonfibrous character.

THE AMERICAN MINERALOGIST, VOL. 43, JANUARY-FEBRUARY 1958

MAGNETIC SUSCEPTIBILITIES OF MINERALS IN THE FRANTZ ISODYNAMIC MAGNETIC SEPARATOR[1]

SAM ROSENBLUM, *U. S. Geological Survey Denver Federal Center, Denver, Colorado*[2]

The following list (Table 1) and the accompanying chart (Fig. 1) of magnetic susceptibilities of minerals were compiled to fill the need for a guide in separating minerals in an isodynamic magnetic separator, and were especially designed for the occasional "do-it-yourself" user.

The magnetic susceptibilities on the chart are in terms of increasing amperages on the Frantz separator and are valid only for the tilts indicated: i.e., 15° side, 25° forward. For other settings of tilt, the amperages will serve as relative magnetic susceptibilities of the minerals, and the chart should then be used only as a guide.

The writer worked chiefly with grains in the 100–150 mesh size range, but found the same results are obtained with grains in the 65–100 mesh and 150–200 mesh ranges. No data are available for mesh ranges other

---

[1] Publication authorized by the Director, U. S. Geological Survey.

[2] Present address: ICA/MSM-China, APO 63, San Francisco, California.

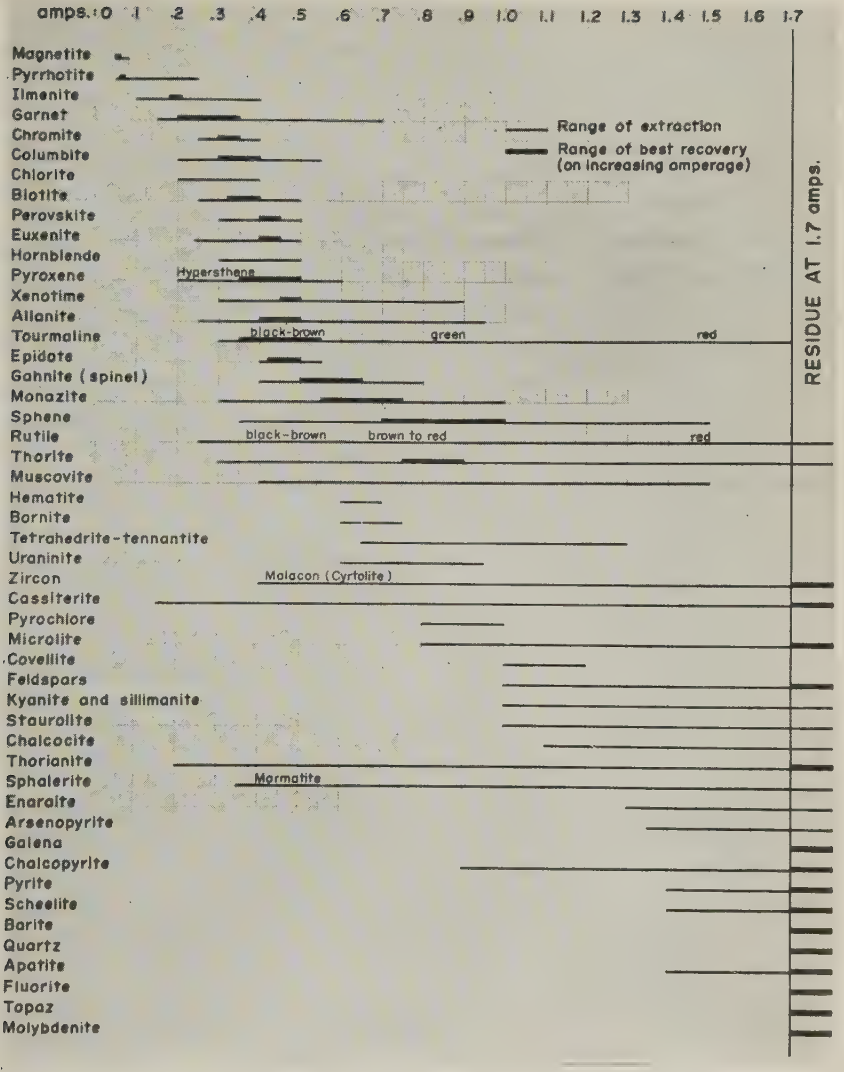

FIG. 1. Magnetic susceptibilities of minerals in Frantz isodynamic magnetic separator (side tilt 15°; forward tilt 25°; dried grains in 100–150 mesh range).

than these. The 100–150 mesh range is probably best for most crushed medium-grained rock samples, as the percentage of locked grains is generally small, and the grains are easier to manipulate and identify than smaller sizes under the binocular and petrographic microscopes.

TABLE 1

Mineral	Extraction range (amps.)	Best extraction range (amps.)
Allanite	.25–.95	.40–.50
Apatite	1.4–1.7+	1.7+
Arsenopyrite	1.35–1.7+	
Barite	1.7+	
Biotite	.25–.50	.32–.40
Bornite	.60–.75	
Cassiterite	.15–1.7+	1.7+
Chalcocite	1.1–1.7+	
Chalcopyrite	.9–1.7+	1.7+
Chlorite	.20–.40	
Chromite	.25–.40	.30–.35
Columbite	.20–.55	.30–.40
Covellite	1.0–1.2	
Enargite	1.3–1.7+	
Epidote	.40–.55	
Euxenite	.24–.50	.40–.45
Feldspars	1.0–1.7+	1.7+
Fluorite	1.7+	
Gahnite	.40–.80	.50–.65
Galena	1.7+	
Garnet	.15–.70	.20–.35
Hematite	.60–.70	
Hornblende	.30–.50	
Ilmenite	.10–.40	.18–.21
Kyanite and sillimanite	1.0–1.7+	
Magnetite	0 – .05	.02(−)
Microlite	.80–1.7+	1.7+
Molybdenite	1.7+	
Monazite	.30–1.0	.55–.75
Muscovite	.40–1.5	
Perovskite	.30–.50	.40–.45
Pyrite	1.4–1.7+	1.7+
Pyrochlore	.80–1.0	
Pyroxene	.20–.60	.35–.50
Pyrrhotite	0 – .25	.02–.04
Quartz	1.7+	
Rutile	.25–1.7+	
Scheelite	1.4–1.7+	1.7+
Sphalerite	.35–1.7+	
Sphene	.35–1.5	.70–1.0
Staurolite	1.0–1.7+	
Tetrahedrite-tennantite	.65–1.3	
Thorianite	.20–1.7+	1.7+
Thorite	.30–1.7+	.75–.90
Topaz	1.7+	
Tourmaline	.30–1.7	.35–.55
Uraninite	.60–.95	
Xenotime	.30–.90	.45–.50
Zircon	.40–1.7+	1.7+

It is suggested that removal of magnetite and pyrrhotite is most efficiently accomplished with a hand magnet and it will avert clogging in the Frantz separator.

Most of the data were determined by the writer; those for the ore sulfides and the columbates were taken from articles by Gaudin and Spedden (1943), and Jacobson, Cawley, and Macleod (1951). Data for fluorite, kyanite and sillimanite, molybdenite, staurolite, topaz and uraninite were supplied by David Gottfried (written communication, 1957) of the U. S. Geological Survey.

The purpose of this note is two-fold: (1) to present data available on some of the common rock-forming and ore minerals, and (2) to urge others to present similar data for other minerals. The isodynamic magnetic separator is a most useful tool in the mineralogical laboratory and its characteristics in the separation of minerals do not seem to differ appreciably from one instrument to another. A more complete chart of magnetic susceptibilities for this instrument is desirable and may in some cases be useful in determinative mineralogy. Additions to the following list will be welcome.

References

Gaudin, A. M., and Spedden, H. R. (1943), Magnetic separation of sulphide minerals: *Am. Inst. Min. Met. Eng. Tech.* Paper No. **1549,** 13 p.

Jacobson, R. R. E., Cawley, A., and Macleod, W. N., (1951), The occurrence of columbite in Nigeria: *Geol. Survey Nigeria,* Occas. Paper No. **9,** 11 p.

The Department of Mineralogy and Petrography, Harvard University, made a substantial contribution toward the cost of the enlarged November-December 1957 issue of the *American Mineralogist.*

Dr. Paul F. Kerr, Professor of Mineralogy at Columbia University, has been presented with the third K. C. Li Medal. This medal is awarded for "Meritorious achievement in advancing the science of tungsten." The two former recipients are Dr. William D. Coolidge, Director Emeritus of the General Electric Research Laboratory, and Dr. Thomas B. Nolan, Director of the U. S. Geological Survey.

Professor W. N. Benson, of the University of Otago, Dunedin, New Zealand, died August 20, 1957, at the age of 72.

National Science Foundation Grant

The National Science Foundation will award grants to partially defray travel expenses for a limited number of American scientists wishing to participate in the meetings of the International Federation of Electron Microscope Societies. This meeting is to be held in Berlin, Germany, 10–17 September, 1958.

Application blanks may be obtained from the National Science Foundation, Washington 25, D. C. Completed application forms must be submitted by 15 February, 1958.

THE AMERICAN MINERALOGIST, VOL. 43, JANUARY-FEBRUARY 1958

THE STRUCTURE AND PROPERTIES OF NATURAL AND SYNTHETIC MINERALS

An invitation conference on the above theme was held at the College of Mineral Industries, The Pennsylvania State University, from July 5 to 8, 1957. Five sessions were held on the following subjects:

Polymorphism and polytypism
Calcium silicate hydrates, serpentines and chlorites
Feldspars and micas
Ferroelectric and ferromagnetic materials
Zeolites and phase-equilibrium investigations

The first, second and fourth sessions will be reported in the *Bulletin of the American Ceramic Society,* while the third and fifth sessions are reported here.

Third Session:

Dr. W. F. Bradley (Illinois Geological Survey) proposed a structure for muscovite in which the deviation from the ideal hexagonal layers was obtained from a consideration of the geometrical restrictions imposed by the necessity for a fit between the tetrahedral and octahedral groups. The resulting distortion was in good agreement with the observed geometry of muscovite. Dr. Bradley pointed out that this idea could be extended to other minerals and might well prove to be an an important principle in crystal chemistry.

Two contributions to the long-standing problem of the structure of the intermediate plagioclases were given. X-ray photographs reveal pairs of reflections whose separation varies with the An-content and whose sharpness varies with the thermal and petrological history. Their origin is as yet unexplained though some sort of ordering and/or segregation is thought to be responsible. Dr. F. Chayes (Geophysical Laboratory) described the results obtained from a simple diffraction apparatus in which a grating containing "ordered and disordered" points was used. This gave the doubled pairs of reflections seen in photographs of plagioclase and promised to give a rapid check of any models proposed for the plagioclase structure. In addition, Dr. Chayes applied his statistical skill to an analysis of the different ways, the runs and the sequences obtained when two types of atoms are placed on a single array of points. Dr. H. D. Megaw (University of Cambridge, England) has used the mathematical theory of A. J. C. Wilson to approach the problem and obtained fairly good agreement by using a different model for each of the three principal axes. The two approaches paralleled each other and the partial success so far achieved leads to the hope that a complete solution of this intriguing phenomenon will not be far waay.

Professor J. Wyart (Paris, France) described experiments in which alkali feldspars had been subjected to heat treatment in the presence of mixtures of NaCl and KCl under dry and aqueous conditions. The products were indentified by x-ray powder patterns. Under dry conditions low albite and adularia (orthoclase) could be interchanged, as could sanidine and analbite (high albite). Under wet conditions the low feldspars were transformed into high feldspars. The experiments under dry conditions promised to lead to a determination of the extent of solid solution, for discontinuities were observed in the plots of NaCl:KCl ratio versus composition of the alkali feldspar deduced from the powder patterns. Discussion centered on the question of whether the conversion of the low feldspars to the high feldspars under aqueous conditions at the comparatively low temperatures of experimentation ($\sim$400° C.) represented equilibrium conditions or merely solution of the feldspar in the fluid with recrystallization in the disordered state (as observed by Goldsmith for microcline).

Dr. H. S. Yoder, Jr. (Geophysical Laboratory, Washington D. C.) described the phase equilibrium studies on alkali and ternary feldspars carried out by himself, and Drs. D. B. Stewart and J. R. Smith. Under the high pressure of water used in the bombs (5000 bars), the unmixing solvus of the alkali feldspars intersected the liquidus-solidus curves at $Or_{34}Ab_{66}$ $Or_{58}Ab_{42}$ and 698° C. The crest of the solvus differed by 40° C. from that obtained by Bowen and Tuttle and this was attributed to the effect of pressure. Dr. Tuttle, however, suggested that it may be the result of a change in the structural state of the feldspar. Dr. J. V. Smith (Penn. State) described the studies carried out in collaboration with Dr. Wm. Scott MacKenzie (University of Manchester, England) on alkali feldspars from igneous rocks, selected to represent the trend from volcanic through hypabyssal to plutonic conditions. A series of phase diagrams for the various cooling rates was proposed.

Dr. F. Laves (Zürich) described the results obtained by the application of infra-red absorption methods to alkali feldspars. The low temperature feldspars show a multiple set of absorptions near 11μ in contrast to the more uniform change of absorption for the high-temperature feldspars.

Fifth Session:

Dr. D. W. Breck (Linde Air Products Company, Tonawanda, N. Y.) reported on recent studies on the zeolites. About thirty zeolites are known to occur in nature and about twenty more have been synthesized in the Linde and other laboratories. Some of the zeolites have large inter-connected cavities in the framework of Si, Al tetrahedra, which lead to remarkable absorption and sieve-like properties. In particular, Dr. Breck described the properties of the Type-A synthetic zeolite whose synthesis and crystal structure were recently established at Linde. It contains large cavities 11.4 and 6.6 Å in diameter interconnected by openings 4.2 Å in diameter. Among its capabilities is the power of separating straight chain from branched chain hydrocarbons.

Professor W. Nowacki (Bern, Switzerland) described the structure of faujasite, another zeolite that contains large cavities. Professor H. O'Daniel and Dr. K. Fischer (Frankfurt, Germany) in a written communication described recent work in which faujasite has been assigned the formula $(Ca, Mg, Na_2)Al_2Si_4O_{12} \cdot 8H_2O$, herschelite has been found to be twinned chabazite with one-dimensional disorder and the structure of gmelinite has been determined.

Mr. P. Saha (Penn. State) described syntheses of analcite and other zeolites from compositions ranging from albite to nepheline. His discovery that analcite can be formed with the composition $NaAlSi_3O_8$ (albite) led to the suggestion that some authigenic albite might represent the breakdown of analcite solid solution. Dr. L. Sand (University of Utah) mentioned the occurrence of enormous deposits of mordenite-ptilolite in the western United States.

Dr. R. Roy (Penn. State) discussed the nature of the polytypic changes in mica and examined the experimental evidence for the existence of a difference in free energy between different polytypes. Mr. F. Dachille (Penn. State) described results obtained from high-pressure squeezer type equipment: P, T data for the coesite form of BeF_2 and the high-pressure form of B_2O_3 among others were presented. There has been some controversy concerning the effective cross-section between the pistons of the apparatus and Mr. Dachille suggested that the pressure must be carried by the whole cross section in runs made at high T and P because the metal of the jaws was found to be deformed after the runs. An attempt to determine the nature of infra-red absorption patterns, and in particular their suitability for the estimation of ionic coordination, by the use of model structures and polymorphs was described.

P. Saha and J. B. Smith

BOOK REVIEWS

TABLES FOR THE MICROSCOPIC AND X-RAY DETERMINATION OF THE OPAQUE MINERALS ("TABLAS PARA LA DETERMINACIÓN MICROSCÓPICA Y RAYOS X DE MINERALES OPACOS") 2d enlarged edition, by Alejandro Novitzky. Universidad Técnica de Oruro, Biblioteca de Estudios Técnicos No. 2, Oruro, Bolivia, 1957, 268 pages, 13×10 inches. Price $12.00.

This work is a compilation of nearly all existing data for the microscopic and *x*-ray determination of 298 opaque minerals. An introductory table of six pages lists all of the minerals, arranged in groups of isotropic, weakly anisotropic, strongly anisotropic, and minerals frequently showing internal reflections. Each group is divided into three sub-groups according to "polishing hardness," with galena and chalcopyrite as index minerals for comparison. Each sub-group of the weakly anisotropic minerals is further divided into three categories showing very weak, weak, and noticeable birefringence. The groups are divided into 17 columns by color. This arrangement, into some 130 sub-groups, facilitates the use of the main tables which follow, each of which deals with one of the 17 color classes. In the second group of tables, each mineral is named, and its composition, crystal system, density, hardness, magnetism, macroscopic observations—color and cleavage—color 'hue' or tint, with comparison to other minerals, reflectivity, pleochroism, zoning, cleavage, Talmage and polishing hardness, optical phenomena in cedar oil such as color, reflectivity, and pleochroism are given. These data all refer to observations under parallel nicols, and are followed by similar data under crossed nicols, in air and cedar oil, of anisotropy, internal reflections, and twinning. Next, a list of associated minerals, diagnostic criteria, and provenance are tabulated.

These tables, including the six introductory pages, comprise 95 pages of the work. There follows a seven page section on microchemical reactions of the various metals present in ore minerals. Then 28 pages give for each such metal a tabular list of minerals containing it, with brief diagnostic microscopic criteria. Forty-five pages follow on etch-reactions, first arranged according to reagents employed, then there is an alphabetical listing of minerals giving their specific etch-reactions. Eighteen pages contain reflection data, in air and oil, by photo-electric cell and photometric ocular (data for O and E), for various wave lengths of light. The *X*-ray Section of 73 pages concludes the book. The first four pages list all the minerals in order of the strongest of the three main lines of the diffraction pattern. The other 69 pages give complete powder data for each mineral, with reference to the source of the data.

Evidently, Novitzky has compiled in one volume for Spanish speaking workers the data of Short, Harcourt and Uytenbogardt, in English, and of Schneiderhöhn and Ramdohr in German, as well as information from other sources. There is little outside of some of the *x*-ray data not already available in the several standard works mentioned, but it is convenient to have it all in classified tabular form in a single volume.

The typography and grade of paper are good, though the paper cover may require re-enforcement if the book is to be used steadily for reference.

For Spanish speaking mineralogists, to whom the English and German texts are not readily available, and where an *x*-ray diffraction film library is lacking, Novitzky's work will be especially useful and welcome.

Earl Ingerson
U. S. Geological Survey,
Washington 25, D. C.

KLEINE METEORITEKUNDE by Fritz Heide (Second Edition). vii+142 pages, 107 figures. Springer Verlag, Reichpietscufer 20, Berlin W 35, Germany, 1957. Price D.M. 7.80 (ca $1.90).

This little book is Volume 23 in Springer's popular science series. It is considerably larger than the first (1934) edition, having had 23 pages of text and 15 illustrations added.

The new edition has the same chapters and sections as the original one; additional material has been added to individual sections. The chapter headings are Fall Phenomena, Material of Meteorites, and Source and Origin of Meteorites. An appendix gives a list of German collections of meteorites, a table of the concentrations of the elements in meteorites, a table of the minerals of meteorites, and a four page section on tektites.

The book is a compact summary of general information on meteorites. It is well illustrated with pictures of many types of meteorites and their thin and polished sections. A map shows the distribution of the principal meteorite craters of the world and there are photographs, diagrams, cross sections, and detailed maps for more than half of these.

Earl Ingerson
U. S. Geological Survey,
Washington 25, D. C.

THE LIVING ROCKS. Photographs by Stévan Célébonovic; preface by Andre Maurois; commentary by Geoffrey Grigson; translation by Joyce Emerson and Stanley A. Pocock. The Philosophical Library, 15 East 40th St., New York 16, N. Y., 1957. 94 pages, 64 plates. Price, $6.00.

The Living Rocks is a photographic essay by Stevan Célébonovic based on specimens in the Museum d'Histoire naturelle de Geneve, the Museum National d'Histoire naturelle de Paris, the British Museum (Natural History) and the Geological Survey and Museum in London. It is intended as the first of an *Art and Nature Series* to be photographed by Célébonovic, with future volumes to consist of a pictorial survey of natural and man-made materials, both living and inorganic, both ancient and modern.

The full page photographs (quarto size), which are bled into the margins, are in two groups: Nos. 1–24 of minerals and Nos. 25–64 of fossils. Illustrations of minerals, which include opal, limonite, anatase, malachite, axinite, pseudomalachite, aragonite, copper, silver, vanadinite, pyrrhotite, stibnite, clinochlore and quartz, serpentine, heulandite, and scolectite, epidote and calcite, fluorite, pennine, manganite, descloisite, manganese dendrites, and collinsite, under from 4–20× magnification and skillful lighting, are a phantasmagoria of forms and groups, sharply etched in shade and sheen. Although chosen principally for the stunning optical effects of their shapes and patterns, many photographs also are resplendent in crystallographic and paragenetic details.

The collection of fossils photographed in equally effective not only in satisfying the eye but also in restoring to a thought of life the creatures whose remains are registered. This section contains a simplified geologic column.

The text, a short delightful discourse prepared for the layman, proves more than just edible to the mineralogist or paleontologist and in many places is beautifully phrased. Most of the localities to which reference is given are in England.

E. Wm. Heinrich
University of Michigan,
Ann Arbor, Michigan

STRUKTUR UND EIGENSCHAFTEN DER KRISTALLE by Helmut G. F. Winkler, pp. viii+314, 111 illustrations, 82 tables, 2 plates, Springer Verlag, Berlin-Göttingen-Heidelberg, 1955. Price 2.80 D.M. (stiff binding), 29.60 D.M. (linen).

The first edition of this book was reviewed in Volume 37 of this journal (pp. 132–133, 1952). The second edition is a considerably expanded (20 per cent) and revised book. There are 49 additional illustrations.

Part A, entitled "Einführung und Kristallgeometrische Grundlagen," consists of a revision of the former parts, entitled "Einführung und Anhang-Erläuterung einiger krystallographischer Begriffe und Symbole," and presents a general introduction to crystallography with emphasis on considerations pertaining to the space groups. These sections are now illustrated and contain 27 figures and 2 photographs.

Part B is entitled "Kristallstrukturen und Eigenschaften" and deals with six different kinds of bonding in crystals, isomorphism, polymorphism, and ideal and real crystals.

Part C, entitled "Eigenschaft und Kristallstrukturen," takes up the physical properties of crystalline substances (thermal conductivity, compressibility, thermal expansion, optical properties, hardness, and cleavage) and relates them to the crystal structures of the substances concerned. Those who studied physical crystallography or crystal physics 25 years or more ago will recognize in this section a clear presentation of the modern approach to the subject.

This book should appeal especially to professors teaching courses in advanced mineralogy and crystal chemistry, and to their graduate students.

George T. Faust
Washington, D. C.

DIE SILIKATISCHEN TONMINERALE by K. Jasmund: 2nd enlarged edition, Monograph No. 60 "Angewandte Chemie" und "Chemie-Ingenieur-Technik." Verlag Chemie, G.M.B.H., Bergstrasse, Weinheim, Germany, 1955, 192 pp., 43 fig., 74 tables, Price 17.80 D.M.

The first edition of this book was reviewed in Volume 36 of this journal on page 924. This reviewer can only laud still further the excellence of this new edition. Jasmund has made a thorough search of the literature and has added about 277 new references, of which 45 have been added as lettered variants of a given number such as 393, 393a, 393b. The book has been increased by about one-third the number of pages in the first edition. References include some papers as late as 1954.

In writing this book, Jasmund has prepared a text which will appeal particularly to mineralogists and petrologists. The organization, arrangement, and presentation are well done. It is difficult to keep a book up-to-date in a field, such as clay mineralogy, which is changing so rapidly. Despite this handicap, Jasmund has written an excellent treatise. The reviewer strongly recommends this book.

George T. Faust
Washington, D. C.

S. JAMES SHAND MEMORIAL VOLUME. Annals of the University of Stellenbosch, Volume 33, Section A, Nos. 1–11, 575 pp., edited by M. S. Taljaard, 1957.

Attention should be called to this volume which presents a collection of significant, well-illustrated papers dealing mainly with regional studies in South Africa. The articles are of special interest in the fields of petrology, tectonics, geomorphology, stratigraphy, and economic geology.

A Critical Review of Superimposed and Antecedent Rivers in Southern Africa..by S. Maske
The Diorites of Yzerfontein, Darling, Cape Province....................by S. Maske
On the Tectonic History and Some Related Sedimentational Aspects of the Witwatersrand

and Ventersdoys Systems in the Far East Rand, During Upper-Witwatersrand, Pre-Transvaal Time . . . . by A. F. Cluver
Morphological Reconstruction of the Kimberley-Elsburg Series, with special reference to the Kimberley Group of Sediments in the East Rand Basin . . . . . by F. S. J. de Jager
The River Evolution and the Remnants of the Tertiary Surfaces in the Western Little Karoo . . . . by C. J. Lenz
The Mineralogy and Genesis of the Lead-Zinc-Vanadium Deposit of Abenab West in the Otavi Mountains, South West Africa . . . . by W. J. Verwoerd
The Application of the "Stereographic Projection" to Problems in Structural Geology . . . . by V. Vellet
The Dyke Rocks of Cape St. Martin . . . . by J. D. T. Otto
The Geology of the Klein Letaba Gold Mine, Sutherland Range, North-East Transvaal . . . . by B. F. Weilers
A Petrographic Study of the Waterfall Gorge Profile at Insizwa . . . . by D. Bruynzeel
On the Granite-Hornstone Contact at Slippers Bay . . . . by J. R. McIver

The volume (paper-bound) may be obtained through the Registrar, University of Stellenbosch, Stellenbosch, South Africa. Price £5-5-0.

WILLIAM C. KELLY
University of Michigan,
Ann Arbor, Michigan

NEW MINERAL NAMES

Francevillite

Georges Branche, Marie-Edith Ropert, Francis Chantret, Bernard Morignat, and Robert Pouget, La francevillite, nouveau minéral uranifère. *Compt. rend.*, **245**, No. **1**, p. 89–91 (1957).

Analyses of four samples gave UO_3 55.5, 54.9, 55.0, 55.4, V_2O_5 17.5, 17.6, 17.8, 17.5; BaO 9.8, 10.1, 10.2, 10.3; PbO 7.2, 7.5, 7.5, 7.4; H_2O 8.7, 8.7, 8.7, 8.7; sum 98.7, 98.8, 99.2, 99.3%; these after eliminating impurities amounting to about .0.2% of SiO_2 and Al_2O_3 and about 0.1% of Na_2O, MgO, and Fe_2O_3. Spectrographic analysis showed K 400–600 p.p.m., Ca and Sn 200–400 p.p.m. Mo 100–200 p.p.m. Ti, Mn, and Cu about 50 p.p.m. The analyses correspond to $(Ba, Pb)(UO_2)_2(VO_4)_2 \cdot 5H_2O$ with Ba:Pb=2:1. A sample from another locality, "d'origine metropolitaine," contained no Pb (microchemical test) and apparently is the barium end-member.

The mineral loses 7.8% H_2O up to 225° and 8.7% up to 520°, but heating for three hours at 225° drove off 8.6%. *X*-ray patterns of material heated at 520° showed no change, and the mineral rehydrates on being allowed to stand in the laboratory atmosphere. A D.T.A. curve shows a large endothermal effect at about 150–200°, smaller ones at 680° and 900°.

The mineral is orthorhombic with a perfect cleavage, (001). The faces (111), and especially (100) and (010) are rare. Optically biaxial, negative, with indices: (Pb-free) $\alpha 1.750 \pm 0.010$, $\beta 1.910 \pm 0.005$, $\gamma 1.945 \pm 0.005$, 2V (calcd.) $46 \pm 2°$; (lead-bearing) $\alpha 1.785$, $\beta 1.952$, $\gamma 2.002$, each ± 0.005, 2V (calcd) $53 \pm 1°$ (measured $52 \pm 1°$. $X=c$, $Y=b$. Pleochroic, with X colorless, Y and Z yellow. Does not fluoresce in ultra-violet light. Hardness 3. G. (lead-bearing) 4.55.

An unindexed powder pattern is given. The strongest lines (*d* in Å) and intensities are: 8.30–10, 2.98–8, 4.17–6, 2.57–6, 2.10–5, 3.27–4, 2.01–4. The pattern resembles that of meta-tyuyamunite.

The mineral occurs as impregnations, as cryptocrystalline veinlets, and as crystal-plates several mm. in thickness in sandstones in the region of Franceville, French Equatorial Africa.

The name is for the locality.

Discussion—This is apparently the barium analog of meta-tyuyamunite.

Michael Fleischer

Bonattite

Carlo L. Garavelli, Bonattite: Un nuovo minerale di alterazione del giacimento Elbano di Capo Calamita. *Rend . soc. mineralog. ital.* **13,** 268 (1957).

The name bonattite is given to $CuSO_4 \cdot 3H_2O$, found as a secondary mineral in the deposits of Cape Calamita, Elba. Chemical analysis (not given) corresponds to 85% $CuSO_4 \cdot 3H_2O$, 15% $CuSO_4 \cdot 5H_2O$, with a little Fe and Mg present. The mineral is in the form of concretions composed of minute individuals. Artificial crystals are monoclinic, domatic, with $a:b:c=0.432:1:0.552$, β 96°25′. The strongest lines of the *x*-ray powder pattern are 4.40 (100), 3.24 (67), 3.65 (54), and 3.42 (50). Mean indices of the natural material ranged from 1.578 to 1.601; the artificial material had *n*s, α 1.554, β 1.577, γ 1.618.

Origin of the name is not stated; perhaps named for Prof. Stefano Bonatti of Pisa.

M.F.

SCOTT J. WILLIAMS
Mineralogist
offers
NEW MINERAL CATALOG 25¢

Specializing in Specimens for
Collections, Museums, Research and Teaching Purposes

Specimens for Sale or Exchange

2346 S. Scottsdale Road **Scottsdale, Arizona, U.S.A.**

Notice

MICROTEXT EDITION OF OUT OF PRINT ISSUES

All out of print issues of the American Mineralogist are now available in microtext edition as indicated below. The microtext is furnished on 3x5-inch cards, each card containing 48 pages of text material. A heading on each card in regular size type indicates the volume, number, pages, and date. All orders that include out of print issues will be filled with the microtext edition unless it is specifically stated that it is not desired. The cost of the microtext edition is the same as the cost of the regular issue. The following issues are available.

1-5	complete volume only	1916-1920
9	3	1924
10	3	1925
26	1-3, 6-8, 12	1941
27	1-9, 11	1942
28	1-8	1943
29	1-8	1944
30	1-4	1945
31	1-4	1946
32	1-2	1947

Send all orders to

MINERALOGICAL SOCIETY OF AMERICA
Earl Ingerson, Treasurer
U. S. Geological Survey
WASHINGTON 25, D.C.

RECENT ACQUISITIONS

Aragonite. Sicily. A group of large pseudohexagonal crystals, creamy white in color, partly transparent, 11½ x 12 x 6½", *$75.00*

Beryl. Quebec. Blue xline in pegmatite. 5 x 7", *$7.50*

Bournonite. Germany. Xled with chalcopyrite, xled siderite on xline siderite 5 x 6½", *$35.00*

Celestite. Sicily. Choice xled, white, with sulfur 5 x 5" to 5 x 6", *$25.00* to *$35.00*

Cerussite. New South Wales. A group of reticulated crystals coated with anglesite 4 x 5", *$15.00*

Cerussite. Southwest Africa. Twinned crystals on xline cerussite 4½ x 5½", *$25.00;* small twinned crystals on bright green malachite, a museum piece, 8½ x 12", *$200.00*

Iron, Meteoritic, var. *Siderolite.* First found in 1882, examples of this stony-iron meteorite are outstanding for exhibition or study. A polished slab, S 10.56, 254.29 grams, *$50.84* (This is only one of our meteorite specimens. Write for catalog *FM 10*)

Molybdenite. Quebec. Rich xline with pyrite, etc. 4 x 5", *$7.50, $10.00*

Monticellite. California. Brown xline, partly xled in blue calcite 4½ x 5½", *$7.50*

Phosgenite. Sardinia. Partly xled 2 x 2", *$15.00*

Quartz, var. *Rock Crystal.* Switzerland. A large water clear crystal with attractive chlorite phantoms. Rhombohedral faces have been polished. 3½ x 11¼", *$75.00*

Scapolite. Quebec. Gray xline with pyroxene, salmon calcite, molybdenite 3½ x 8", *$5.00*

Siderite. Germany. Group of light brown rhombohedral crystals 3½ x 4½", *$15.00*

Silicified Wood. Arizona. Exceptional polished complete trunk section, brown, tan, gray, shows grain beautifully. A museum piece. 11 x 13½ x 1¾", *$75.00*

Sphalerite. Colorado. Medium sized, brown crystals with galena on rock 9 x 12½", *$10.00*

Uranophane. Texas. Yellow tufted in vesicular rhyolite, attractive. 2 x 3", *$4.00,* 3 x 4", *$7.50*

Uranothorite. Ontario. Rich uranothorite ore showing brown uranothorite, zircon, allanite, pyroxene, etc. 3 x 4", *$7.50*

Vanadinite. Southwest Africa. A large group of crystals coated with descloizite. Majority of crystals show orange red vanadinite core. 5 x 7½", *$50.00*

Wolframite. Japan. A large crystal pseudomorphed after scheelite (Reinite) 1½ x 2", *$17.50*

CRYSTALLOGRAPHIC AIDS

There is nothing finer for lecture demonstration or laboratory study than the crystallographic models that are prepared in the Krantz laboratories. Accurately cut pearwood models are available to illustrate 282 different crystal forms and combinations in the popular Dana series. Large models of glass and cardboard simplify lecture work. A wide series of crystal structure models includes a very popular set of 6 Si 0 models. (Write for new price list.)

CATALOGS

Ward's Geology Catalog: a complete listing of collections, bulk minerals and rocks, student specimens, color slides, models and equipment for field and laboratory. Sent free if requested on school or business letterhead.

Ward's Specimen Catalog—FM 10—A recent listing of individual mineral specimens and popular collections.

WARD'S *NATURAL SCIENCE ESTABLISHMENT, INC.*
3000 RIDGE ROAD EAST **ROCHESTER 9, N.Y.**

GEORGE BANTA COMPANY, INC., MENASHA, WISCONSIN, U.S.A.